ONTOGENY OF UPPER CRETACEOUS (TURONIAN-SANTONIAN) SCAPHITID AMMONITES FROM THE WESTERN INTERIOR OF NORTH AMERICA: SYSTEMATICS, DEVELOPMENTAL PATTERNS, AND LIFE HISTORY

NEIL H. LANDMAN

BULLETIN
OF THE
AMERICAN MUSEUM OF NATURAL HISTORY
VOLUME 185 : ARTICLE 2 NEW YORK : 1987

ONTOGENY OF UPPER CRETACEOUS (TURONIAN-SANTONIAN) SCAPHITID AMMONITES FROM THE WESTERN INTERIOR OF NORTH AMERICA: SYSTEMATICS, DEVELOPMENTAL PATTERNS, AND LIFE HISTORY

NEIL H. LANDMAN
Assistant Curator, Department of Invertebrates
American Museum of Natural History

BULLETIN OF THE AMERICAN MUSEUM OF NATURAL HISTORY
Volume 185, article 2, pages 117–241, figures 1–82, tables 1–25
Issued April 10, 1987
Price: $11.50 a copy

ISSN 0003-0090

CONTENTS

ABSTRACT

Scaphites are a group of Late Cretaceous heteromorphic ammonites in which the final body chamber partially uncoils, thereby marking the attainment of the adult stage. This distinctive change in shape permits unequivocal separation of variation due to developmental stage from phenotypic variation among adults. In the Western Interior of North America, scaphites are represented by a wide diversity of endemic species. Many of these species are abundant and well preserved and, therefore, are especially suitable for a detailed investigation of ontogenetic development. I studied the ontogeny of several species of Turonian-Santonian scaphites in the genera *Scaphites, Clioscaphites,* and *Pteroscaphites,* utilizing both whole fossils and polished sections. The study of their ontogeny bears on the questions of scaphite systematics and morphological development, and ammonite life history in general.

The initial whorls of scaphites, as in other ammonites, consist of a bulbous protoconch and part of a planispiral whorl (referred to as the ammonitella). The ammonitella displays a uniform tuberculate micro-ornamentation extending 0.75 whorls to a depression (primary constriction) after which growth lines appear. The shell wall is prismatic in microstructure and nacre first appears at the constriction where it forms an internal pad (primary varix). These morphological observations support a scheme of direct development in which the constriction marks the aperture of the embryonic shell. Preserved ammonitellas of *Scaphites ferronensis* and *Baculites* cf. *B. asper, B. codyensis* suggest that hatching may have occurred after the development of the proseptum. In scaphites, the proseptum displays a unique necklike attachment that appears as a superimposed saddle on the prosuture. The caecum and its prosiphonal attachment are similar among all the species studied. The diameter of the embryonic shell averages 700 μm and ranges from approximately 600 to 800 μm. The ammonitella angle averages 270°, which is similar to the angular length of the juvenile body chamber. Unlike modern *Nautilus,* the embryonic shell is comparable in size to the young of many Recent dibranchiate cephalopods and may have followed a planktonic mode of life immediately after hatching.

The juvenile shell conforms to a logarithmic spiral but exhibits a conspicuous change in morphology at approximately 3–4 mm diameter corresponding to two whorls from the primary constriction. The change involves modifications in the growth patterns of the umbilical diameter and spiral radius and coincides with the first appearance of macro-ornamentation. It also corresponds to a minimum in septal spacing and the attainment of a stable, ventral position of the siphuncle. These changes may indicate a transition from a passive planktonic to a more active mode of life. Similar morphometric changes occur in many other ammonites at this approximate size and whorl number and may represent a common developmental pattern. In micromorph scaphites of the genus *Pteroscaphites,* this whorl size coincides with the initiation of an accelerated maturity. As in modern *Nautilus,* the period of septal secretion in scaphites and other ammonites was probably dependent on the rate of apertural growth and buoyancy requirements rather than external astronomical rhythms. The period may also have displayed an increase over ontogeny, although the absolute rate of growth is unknown.

Maturity is expressed by the development of an uncoiled body chamber, although the degree of uncoiling varies widely among species. Interspecific comparisons are therefore facilitated by examination of the more similarly shaped phragmocones. Within species, histograms of adult phragmocone diameter form unimodal distributions although a well-marked sexual dimorphism appears in many species. The ratio of maximum to minimum phragmocone diameter ranges from 1.7 in *S. preventricosus* to 4.6 in *S. carlilensis.* The diameter of the adult phragmocone and the number of postembryonic whorls exhibit a positive correlation within and among species. The adult size and the extent to which the mature body chamber uncoils also covary within and among species. Evolutionary changes in size, with concomitant changes in the timing of sexual maturation, may thus explain interspecific variation in the degree of mature uncoiling.

INTRODUCTION

Scaphites are heteromorphic ammonites: the shape of their shell changes markedly during growth. Their final body chamber partially uncoils, but remains in the same plane of growth and reflexes hooklike upon the earlier secreted phragmocone. Although scaphites, like other externally shelled molluscs, preserve in their shells a record of their on-

togeny, this ultimate change in shape reflects determinate growth and provides a conspicuous criterion for comparative study. The uncoiling of the final body chamber is interpreted as the attainment of maturity and, indeed, in many species, the hooklike recurvature brings the aperture so closely against the phragmocone that further growth is clearly precluded. This morphologic change facilitates ontogenetic study and permits unequivocal separation of variation due to disparity in developmental stage from phenotypic variation among adults. This distinction is fundamental to scaphite systematics.

Scaphitid ammonites occur on all continents except Antarctica but display a concentration of species in the Northern Hemisphere. They range in age from the latest Albian to the latest Maastrichtian and are among the last ammonites to become extinct. In the Western Interior of North America, they are represented by a wide diversity of species ranging in age from the latest Cenomanian to the late Maastrichtian, a period of approximately 35 million years.

This study is based on the scaphite species endemic to the Western Interior during Turonian-Santonian time, which is also known regionally as middle and late Coloradoan age (Cobban, 1951). This interval equals approximately 6 million years ranging from 89 to 83 my B.P. (Obradovich and Cobban, 1975; Kaufmann, 1979). More than 50 species occur constituting four different genera: *Scaphites, Clioscaphites, Desmoscaphites* and *Pteroscaphites. Pteroscaphites,* distinguished as a separate genus by Wright (1953), consists of rare micromorph species with apertural lappets. Cobban (1951) illustrated and described all these species, documented their biostratigraphic zonation, and discussed their phylogenetic relationships based on their ranges and adult morphology.

These Turonian-Santonian scaphites exhibit a broad geographic distribution within the Western Interior, ranging from New Mexico to Montana and from Wyoming to Greenland. Their distribution reflects the configuration and environment of the epeiric seaway. The most fossiliferous sections occur along the periphery of the Black Hills in Wyoming and South Dakota and on the Sweetgrass arch in north-central Montana (figs. 1, 2; Cobban, 1951, 1956; Cobban et al., 1959, 1976; Rice and Cobban, 1977). In the Black Hills region these formations include the top of the Greenhorn Limestone and the Carlile Shale, yielding the sequence of species from *S. delicatulus* to *S. corvensis* of Turonian age. *S. ferronensis* is absent here but occurs elsewhere in Wyoming, Utah, and New Mexico between the ranges of *S. warreni* and *S. whitfieldi.* On the Sweetgrass arch, scaphites are abundant in the Marias River Shale starting with *S. nigricollensis* and including most of the Coniacian and Santonian species. *S. depressus,* which occurs between the ranges of *S. ventricosus* and *C. montanensis,* is absent here but occurs just west of the Sweetgrass arch in the Glacier Park area (Cobban et al., 1958) and in the Cody Shale of the Bighorn Basin, Wyoming. The fauna associated with these species is predominantly molluscan and includes many bivalves and gastropods as well as many other ammonites such as *Collignoniceras, Prionocyclus,* and *Baculites,* another common heteromorph.

In addition to their abundant spatial and temporal distribution, many of these scaphites are beautifully preserved, retaining their original aragonitic shell, and therefore, lend themselves to a detailed investigation of ontogenetic development. This investigation had three aims. (1) Description of the ontogeny of individual species to supplement systematic descriptions that have been based mostly on adult morphology. I examined many characters and their ontogenetic transformations, thereby providing a firmer basis for the construction of testable hypotheses of evolutionary descent. Morphologic comparison with other ammonites also indicated character states unique to scaphites that could be used to establish monophyly. (2) Study of the developmental or morphological constraints in scaphitid ontogeny. For example, does the size of the embryonic shell influence the size of the mature conch? How do changes in one morphologic feature correlate with changes in others during the course of ontogeny? (3) Study of the patterns of ontogeny among species to reveal similarities in development and mode of life. The identifica-

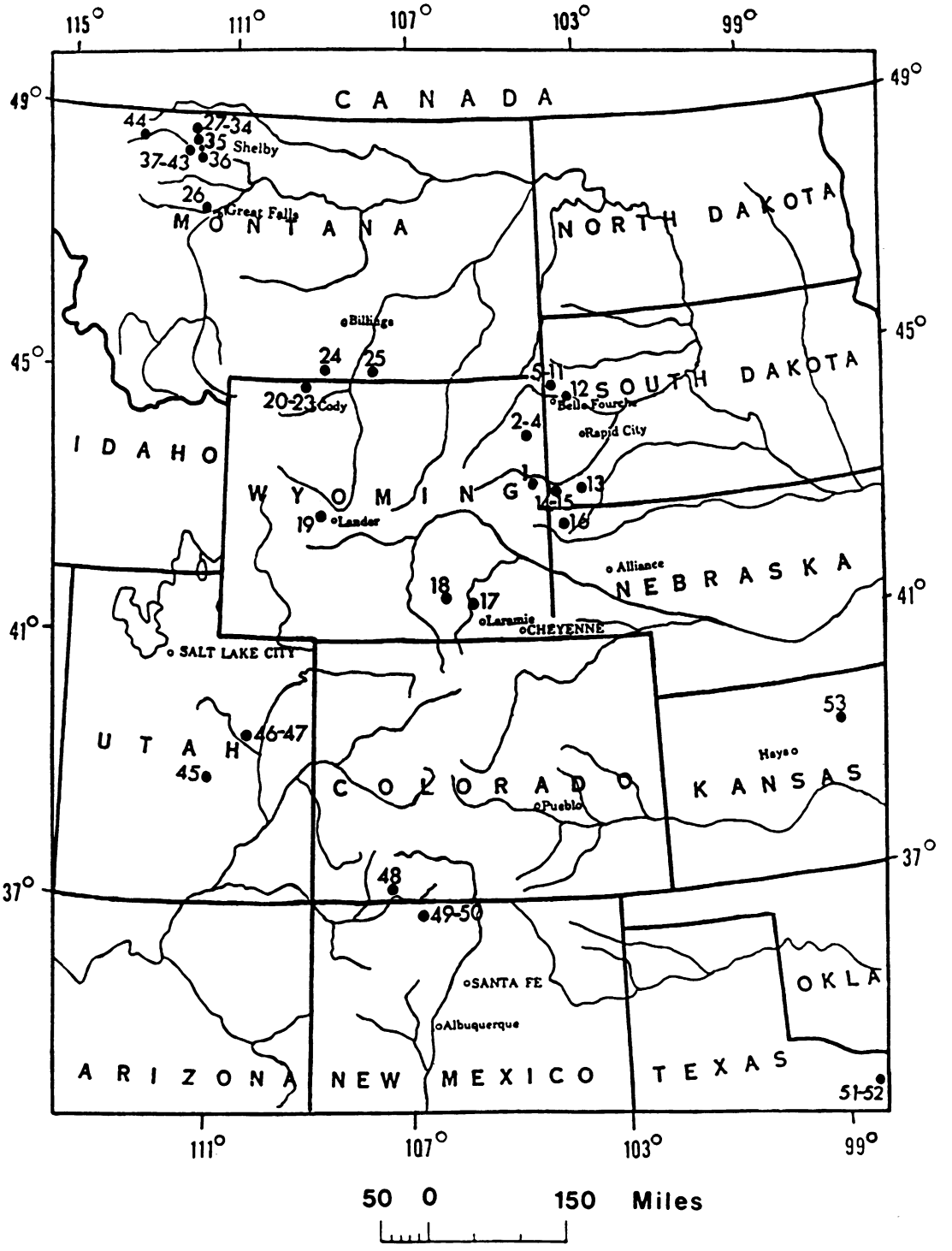

Fig. 1. Map of the Western Interior of North America illustrating the fossil localities mentioned in the text. Numbers refer to Appendix I.

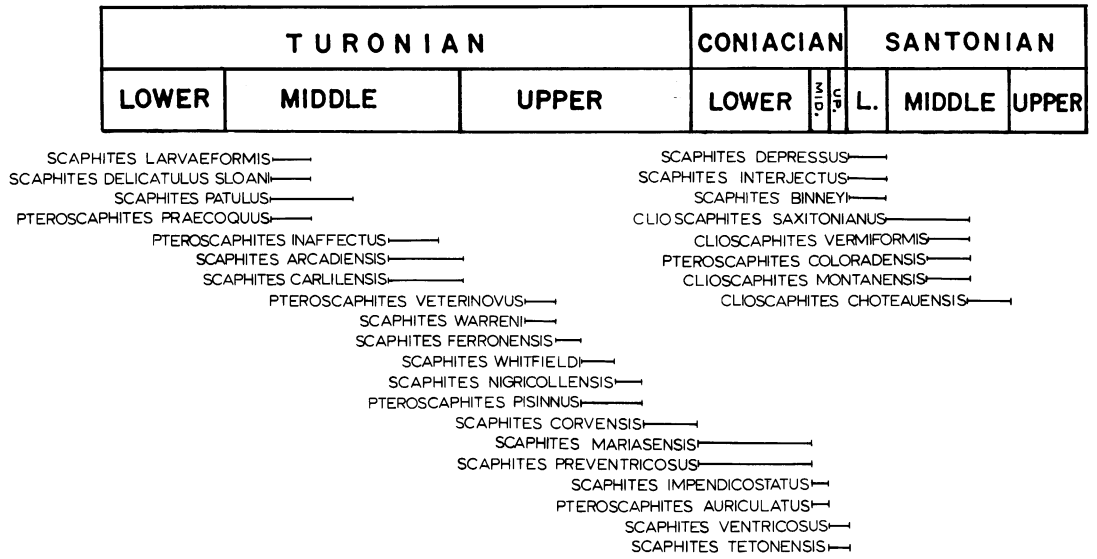

Fig. 2. Age distribution of "Coloradoan" (Turonian-Santonian) scaphites in the Western Interior of North America.

tion of developmental stages provides homologous points of comparison and facilitates study of the mechanisms of developmental modification. Such changes are not always confined to the adult, but often appear in early ontogeny and affect the whole course of subsequent development.

Two approaches were used to study ontogeny. The first involved examination of the preserved ontogenetic record of mature individuals to reconstruct the pattern of growth at earlier stages. Shells were broken down or sectioned to expose the embryonic or juvenile whorls. The second approach relied on specimens preserved intact at various stages of development. Such specimens yield unique information not recoverable using the first approach. Both approaches are mutually reinforcing, of course, and were used throughout my study.

Specimens of various scaphite species were collected in South Dakota, Wyoming, and Montana and were supplemented by generous loans of specimens from W. A. Cobban (United States Geological Survey, Denver, Colorado). The locality and stratigraphic data for these specimens are described in the appendix (fig. 1). I concentrated on four species of scaphites that comprised the most abundant and well-preserved specimens: *S. larvaeformis* from the middle Turonian, *S. whitfieldi* from the upper Turonian, *S. preventricosus* from the lower Coniacian, and *C. vermiformis* from the middle Santonian. The study of the ontogeny of these four species was frequently supplemented by the study of other scaphite species and *Baculites*. Illustrated specimens are reposited in the Yale Peabody Museum (YPM) and the American Museum of Natural History (AMNH).

Measurements of morphology were made on whole fossils and polished sections. Approximately 1000 median and dorsoventral sections were prepared for examination. I measured several parameters including whorl height, whorl width, cross-sectional area, umbilical diameter, siphuncular diameter, septal number, septal spacing, spiral radius, protoconch diameter, protoconch width, ammonitella angle, and ammonitella diameter. Suture patterns were not described because they are well illustrated in Cobban (1951) and will be examined in detail in a future study. Data were interpreted using several statistical tests including F-tests to evaluate similarities in the variances of the measured parameters, Student's t-tests to compare means, and Z-tests to determine positive or negative allometry. Linear regressions were also calculated using least squares.

This paper is organized into seven parts covering embryonic development, early postembryonic growth, and maturity. The micromorphs are treated in a separate section near the end. This section is followed by the conclusions and a systematic description of the four scaphite species most closely studied.

Acknowledgments

This research has benefited principally from the generous help of Karl Waage (Yale University) and William Cobban (United States Geological Survey, Denver, Colorado). Many other individuals have contributed their ideas and time including Donald Rhoads (Yale University), David Schindel (Yale University), Danny Rye (Yale University), Karl Turekian (Yale University), Kirk Cochran (SUNY, Stony Brook), and Peter and Neal Larson (Black Hills Institute of Geological Research). Several people have revised and improved this manuscript. I thank William Cobban, Andrew Swan (University of Swansea), John Chamberlain (Brooklyn College, CUNY), Michael McKinney (University of Tennessee), Roger Hewitt (McMaster University), Gerd Westermann (McMaster University), Niles Eldredge (AMNH), and W. James Kennedy (Oxford University). In my fieldwork I was helped by many friends including Karl Waage, Susan Kidwell, Diana Gibson, David Jablonski, David Schindel, Danita Brandt, Susse Wright, John Kurtz, Tim White, and Marcus Key. Specimens were prepared by Wally Phelps, Jean Lawless, and Susan Klofak. Photographs and figures were prepared by Carol Phelps, Beverly Heimberg, and Stephen Butler. The manuscript was typed by Diane Bennett and Stephanie Crooms. This research was supported by grants from the Geological Society of America, the National Science Foundation (Grants No. DEB78-12518 and EAR-8302093), Sigma Xi, the Woman's Seamen's Society of Connecticut, and the Charles Schuchert Fund of Yale Peabody Museum.

EMBRYONIC DEVELOPMENT

Basic Terminology

The early whorls of scaphites, other heteromorphs, and more normally coiled ammonites are similar in morphology and are referred to as the ammonitella (fig. 3; Druschits and Khiami, 1970; Druschits et al., 1977a; Tanabe et al., 1981). Any deviation in structural plan during the course of ontogeny occurs only after the formation of the ammonitella. It consists of a spheroidal or ellipsoidal initial chamber called the protoconch followed by approximately one planispiral whorl (fig. 3). This whorl terminates in the primary constriction and accompanying varix, which consists of a thickening of the outer wall. Internally, septa subdivide the shell into chambers. The first septum is called the proseptum and differs in shape from all subsequent septa. The siphuncle, a secretion of the posterior part of the body, runs through all of the chambers. The siphuncle originates in the protoconch as a small swelling, known as the caecum, which is attached to the protoconch walls by means of prosiphonal sheets.

External Appearance of the Ammonitella

Under scanning electron microscopy, the ammonitellas of the Turonian-Santonian scaphites from the Western Interior display a consistent distribution of tuberculate sculpture (fig. 4). The scaphite species examined were *S. whitfieldi, S. preventricosus, C. vermiformis,* and *P. auriculatus.* Similar micro-ornament has been observed previously on the ammonitellas of several other ammonite species. This micro-ornament was first reported on the early whorls of *Baculites compressus* and described as "minute tuberculations of irregular shape" (Brown, 1892). Later, J. P. Smith (1901) observed this micro-ornament on the early coil of another species of *Baculites, B. chicoensis,* from the Upper Cretaceous of California. He wrote that "the pustules gave the shell a granulated appearance and did not extend beyond the constriction." W. D. Smith (1905) first documented this micro-ornament on the early whorls of scaphites in the species *Scaphites nodosus* from the Western Interior of North America.

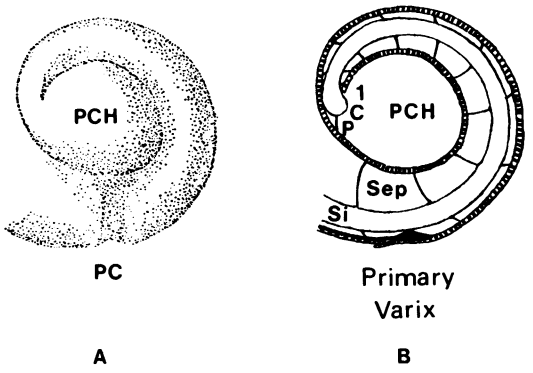

Fig. 3. **A.** View of the early whorls (ammonitella) of an adult scaphite showing the protoconch (PCH), first planispiral whorl, and primary constriction (PC). **B.** Median section of the same specimen reveals the siphuncle (Si), first septum or proseptum (1), subsequent septa (Sep), caecum (C), prosiphon (p), and primary varix.

He noted "regular rows of small pustules . . . ceasing abruptly at a constriction." More recently, this micro-ornament has been observed on the ammonitellas of *Quenstedtoceras* and *Kosmoceras* from the Callovian of Poland (Kulicki, 1979; Bandel et al., 1982); *Discoscaphites conradi, Hoploscaphites nicolleti, Hoploscaphites* sp. juveniles, and *Sphenodiscus lenticularis* from the Maastrichtian of the Western Interior of North America (Bandel et al., 1982); *Baculites chicoensis* from the Campanian of California (Bandel et al., 1982); and *Baculites* sp. from the Campanian and Maastrichtian of north Jordan (Bandel et al., 1982; Bandel, 1982).

On the Turonian-Santonian scaphites from the Western Interior, the tubercles are irregularly distributed over and restricted to the exposed portions of the ammonitella. They occur at random and some areas lack tubercles altogether. The distribution of tubercles is similar among all the species studied. The tubercles are more subdued on the protoconch but this may be an artifact of preservation because the tubercles on the ammonitellas of *Hoploscaphites nicolleti* and other species are as prominent on the protoconch as on the rest of the ammonitella (Bandel et al., 1982: figs. 1, 2). The tubercles may disappear at the adapical edge of the primary constriction, within its shallow depression, or on the narrow extension of the shell adoral to the constriction (fig. 4A, B). The subsequent shell is smooth and commonly marked by very fine transverse ridges that probably represent growth lines (fig. 4A, B).

In well-preserved ammonites, the tubercles consist of sectors of spherules (Bandel et al., 1982). In thin sections of the outer wall of *Quenstedtoceras* sp. the tubercles display a spherulitic structure (Kulicki, 1979). In the Turonian-Santonian scaphites from the Western Interior, the tubercles appear to be emergent ends of single large prisms (figs. 4C, 5). Originally, these tubercles may have been spherulitic, but recrystallization may have obliterated the structural detail. The height of the tubercles is approximately 2 μm. The tubercles range in diameter from approximately 4 to 8 μm within and among the species studied (fig. 4C, D). They are similar in diameter to the tubercles in *Baculites* but larger than those in *Sphenodiscus* and *Quenstedtoceras,* which average 2 to 3 μm.

The early whorls of other ammonites have been reported as smooth (Druschits et al., 1977: 197; Druschits and Khiami, 1970: 27), although this may be due to the difficulty of detecting tubercles in thin and polished cross-sections. However, the diversity of ammonites that display tuberculate micro-ornament indicates that this kind of sculpture is widespread. On the other hand, Paleozoic ammonites exhibit at least one other kind of ornament. House (1965: 87) described the ornament on the early whorls of the Devonian genus *Tornoceras* as consisting of "convex evenly spaced lirae" which extend to the primary constriction where they are replaced by "biconvex lirae which show a prominent ventrolateral salient and a deeper, narrower, ventral sinus."

Structure of the Outer Wall of the Ammonitella

In the Turonian-Santonian scaphites from the Western Interior, as in all other ammonites, the wall of the protoconch and first whorl is prismatic (fig. 5). The wall of the protoconch ranges in thickness from approximately 1.8 μm at its proximal end to approximately 8.5 μm at its distal end. According to Birkelund and Hansen (1974), a new shell layer appears at the beginning of the first

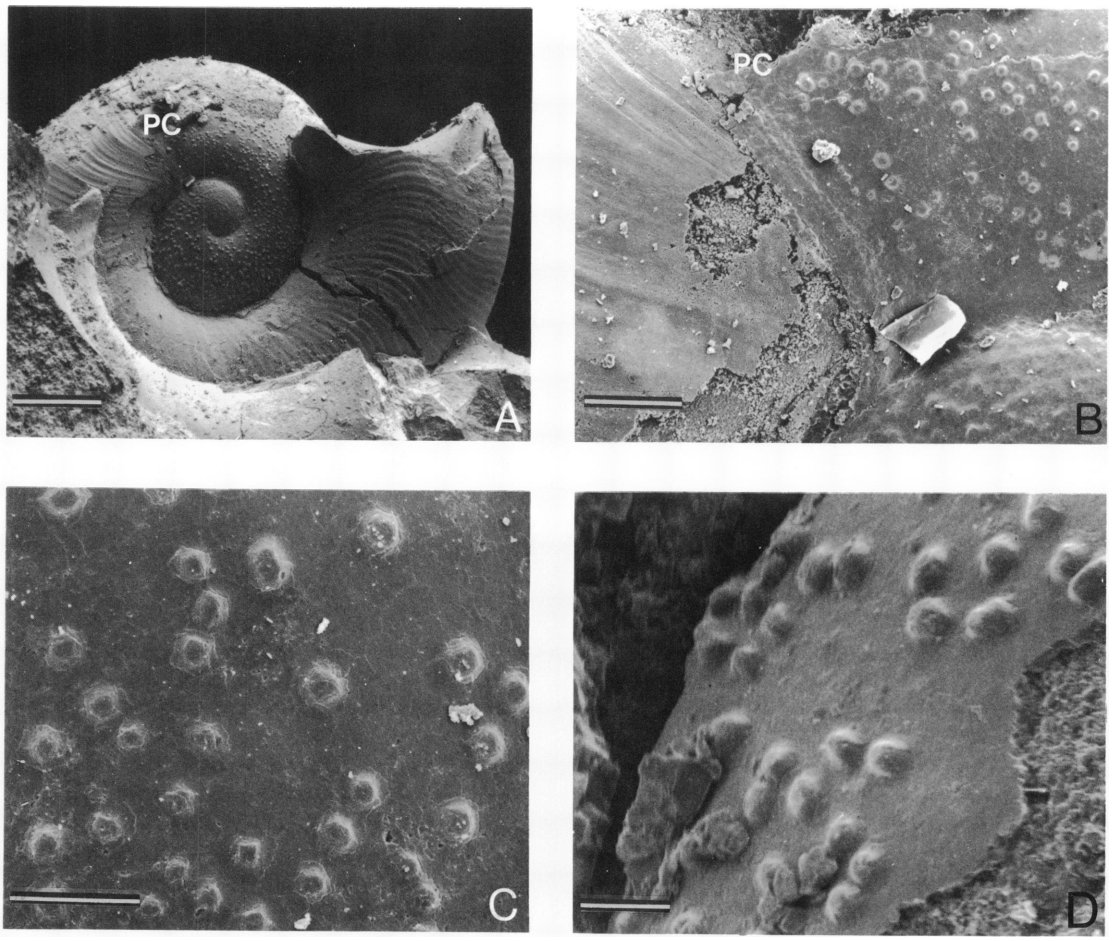

Fig. 4. Micro-ornament on the ammonitellas of two species of scaphites. **A.** *Clioscaphites vermiformis* (AMNH 43033). The ornamentation extends to the primary constriction. Scale bar = 200 μm. **B.** Close-up of same specimen. The tuberculate micro-ornamentation ends at the primary constriction and growth lines appear. Scale bar = 40 μm. **C.** Close-up of the tubercles on same specimen. Scale bar = 20 μm. **D.** Close-up of the tubercles on a specimen of *Pteroscaphites auriculatus* (AMNH 43034). Scale bar = 10 μm.

whorl and grows in thickness at the expense of the protoconch layer, which soon wedges out. The wall of the first whorl consists of two sublayers; the inner sublayer is more coarsely crystalline than the outer sublayer. Kulicki (1979) has interpreted the outer sublayer as the dorsal wall of the next whorl.

The primary varix and accompanying constriction occur at the end of the first whorl (figs. 6, 7). Scanning electron microscopy of the microstructure of the outer wall of the ammonitella in scaphites, as in all other ammonites, reveals a remarkable change at this point. The prismatic layer forming the first whorl thins out and beneath it, a pad of nacre develops, i.e., the primary varix. This feature has been illustrated in many ammonites including *Saghalinites wrighti, Discoscaphites* sp., *Hypophylloceras* (*Neophylloceras*) *groenlandicum* (fig. 5, pl. 2a, Birkelund and Hansen, 1974); *Eleganticeras elegantulum, Scaphites* sp., *Androgynoceras* cf. *planicosta, Spinicosmoceras* sp., *Aconeceras trautscholdi* (pl. 9, Erben et al., 1969); *Kosmoceras* sp. and *Quenstedtoceras* sp. (pl. 45, Kulicki, 1979) and *Luppovia* sp. (Doguzhayeva and Mikhailova, 1982).

The primary varix parallels the external

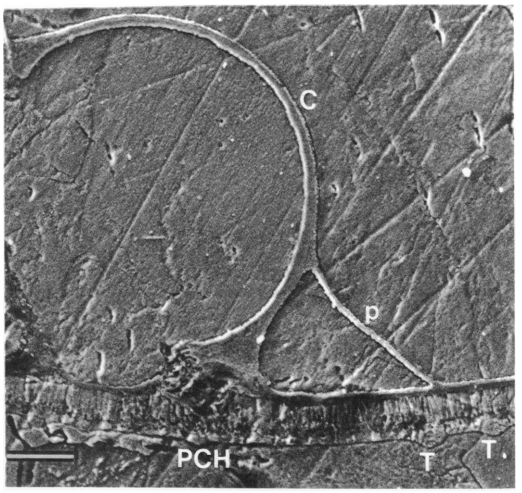

Fig. 5. Median cross section of a specimen of *Scaphites preventricosus* (AMNH 43035) illustrating part of the wall of the protoconch (PCH), caecum (C), prosiphon (p), and two tubercles (T). Scale bar = 10 μm.

constriction and lies close to its adapical side. Grandjean (1910: 512) called this feature his "première varice" and noted, "The form of this varix, in median section, varies little: it is always an abrupt thickening of the shell accompanied by a more or less marked undulation [author's translation]." The post-ammonitella shell which emerges from beneath the primary varix is composed of both prismatic and nacreous layers.

Landman and Waage (1982) have pointed out that "Some investigators have used the term primary varix for the depression the nacreous welt leaves on the steinkern, but this is a misapplication of Grandjean's usage and etymologically an incorrect use of the term varix (L = dilation, as of a vein)." The term "varix trace" was introduced by Landman and Waage (1982) for this depression. It is not a morphological feature of an ammonite but rather an impression of one and cannot be interpreted as a constriction or varix.

The term "nepionic" commonly used to describe both the constriction and accompanying varix is derived from the Greek word for infant and connotes a postembryonic or larval stage (Landman and Waage, 1982). The term was introduced by Hyatt (in Jackson, 1890: 290 footnote) and subsequently used by Smith (1898, 1901) although neither specifically applied it to the ammonite constriction or varix. Willey (1897a) in his study of juvenile *Nautilus* borrowed the term to describe a shell feature which he interpreted to mark the end of the embryonic stage. The primary constriction and varix occur early in ontogenetic development and, therefore, I prefer the descriptive adjective "primary" which avoids interpretation.

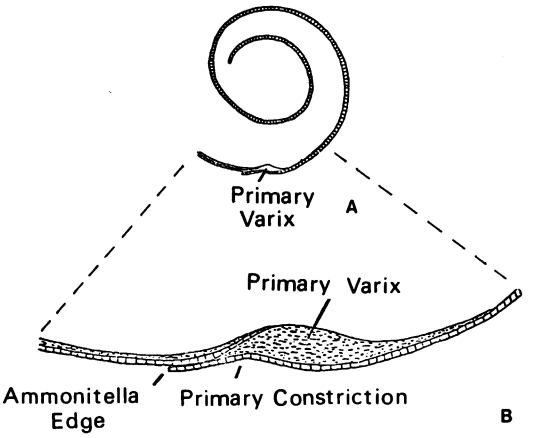

Fig. 6. Schematic diagram of the morphology near the aperture of the ammonitella. **A.** Median cross section of an ammonitella (without septa). **B.** Enlargement of the shell wall at the aperture.

Proseptum and Second Septum

Schindewolf (1954) referred to the initial two septa in ammonites as the proseptum and

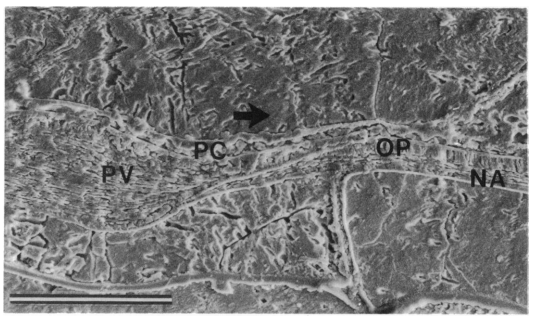

Fig. 7. Median cross section of the shell wall at the primary constriction (PC) and accompanying varix (PV) of a specimen of *Scaphites preventricosus* (AMNH 43036). The shell wall adoral of the constriction consists of an outer prismatic (OP) and inner nacreous layer (NA). Scale bar = 40 μm.

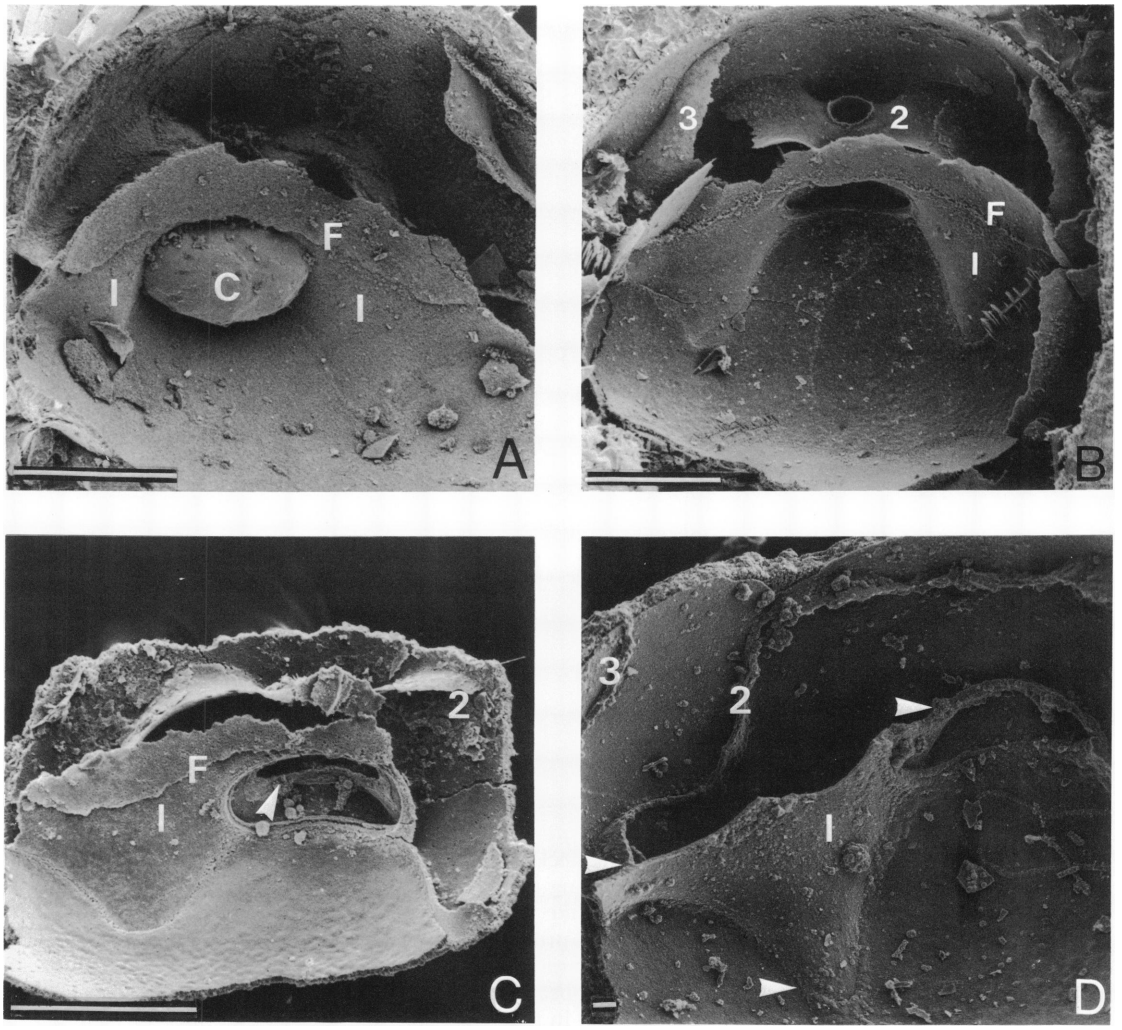

Fig. 8. **A.** Fragment of a protoconch dissected from a specimen of *Scaphites* cf. *whitfieldi* free of matrix (AMNH 42899). The proseptum (1), caecum (C), and flange (F) are visible. Scale bar = 100 μm. **B.** Interior of the protoconch and part of the first whorl of a specimen of *S.* cf. *whitfieldi* (AMNH 43037) showing the proseptum (1), flange (F), proseptal opening, second (2) and third septa (3), and the septal neck of the second septum. Scale bar = 100 μm. **C.** Interior of the protoconch and part of the first whorl of a specimen of *S.* cf. *whitfieldi* (AMNH 42900) showing the proseptum (1), flange (F), opening of the proseptum with its necklike attachment (arrow), and the second septum (2). Scale bar = 100 μm. **D.** View into the interior of the protoconch and part of the first whorl of a specimen of *S.* cf. *whitfieldi* (YPM 6240) reveals the proseptum (1), part of its necklike attachment (upper arrow), and the ventral traces of the second (2) and third (3) septa. Note that the second septum only intersects the proseptum at the extreme lateral margins (middle arrow). A prismatic ridge occurs at the base of the proseptum (lower arrow). Scale bar = 10 μm.

primary septum, respectively. According to Erben et al. (1969), the proseptum and the primary septum are prismatic in the Jurassic genera *Xipheroceras, Androgynoceras, Eleganticeras, Quenstedtoceras,* and *Pavlovia.* They observed nacre in the third septum and therefore called it the first nacroseptum. Landman and Bandel (1985) also documented that the proseptum is invariably prismatic. However, they indicated that the pri-

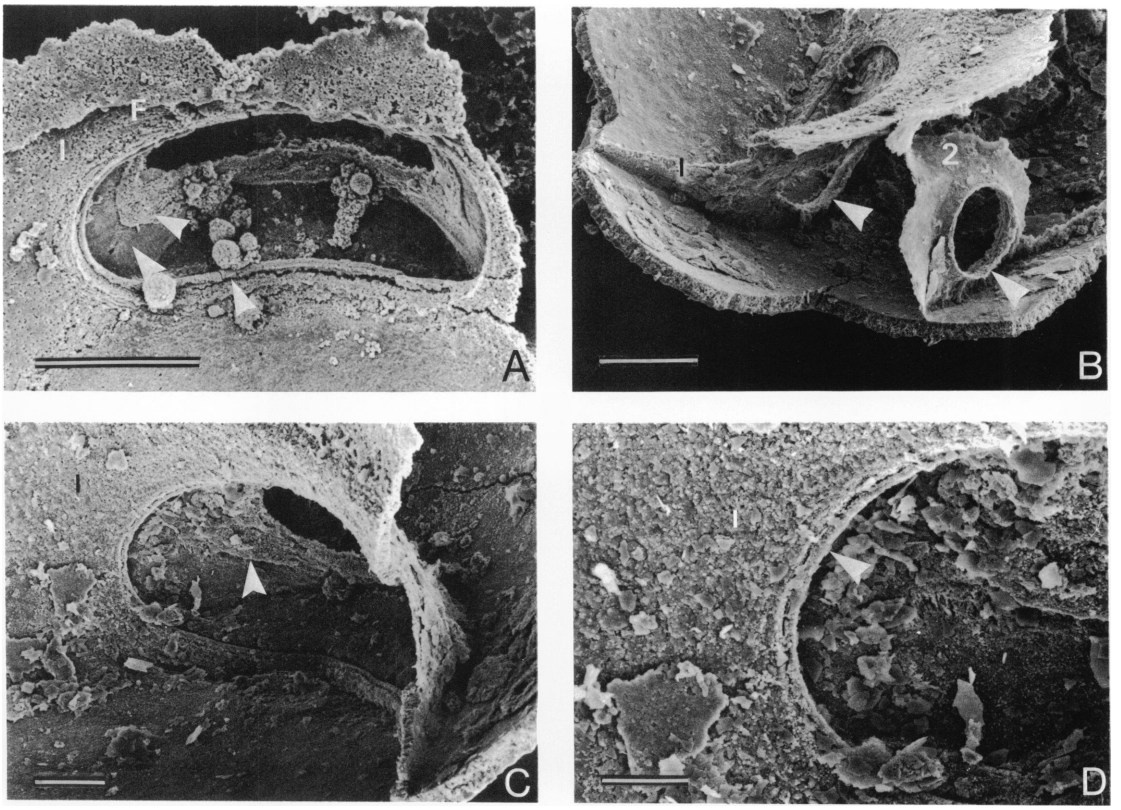

Fig. 9. **A.** Close-up of the specimen of *Scaphites* cf. *whitfieldi* illustrated in figure 8C reveals the opening of the proseptum (1), flange (F), and the necklike attachment of the proseptum (middle arrow). A groove (lower arrow) occurs around the opening of the proseptum. Prismatic attachment deposits (upper arrow) of the siphuncle occur on the necklike attachment of the proseptum. Scale bar = 40 μm. **B.** View from the first whorl looking back into the protoconch of a specimen of *S.* cf. *whitfieldi* (AMNH 42901). The proseptum (1) and its necklike attachment (left arrow) are visible. The second septum (2) with its prochoanitic septal neck (right arrow) appears in the foreground. Scale bar = 40 μm. **C.** The proseptum (1) and part of its necklike attachment in the same specimen of *S.* cf. *whitfieldi* illustrated in figure 9B. Prismatic attachment deposits (arrow) occur on the necklike attachment of the proseptum. Scale bar = 20 μm. **D.** Close-up of the specimen illustrated in figure 9B and C reveals a groove (arrow) around the opening of the proseptum (1). Scale bar = 10 μm.

→

Fig. 10. Five serial sections of the same specimen of *Scaphites preventricosus* (AMNH 42902) prepared parallel to the median plane. **A.** The most lateral section shows the proseptum (1), flange (F), and first nacreous septum (2). Scale bar = 20 μm. **B.** In this section the necklike attachment (arrow) of the proseptum (1) begins to develop. Scale bar = 20 μm. **C.** In this section the proseptum (1) and its necklike attachment (arrow) display an incipient separation. Scale bar = 20 μm. **D.** In the next to last section, the proseptum (1) has opened to reveal part of the caecum (C). The necklike attachment (arrow) of the proseptum is still unbroken. Scale bar = 20 μm. **E.** The final median section reveals the flange (F), caecum (C), siphuncle (S), proseptum (1), necklike attachment of the proseptum (left arrows), and the second septum (2) with its septal neck (right arrows). Scale bar = 20 μm. **F.** Close-up of the dorsal part of the proseptum (1) reveals the flange (F), necklike attachment of the proseptum (upper arrow), caecum (C), siphuncle (S), and additional prismatic attachment deposits of the caecum and siphuncle (lower arrows). Scale bar = 20 μm (from Landman and Bandel 1985).


2
F
I
A

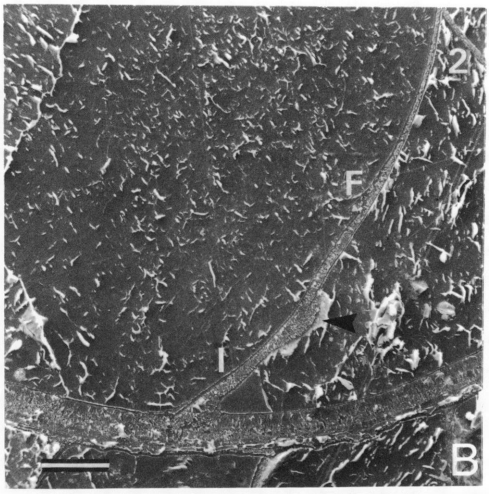
2
F
I
B

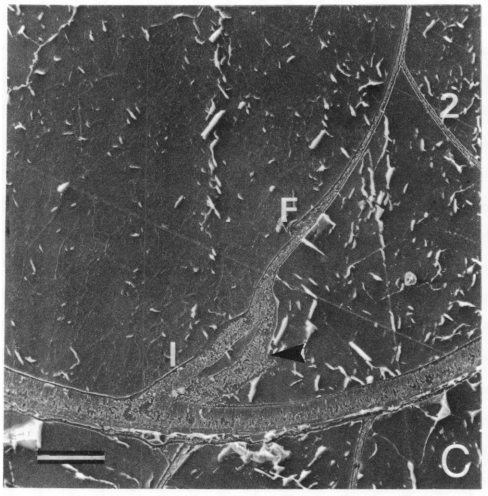
2
F
I
C

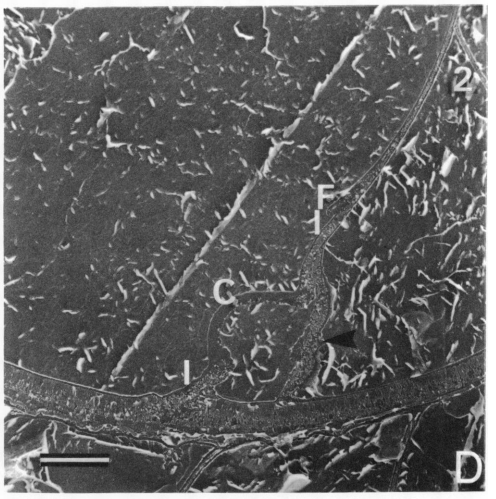
2
F
C
I
D


C
F
I
2
S
S
2
I
E

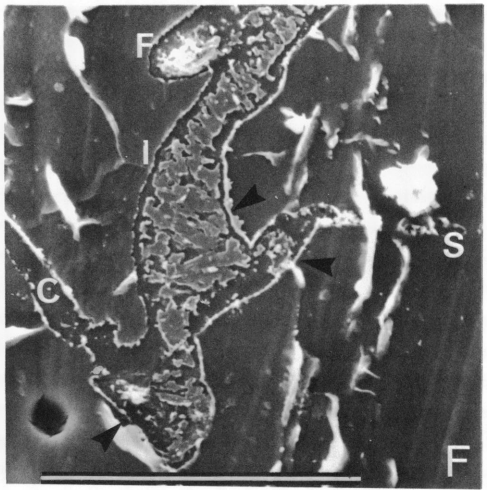
F
I
S
C
F

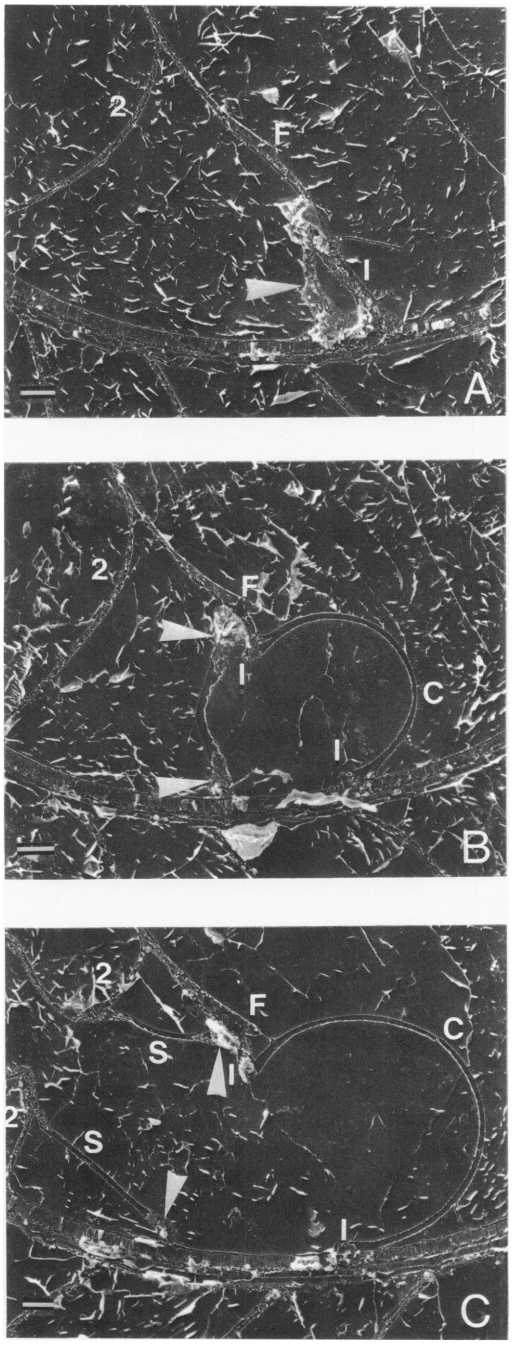

Fig. 11. Three serial sections of the same specimen of *Clioscaphites vermiformis* (AMNH 43200) prepared parallel to the median plane. **A.** The most lateral section shows the proseptum (1), flange (F), necklike attachment (arrow) of the proseptum, and first nacreous septum (2). Scale bar = 10 μm. **B.** In this section the proseptum (1) and the necklike attachment (arrows) of the proseptum open to reveal part of the caecum (C). Scale bar = 10 μm. **C.** The final median section reveals the caecum (C), proseptum (1), necklike attachment (arrows) of the proseptum and siphuncle (S). The second septum (2) is slightly convex toward the aperture and displays a prochoanitic septal neck. Scale bar = 10 μm.

mary septum is already nacreous in *Quentstedtoceras, Kosmoceras, Euhoplites, Baculites, Hypacanthoplites,* and *Scaphites* and allied genera. To avoid nomenclatural confusion, they simply referred to these initial septa in numerical sequence starting with the proseptum as the first septum. All septa may exhibit additional prismatic deposits which have been termed false septal necks (Birkelund and Hansen, 1974), cuffs (Druschits et al., 1977a), auxiliary deposits (Kulicki, 1979), and prismatic attachment deposits (Bandel, 1982). These serve to attach the caecum or siphuncle to the septa.

The structural arrangement of the first few septa in scaphites is difficult to resolve from thin sections alone. However, specimens of *Scaphites whitfieldi* free of matrix from locality B198a have also been used. Within the protoconchs of these specimens, the caecum, flange, and proseptum are visible (figs. 8, 9). The proseptum surrounds and cups the caecum to form a median saddle. If the caecum is removed or destroyed due to diagenesis, the proseptum, proseptal opening, and second septum become visible. A necklike attachment of the proseptum appears near the median plane and extends adorally from the proseptum, surrounding the smaller end of the caecum. It rides ventrally on the interior of the wall of the first whorl and precedes the second septum.

The shape and arrangement of the proseptum and its necklike attachment may be studied further using serial sections prepared parallel to the median plane and viewed under scanning electron microscopy. The series of sections illustrated in figures 10 and 11 were prepared from a specimen of *S. preventricosus* and a specimen of *C. vermiformis.* In these sections, the wall of the protoconch is prismatic in structure and passes into the wall of the first whorl. In the most lateral section,

the prismatic proseptum forms an unbroken structure followed by the first nacreous septum. In the next section, the prismatic necklike attachment of the proseptum appears as either an outgrowth of the proseptum or as a separate structure. The proseptum and its necklike attachment subsequently separate except at their dorsal and ventral ends. Nearer the median plane, the caecum appears through the opening of the proseptum. The opening of the proseptum is wider than that of its necklike attachment and, therefore, the necklike attachment is still unbroken. In the last median section, the proseptum and its necklike attachment are only visible on the dorsal and ventral ends. They are less conspicuous on the venter and are widely separated, having diverged toward the median plane.

The flange is visible on all lateral sections but is most conspicuous on the median section (figs. 10, 11). It is the blind proximal end of the protoconch wall but in some specimens the flange and the wall of the protoconch appear separated for a short adoral distance. The flange is clearly visible on specimens free of matrix (figs. 8, 9).

The proseptum and its necklike attachment are prismatic. A prismatic ridge also occurs at the base of the proseptum (fig. 8D). Additional prismatic deposits connect the proseptum and its necklike attachment to the siphuncle and caecum. In median section, these deposits are especially well developed on the dorsal side and are also conspicuous on the necklike attachment of the proseptum in specimens free of matrix (figs. 9, 10F). A groove appears around the opening of the proseptum (fig. 9).

The first nacreous septum, that is, the second septum, is a moderate distance from the proseptum and its necklike attachment. It is slightly convex toward the aperture. It contacts the proseptum at the extreme lateral margins, as illustrated in figure 8. The second septum exhibits a prochoanitic neck and is generally thinner than the proseptum and its associated structure. On median sections of *S. preventricosus* and *C. vermiformis,* the proseptum and its necklike attachment each measure approximately 3–4 μm in thickness whereas the nacreous septum measures approximately 1.5 μm in thickness. The latter value compares to a thickness of 3 μm for the first nacreous septum in *Discoscaphites* sp. (Birkelund and Hansen, 1974). However, on lateral sections, the proseptum and its necklike attachment become thicker whereas the second septum retains the same thickness. This discrepancy is due to the oblique angle of the lateral section through the septa.

TABLE 1
Septal Spacing of the Initial Five Septa in Three Specimens of *C. vermiformis*[a]

B239a 1		21425		B235a 7	
Septum	Angle	Septum	Angle	Septum	Angle
ps(1)	0.0	ps(1)	0.0	ps(1)	0.0
neck	19.6	neck	14.5	neck	15.2
2	17.5	2	18.5	2	16.0
3	23.8	3	29.9	3	18.0
4	22.7	4	26.8	4	21.8
5	24.6	5	29.2	5	21.8

[a] ps(1) = proseptum; neck = necklike attachment of the proseptum.

The angular distances between the proseptum, its necklike attachment, and the second septum in three specimens of *C. vermiformis* are presented in table 1. The angles are measured along the venter on the median plane. Each value represents the average of four measurements. The angular distance between the necklike attachment and the proseptum is sometimes slightly less, and sometimes slightly more, than the angular distance between the necklike attachment and the second septum. The distances between the second and third septa and between the third and fourth septa are usually larger than the aforementioned values. On lateral sections parallel to the median plane, the angular distance between the proseptum and its necklike attachment reduces to zero but the distance between the necklike attachment and the second septum increases. All the other angular distances remain approximately the same.

The marginal plications of the proseptum and its necklike attachment appear as the prosuture and a superimposed ventral saddle (figs. 12, 13). The prosuture is angustisellate and consists of a ventral and dorsal saddle separated by two lobes and one umbilical saddle. The necklike attachment produces a ventral saddle above the saddle formed by

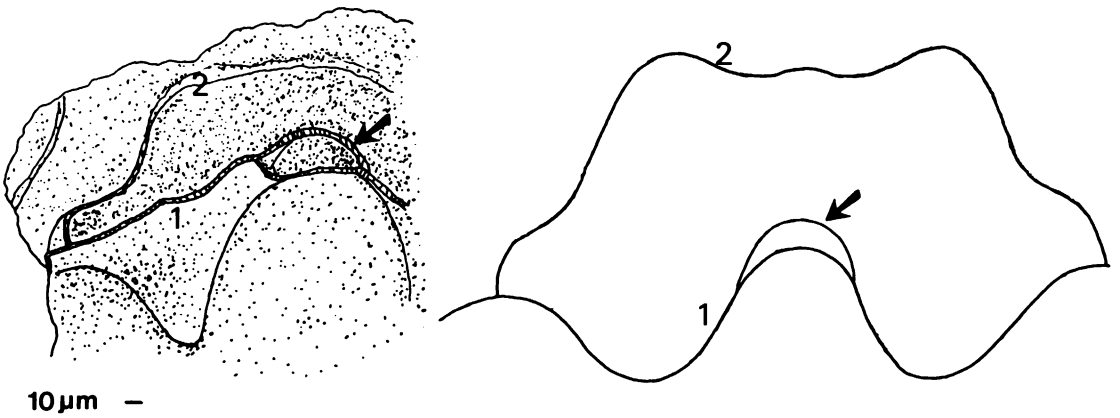

Fig. 12. Drawing of the specimen illustrated in figure 8D showing the proseptum (1), necklike attachment of the proseptum (arrow), and second septum (2), and their corresponding sutures. Scale bar = 10 μm.

the proseptum (fig. 12). On the dorsal side, the necklike attachment coincides with the proseptum. The ventral suture of the first nacreous septum contacts the prosuture at the lateral margins (fig. 13).

The necklike attachment of the proseptum may be unique to scaphites. It occurs in all the scaphites studied in the genera *Scaphites, Clioscaphites,* and *Pteroscaphites.* In a brief survey of younger scaphites from the Upper Cretaceous of the Western Interior, I observed this structure in *Hoploscaphites* sp. from the *Baculites reesidei* Range Zone from the Pierre Shale (USGS loc. D4440) and *Hoploscaphites nicolleti, H. nebrascensis,* and *Discoscaphites conradi* from the Fox Hills Formation. It also occurs in *Discoscaphites* sp. from the Maastrichtian of Greenland. It is absent in other ammonites including *Saghalinites* sp. from the Maastrichtian of Greenland (a lytoceratid), *Baculites* sp. from the Santonian of the Western Interior (an ancyloceratid), *Neophylloceras ramosum* from the Upper Cretaceous of California (a phylloceratid), *Euhoplites* from the Albian of England (an ammonitid), *Hypacanthoplites* from the Aptian of Germany (an ancyloceratid), and *Quenstedtoceras* and *Kosmoceras* from the Callovian of Poland (both ammonitids). Branco (1879, pl. 8, illus. 3; pl. 9, illus. 1, 3) illustrated specimens in which the second suture contacted the prosuture. This is common among ammonites and appears in scaphites. However, it does not relate to the necklike attachment of the proseptum.

The necklike attachment of the proseptum may represent a unique derived character among all scaphites (a synapomorphy). On the other hand, it may be restricted to Western Interior and Greenland scaphite species of close affinity. This feature may help establish monophyly for scaphites and serve as a criterion for membership in the group. For example, *Worthoceras* has been excluded from the scaphites by Wiedmann (1965) but Henderson (1973) has argued for inclusion, and, indeed, a decision based on adult morphology seems problematic. However, simple inspection of the prosuture in *Worthoceras* to determine the presence or absence of a superimposed ventral saddle may help resolve this dilemma.

Caecum and Prosiphon

The caecum is the bulbous beginning of the siphuncle, originating in the protoconch. The morphology of the caecum is similar among the Turonian-Santonian scaphites from the Western Interior. In median cross section, it is semicircular in outline and resembles the caecum in several species of scaphites from Japan as well as in many other species within the order Ancyloceratina (fig. 10; Tanabe et al., 1979; Tanabe and Ohtsuka, 1985). In specimens of *S. whitfieldi* free of matrix, the caecum appears as an oblate ellipsoid nestled in the median saddle of the proseptum (fig. 8A). The caecum is devoid of ornament and its microstructure in median

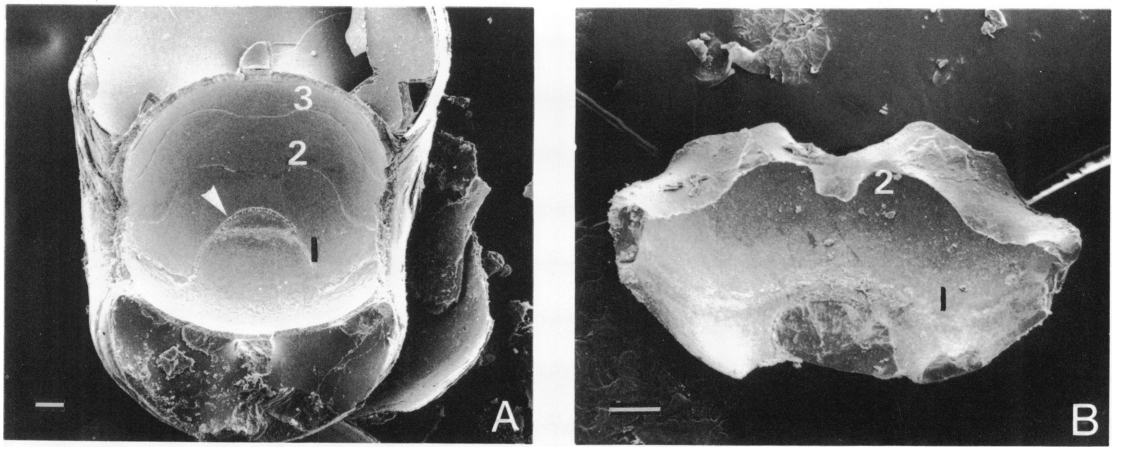

Fig. 13. **A.** Ventral view of the prosuture (1), suture formed by the necklike attachment of the proseptum (arrow), second suture (2) and third suture (3) of a specimen of *Scaphites* cf. *whitfieldi* (AMNH 42903). **B.** Dorsal view of a steinkern of *S.* cf. *whitfieldi* (AMNH 42904) shows that the prosuture (1) and second suture (2) are distinctly separated.

cross section and on fractured surfaces appears to be homogeneous. It probably is composed of the same organic material as the siphuncle. The thickness of the caecal wall along its convex adapical side averages 2.5 μm in a specimen of *S. whitfieldi* and a specimen of *S. preventricosus* (figs. 14 and 15).

The caecum is not surrounded by a calcareous sheath although such a structure has been observed in several species of scaphites from Japan including *S. planus, S. pseudoequalis, Otoscaphites puerculus,* and *O. klamathensis* (Tanabe et al., 1979). This thin calcareous sheath is comparable in cross-sectional thickness with what I am interpreting as the caecal wall and exhibits a massive microstructure upon etching with weak acid. The caecal wall in the Japanese scaphites is much thicker than the wall I observed, approximately 20 μm in thickness, and is characterized by a multilayered microstructure. These differences may be explained by diagenesis (see Tanabe and Ohtsuka, 1985). The scaphites do not exhibit any elaborate structure housing the caecum as in *Desmophyllites* (Zakharov, 1972).

The caecum illustrated in figure 14 in a specimen of *S. whitfieldi* measures 142 μm in length along its long axis. The maximum diameter of the caecum was measured on photographs of median sections of ten specimens of *S. preventricosus* and *C. vermiformis.* The maximum diameter averages 68 μm (SD = 5.58, CV = 8.20) measured from the dorsal part of the proseptum to the opposite side of the caecum. The ratio of the length of the caecum to its maximum diameter equals approximately 2.0.

The caecum is attached to the wall of the protoconch chiefly by means of prosiphons. These structures are similar in size and shape among all the scaphite species studied. As illustrated in a specimen of *S. whitfieldi* free of matrix (fig. 14), the prosiphon extends as a nearly continuous apron along the convex surface of the caecum adapical of the proseptum. The prosiphon consists of several prominent extensions in the form of bands or folds that are attached to the interior of the protoconch wall. The adapical ends of these extensions are directed slightly toward the median plane in a convergent fashion.

Scanning electron micrographs of serial sections prepared parallel to the median plane of a specimen of *S. preventricosus* allow further study of the prosiphonal configuration (fig. 15). In a lateral section, the prosiphon and caecum form a swollen attachment near the ventral part of the proseptum. Dorsally, the caecum rests against the dorsal part of the proseptum. One-third way up the caecum, a long prosiphonal strand extends to the wall of the protoconch creating an open space. Nearer the median plane a small opening develops near the dorsal part of the proseptum and an organic connection extends almost to

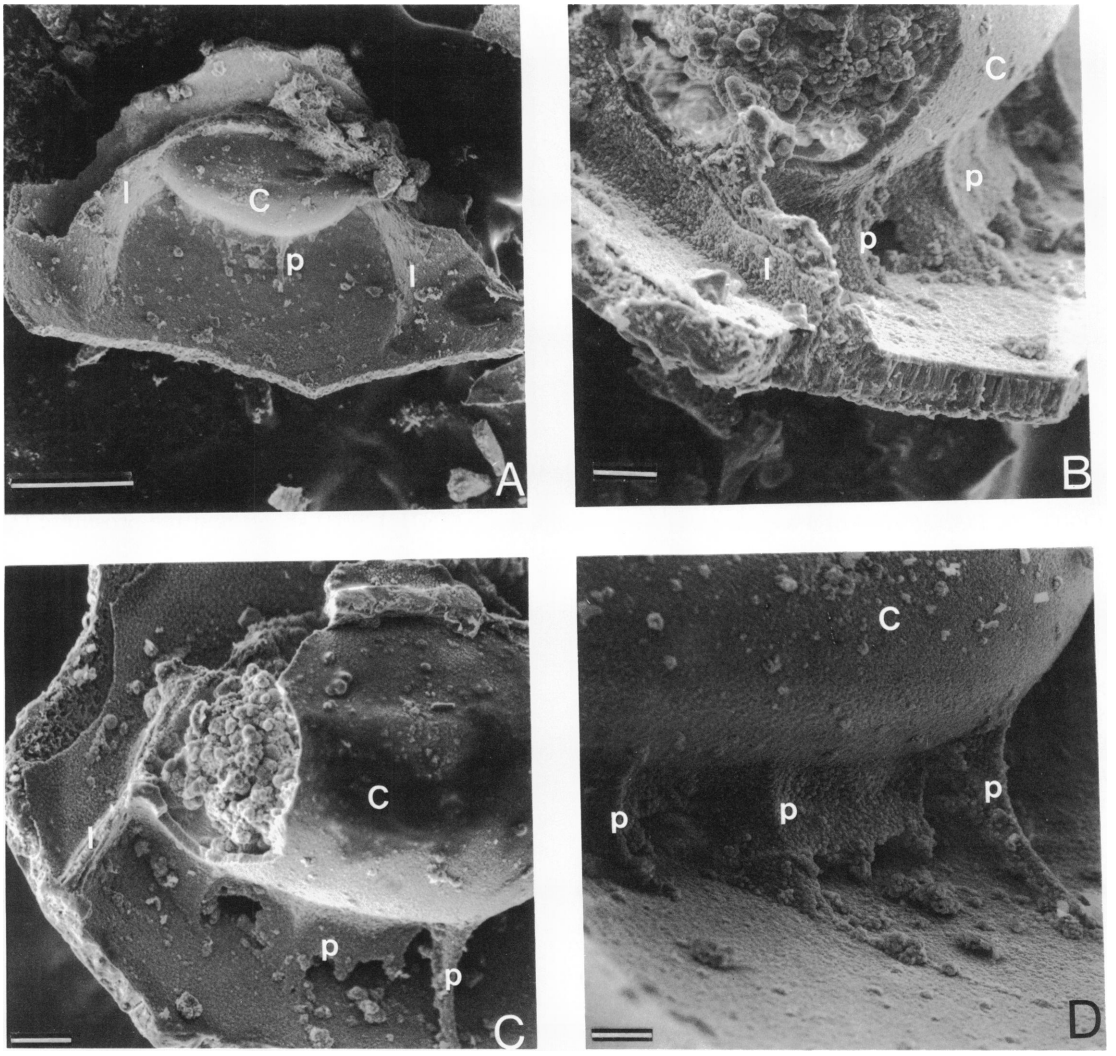

Fig. 14. **A.** Caecum (C) and prosiphonal attachment sheets (p) in a specimen of *Scaphites* cf. *whitfieldi* (YPM 6239). Scale bar = 100 μm. **B.** View of the fractured surface of the caecum (C) in the same specimen. Scale bar = 10 μm. **C.** Another view of the same caecum (C) and prosiphonal attachment sheets (p) in the same specimen. Scale bar = 10 μm. **D.** Close-up of the prosiphons (p). Scale bar = 10 μm.

the flange. Commonly, the caecum will touch the flange if this structure is very prominent. Ventrally, a small prosiphonal strand appears. The long prosiphonal strand previously observed is still present. The maximum length of this long strand in two specimens of *S. preventricosus* averages 30.5 μm. It is shorter than the prosiphonal strands observed in *S. planus, S. pseudoequalis,* and *O. klamathensis,* which range from 83 to 120 μm (Tanabe et al., 1979). On the median plane, a third much smaller strand develops near the ventral part of the proseptum creating another open space. Such small strands have been called partial septa by Shimizu (1929) and compose part of the larger prosiphonal attachment complex (see Grandjean, 1910; Druschits and Doguzhayeva, 1974; Tanabe et al. 1979).

A similar arrangement of the prosiphon

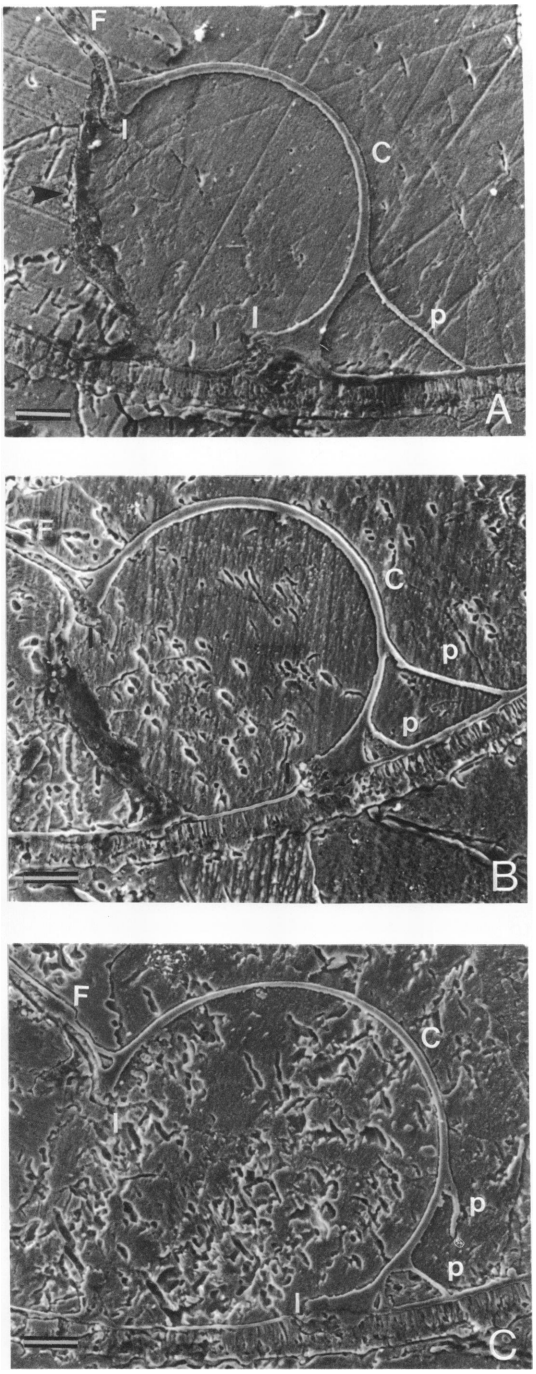

Fig. 15. Three serial sections of the same specimen of *Scaphites preventricosus* (AMNH 43035) prepared parallel to the median plane illustrating the caecum (C) and prosiphonal attachment sheets (p). **A** is the most lateral section and **C** is the median section. Scale bar = 10 μm.

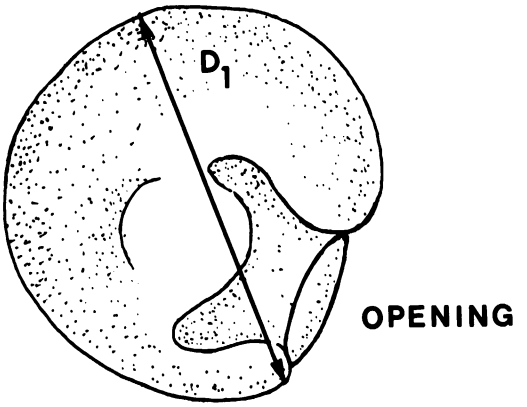

Fig. 16. Diagrammatic side view of a protoconch of *Clioscaphites vermiformis* illustrating measurement of the maximum diameter (D_1). Note the opening of the proseptum.

and caecum to that in figure 15 has been illustrated previously in a specimen of *Discoscaphites* sp. from Greenland (Birkelund and Hansen, 1968). According to Tanabe et al. (1979) and Tanabe and Ohtsuka (1985) short, adorally convex prosiphons are common in scaphites as well as in many other species within the order Ancyloceratina.

Shape and Dimensions of the Protoconch

In the Turonian-Santonian scaphites from the Western Interior, the protoconch is an oblate ellipsoid (fig. 16). The protoconch was measured in three ways (figs. 16, 17). First, the maximum diameter of the protoconch was measured on a median cross section. The maximum diameter is defined as the distance from the adapical ventral edge of the proseptum through the center of the protoconch to the opposite side, excluding the thickness of the outer walls. Second, the minimum diameter of the protoconch was measured on a median cross section. It runs perpendicular to the maximum diameter and through the center of the protoconch. Third, the maximum width of the protoconch was measured on a dorsoventral section.

The choice to exclude the thickness of the outer walls in measuring the maximum diameter of the protoconch permits comparisons with published protoconch measurements, which are normally made on

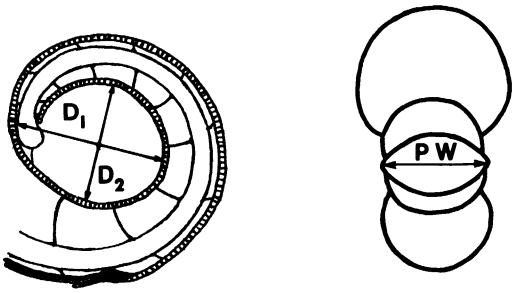

Fig. 17. Measurements of maximum (D_1) and minimum (D_2) diameter of the protoconch on a median section. Protoconch width (PW) is measured on a dorsoventral section.

steinkerns without shell (e.g., Palframan, 1967). Even so, my definition of maximum diameter differs from that of Tanabe et al. (1979) who run their line of measurement through the apical tip of the caecum. However, as Druschits and Khiami (1970: 30) point out in regard to using the caecum as a standard reference point, "it is comparatively rare for the caecum to be preserved, and even when it is, its shape and size vary widely even in members of a single species [especially because of differences in preservation]. On the other hand, it is possible to determine where a spiral whorl starts and the position of the first septum even in the absence of a caecum." Measurements of the same specimens using the two techniques indicate that my method yields comparable or only slightly larger values than the method of Tanabe et al. (1979).

The size of the protoconch varies slightly among scaphite species. The maximum and minimum diameters are listed in table 2. The individual measurements of maximum diameter range from 250 to 469 μm. The means range from 313 μm for individuals of *S. whitfieldi* from a single concretion and individuals of *S. warreni* from one locality, to 365 μm and 366 μm for individuals of *S. nigricollensis* and *S. depressus,* respectively from various localities. The coefficients of variation vary widely and are highest in samples from mixed localities. However, a sample of *S. warreni* from a single locality exhibits an anomalously high coefficient of variation because the specimens are very poorly preserved. An *F*-test to determine the equality of variances of the maximum diameter of the protoconch among species based on samples from all localities reveals significant differences at the 1, 2, and 5% levels (table 3). The only nonsignificant differences occur between *C. vermiformis* and *S. whitfieldi, S. larvaeformis* and *S. whitfieldi, S. larvaeformis* and *S. nigricollensis,* and *S. larvaeformis* and *S. preventricosus.* Performing a Student's *t*-test (table 4) among these four pairs of species to determine the equality of means of the maximum protoconch diameter yields a nonsignificant difference between *S. larvaeformis* and *S. whitfieldi* but significant differences at the .2% level between *S. larvaeformis* and *S. nigricollensis, S. larvaeformis* and *S. preventricosus,* and *S. whitfieldi* and *C. vermiformis.* These results approximately imply that the maximum diameter of the protoconch is significantly different among all the species tested except for the pair *S. larvaeformis* and *S. whitfieldi.* However, *C. vermiformis* is not significantly more different than the other species tested within the genus *Scaphites.*

Tanabe et al. (1979) reported a slightly more elevated range of the maximum diameter of the protoconch in four Turonian scaphite species from Japan. The maximum protoconch diameter in these species, *Scaphites planus, S. pseudoequalis, Otoscaphites puerculus,* and *O. klamathensis* ranges from 351 to 581 μm. In general, these protoconchs are small relative to those in most other ammonites (Druschits et al., 1977a). For example, in *Gaudryceras* sp. and *Tragodesmoceras* sp. within the Lytoceratina, the diameter of the protoconch averages 800–900 μm (Tanabe et al., 1979).

The minimum diameter of the protoconch is only reported for *C. vermiformis.* It averages 270 μm for individuals from locality B235a (table 2). The coefficient of variation equals 8.80 and is comparable to that for the maximum diameter of the protoconch. Tanabe et al. (1979) report much higher values for the minimum diameter of the protoconch in four individuals of the four Turonian species listed above (413–509 μm). The discrepancies are very large and are probably not due to minor differences in measuring technique. The ratio of maximum to minimum diameter of the protoconch in *C. vermiformis* equals 1.24.

TABLE 2
Maximum and Minimum Diameters of the Protoconch in Turonian-Santonian Scaphite Species from the Western Interior

	Mean (μm)	SD (μm)	CV	Range (μm)
Maximum diameter of protoconch (D_1)				
S. larvaeformis adults				
N = 36 (all available localities)	318.7	17.96	5.64	281.4–361.8
S. warreni adults				
N = 9 (locality B191b)	313.2	37.86	12.09	268.0–375.2
N = 15 (all available localities)	335.0	40.71	12.15	268.0–388.6
S. whitfieldi adults and juveniles				
N = 113 (single concretion, locality B176a)	313.2	23.05	7.36	247.9–375.2
N = 183 (all available localities)	320.1	29.09	9.09	247.9–402.0
S. nigricollensis adults				
N = 16 (locality B240)	358.0	11.72	3.27	335.0–375.2
N = 35 (all available localities)	364.7	15.78	4.33	335.0–402.0
S. corvensis adult				
N = 1 (USGS locality near Lander, Wyo.)	314.9			
S. preventricosus adults and juveniles				
N = 39 (locality B228a)	342.6	18.14	5.29	294.8–388.6
N = 61 (all available localities)	343.5	21.80	6.34	294.8–415.4
S. depressus adults				
N = 3 (localities B253, USGS localities D4630 and 17957)	366.3	40.94	11.18	321.6–402.0
C. vermiformis adults and juveniles				
N = 44 (locality B235a)	334.6	28.92	8.64	289.3–435.6
N = 67 (all available localities)	337.5	28.58	8.47	289.3–435.6
Minimum diameter of protoconch (D_2)[a]				
C. vermiformis adults and juveniles				
N = 44 (locality B235a)	270.1	23.77	8.80	233.2–371.8

[a] Maximum diameter/minimum diameter = 1.24.

Measurements of protoconch width are listed in table 5. The means range from a low of 404 μm in *S. larvaeformis* to a high of 532 μm for individuals of *C. vermiformis* from localities B203–B205. The coefficients of variation are comparable or perhaps slightly smaller than those for the maximum diameter of protoconch. The individual measurements of protoconch width range from 395 to 592 μm. I performed an *F*-test (table 6) to evaluate the equality of variances of the protoconch width among species based on pooled

TABLE 3
F-Tests of the Maximum Diameter of the Protoconch Among Species[a]

	S. warreni	*S. whitfieldi*	*S. nigricollensis*	*S. preventricosus*	*C. vermiformis*
S. larvaeformis	$F = 5.138$ (14, 35) sig. at 1%	$F = 1.647$ (182, 35) nonsig.	$F = 1.295$ (35, 34) nonsig.	$F = 1.473$ (60, 35) nonsig.	$F = 2.580$ (66, 35) sig. at 2.5%
S. warreni		$F = 1.958$ (14, 182) sig. at 5%	$F = 6.656$ (14, 34) sig. at 1%	$F = 3.487$ (14, 60) sig. at 5%	$F = 2.029$ (14, 66) sig. at 2.5%
S. whitfieldi			$F = 3.398$ (182, 34) sig. at 1%	$F = 1.781$ (182, 60) sig. at 5%	$F = 1.036$ (182, 66) nonsig.
S. nigricollensis				$F = 1.908$ (60, 34) sig. at 5%	$F = 3.280$ (66, 34) sig. at 1%
S. preventricosus					$F = 1.719$ (66, 60) sig. at 5%

[a] Tests are based on samples from all localities unless otherwise indicated in the text. Numbers in parentheses refer to the degrees of freedom.

samples (individuals from all available localities). I excluded individuals of *C. vermiformis* from localities B203–B205 because of their anomalously high standard deviation which is probably due to wide variation in their state of preservation. The results of the *F*-tests reveal no significant differences except between *C. vermiformis* and all other species. A Student's *t*-test to evaluate the equality of means of the protoconch width among all species except *C. vermiformis* yields significant differences at the .2, 1, and 5% levels. The only nonsignificant differences occur between *S. warreni* and *S. nigricollensis, S. warreni* and *S. preventricosus,* and *S. preventricosus* and *S. nigricollensis* (table 7). An approximate interpretation of these results implies that the protoconch width is significantly different among all species tested except within the group *S. warreni, S. nigricollensis,* and *S. preventricosus.* No data are available on protoconch widths from European or Japanese scaphites to permit a comparative study.

The ratio of the average width of the protoconch to the average maximum diameter of the protoconch for each species is listed below. The difference between the average width and the average diameter is also calculated.

	Width/ diameter	Width − diameter (μm)
S. larvaeformis	1.27	85.1
S. warreni	1.44	147.4
S. whitfieldi	1.39	123.9
S. nigricollensis	1.30	109.6
S. preventricosus	1.34	116.4
C. vermiformis	1.31	105.9

Protoconch width averages approximately 1.3 maximum protoconch diameter; protoconchs are slightly more spheroidal in *S. larvaeformis* and slightly more ellipsoidal in *S. warreni.* The protoconchs in younger scaphite genera such as *Hoploscaphites* are similar in shape although they are much more ellipsoidal in *Discoscaphites* sp. (Waage and Landman, in prep.).

Based on the difference between protoconch width and diameter, Druschits et al. (1977a) subdivided the protoconchs of Cretaceous ammonites into three shape categories: spherical in which $W - D = 100$ μm, "ridge-like" in which $W - D = 101$–200 μm, and fusiform in which $W - D = 201$ μm. According to this classification, the scaphite protoconch is "ridge-like" although I prefer the more general adjective, oblate ellipsoid.

Figure 18 is a plot of the average proto-

TABLE 4
t-Tests of the Maximum Diameter of the Protoconch Among Species[a]

	S. whitfieldi	*S. nigricollensis*	*S. preventricosus*	*C. vermiformis*
S. larvaeformis	nonsig.	sig. at .2%	$t = 5.765$ df = 95 sig. at .2%	
S. whitfieldi				$t = 4.208$ df = 248 sig. at .2%

[a] Tests are based on samples from all localities unless otherwise indicated in the text.

TABLE 5
Protoconch Width in Turonian-Santonian Scaphite Species from the Western Interior

	Mean (μm)	SD (μm)	CV	Range (μm)
S. larvaeformis adults				
N = 10 (locality B189)	418.2	26.16	6.25	394.8–460.6
N = 16 (all available localities)	403.8	33.38	8.27	361.9–460.6
S. warreni adults				
N = 11 (all available localities)	482.4	45.89	9.51	427.7–565.9
S. whitfieldi adults				
N = 28 (single concretion, locality B176a)	437.0	25.43	5.82	394.8–503.4
N = 37 (localities B176, B176a)	443.5	29.55	6.66	394.8–503.4
N = 56 (all available localities)	444.0	34.85	7.85	355.3–519.8
S. nigricollensis adults				
N = 10 (locality B240)	463.2	24.11	5.20	427.7–493.5
N = 18 (all available localities)	474.3	29.66	6.25	427.7–526.4
S. preventricosus adults and juveniles				
N = 21 (locality B228a)	458.9	23.43	5.11	394.8–493.5
N = 32 (all available localities)	459.9	32.23	7.01	394.8–559.3
S. impendicostatus adults				
N = 2 (locality B225a and USGS locality 23938)	439.2	30.26	6.89	417.8–460.6
C. vermiformis adults and juveniles				
N = 18 (locality B235a)	442.5	15.73	3.55	427.7–460.6
N = 8 (localities B203–B205)	532.2	52.80	9.92	427.7–592.2
N = 19 (all available localities excluding B203–B205)	443.4	15.84	3.57	427.7–460.6
C. montanensis var. *hesperius* adult				
N = 1 (locality B235a)	460.6			

TABLE 6
F-Tests of the Protoconch Width Among Species[a]

	S. warreni	*S. whitfieldi*	*S. nigricollensis*	*S. preventricosus*	*C. vermiformis*
S. larvaeformis	$F = 1.890$ (10, 15) nonsig.	$F = 1.090$ (55, 15) nonsig.	$F = 1.266$ (15, 17) nonsig.	$F = 1.073$ (15, 31) nonsig.	$F = 4.441$ (15, 18) sig. at 1%
S. warreni		$F = 1.734$ (10, 55) nonsig.	$F = 2.394$ (10, 17) nonsig.	$F = 2.027$ (10, 31) nonsig.	$F = 8.393$ (10, 18) sig. at 1%
S. whitfieldi			$F = 1.380$ (55, 17) nonsig.	$F = 1.169$ (55, 31) nonsig.	$F = 4.840$ (55, 18) sig. at 1%
S. nigricollensis				$F = 1.181$ (31, 17) nonsig.	$F = 3.506$ (17, 18) sig. at 1%
S. preventricosus					$F = 4.140$ (31, 18) sig. at 1%

[a] Tests are based on samples from all localities unless otherwise indicated in the text. Numbers in parentheses refer to the degrees of freedom.

conch width versus the average protoconch maximum diameter for six species. These values are based on samples from all available localities except for *C. vermiformis,* which only represents specimens from locality B235a. The protoconch of *C. vermiformis* is similar to that of co-occurring specimens of *Baculites* (table 8). In juvenile specimens of *Baculites* cf. *B. asper, B. codyensis,* the maximum diameter of the protoconch averages 340 μm, the minimum diameter averages 284 μm, and the protoconch width averages 475 μm. It would be difficult to distinguish the two genera on the basis of these measurements.

Size and Shape of the Ammonitella

The ammonitella was measured in two ways (fig. 19). First, the diameter of the ammonitella (A.D.) was measured on a median section. The diameter is defined as the distance

TABLE 7
t-Tests of the Protoconch Width Among Species[a]

	S. warreni	*S. whitfieldi*	*S. nigricollensis*	*S. preventricosus*
S. larvaeformis	$t = 5.163$ df = 25 sig. at .2%	$t = 4.106$ df = 70 sig. at .2%	$t = 6.522$ df = 32 sig. at .2%	$t = 5.560$ df = 46 sig. at .2%
S. warreni		$t = 3.167$ df = 65 sig. at 1%	$t = 0.580$ df = 27 nonsig.	$t = 1.786$ df = 41 nonsig.
S. whitfieldi			$t = 3.319$ df = 72 sig. at .2%	$t = 2.115$ df = 86 sig. at 5%
S. nigricollensis				$t = 1.559$ df = 48 nonsig.

[a] Tests are based on samples from all localities unless otherwise indicated in the text.

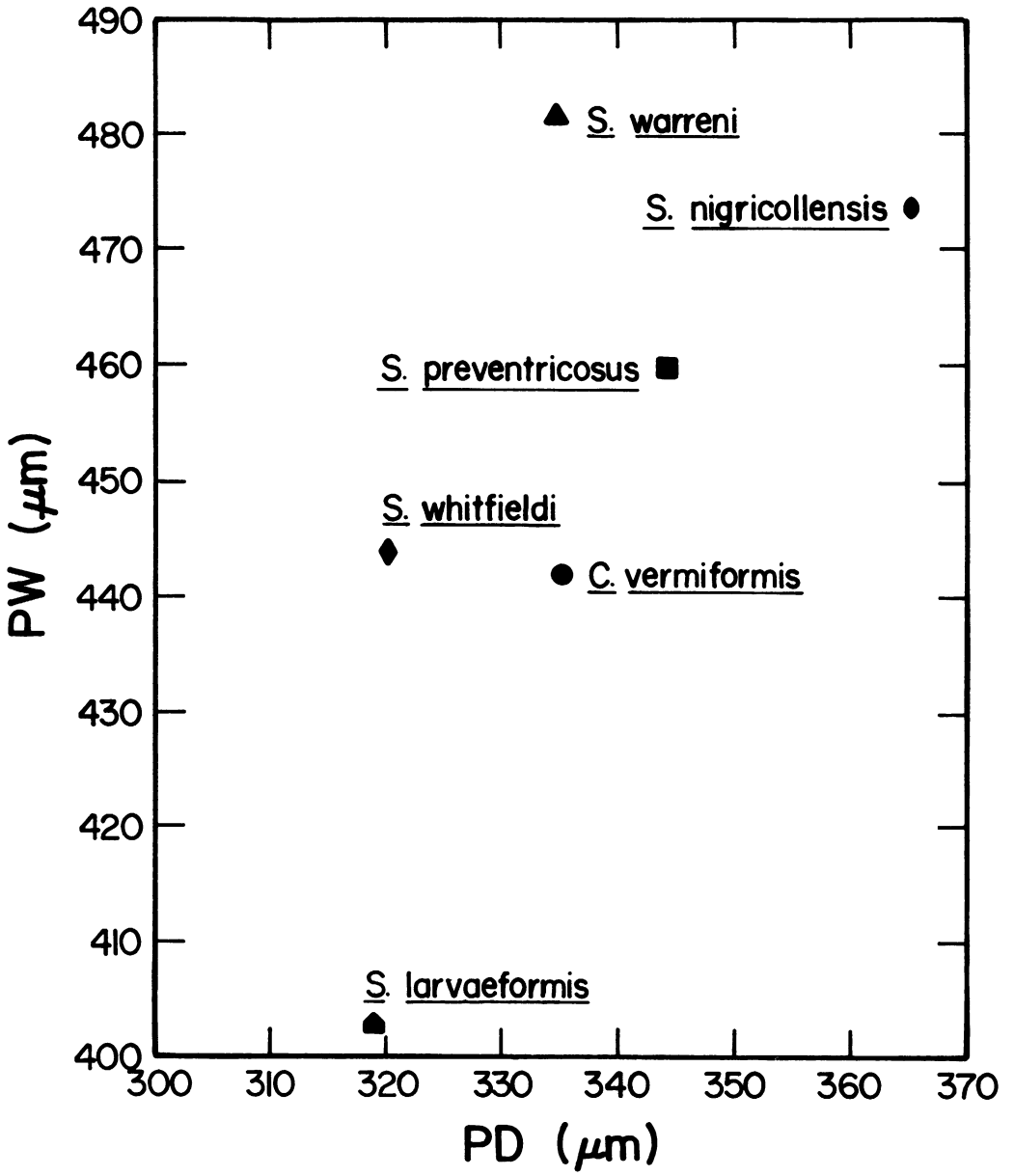

Fig. 18. Plot of mean protoconch width (PW) versus mean protoconch maximum diameter (PD) for six species.

TABLE 8

Diameter and Width of the Protoconch in *Baculites* sp. cf. *B. asper, B. codyensis* from Locality B235a

	Mean (μm)	SD (μm)	CV	Range (μm)
Maximum diameter (D_1)[a]	340.5	18.27	5.36	308.7–382.1
Minimum diameter (D_2)[a]	284.2	16.81	5.92	255.2–320.1
Protoconch width[b]	475.1	42.48	8.94	427.7–526.4

[a] Locality B235a; N = 18; $\bar{D}_1/\bar{D}_2 = 1.20$.

[b] Locality B235a; N = 5.

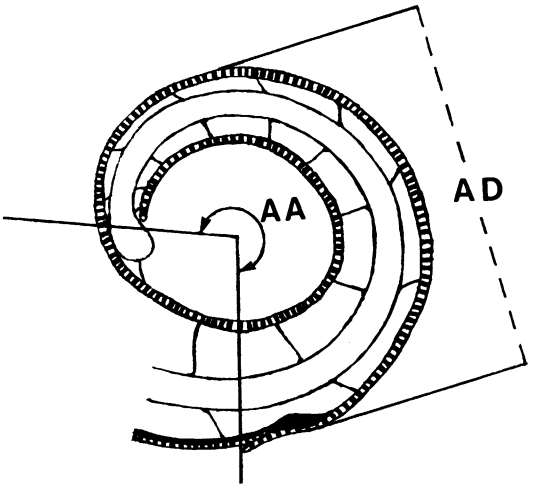

Fig. 19. Median section of an ammonitella illustrating the measurement of ammonitella angle (AA) and ammonitella diameter (AD).

from the end of the primary constriction and its accompanying varix through the center of the protoconch to the opposite side. Second, the angle of the ammonitella was measured on a median section. The apex of the angle is located at the center of the protoconch and its two legs are positioned at the ventral part of the proseptum and the ventral edge of the ammonitella.

This last measurement differs slightly from that of Grandjean (1910) who measures "the angle of involution corresponding to the primary varix" from the middle of the caecum to the middle of the primary varix [author's translation]. Druschits and Khiami (1970) note that the caecum is rarely preserved and prefer to measure "the angle of the primary varix" from the proseptum to the middle of the primary varix. This practice is also followed by Tanabe et al. (1979), although Tanabe and Ohtsuka (1985) later extend their measurement to the end of the primary varix. I also use the proseptum and end of the primary varix as markers because they may be easily and consistently spotted.

The measurements of ammonitella diameter are listed in table 9. The ammonitella diameter varies slightly among the Turonian-Santonian scaphite species from the Western Interior. The means range from a low of 582 μm in *S. larvaeformis* to more than 750 μm in samples of *S. depressus, C. vermiformis,* and *C. montanensis.* The coefficients of variation are comparable to those for the measurements of the protoconch. An *F*-test was performed to compare the variances of the ammonitella diameter among species based on pooled samples (table 10). I excluded the sample of *S. depressus* because of its high coefficient of variation, which may be due to wide variation in the state of preservation of these specimens. Similarly, *C. vermiformis* was restricted to include all samples except B203, B204, and B205 because of their unusually high joint mean. The results of the *F*-test yield no significant differences among species with two exceptions: between *S. preventricosus* and *S. whitfieldi* and between *S. preventricosus* and *C. vermiformis.* These differences are significant at the 2.5% level and are due to the low variability of the pooled *S. preventricosus* sample. A Student's *t*-test (table 11) to compare the mean ammonitella diameter among species indicates significant differences at the 2.5 and 5% levels. The only exceptions are between *S. preventricosus* and *S. warreni* (which were nonsignificant with regard to their protoconch width as well) and between *S. nigricollensis* and *C. vermiformis.*

The individual measurements of ammonitella diameter range from 525 to 831 μm with one specimen of *C. montanensis* var. *hesperius* at 908 μm. Tanabe et al. (1979) report a slightly more elevated range from 641 to 949 μm in the four Turonian scaphite species they studied. Nevertheless, the ammonitella in scaphites is small compared to those of other Cretaceous ammonites, which may approach a diameter of 1500 μm (Druschits et al., 1977a). The ammonitella in baculites is larger than that in scaphites. The diameter of the ammonitella of 19 baculite specimens from locality B235a averages 775 μm and ranges from 707 to 834 μm (table 12). The means are significantly different from those in the co-occurring scaphites at the .2% level ($t = 11.288$, df = 64). *Collignoniceras woollgari,* which co-occurs with *S. larvaeformis,* exhibits a slightly larger ammonitella (820 μm versus 582 μm; Tanabe et al., 1979). On the other hand, the ammonitellas of placenticeratids and sphenodiscids, which co-occur with scaphites in the Campanian and Maastrichtian approximate 1.5 mm in diameter.

The ammonitella angle measured from the proseptum to the ammonitella edge varies little among the scaphite species studied (table 13). The means range from 267° for one sample of *S. nigricollensis* to 289° for one sample of *C. vermiformis*. The coefficients of variation are smaller than those for the other protoconch and ammonitella dimensions and average approximately 3.6. Nonetheless, an *F*-test to evaluate the variances of the ammonitella angle among species based on pooled samples reveals significant differences between *S. nigricollensis* and *S. larvaeformis, S. nigricollensis* and *S. preventricosus,* and *S. preventricosus* and *S. whitfieldi* (table 14). A Student's *t*-test evaluating the equality of means among species, excluding the three pairs of species above, indicates significant differences at the .2 and 1% levels (table 15). Nonsignificant differences occur between *S. larvaeformis* and *S. warreni, S. warreni* and *S. nigricollensis, S. warreni* and *S. preventricosus,* and *S. whitfieldi* and *C. vermiformis.*

Druschits and Khiami (1970) assert that the angle of the ammonitella varies widely among ammonites. In phylloceratids and ammonitids, the angle ranges from 260 to 377° (see also Tanabe et al., 1979). However, at lower taxonomic levels, the variation is more restricted. Indeed, Tanabe et al. (1979) report similar angles of 280–295° for four specimens of four scaphite species from Japan.

The angle of the ammonitella in scaphites is small compared to that in other ammonites. Among baculites, the ammonitella angle is higher and represents the most obvious difference between baculites and scaphites at this stage of development. For example, the ammonitella angle of baculites from locality B235a averages 331° whereas it averages 289° in the co-occurring scaphites (table 12). The relationship between the ammonitella diameter and angle in scaphites and baculites is illustrated in figure 20. The two groups are clearly separated on the basis of these two measurements.

Within either group, ammonitella angle does not covary with ammonitella diameter. For example, in *C. vermiformis,* the coefficient of correlation equals −.0545. Large ammonitellas may or may not possess large ammonitella angles. This relationship is further demonstrated in figure 21. This figure represents a plot of mean ammonitella diameter versus mean ammonitella angle for samples of seven species from all localities and indicates zero correlation. Tanabe and Ohtsuka (1985) documented a similarly poor correlation ($r = .433$) between ammonitella diameter and ammonitella angle within and among many other ammonite species.

The statistical comparisons of the measurements for the protoconch and ammonitella among species are summarized in table 16. This table presents the results of *t*-tests of the four measured dimensions: protoconch diameter (P.D.), protoconch width (P.W.), ammonitella diameter (A.D.), and ammonitella angle (A.A.). Samples of species with anomalously high or low variances, however, were not included in this comparison.

In general, the differences are significant among species. The pair *S. larvaeformis* and *S. preventricosus* exhibit the most significant differences; all of their measurements consistently differ at the .2% level. Significant differences at the .2% level also occur between *S. larvaeformis* and *C. vermiformis, S. larvaeformis* and *S. nigricollensis,* and *S. nigricollensis* and *S. whitfieldi.* Significant differences at the 1 and 5% levels occur between *S. whitfieldi* and *S. warreni* and between *S. warreni* and *C. vermiformis.* Significant differences also occur among species for some measurements but not others. For example, *S. larvaeformis* is significantly different at the .2 and 5% levels from *S. whitfieldi* for protoconch width, ammonitella diameter, and ammonitella angle but not for protoconch diameter. In contrast, no significant differences occur between the species pair *S. warreni* and *S. preventricosus.*

Correlations Between the Protoconch and Ammonitella

The ratio of ammonitella diameter to protoconch diameter is similar among the scaphites studied. The values below represent the ratios between mean ammonitella diameter and mean protoconch diameter for pooled samples of each species.

S. larvaeformis	1.83
S. warreni	1.92
S. whitfieldi	1.93

TABLE 9
Ammonitella Diameter in Turonian-Santonian Scaphite Species from the Western Interior

	Mean (μm)	SD (μm)	CV	Range (μm)
S. larvaeformis adults				
N = 38 (all available localities)	582.0	34.22	5.88	525.0–649.0
S. carlilensis adults				
N = 2 (USGS localities 22608 and 6245)	596.3	9.48	1.59	589.6–603.0
S. warreni adults				
N = 8 (locality B191b)	649.9	47.51	7.31	603.0–723.6
N = 14 (all available localities)	642.7	39.06	6.08	603.0–723.6
S. whitfieldi adults and juveniles				
N = 119 (single concretion B176a)	609.2	32.23	5.29	547.0–683.0
N = 25 (locality B176)	663.2	53.15	8.01	549.4–737.0
N = 144 (localities B176, B176a)	618.6	41.85	6.76	547.0–737.0
N = 4 (locality B177)	671.1	26.87	4.00	643.2–696.8
N = 29 (locality B192)	620.2	40.83	6.58	546.1–707.4
N = 2 (locality B193)	658.3	2.37	0.36	656.6–660.0
N = 179 (localities just south of Black Hills: B176, B176a, B177, B192, B193)	620.2	41.82	6.74	547.0–737.0
N = 8 (locality B198b)	582.2	32.14	5.52	522.6–639.8
N = 198 (all available localities)	619.0	42.49	6.86	547.0–737.0
S. nigricollensis adults				
N = 16 (locality B240)	676.0	37.84	5.60	603.0–737.0
N = 18 (localities B185–B188)	678.2	32.60	4.81	633.2–737.0
N = 41 (all available localities)	678.2	36.92	5.44	603.0–755.3
S. corvensis adult				
N = 1 (USGS locality near Lander, Wyo.)	670.0			
S. preventricosus adults and juveniles				
N = 39 (locality B228)	646.0	28.02	4.34	575.0–696.8
N = 61 (all available localities)	644.6	31.00	4.81	575.0–713.6
S. depressus adults				
N = 4 (locality B253, USGS localities D4630, D4636, and 17957)	754.6	69.17	9.17	676.7–830.8
C. vermiformis adults and juveniles				
N = 14 (locality B239a)	695.0	49.05	7.06	639.8–763.8

TABLE 9—(*Continued*)

	Mean (μm)	SD (μm)	CV	Range (μm)
N = 47 (locality B235a)	659.0	37.76	5.73	603.0–809.0
N = 9 (locality 21425)	671.8	38.96	5.80	629.8–737.0
N = 16 (localities B203–B205)	765.3	45.21	5.91	607.0–817.4
C. vermiformis adults and juveniles				
N = 89 (all available localities)	685.4	56.65	8.26	603.0–817.4
N = 73 (all localities excluding B203–B205)	667.9	42.04	6.30	603.0–809.0
C. montanensis var. *hesperius* adult				
N = 1 (locality B205)	907.85			

S. nigricollensis	1.86
S. preventricosus	1.88
C. vermiformis	2.03

The ratios range from 1.8 to 2.0. Taking the reciprocals of these ratios implies that diameter of the protoconch represents .5 to .6 the diameter of the ammonitella. Simplistically assuming spherical shapes for the protoconch and ammonitella, these values suggest a volume ratio of 1:8. In *Baculites* cf. *B. asper, B. codyensis,* the ratio of mean ammonitella diameter to mean protoconch diameter equals 2.04. Taking the reciprocal of this ratio implies that the protoconch represents .49 the diameter of the ammonitella.

The relationship between protoconch and ammonitella diameter is also illustrated in figures 22 and 23, which represent plots of these measurements for *S. larvaeformis* from all available localities, *S. preventricosus* from locality B228a, and *C. vermiformis* from locality B235a. The equations of the lines of best fit through the measurements of each

TABLE 10
***F*-Tests of the Ammonitella Diameter Among Species[a]**

	S. warreni	*S. whitfieldi*	*S. nigricollensis*	*S. preventricosus*	*C. vermiformis*
S. larvaeformis	$F = 1.303$ (13, 37) nonsig.	$F = 1.542$ (197, 37) nonsig.	$F = 1.164$ (40, 37) nonsig.	$F = 1.218$ (60, 37) nonsig.	$F = 1.509$ (73, 37) nonsig.
S. warreni		$F = 1.183$ (197, 13) nonsig.	$F = 1.117$ (40, 13) nonsig.	$F = 1.588$ (60, 13) nonsig.	$F = 1.158$ (72, 13) nonsig.
S. whitfieldi			$F = 1.324$ (197, 40) nonsig.	$F = 1.879$ (197, 60) sig. at 2.5%	$F = 1.022$ (72, 197) nonsig.
S. nigricollensis				$F = 1.418$ (40, 60) nonsig.	$F = 1.296$ (72, 40) nonsig.
S. preventricosus					$F = 1.839$ (72, 60) sig. at 2.5%

[a] Tests are based on samples from all localities unless otherwise indicated in the text. Numbers in parentheses refer to the degrees of freedom.

TABLE 11
t-Tests of the Ammonitella Diameter Among Species[a]

	S. warreni	*S. whitfieldi*	*S. nigricollensis*	*S. preventricosus*	*C. vermiformis*
S. larvaeformis	$t = 5.463$ df = 50 sig. at .2%	$t = 5.059$ df = 234 sig. at .2%	$t = 11.984$ df = 77 sig. at .2%	$t = 9.388$ df = 97 sig. at .2%	$t = 10.855$ df = 109 sig. at .2%
S. warreni		$t = 2.027$ df = 210 sig. at 5%	$t = 3.062$ df = 53 sig. at 1%	$t = 0.197$ df = 73 nonsig.	$t = 2.076$ df = 85 sig. at 5%
S. whitfieldi			$t = 8.293$ df = 237 sig. at .2%		$t = 8.429$ df = 269 sig. at .2%
S. nigricollensis				$t = 4.987$ df = 100 sig. at .2%	$t = 1.310$ df = 112 nonsig.
S. preventricosus					

[a] Tests are based on samples from all localities unless otherwise indicated in the text.

species are listed below where A equals ammonitella diameter and P, protoconch diameter.

Species	N	Equation of the line of best fit	Coefficient of correlation
S. larvaeformis	36	$A = 1.00P + 259.6$	.525
S. preventricosus	39	$A = 1.23P + 224.0$	.796
C. vermiformis	44	$A = 1.06P + 303.8$	.812

The slopes of the lines are similar and the intercepts are all positive. In general, large protoconchs correlate with large ammonitellas. A plot of mean protoconch diameter versus mean ammonitella diameter for six scaphite species also reveals a positive correlation (fig. 24). Similar correlations have been documented within and among many other ammonite species (Tanabe and Ohtsuka, 1985; Tanabe et al., 1979).

TABLE 12
Ammonitella Diameter and Angle in *Baculites* sp. cf. *B. asper, B. codyensis*[a]

	Mean	SD	CV	Range
Ammonitella diameter (μm)	775	37.90	4.89	707–834
Ammonitella angle (°)	331	7.94	2.40	320–342

[a] Locality B235a; N = 18.

Although this correlation is positive, the relationship between ammonitella and protoconch diameter is negatively allometric within species. In other words, the ratio of ammonitella diameter to protoconch diameter decreases with increasing protoconch diameter. If measurements of the protoconch and ammonitella diameter of two species are plotted on the same graph, the slope of the line of best fit through the measurements of both species is higher than the slopes of the lines of best fit through the measurements of the individual species. For example, figure 22 represents measurements for both *S. larvaeformis* and *S. preventricosus*. Although the slopes of the lines of best fit through the measurements of the individual species equal 1.00 and 1.23, respectively, the slope of the line of best fit through the measurements of both species equals 1.65; the *y* intercept is 66.8 and the coefficient of correlation is .797.

Figure 23 includes a plot of the measurements of protoconch diameter versus ammonitella diameter for individuals of *Baculites* cf. *B. asper, B. codyensis* from locality B235a. The line of best fit through the measurements of these species exhibits a slope of

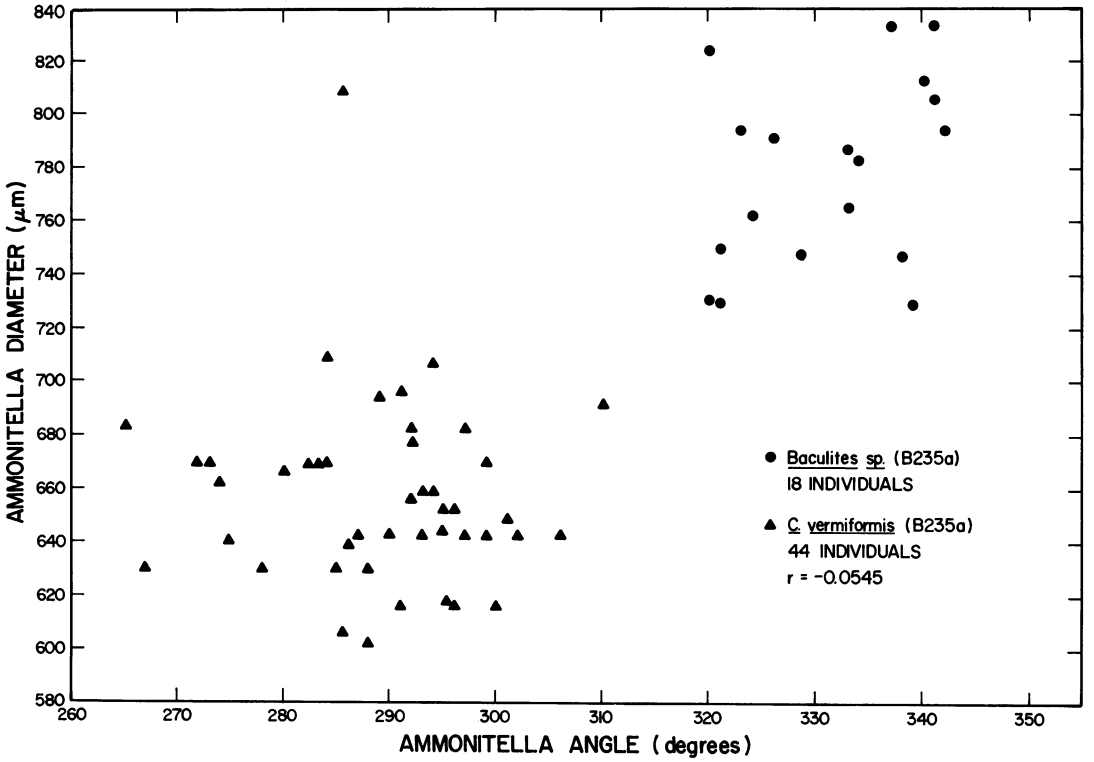

Fig. 20. Plot of ammonitella diameter versus ammonitella angle for 44 specimens of *Clioscaphites vermiformis* and 18 specimens of *Baculites* cf. *B. asper, B. codyensis* from locality B235a indicates a clear separation in these dimensions for the two genera.

1.38, a y intercept of 302.2 and a coefficient of correlation of .665. The value of the y intercept is similar to that for the line of best fit through the measurements of the species *C. vermiformis.* However, the slope of the line is higher for *Baculites* sp. and indicates that the same size protoconch will be associated with a larger ammonitella in *Baculites* sp. than in *C. vermiformis.* Several ammonitellas of *C. vermiformis* that attain large sizes, however, do not fall on the line of best fit for *Baculites* sp., but more nearly conform to the line of best fit for *C. vermiformis.* These large ammonitellas of *C. vermiformis* all retain ammonitella angles common for this species, that is, 290°.

In contrast to the positive correlation between protoconch and ammonitella diameter, the relationship between protoconch diameter and ammonitella angle exhibits no correlation within and among species. For example, a plot of the measurements of protoconch diameter versus ammonitella angle within *C. vermiformis* yields a coefficient of correlation of −.1512. Similarly, ammonitella angle bears no correlation with ammonitella diameter, as previously described.

Mode of Early Development

Based on the morphology of the initial whorls of scaphites and other ammonites, what is the mode of early development? The similarity in the morphology of the initial whorls among all ammonites suggests a common developmental scheme (Druschits et al., 1977a; Doguzhayeva and Mikhailova, 1982). Two interpretations of early ontogenetic development have been suggested. The first interpretation includes a larval stage (Erben et al., 1969; Palframan, 1967; fig. 2). According to this view, hatching occurs after the formation of the protoconch, which, therefore, represents the end of the embryonic stage. This is followed by a larval stage of the veliger type during which time the shell grows to the

TABLE 13
Ammonitella Angle in Turonian-Santonian Species from the Western Interior

	Mean (°)	SD (°)	CV	Range (°)
S. larvaeformis adults				
N = 36	279.7	9.19	3.28	266.0–300.0
(all available localities)				
S. carlilensis adult				
N = 1	274.0			
(USGS locality 6245)				
S. warreni adults				
N = 12	276.5	10.45	3.78	266.0–290.0
(all available localities)				
S. whitfieldi adults and juveniles				
N = 105	287.4	10.41	3.62	266.0–308.0
(single concretion, locality B176a)				
N = 123	285.9	11.19	3.91	260.0–308.0
(localities B176, B176a)				
N = 18	277.2	11.89	4.29	260.0–300.0
(locality B176)				
N = 32	279.0	10.85	3.89	260.0–301.0
(locality 192)				
S. whitfieldi adults and juveniles				
N = 148	284.0	11.90	4.19	260.0–308.0
(all localities just south of the Black Hills: B176, B176a, B177, B192, B193)				
N = 11	284.7	4.18	1.47	279.0–291.0
(locality B198b)				
N = 168	284.0	11.68	4.11	260.0–308.0
(all available localities)				
S. nigricollensis adults				
N = 15	276.2	9.48	3.43	264.0–300.0
(locality B240)				
N = 16	266.6	9.67	3.63	253.0–287.0
(localities B185–B188)				
N = 34	273.0	12.49	4.57	253.0–308.0
(all available localities)				
S. corvensis adult				
N = 1	282.0			
(USGS locality near Lander, Wyo.)				
S. preventricosus adults and juveniles				
N = 39	273.4	8.63	3.16	256.8–292.0
(locality B228a)				
S. preventricosus adults and juveniles				
N = 61	273.8	8.01	2.93	256.8–292.0
(all available localities)				
S. impendicostatus adults				
N = 2	282.5	8.48	3.00	276.5–288.5
(locality B228a and USGS locality 23938)				
S. depressus adults				
N = 3	288.3	5.51	1.91	282.0–292.0
(locality B253, USGS localities D4630 and 17957)				
C. vermiformis adults and juveniles				
N = 12	280.1	13.05	4.66	259.2–296.0
(locality B239a)				

TABLE 13—(*Continued*)

	Mean (°)	SD (°)	CV	Range (°)
N = 46 (locality B235a)	289.1	9.46	3.27	265.0–306.0
N = 9 (locality 21425)	287.2	8.40	2.92	273.0–300.0
N = 15 (localities B203–B205)	282.7	7.02	2.48	268.0–296.0
C. vermiformis adults and juveniles				
N = 86 (all available localities)	286.2	9.88	3.45	259.2–306.0
N = 71 (all available localities excluding B203–B205)	286.9	10.28	3.58	259.2—306.0

end of the primary constriction (fig. 3). At this point, metamorphosis occurs and produces the primary varix.

This interpretation was based on studies of the morphology of bactritids and goniatites in analogy with prosobranch gastropods and Recent *Nautilus*. It interpreted the changes in the morphology of the initial whorls at the end of the protoconch and at the primary constriction. Erben et al. (1969) and subsequently Birkelund and Hansen (1974) observed that a new shell layer appears at the beginning of the first whorl and grows in thickness at the expense of the protoconch layer, which soon wedges out. Erben also noted that a ventral modification of the aperture is absent on the protoconch, whereas on the following whorl, a wide ventral sinus appears in the growth lines of primitive ammonites. He interpreted this feature as indicating the position of a locomotor organ such as a velum. Erben further pointed out that nacre first appears in ammonites at the end of the first whorl whereas in *Nautilus* it is present from the start of the shell without any indication of a subsequent metamorphosis in shell struc-

TABLE 14
***F*-Tests of the Ammonitella Angle Among Species[a]**

	S. warreni	*S. whitfieldi*	*S. nigricollensis*	*S. preventricosus*	*C. vermiformis*
S. larvaeformis	$F = 1.293$ (11, 35) nonsig.	$F = 1.615$ (167, 35) nonsig.	$F = 1.847$ (33, 35) sig. at 5%	$F = 1.316$ (35, 60) nonsig.	$F = 1.156$ (85, 35) nonsig.
S. warreni		$F = 1.249$ (167, 11) nonsig.	$F = 1.428$ (33, 11) nonsig.	$F = 1.702$ (11, 60) nonsig.	$F = 1.119$ (11, 85) nonsig.
S. whitfieldi			$F = 1.144$ (33, 167) nonsig.	$F = 2.126$ (167, 60) sig. at 1%	$F = 1.398$ (167, 85) nonsig.
S. nigricollensis				$F = 2.431$ (33, 60) sig. at 1%	$F = 1.598$ (33, 85) nonsig.
S. preventricosus					$F = 1.521$ (85, 60) nonsig.

[a] Tests are based on samples from all localities unless otherwise indicated in the text. Numbers in parentheses refer to the degrees of freedom.

TABLE 15
t-Tests of the Ammonitella Angle Among Species[a]

	S. warreni	*S. whitfieldi*	*S. nigricollensis*	*S. preventricosus*	*C. vermiformis*
S. larvaeformis	$t = 1.010$ df = 46 nonsig.	$t = 2.074$ df = 202 sig. at 5%		$t = 3.317$ df = 95 sig. at .2%	$t = 3.381$ df = 120 sig. at .2%
S. warreni		$t = 2.162$ df = 178 sig. at 5%	$t = 0.868$ df = 44 nonsig.	$t = 1.014$ df = 71 nonsig.	$t = 3.164$ df = 96 sig. at 1%
S. whitfieldi			$t = 4.950$ df = 200 sig. at .2%		$t = 1.494$ df = 252 nonsig.
S. nigricollensis					$t = 6.104$ df = 118 sig. at .2%
S. preventricosus					$t = 8.093$ df = 145 sig. at .2%

[a] Tests are based on samples from all localities unless otherwise indicated in the text.

ture. Because a free-living larval stage is absent in Recent *Nautilus,* Erben postulated that it was present in ammonites.

The interpretation of a three stage developmental scheme including a larval stage was proposed earlier by Hyatt (1894) and Smith (1901). Hyatt formulated his scheme based largely on sutural patterns. He introduced terms such a nepionic and neanic to subdivide early ontogeny into as many sequential stages as possible thereby facilitating comparisons between ontogeny and phylogeny. Smith (1901) inferred a three stage developmental scheme in his study of *Baculites chicoensis.* He considered that the protoconch represented the embryonic stage and the shell extending to the end of the primary constriction represented the first postembryonic (ananepionic) larval stage. However, in his studies of *Phylloceras* and *Lytoceras* Smith (1898) interpreted the primary constriction as marking the paranepionic and the end of the metanepionic stages, respectively. Other developmental interpretations include those of Branco (1879) who supposed that only part of the protoconch formed during the embryonic stage, Schindewolf (1929) who believed that the entire protoconch developed during the embryonic stage, and Arkell (1957) who considered that the protoconch grew during a larval stage.

In contrast to these interpretations is the scheme of simple direct development comprising only two stages: embryonic and postembryonic. According to this view, the embryonic stage consists of the protoconch and first whorl terminating at the end of the primary constriction. This developmental scheme has been discussed previously by a number of authors (Grandjean, 1910; Druschits and Khiami, 1970; Druschits et al., 1977a; Kulicki, 1974, 1979; Birkelund and Hansen, 1974; and Bandel, 1982, 1986). It is supported by the fact that the tuberculate sculpture on the ammonitellas of scaphites and other ammonites is distributed without interruption to the end of the primary constriction (Kulicki, 1974, 1979; Bandel et al., 1982; Bandel, 1982, 1986). The uniform surface of the ammonitella argues against an intervening larval stage after formation of the protoconch. The ammonitella also lacks ribs, characteristic of later ontogeny, whose formation requires an unconstrained position of the pallial margin.

The ammonitellas of scaphites and other Mesozoic ammonites also lack growth lines. Their absence may be due to the rapid min-

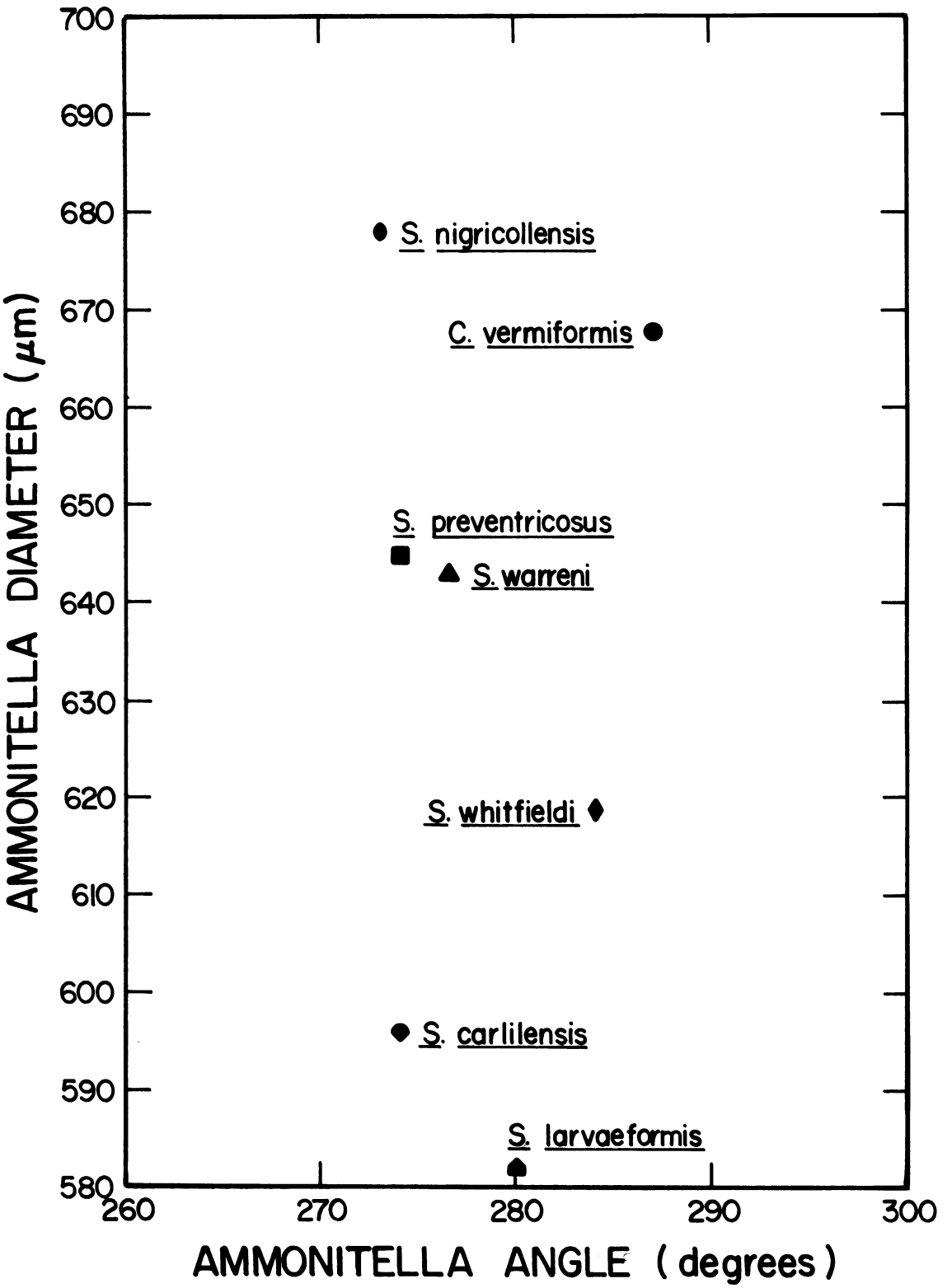

Fig. 21. Plot of mean ammonitella diameter versus mean ammonitella angle for seven species exhibits no correlation.

TABLE 16

t-Tests of the Dimensions of the Protoconch and Ammonitella Among Species[a]

	S. warreni	*S. whitfieldi*	*S. nigricollensis*	*S. preventricosus*	*C. vermiformis*
S. larvaeformis		P.D. nonsig.	P.D. sig. at .2%	P.D. sig. at .2%	
	P.W. sig. at .2%	P.W. sig. at .2%	P.W. sig. at .2%	P.W. sig. at .2%	
	A.D. sig. at .2%	A.D. sig. at .2%	A.D. sig. at .2%	A.D. sig. at .2%	A.D. sig. at .2%
	A.A. nonsig.	A.A. sig. at 5%		A.A. sig. at .2%	A.A. sig. at .2%
S. warreni		P.W. sig. at 1%	P.W. nonsig.	P.W. nonsig.	
		A.D. sig. at 5%	A.D. sig. at 1%	A.D. nonsig.	A.D. sig. at 5%
		A.A. sig. at 5%	A.A. nonsig.	A.A. nonsig.	A.A. sig. at 1%
S. whitfieldi					P.D. sig. at .2%
			P.W. sig. at .2%	P.W. sig. at 5%	
			A.D. sig. at .2%		A.D. sig. at .2%
			A.A. sig. at .2%		A.A. nonsig.
S. nigricollensis				P.W. nonsig.	
				A.D. sig. at .2%	A.D. nonsig.
					A.A. sig. at .2%
S. preventricosus					A.A. sig. at .2%

[a] Tests are based on samples from all localities unless otherwise indicated in the text. P.D. = protoconch diameter; P.W. = protoconch width; A.D. = ammonitella diameter; A.A. = ammonitella angle.

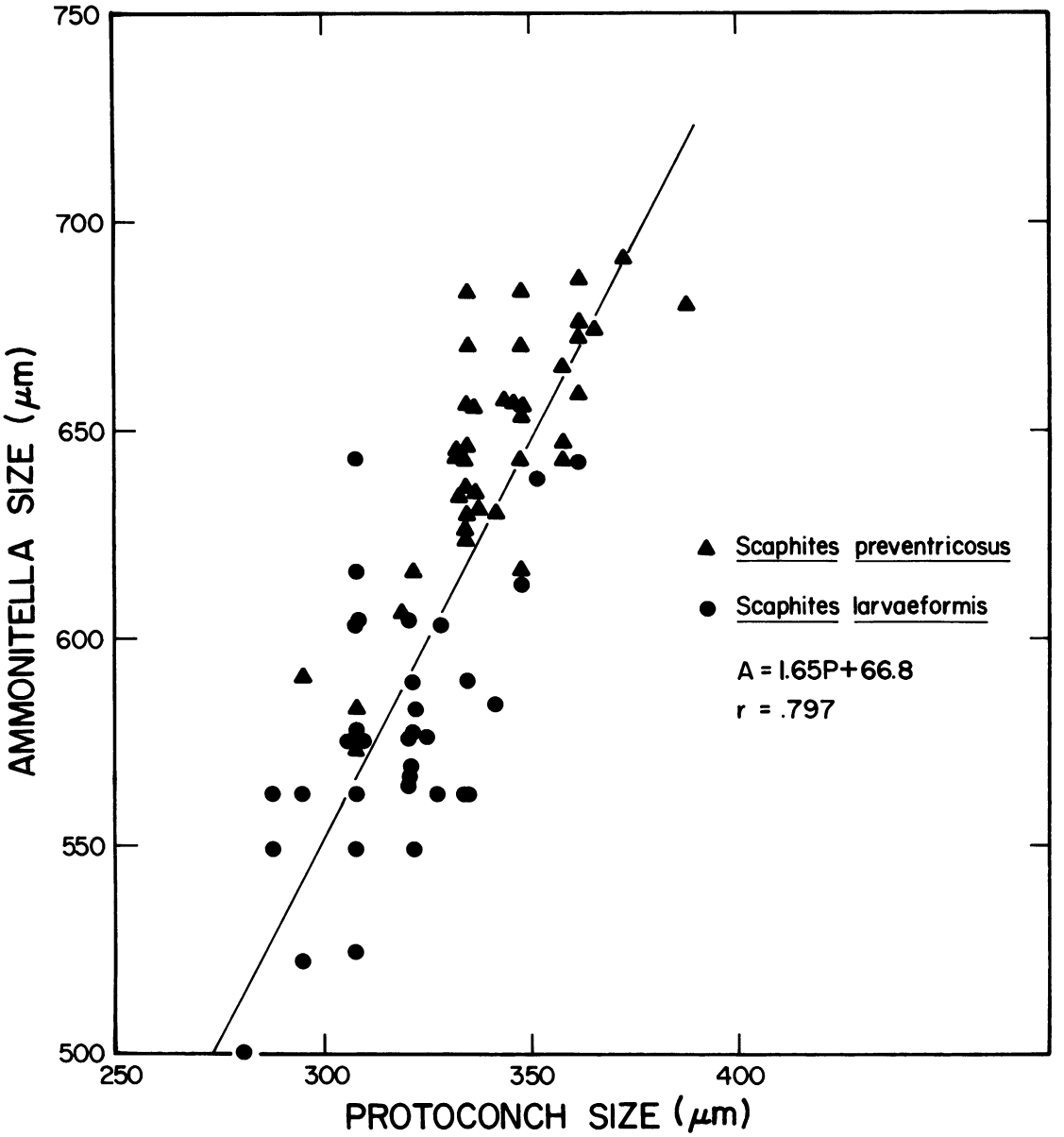

Fig. 22. Plot of protoconch size versus ammonitella size for 33 specimens of *Scaphites larvaeformis* from all localities and 39 specimens of *S. preventricosus* from locality B228a indicates a positive correlation.

eralization of an originally organic shell similar to that which occurs in modern archaeogastropods (Bandel, 1975, 1982, 1986). According to this hypothesis, the originally organic shell is mineralized by prismatic needles of aragonite to form an initial layer of uniform thickness that preserves the original ornamentation of the organic shell (Bandel, 1975: 50–52). Subsequently, other mineral layers were deposited from the interior, increasing the thickness of the outer wall. In contrast, the embryonic shells of molluscs that grow by secreting mineralized shell increments from the beginning usually exhibit growth lines (Bandel, 1982; Bandel et al., 1982). Growth lines are also present on the

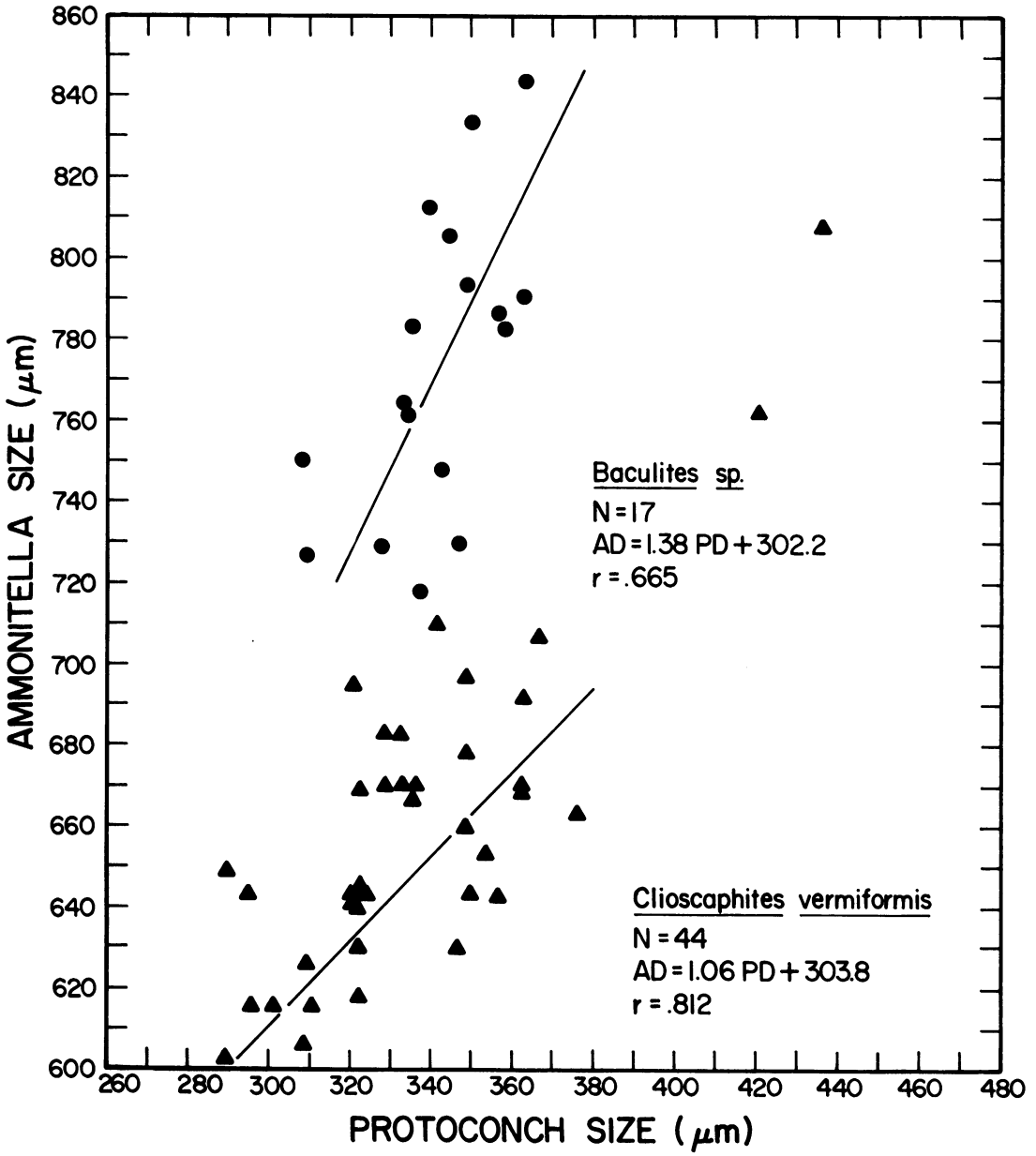

Fig. 23. Plot of protoconch size versus ammonitella size for 44 specimens of *Clioscaphites vermiformis* and 17 specimens of *Baculites* cf. *B. asper, B. codyensis* from locality B235a.

larval shells of bivalves and gastropods that include a free-living larval stage as part of their development.

Whether the primary varix formed before or after hatching is unknown. Druschits et al. (1977a) believed that the primary varix formed after hatching. "It was formed by the nacreous layer during adaptation of the ammonitella to the new habitat and the associated interruption in accretion." In contrast, Kulicki (1979: 128) believed that it formed before hatching: "The swelling formed during a phase when the margin of the nacre halted or even retreated, together with a change in the secretion of the posterior subzone of the mantle margin. The differences in secretory

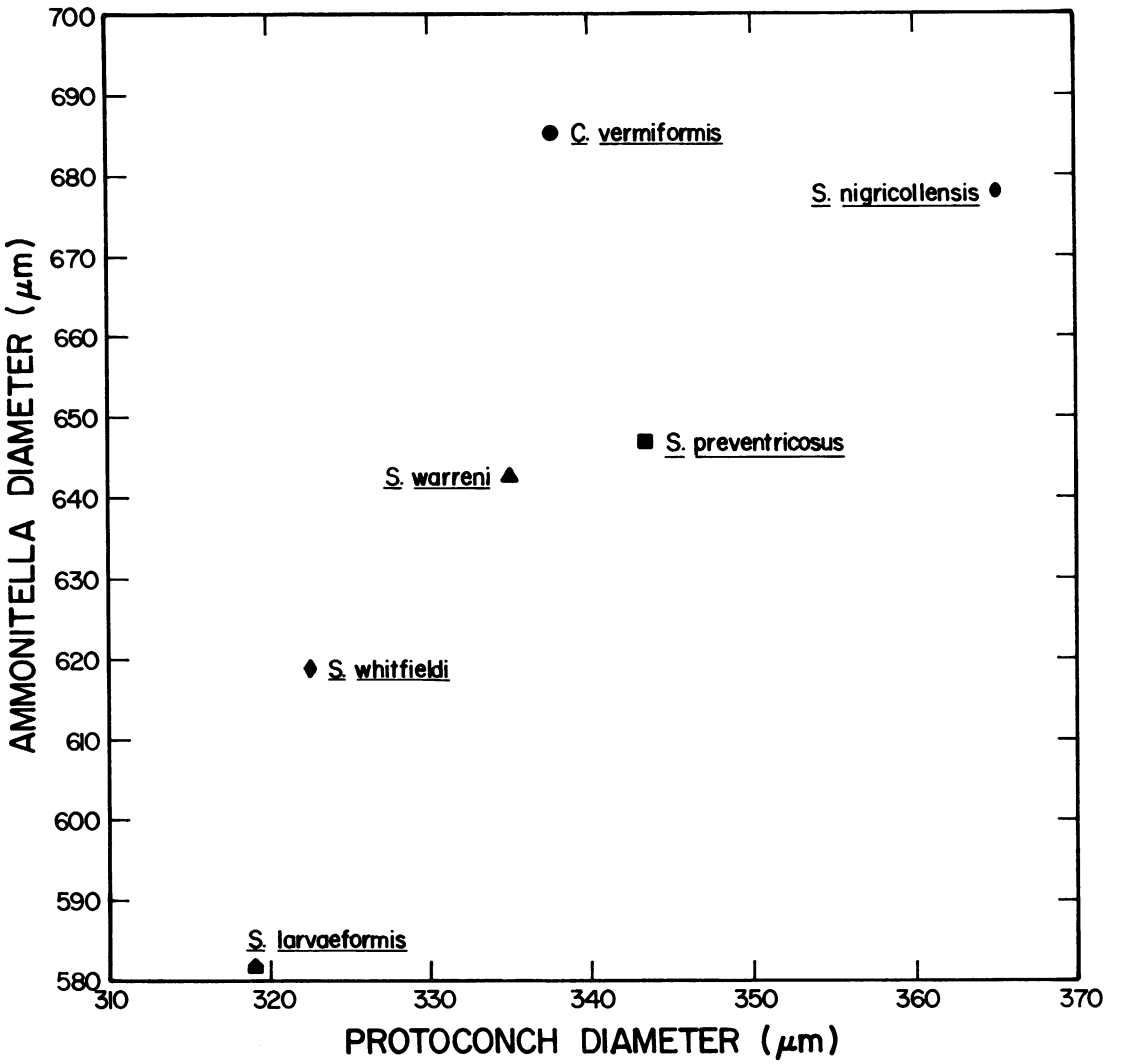

Fig. 24. Plot of mean ammonitella diameter versus mean protoconch diameter for six species exhibits a positive correlation.

products of the posterior subzone may result from, and be correlatable with, processes acting just before hatching." This latter interpretation is supported by finds of preserved ammonitellas with completely formed primary varices.

A scheme of direct development in ammonites is supported further by the fact that all cephalopods whose early ontogeny is known exhibit direct development. In all species of *Nautilus,* development is direct without an intervening larval phase. Although hatching has never been observed in any *Nautilus* species, early embryonic stages of *N. belauensis* have been obtained in aquarium studies (Arnold and Carlson, 1986). Based on the morphology of the nautilus shell, the oxygen isotopic composition of its septa, and the size of its egg capsules, hatching is presumed to occur at a diameter of approximately 26 mm in all species (Cochran et al., 1981; Taylor and Ward, 1983; Landman et al., 1983; Crocker et al., 1985). Externally, the point of hatching is marked by a shallow groove called the nepionic line or constriction (Willey, 1897b). The first appearance of broken growth lines and repaired former apertural margins occur only after the formation

of the nepionic constriction (Stenzel, 1964). The outer wall possesses all three aragonitic layers from the shell apex: outer prismatic, nacreous, and inner prismatic. Internally, the constriction corresponds with an approximation between septa 7 and 8 and a change from thin, widely spaced to thick, closely spaced septa (Naef, 1923; Stenzel, 1964; Willey, 1897b; Westermann, 1973; Stumbur, 1975).

Development is also direct in the coleoids (Arnold and Williams-Arnold, 1977; Wells and Wells, 1977; Bandel and Boletzky, 1979). The term "larvae" is sometimes used to describe early ontogeny but it refers here to underdeveloped individuals immediately after hatching. For example, Wells and Wells (1977) state that the young of octopus species like those of *Octopus vulgaris* normally spend some time in the plankton and are commonly referred to as larvae. However, these young do not undergo an abrupt metamorphosis and the authors suggest that the term "larva" should be avoided. Larval stages are also absent in decapods, squids, and cuttlefish. "Development is direct to a miniature adult which may or may not enter into a planktonic type or existence before forming the typical schools or sedentary life style" (Arnold and Williams-Arnold, 1977).

Number of Septa at Hatching

During growth, the continuous addition of new internal structures obscures the identity of those characteristic of any one stage of ontogeny. Therefore, the description of the internal features at the embryonic stage of development based on the inspection of later stages is difficult. For example, how is the embryonic part of the siphuncle identified? The siphuncle is continuously lengthened during growth and does not display any obvious break which may be confidently relied upon to subdivide its length into embryonic and postembryonic parts. This is also true of the number of embryonic septa. Growth is marked by the steady addition of new septa obscuring the number occurring at any one stage.

Two approaches may be used to determine the number of embryonic septa in scaphites and other ammonites. The first approach relies on the study of the embryonic whorls of juvenile and mature specimens. These studies cannot yield definite answers but rather provide the morphological information on which the identification of embryonic septa may be confidently based. For example, study of the first few septa in scaphites indicates that the proseptum is prismatic and all subsequent septa are nacreous. This difference in microstructure may demarcate the embryonic from postembryonic septa. The shell wall of the ammonitella is entirely prismatic until the primary varix and, therefore, the septa secreted by the posterior part of the soft body may also have been composed of this same microstructure. Similarly, because the postembryonic shell wall is composed partly of nacre, all the nacreous septa may have developed postembryonically. Therefore, according to this criterion, the embryonic scaphite would have possessed only a proseptum.

A similar viewpoint is expressed by Druschits and Khiami (1970) and Druschits et al. (1977a, 1977b). These authors believed that the ammonitella is characterized by only one septum, that is, the proseptum, or less commonly two septa in species in which the second septum is also prismatic; the first nacreous septum develops only after hatching. Birkelund and Hansen (1974) reached similar conclusions based on their study of *Saghalinites, Discoscaphites,* and *Hypophylloceras.*

Study of the early septa in scaphites also indicates that these septa are unevenly spaced. In analogy with modern *Nautilus* and *Sepia,* a reduction in septal spacing may indicate the last embryonic and first postembryonic septa. In *Nautilus,* hatching is marked by a closer spacing between septa 7 and 8 (Stenzel, 1964; Cochran et al., 1981). This septal approximation coincides with a change in the pattern of septal thickness although the septal microstructure remains the same (Westermann, 1973). A reduced septal spacing has also been observed in *Sepia officinalis* and *S. esculenta.* In these two species, the eighth septum also occurs at a reduced distance from the preceding septum (Denton and Gilpin-Brown, 1966).

However, this criterion of septal spacing may yield results in conflict with those based on septal microstructure. For example, Ku-

licki (1974) determined the number of septa in the embryonic shell of *Quenstedtoceras* by measuring the septal spacing of the first few septa, excluding the proseptum. A reduction in septal spacing was interpreted as indicating the last embryonic and first postembryonic septa. Kulicki also reported that the angular length of the whorl from the septum preceding the reduced chamber to the edge of the ammonitella approximated the angular length of the juvenile body chamber. He therefore concluded that at least three septa characterized the embryonic shell although only the proseptum is prismatic.

Measurement of septal spacing also poses operational difficulties. For example, the table below presents measurements made on a polished median section of a juvenile specimen of *Baculites* with nine septa.

Septa	Ang. distance betw. septa
1 and 2	8.5°
2 and 3	21.5°
3 and 4	36.0°
4 and 5	25.0°
5 and 6	22.5°
6 and 7	24.5°
7 and 8	26.0°
8 and 9	25.0°

The angular distance between the proseptum and the second septum equals 8.5°, the smallest angular distance. This reduced distance is due to the inverted shape of the proseptum. On a median section, the proseptum is strongly bent anteriorly and the second septum posteriorly forming a ventral saddle and lobe, respectively. However, measurements of the septal spacing on the same specimen from a parallel, more lateral section transecting approximately saddle *E/L* of the second septum and lobe 1, which corresponds to it on the proseptum, yields different values, which are listed below.

Septa	Ang. distance betw. septa
1 and 2	37.5°
2 and 3	26.0°
3 and 4	35.6°
4 and 5	27.65°
5 and 6	22.55°

The angular distances between most septa are approximately the same whereas the distance between the first two septa is markedly different. Kulicki (1974) recognized this difficulty in his study of *Quenstedtoceras* and, therefore, did not consider the angular distance between the proseptum and second septum. Instead, he selected the next available reduced distance as indicating the last embryonic and first postembryonic septa, namely, septa 3 and 4. In my baculite example he would have chosen the reduced distance between septa 2 and 3. Nevertheless, it is possible that only the proseptum developed in the embryonic stage. An alternative approach using, for example, volume, may better represent septal spacing. Volumes could be estimated in specimens free of matrix or through a calibrated series of sections prepared parallel to the median plane.

The second approach to determine the number of embryonic septa relies on the study of preserved ammonitellas, which are identified based on their external morphology as previously described. They consist of the protoconch and first whorl terminating at the primary constriction. Such shells, which provide the best data for determining the number of embryonic septa, are known from approximately ten localities around the world. Landman (1985) described preserved ammonitellas of *S. ferronensis* from the top of the Juana Lopez Member of the Mancos Shale (fig. 25, USGS locality no. D6022). Several thousand specimens occurred in the body chambers of 15 adults. These small shells, which measured 650 μm in diameter, terminated at the end of the primary constriction and accompanying varix or at the varix trace but did not preserve a caecum or siphuncle. They were assigned to *S. ferronensis* because this was the only ammonite species present and because their protoconchs and ammonitellas were similar in size to those of this species. The outer surfaces of the ammonitellas also exhibited the same micro-ornamentation as that present on the embryonic whorls of this species.

A sample of 50 shells that ended at the primary constriction displayed variation in the number of septa. Most shells possessed only a proseptum with body chamber angles ranging from approximately 270 to 310° (av-

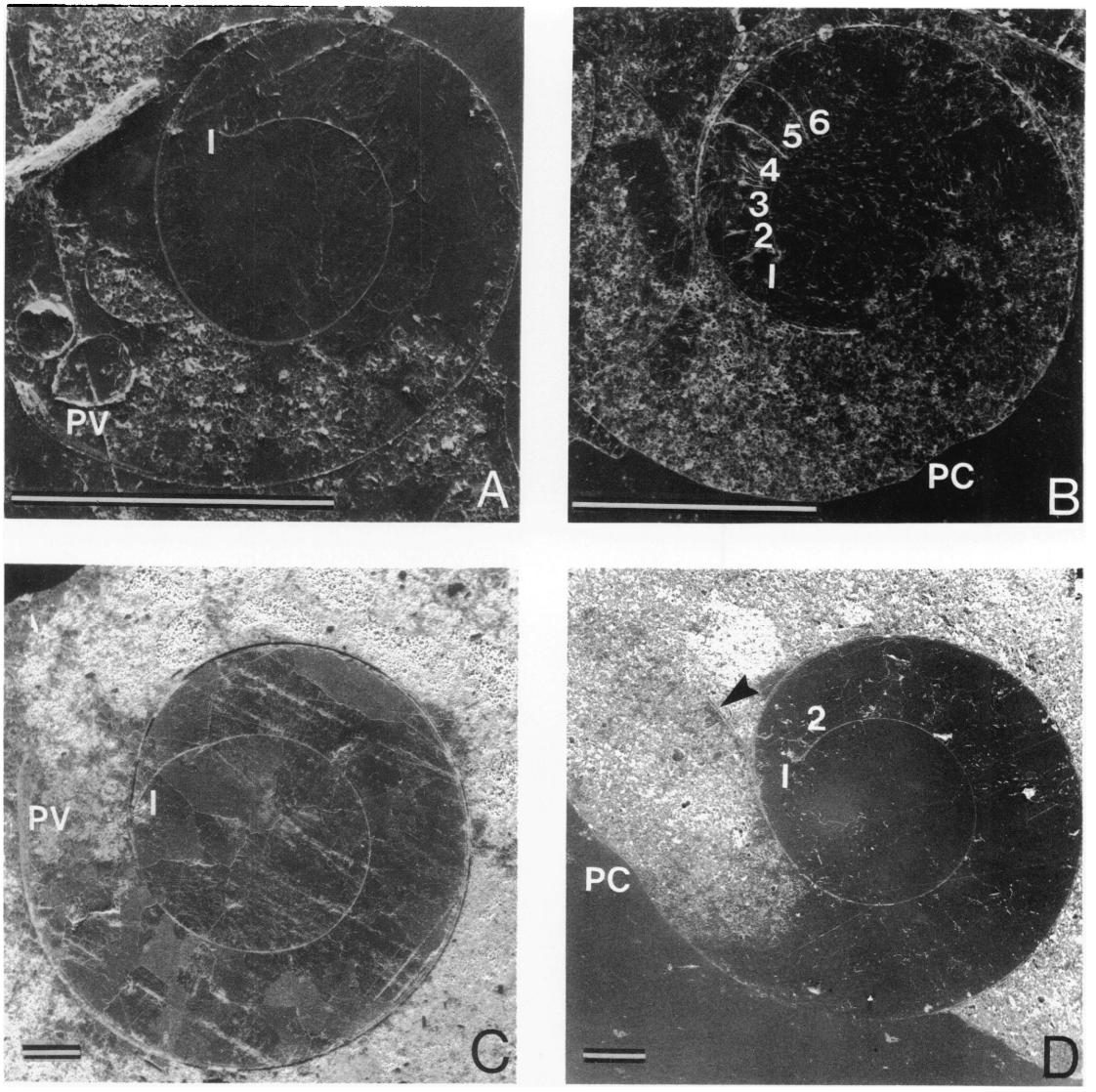

Fig. 25. **A.** Preserved ammonitella of *Scaphites ferronensis* (AMNH 43201) with only a proseptum. **B.** Young postembryonic specimen of *S. ferronensis* (AMNH 43202) with six septa. **C.** Preserved ammonitella of *Baculites* cf. *B. mariasensis, B. sweetgrassensis* (AMNH 43203) with only a proseptum. **D.** Young postembryonic specimen of *Baculites* cf. *B. asper, B. codyensis* (AMNH 42907) with two septa. PV and PC represent the primary varix and constriction, respectively.

erage approximately 290°), similar to the body chamber angles in older juveniles. Fewer specimens possessed two to eight septa with body chamber angles ranging from less than 150 to approximately 260°. However, some of these specimens were clearly fragments of young postembryonic shells because their primary constriction and accompanying varix were broken. In fact, the body chamber angles of young postembryonic shells with a comparable number of septa ranged from 220 to 280°. This interpretation was further supported by the presence of shells completely filled with septa yielding body chamber angles of less than 60°. The edges of many of these shells appeared intact although in other specimens the primary constriction was obviously broken and stray fragments of shell

were located nearby. Evidently, the junction between embryonic and postembryonic shell is a natural point for postmortem breakage and separation. This observation lends support to the contention that the shells with more than a proseptum actually represent fragments of larger shells; only the proseptum appears in the embryonic stage.

Two studies of embryonic baculites provide further support for this hypothesis. Smith (1901) illustrated a nearly complete ammonitella of *Baculites chicoensis* from the Campanian of California that possessed only a proseptum. It is a steinkern but does not display a varix trace because it is broken at its edge. Preserved ammonitellas of *Baculites* were also described from two horizons in the Marias River Shale co-occurring with two scaphite species (fig. 25; Landman, 1982). One ammonitella was discovered in the broken septate portion of an adult specimen of *S. preventricosus* from locality B230. The co-occurring species of *Baculites* consisted of *B. mariasensis* and *B. sweetgrassensis.* The other embryonic shells were collected from locality B235a together with *Clioscaphites vermiformis, Baculites codyensis,* and *B. asper.*

These shells were assigned to *Baculites* because their protoconchs and ammonitellas were similar in size to those of this genus. They measure approximately 750 μm in diameter with body chamber angles averaging approximately 330°. They terminate at the primary constriction and accompanying varix and possess only a proseptum (fig. 25). Several young postembryonic shells that had developed beyond the primary constriction displayed nacreous septa in addition to the proseptum (fig. 25). Other reports of preserved ammonitellas from the Lower Aptian of Ul'yanovsk display only a proseptum (Druschits and Khiami, 1970: 36).

In contrast to these ammonitellas, Bandel (1982) has documented intact ammonitellas of *Baculites* from the Campanian of Jordan with five to seven septa and body chamber angles of approximately 180°, almost half that of the North American baculite species. This discrepancy may illustrate the natural variation in the number of embryonic septa within different species of the same genus. However, the Campanian specimens were silicified and may represent fragments of larger shells that broke at the primary constriction. Nevertheless, preserved ammonitellas of Jurassic perisphinctids from the Jagua Formation of western Cuba with intact primary varices also exhibited more than one septum, generally four or more (Kulicki and Wierzbowski, 1983). These specimens averaged 720 μm in diameter with body chamber angles of approximately 215°. Similarly, Wetzel (1959) reported preserved embryonic shells from the Jurassic of southern Holstein with one or two septa and Blind (1979) reported embryonic shells of *Quenstedtoceras* with two septa.

These studies indicate that scaphites and other ammonites may have hatched with as few as one septum completed, the prismatic proseptum, although additional septa may also have formed during embryonic development. However, the presence of a single septum would have been sufficient to permit buoyancy regulation. If the newly hatched ammonite only possessed a proseptum, the measurement, ammonitella angle, indicates the body chamber angle of the embryonic animal.

Mode of Life at Hatching

The size of the ammonitella varies among ammonites from 0.5 to 1.5 mm and may imply variation in the mode of life at hatching. A planktonic mode may have been common, especially among ammonites such as scaphites with small embryonic shells (approximately 700 μm in diameter). The shape of these ammonitellas is spherical and may have been an adaptation to life in the plankton. The newly hatched animals may have been passive or capable of weak swimming; their shell may have functioned as a neutrally buoyant hydrostatic organ. As Druschits et al. (1977a) write in reference to ammonites in general, "The protoconch of the ammonitella, which was filled with gas and, possibly partly with liquid, was a float of relatively large diameter. . . . This float maintained the young animal suspended in the water and enabled it to lead a planktonic mode of life for some time."

A planktonic mode of life at hatching is common among many modern coleoids, including planktonic and nektonic squids, sepioids, and benthic octopods with relatively small eggs (Boletzky, 1974, 1977). *Nautilus,* in contrast, hatches at the relatively large size

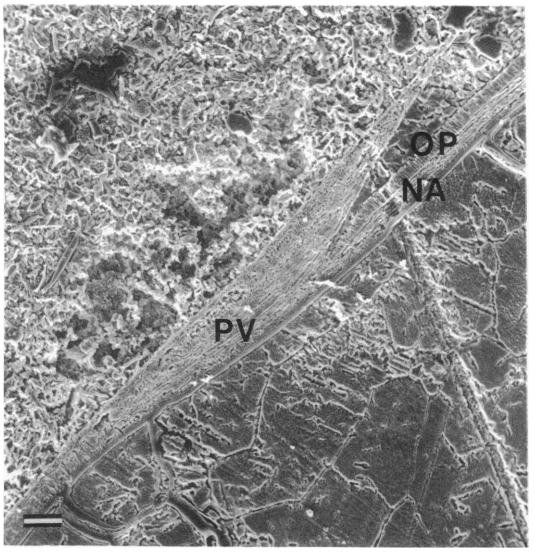

Fig. 26. Median section of a juvenile specimen of *Baculites* cf. *B. asper, B. codyensis* (AMNH 43204) showing the edge of the ammonitella extending beyond the postembryonic shell forming a tapering, unbroken projection. The postembryonic shell which emerges from beneath the primary varix (PV) is composed of an outer prismatic (OP) and inner nacreous layer (NA). Scale bar = 10 μm.

of 26 mm in diameter and is reported to be an active swimmer (Davis and Mohorter, 1973). Commonly, the aperture at hatching is broken and numerous scars appear on the postembryonic shell. In contrast, ammonitellas, which measure less than 4% the size of newly hatched *Nautilus,* rarely display a broken aperture. In fact, in one juvenile of *Baculites* cf. *B. asper, B. codyensis,* the edge of the ammonitella extends above the postembryonic shell and forms a fragile, tapering, but unbroken projection (fig. 26).

A buoyant mode of life at hatching implies a correlation between the volume of the phragmocone and that of the living chamber. Such a relationship appears in the measurements of ammonitella diameter and protoconch diameter for the scaphite species studied as well as for many other ammonites (Tanabe and Ohtsuka, 1985).

The organ responsible for regulating the amount of gas and liquid necessary to maintain buoyancy in the newly hatched ammonite may have been the caecum. This structure and its prosiphonal attachment have been reported from the preserved embryonic shells of at least two ammonite species (Druschits and Khiami, 1970; Landman, 1982). In modern *Nautilus,* the siphuncle is permeable and effects liquid transfer from newly formed chambers (Denton and Gilpin-Brown, 1966; Ward et al., 1980). The ammonite caecum and siphuncle probably performed a similar function and, indeed, Obata et al. (1980) have reported that the siphuncular wall in several Late Cretaceous ammonites resembles the inner conchiolin layer of the siphuncular wall of *Nautilus* in its microstructure and elemental composition. The shape of the caecum further enhances its effectiveness to remove liquid from the protoconch of the embryonic shell. As an oblate ellipsoid, with its length about twice its diameter, it is similar in shape to that of the protoconch and presents a large surface area for the transfer of liquids.

The prosiphonal sheets attached to the caecum also may have helped facilitate cameral liquid removal. They are composed of the same material as the caecum. Although they have traditionally been interpreted as struts to help attach the caecum to the protoconch (Crickmay, 1925), they may also have functioned as part of the hydrostatic regulatory apparatus (Tanabe et al., 1980). They may have acted as wicks to conduct liquid to the caecum or they may have provided a network of tiny openings for interim storage of liquid as it drained from the protoconch. (Such tiny openings are observed to appear and disappear in the series of cross sections of caeca viewed under SEM and called open spaces in fig. 15.) Thus, the prosiphonal sheets may have refined and enhanced the ability of the newly hatched animal to maintain its buoyancy.

Other morphological features of the embryonic shell may also have played a role at hatching. According to Kulicki (1979), the weight of the primary varix may have helped orient the shell in the water. Otherwise, the nearly spherical shape of the ammonitella with the protoconch near the center would result in a coincidence between the centers of gravity and buoyancy, and a consequent loss in static equilibrium. The primary varix may also have reinforced the aperture against breakage. Within the egg capsule, it may have

strengthened the margin of the shell as it pressed against the capsule wall. The actual process of hatching may have been facilitated by the tuberculate micro-ornamentation. In gastropods, for example, hatching is a result not only of enzyme secretion but also of the mechanical action of the embryo against the wall of the capsule leading to its ejection (Jablonski, personal commun.). The granular surface of the ammonitella may have had a similar function.

The fauna associated with preserved embryonic shells includes small clams, gastropods, foraminifera, and juvenile and adult ammonites (Landman, 1985). These associations do not provide any obvious clues about the mode of life of newly hatched ammonites. The accumulations of embryonic scaphites and baculites in the Western Interior occur in relatively offshore habitats several hundred kilometers from the strandline (see Kennedy and Cobban, 1976). Like other finds of preserved embryonic shells (Wetzel, 1959; Druschits and Khiami, 1970; Kulicki, 1979; Birkelund, 1979), they consist of large concentrations of hundreds to thousands of individuals. These concentrations suggest a high mortality and possibly limited dispersal immediately after hatching.

One association of young postembryonic shells that indicates a planktonic or nektonic mode of life shortly after hatching consists of juvenile baculites with shafts up to 1 cm in length from the Upper Cretaceous Sharon Springs Member of the Pierre Shale at Red Bird, Wyoming (see Gill and Cobban, 1966). These shells occur sparsely without any other fossils in small grey limestone concretions. The environment of the Sharon Springs is interpreted as an anaerobic bottom with oxygenated water above, about 300 km from shore (Gill and Cobban, 1966; Byers, 1979). These young baculites must have been planktonic or nektonic shortly after hatching to have lived in this environment.

The small size of the embryonic shell of ammonites compared to that of *Nautilus* apparently correlates with marked differences in their respective number of offspring. In *Nautilus,* Hamada and Mikami (1977) reported that two females laid a total of 17 eggs over seven months. The large size of newly hatched *Nautilus* and their active mode of life, much like that of the adult, may represent an adaptation to a stable deep-water environment (Saunders, 1984). Ammonites, judging from finds of preserved embryonic shells of *Scaphites, Baculites,* and Jurassic perisphinctids, produced hundreds to thousands of young that may have led a planktonic existence. These two kinds of developmental strategy are referred to as K-selected and r-selected, respectively. An r-selected strategy stresses maximization of survivors due to the production of a large number of eggs rather than their protection (Shuto, 1974). Therefore, ammonites closely resemble many Recent dibranchiate cephalopods in their number of offspring and their size and mode of life at hatching. However, they resemble *Nautilus* in their possession of an external shell.

Among ammonites themselves, another more refined r–K continuum may be hypothesized on the basis of variation in the size of the embryonic shell. Species with small ammonitellas may have displayed different environmental tolerances and life histories than species with large ammonitellas. However, determination of the degree of size disparity necessary to result in differences in life history requires further work. In the Upper Cretaceous of Japan, Tanabe and Ohtsuka (1985) have documented that species with smaller embryonic shells ($\sim$ 700 μm) were more restricted in their geographic distribution and display more juveniles in their preserved assemblages than species with larger embryonic shells ($\gtrsim$ 1000 μm). Among the Turonian-Santonian scaphites from the Western Interior, the range in ammonitella diameter is small and suggests that all these species may have shared a common life history. Co-occurring species of *Baculites* and *Collignoniceras* exhibit similar or slightly larger ammonitellas, whereas the ammonitellas of placenticeratids and sphenodiscids from the Campanian and Maastrichtian are two to three times as large.

Correlations between embryonic size and life history commonly appear in gastropods and bivalves, although in these groups a clear dichotomy exists between planktotrophic and nonplanktotrophic larvae. The former are characterized by a long pelagic stage and high dispersal capability. This dichotomy is sharp-

ly reflected in the shape and dimensions of the embryonic shell, which provides a predictive index of developmental type. Small shells are associated with planktotrophic, large shells with nonplanktotrophic, development (Jablonski and Lutz, 1980). In ammonites, however, no dichotomy exists because all species followed the same developmental scheme. Therefore, estimating the length of time an ammonite species may have spent in the plankton on the basis of the size of its ammonitella is more tenuous.

EARLY POSTEMBRYONIC GROWTH

Methodology (Application of the Logarithmic Spiral and Allometry)

The object of this section is to document changes in the shape of the postembryonic scaphite shell that may indicate changes in development or mode of life. The embryonic shell differs from the succeeding whorls in shape but its identification and extent were based mainly on changes in microstructure and micro-ornament. The postembryonic shell, however, is characterized by a uniform microstructure. Therefore, recognizing natural developmental or mode of life changes relies more heavily on a consideration of shape and size with all the attendant problems of standardization and statistical significance.

The form of the juvenile scaphite shell closely conforms to a logarithmic spiral. That a planispirally coiled ammonite approaches a logarithmic spiral was recognized as early as 1838 by Moseley and later on by Thompson (1917), Huxley (1932), and others. The uniqueness of the log spiral is that it accommodates change in size without change in shape (it remains self-similar). This unique property is an outcome of the definition of the spiral. Quoting from Thompson (1917: 753):

> If our point [P] move[s] along the radius vector [r] with a velocity *increasing as its distance from the pole [0],* then the path described is called an equiangular [logarithmic] spiral. Each whorl which the radius vector intersects will be broader than its predecessor in a definite ratio; the radius vector will increase in length in *geometrical* progression, as it sweeps through successive equal angles; and the equation to the spiral will be $r = b^{\theta}$.

θ represents the rotational angle. Introducing a constant a into the equation such that $r = ab^{\theta}$ implies that $r = a$ when $\theta = 0$. The constant b can be expressed as e^{k}, that is, the base of the natural logarithms raised to a constant k. This yields the traditional formula for the log spiral:

$$r_{\theta} = ae^{k\theta} \qquad (1)$$

It is in the form of polar coordinates.

In the context of an ammonite sectioned on a median plane,

- r_{θ} represents the distance between the center of the spiral, approximately the center of the protoconch, and the venter;
- a is the distance between the center of the spiral and the start of the spiral or, in other words, the value of r when $\theta = 0$;
- θ is the rotational angle commonly expressed in π radians, or less commonly in degrees or whorl number with an explicit definition of the point at which $\theta = 0$; and
- k is a constant which uniquely describes the rate of expansion of the spiral. McGhee (1980) called it the specific growth rate constant.

In a logarithmic spiral, such as described by an ammonite, the value k is also equivalent to the cotangent of the angle α formed between a radius to a point on the venter and a tangent to that point. The angle is constant and this property supplies the other name for the spiral, the equiangular spiral.

The constant of spiral expansion relates to the parameter W employed by Raup (1966, 1967). W is defined as the squared ratio of two radii one-half whorl apart.

$$W = (r_1/r_2)^2 \qquad (2)$$

where r_1 equals the radius at some θ and r_2 equals the radius at $\theta - \pi$ radians, a half volution earlier.

From the equation of the log spiral

$$r_1 = ae^{k\theta} \quad \text{and} \quad r_2 = ae^{k(\theta-\pi)} \qquad (3)$$

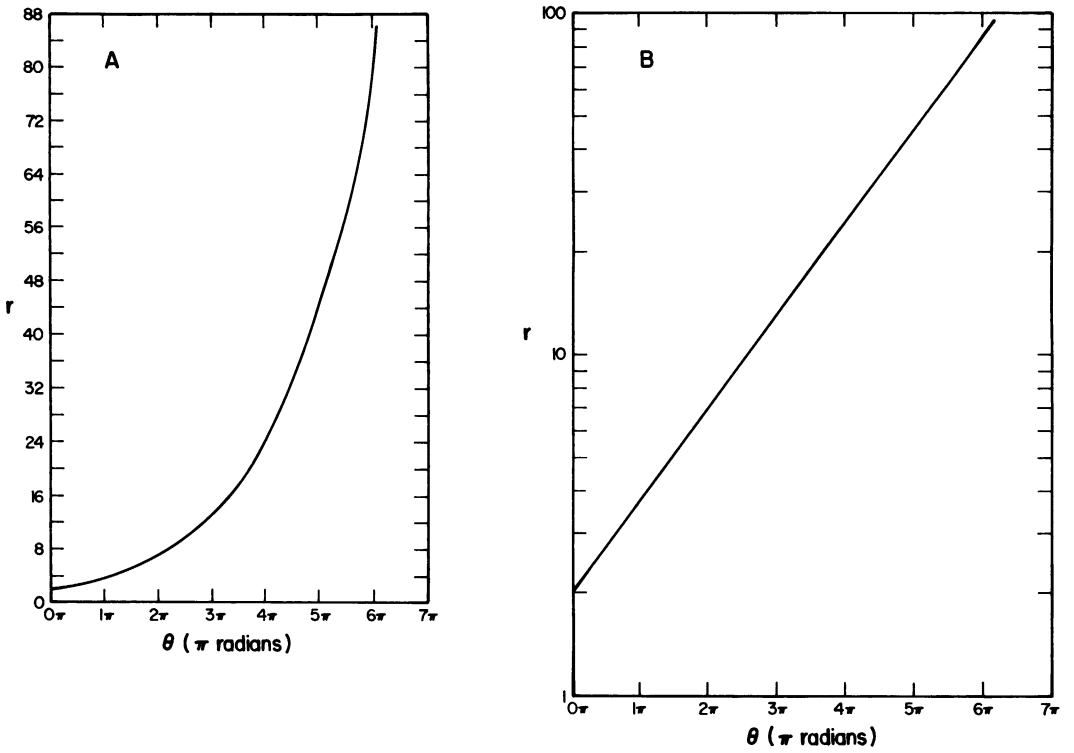

Fig. 27. **A.** Plot of the equation of the logarithmic spiral, $r = 2e^{.2\theta}$, on arithmetic paper. **B.** Plot of the rectified form of the equation, $\ln r = .2\theta + \ln 2$, on semilog paper.

The squared ratio is

$$(ae^{k\theta}/ae^{k\theta}e^{-k\pi})^2 \quad (4)$$

which reduces to

$$e^{2k\pi} \quad (5)$$

If the ammonite shell follows the same spiral throughout growth, W is constant. In my calculations, I use the original form of the spiral equation rather than W because a, the distance between the center and start of the spiral, and k, the expansion rate of the spiral, may be ascertained directly from plotted measurements of the spiral radius as explained below.

Equation 1 can be rewritten by taking the natural logarithm of both sides:

$$\ln r = k\theta + \ln a \quad (6)$$

This is a linear equation which plots as a straight line on semilog paper. The radius r is the dependent variable plotted on the ordinate and θ, the rotational angle, is the independent variable, plotted on the abscissa. The constant k is the slope of the line and a is the intercept. For example, figure 27A and B illustrates the exponential trace of the spiral on arithmetic paper and its rectified form on semilog paper.

The procedures to measure the spiral growth of an ammonite and calculate the constant of spiral expansion are explained in the next few pages. The approach I favor is to take measurements of a specimen sectioned on the median plane. However, measurement of the angle α on the venter is often inexact and nearly impossible. The preferred method involves measurements of r, the distance between the center of the spiral and the ventral edge, versus θ, the rotational angle or whorl number. I recorded radial measurements every ¼ whorl, that is, at ½π intervals between the center of the spiral and the venter (fig. 28A). These measurements were plotted on semilog paper. If the shape of the ammonite *perfectly* conforms to a logarithmic spiral, these measurements will yield a straight line. (Departures from a straight line, that is,

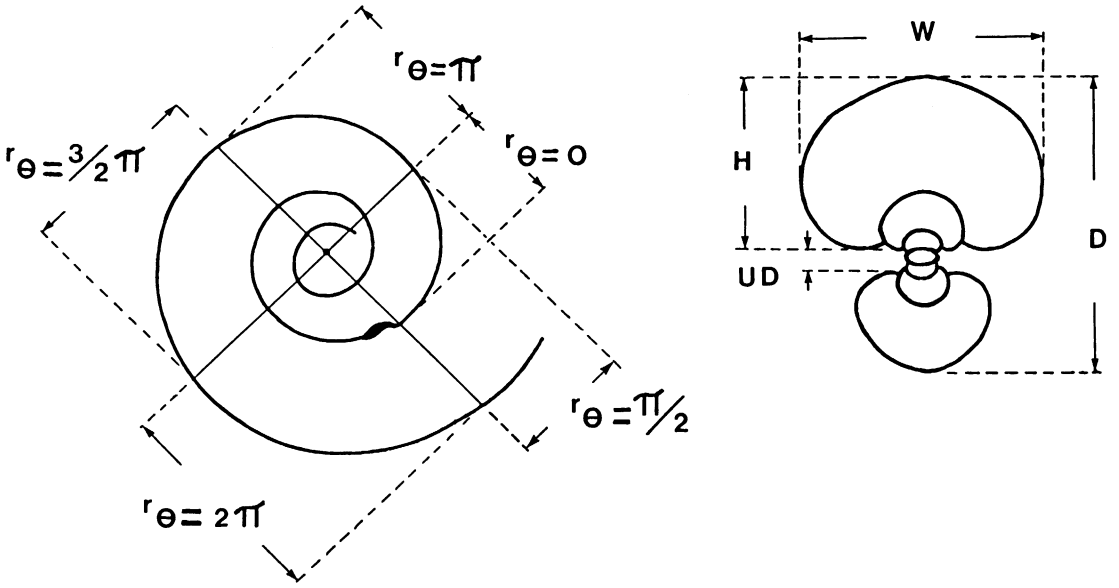

Fig. 28. **Left.** Diagram of a median section of a scaphite illustrating four measurements of the radius of the spiral. **Right.** Diagram of a dorsoventral section of a scaphite illustrating measurements of diameter, whorl width, whorl height, and umbilical diameter.

from a single spiral, are the source and substance of later discussion.) The slope of the line k represents the expansion constant of the spiral and the intercept a represents the distance between the center of the spiral and its start.

This kind of analysis has been called a measure of absolute growth (Kant and Kullmann, 1973; Kullmann and Scheuch, 1972). I presume this description means that this method characterizes growth starting from point 0 ($\theta = 0$). The term "absolute" is probably a misnomer, however, in that growth is still relative, in this case relative to some starting point. The term growth, of course, used here and elsewhere unless otherwise stated, means simply change in shape or size without any implication of growth with respect to time.

This method of "absolute" growth requires recognizing and specifying a starting point, and consistently locating the same starting point in all individuals. McGhee (1980), in a study of convex brachiopod shells, employs the logarithmic spiral but is faced with the difficulty of choosing a starting point. Instead, he chooses an end point; he measures the spiral "backwards" as it were from the commissure in equal angular increments. This requires that the end point of the spiral, the commissure, represent the same growth stage in all individuals. If the pattern of radial increase, that is, the form of the spiral, is slightly different in later growth (the brachiopod becomes more or less convex), measurements

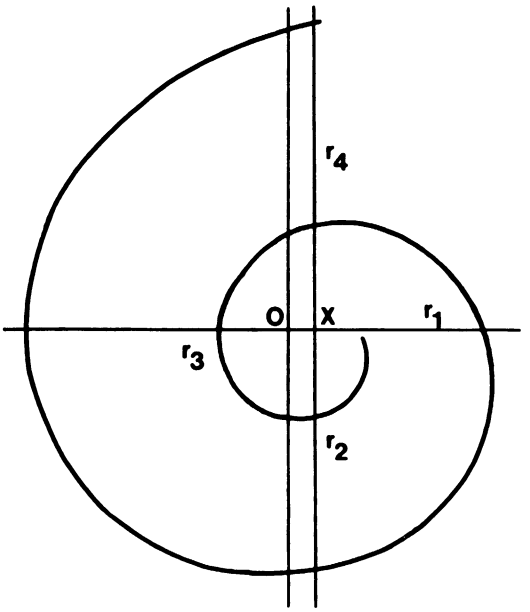

Fig. 29. Consequences of misplacement of the center of the spiral from 0 to X results in anomalously high and low measurements of the spiral radius (see text for discussion).

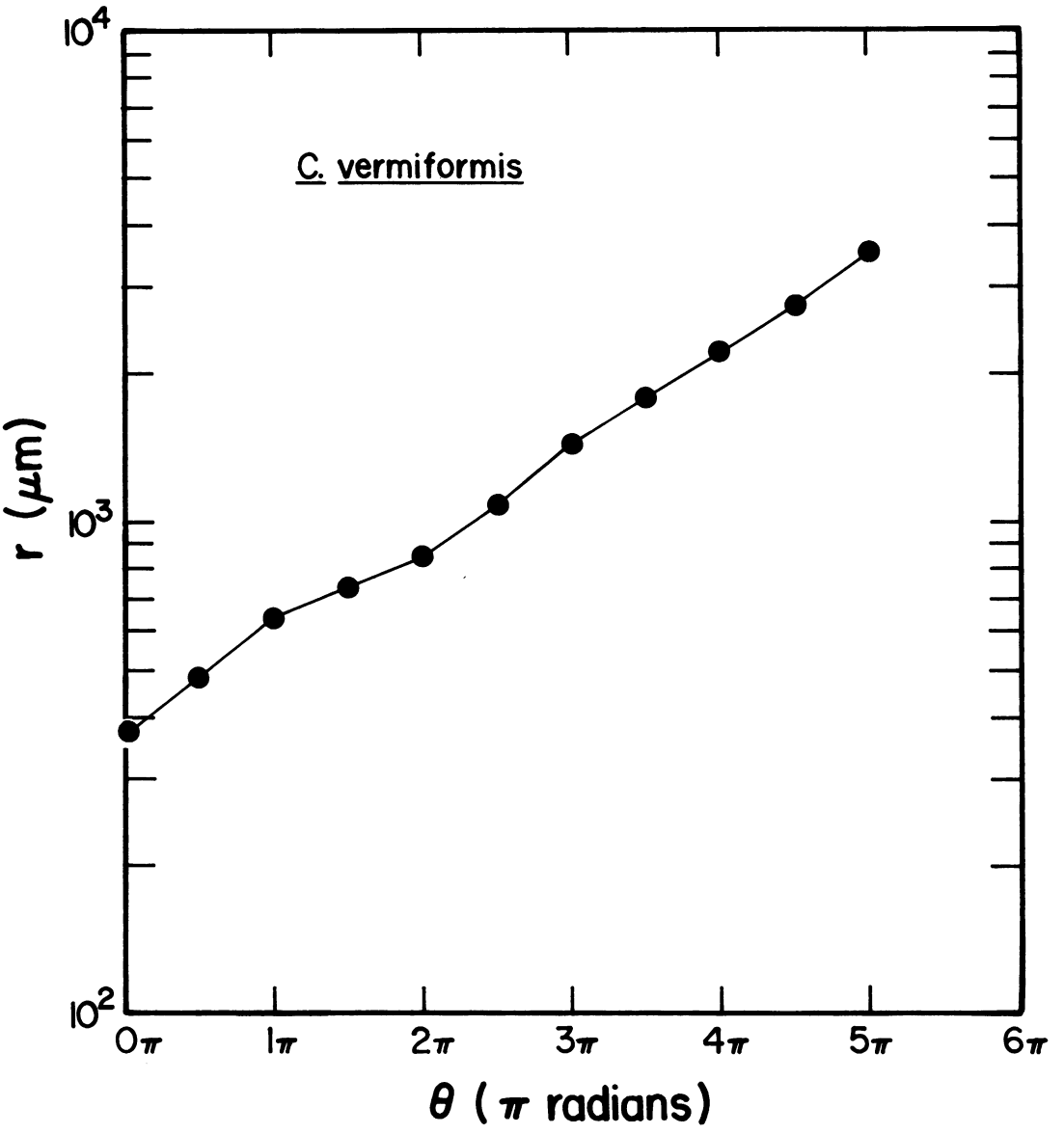

Fig. 30. Plot of the radius of the spiral (r) versus total rotational angle (θ) for a specimen of *Clioscaphites vermiformis*. Measurements were made on a median section in which the center of the spiral was estimated as the center of the protoconch (measurements through 5π).

starting from the commissure of individuals that are at different growth stages will produce confusing results when plotted together. Given, however, that all the individuals are mature, for example, there is another problem in choosing an end point rather than a starting point in scaphites and I will couch my discussion in this context.

Scaphites commonly exhibit variation in the number of whorls at maturity (counting forward from some starting point). Standardizing at maturity and working backwards in equal angular increments may result in equating, for example, the second whorl in one individual with the third whorl in another. If a change in the spiral occurs at a definite whorl number (counting from the beginning), then standardizing from the end and counting backward will obscure this change when the specimens are plotted together.

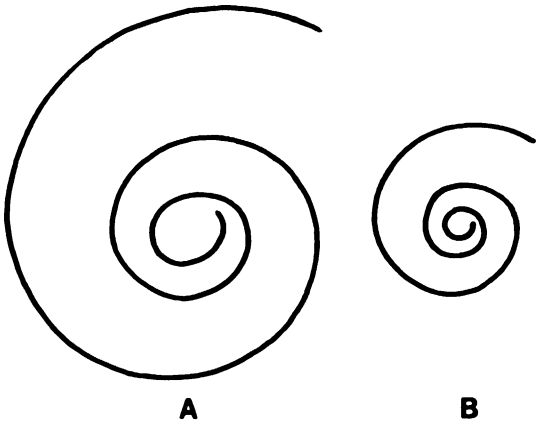

Fig. 31. Technique to accurately pinpoint the center of the spiral. The larger spiral (**A**) is mechanically reduced to a smaller spiral (**B**) which exhibits the same shape but a reduced distance between the origin and the start of the spiral, i.e., a is reduced. By superimposing the reduced spiral onto the original one, a close approximation of the location of the center of the original spiral is obtained.

In my measurements I have chosen as a starting point the start of the postembryonic shell marked by the end of the primary constriction and its accompanying primary varix. This is an easily recognized point of origin that can be detected in all specimens and provides a natural point of departure for a consideration of postembryonic growth (fig. 28A).

The second difficulty in describing the spiral growth of an ammonite is choosing the center of the spiral. This problem is graphically illustrated on median sections where radial measurements are taken every quarter whorl. Figure 29 illustrates how misplacement of the center to the right, for example, will produce anomalously low radial measurements r_1 and r_2 and anomalously high radial measurements r_3 and r_4. The resultant sinusoidal pattern will be most pronounced at small diameters and eventually dampen out. Figure 30 represents a plot of the spiral radius versus the total rotational angle for a specimen of *C. vermiformis* cut exactly on a median plane. The center of the spiral was eyeballed as the center of the protoconch, the usual practice among ammonitologists. If one were inclined, one could discern at least four "growth stages" but to what extent are they an artifact of the mislocation of the center?

D'Arcy Thompson (1917) devotes three pages to a discussion of how to locate the center of the spiral. His suggestions are theoretically sound but in practice very difficult, often yielding too little precision; they have, in fact, generally been ignored. Earlier in his chapter on the equiangular spiral, though, he suggests drawing the outline of a little *Nautilus* shell within a big one. "We know, or we may see at once, that they are precisely the same shape; so that, if we look at the little shell through a magnifying glass, it becomes identical with the big one." This is the clue, I think, to most easily locating the center of the spiral in an ammonite. A *camera lucida* or photograph of the early whorls is made. These approximately conform to a spiral, $r = ae^{k\theta}$, where a represents the distance between the center and the starting point. If we mechanically reduce the drawing, the expansion constant k remains the same but the constant a decreases as one would expect, that is, the starting point is nearer to the center. The two spirals still have the same shape. If the shape of the shell remains approximately the same throughout growth, one can superimpose the enlarged spiral on top of the reduced one and mark the area on the enlarged one near the point at which the smaller spiral begins. This method is illustrated in figure 31 and results in an accurate estimate of the center of the spiral.

The center of the spiral does not occur in the eyeballed center of the protoconch but slightly ventral to it and does not coincide with any morphological feature (fig. 28A). Using this method to locate the center, I replotted r versus θ for the same specimen of *C. vermiformis* illustrated previously (fig. 32). The plot is remarkably smoothed out and the deviations have disappeared. In all specimens in which the spiral radius versus the total rotational angle was measured on the median section, this method was used to locate the center. The distance between the center of the spiral and the start of the spiral (the end of the primary varix) approximately equals 60% of the ammonitella diameter in all species.

Analysis of the growth of the spiral radius versus the total rotational angle may also be based on dorsoventral sections (Kullmann and Scheuch, 1972; Kant and Kullmann, 1973). The ammonite is sectioned so that the

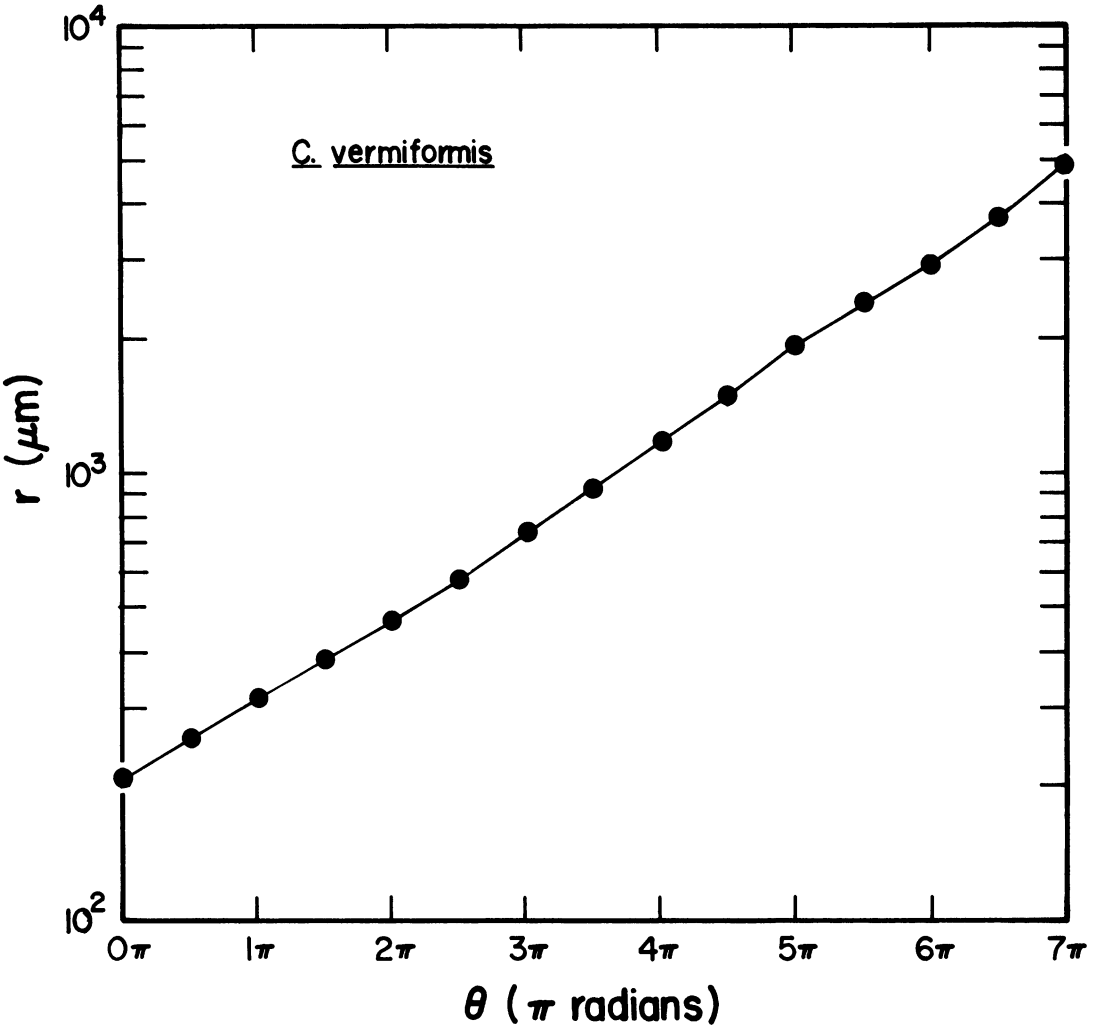

Fig. 32. Replotted measurements of the radius of the spiral (r) versus total rotational angle (θ) for the specimen illustrated in figure 30. The center of the spiral was located using the method described in figure 31. (Measurements through 7π. The values of r plotted are 0.5 times the actual measurements.)

coiling axis lies in the plane of the section (fig. 28B). Measurements are taken between the center and the ventral edge at intervals of 180°. Location of the center of the spiral is slightly easier in this method since it necessarily lies along the line of symmetry. In measurements of diameter rather than radii on dorsoventral sections, the center of the spiral does not have to be located at all. However, use of dorsoventral sections only permits measurements every 2π or 360°. Nor does it allow for the consistent location of the same starting point, that is, the point at which $\theta = 0$. The starting point can vary up to as much as 90° or $\frac{1}{2}\pi$. For example, figure 33 is a median section showing the primary varix and the start of the postembryonic shell. Dorsoventral sections are made perpendicular to this median section and run through the center of the protoconch. They are represented by lines "cutting" into the page. In one such dorsoventral section that fortuitously intersects the end of the primary varix, the first radial measurement, that is, at $\theta = 0$, is r_1 and the second radial measurement made one-half whorl forward is r_2. However, in another dorsoventral section, the line of cut is perpendicular to that in the first section. In this instance, the first radial measurement, r'_1, is offset by 90° from r_1. In this way, two

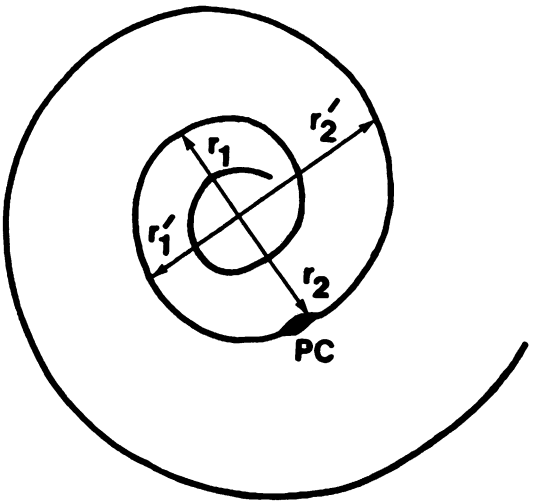

Fig. 33. Diagram of a median section showing the primary constriction (PC) and start of the postembryonic shell. Lines r_1r_2 and $r'_1r'_2$ represent the traces of two dorsoventral planes perpendicular to the median section and running through the center of the protoconch. The two lines are themselves perpendicular to each other and r_1r_2 intersects the primary constriction.

such dorsoventral sections made on identical specimens will yield different results. In other words, both r_1 and r'_1 would be plotted at $\theta = 0$. This problem can be further exacerbated if the early whorls are poorly preserved. In these instances, the choice of the point at which $\theta = 0$ may be off considerably more than 90°. Gutjahr and Hook (1981) described this difficulty in their study of two nautiloid genera in which the early whorls were poorly or not at all preserved. They circumvented the problem by translating the resultant r versus θ patterns for individual specimens along the θ axis until the patterns matched.

The problem of using dorsoventral sections to describe "absolute" growth has been faced in the study of other invertebrates. Cutbill and Forbes (1967), commenting on fusilinids, wrote "In sections containing the coiling axis there is the added complication that while the measurements can be made at precise intervals of whole or half volution, the actual volution number from the first chamber can only be specified to the nearest half volution." The study of fusilinids is further complicated by the presence of microspheric and megalospheric forms in the same species. As Dunbar and Skinner (1937) have eloquently written:

> Truly microspheric forms begin with a small proloculum and pass through several early ontogenetic stages which are completely omitted in the megalospheric shells. The comparison of similarly numbered whorls in the two is, therefore, as indefensible in principle as it is futile in practice; there is no correspondence, even though both represent a single species.

To avoid this difficulty in locating the same starting point for r versus θ measurements, I used median sections.

Median and dorsoventral sections may also be used to study the relative growth of ammonites (fig. 28B). Relative growth, as compared to "absolute" growth, does not rely generally on θ as one of the variables. Nor does it require an explicit choice of a starting point. Usually, one dimension (the dependent variable) is plotted against overall size (the independent variable). I measured the growth patterns of several dependent variables such as whorl height, whorl width, whorl cross-sectional area, umbilical diameter, the expansion rate of the spiral, and siphuncular diameter against overall shell size. The measurements were plotted on log-log paper and commonly describe a straight line although curvilinear patterns may also appear. If the measurements conform to a straight line, their relationship may be represented by a linear equation, $\log y = \alpha \log x + \log b$, where α is the slope and $\log b$ the intercept. This equation is equivalent to the power function $y = bx^{\alpha}$, commonly called the equation of simple allometry (Gould, 1966). The exponent is an index of allometry. Exponents greater than 1.0 indicate positive allometry, that is, the ratio of y to x increases with increasing x. Exponents less than 1.0 imply negative allometry; the ratio of y to x decreases with increasing x. An exponent equal to 1.0 indicates isometry; the ratio of y to x is constant for all x and increase in size does not entail a change in shape.

In measurements of both absolute and relative growth, poor preparation of median and dorsoventral sections will introduce experimental errors. For example, dorsoventral sections may accidentally be cut above or below the axis of coiling. The radii measured

from the center to the ventral edge will, therefore, differ from the corresponding radial measurements made on a section coincident with the axis of coiling and will thus not describe a perfect logarithmic spiral, particularly at small diameters. Gutjahr and Hook (1981) present this explanation to account for oscillations in the growth pattern of the spiral radius of two Ordovician nautiloids measured from dorsoventral sections. The sinusoidal pattern dampens with increasing radius and may be modeled using a cosine expression that simulates periodicity dampening with increasing size. Kullmann and Scheuch (1972) describe another example in which a dorsoventral section is accidentally cut at an angle resulting in distortion in the measurements of whorl width. All these kinds of accidents may also occur in preparing median sections with similar results but the presence of the siphuncle often helps to establish the plane of coiling.

Whorl Width

Whorl width is measured on dorsoventral sections and plotted against shell diameter. The plots indicate a marked change at the embryonic-postembryonic boundary. Even in the absence of other data about microornamentation, this change is dramatic enough to indicate an abrupt shift in development. Figure 34 illustrates measurements for 18 individuals of *S. larvaeformis* from locality B189. Measurements of the whorl width of the embryonic shell, which averages less than 700 μm in diameter, plot almost on a straight line of zero slope. In other words, in embryonic development, whorl width is constant. In postembryonic growth, however, an increase in diameter coincides with an increase in whorl width. This relationship approximates a straight line on log-log paper although the pattern changes slightly at approximately 3 mm. The equation of the line of best fit for postembryonic growth is

$$\log W = 1.134 \log D - .625$$

where W = whorl width, expressed in μm
D = shell diameter, expressed in μm
1.134 = the slope, and
$-.625$ = the intercept.

The correlation coefficient r equals .9880. Rewriting the equation as a power function yields:

$$W = .237D^{1.134}$$

If the measurements were expressed in mm instead of μm, the slope would be the same but the intercept would be different. This equation only applies to postembryonic growth, which begins at approximately 700 μm in shell diameter equal to the diameter of the ammonitella. Below this size, the equation does not apply. The exponent in the power function, 1.134, indicates that this relationship is nearly isometric, only slightly positively allometric. The ratio of whorl width to shell diameter is nearly constant, displaying only a slight increase with increasing diameter. Application of a statistical test developed by Hayami and Matsukuma (1970) to discriminate between allometry and isometry with 95% confidence, indicates positive allometry ($Z = 6.68$, number of data points = 81).

Measurements of the whorl width of 11 specimens of *S. whitfieldi* exhibit a similar pattern with a change in slope between embryonic and postembryonic growth, although it occurs approximately 100 μm later (fig. 35). The equation of the line of best fit is $\log W = .9410 \log D - .050$ or the equivalent power function $W = .892D^{.9410}$ (measurements are expressed in μm). The correlation coefficient equals .9973. Application of Hayami and Matsukuma's statistical test indicates negative allometry with 95% confidence ($Z = -7.92$, number of data points = 86). In other words, the ratio of whorl width to shell diameter decreases with increasing diameter. Measurements of the whorl width of 16 individuals of *S. preventricosus* from locality B228a are illustrated in figure 36. A break in the slope between embryonic and postembryonic growth appears but, as in *S. whitfieldi*, it occurs at a diameter of approximately 800 μm. Postembryonic growth approximates a straight line although a definite sinusoidal pattern occurs with an inflexion point at approximately 3 mm. The equation of the line of best fit is $\log W = 1.026 \log D - .336$ or the equivalent power function $W = .461D^{1.026}$ (measurements are expressed in μm). The correlation coefficient equals

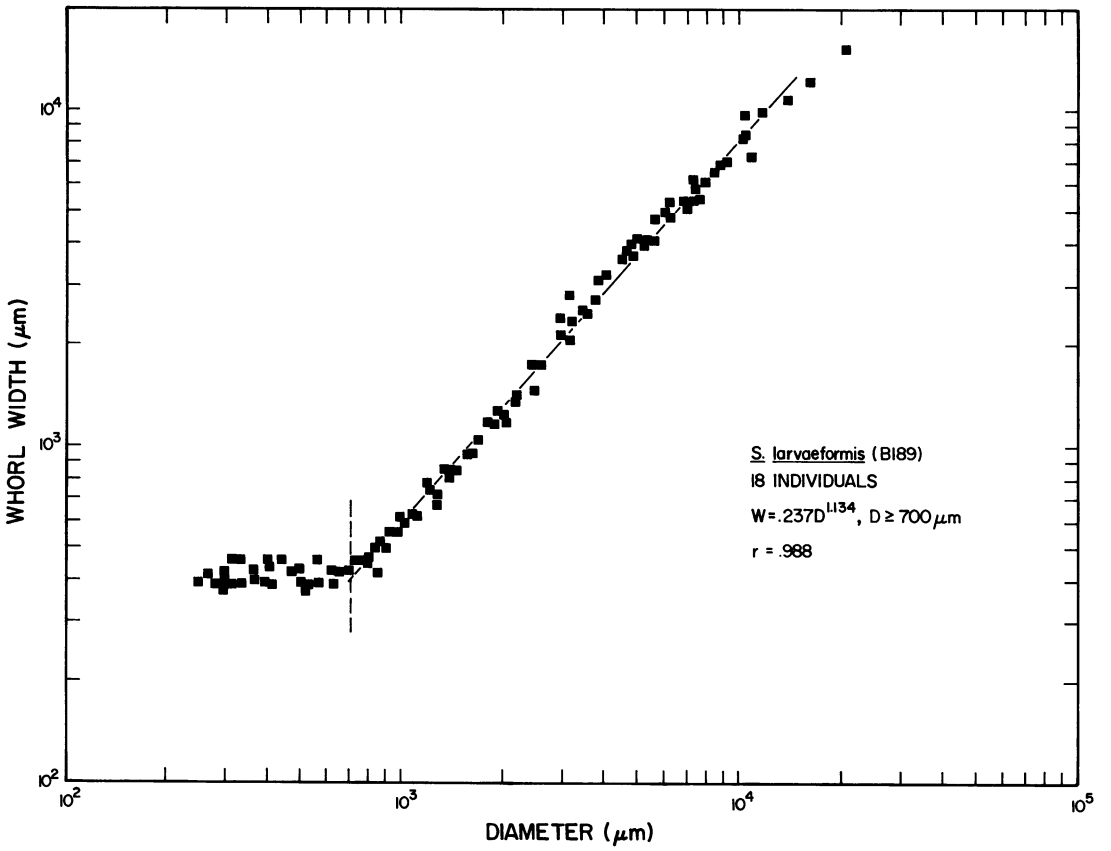

Fig. 34. Plot of whorl width versus shell diameter for 18 specimens of *Scaphites larvaeformis*. The dashed vertical line represents the boundary between embryonic and postembryonic growth.

.9967. Allometry is positive with 95% confidence ($Z = 2.76$, number of data points = 78). Figure 37 illustrates the growth of whorl width versus shell diameter for 11 specimens of *C. vermiformis* from locality B235a. A marked break occurs at the embryonic-postembryonic boundary. Postembryonic growth nearly conforms to a straight line although some departures from linearity appear. At shell diameters less than approximately 2 mm, many points fall below the line of best fit; at shell diameters greater than approximately 4 mm, many points lie above the line of best fit. The equation for postembryonic growth is $\log W = 1.098 \log D - .473$ or the equivalent power function $W = .336D^{1.098}$ (measurements are expressed in μm). The correlation coefficient equals .9891. Application of Hayami and Matsukuma's statistical test reveals positive allometry with 95% confidence ($Z = 4.98$, number of data points = 56).

Thus, the growth pattern of whorl width versus shell diameter for these four species indicates a marked shift at approximately 700–800 μm and is nearly, but not quite, isometric thereafter. The pattern is positively allometric in three species and negatively allometric in one species. The slopes may be statistically compared using a test developed by Imbrie (1956). The test statistic Z is calculated employing the value of the standard error of the slope. The results of this test indicate that each species is significantly different at the 1% level except the species pair *S. larvaeformis* and *C. vermiformis* (table 17).

At least three of the four species display slight departures from linearity in their pattern of postembryonic growth. Many of these changes occur at approximately 3 mm in shell

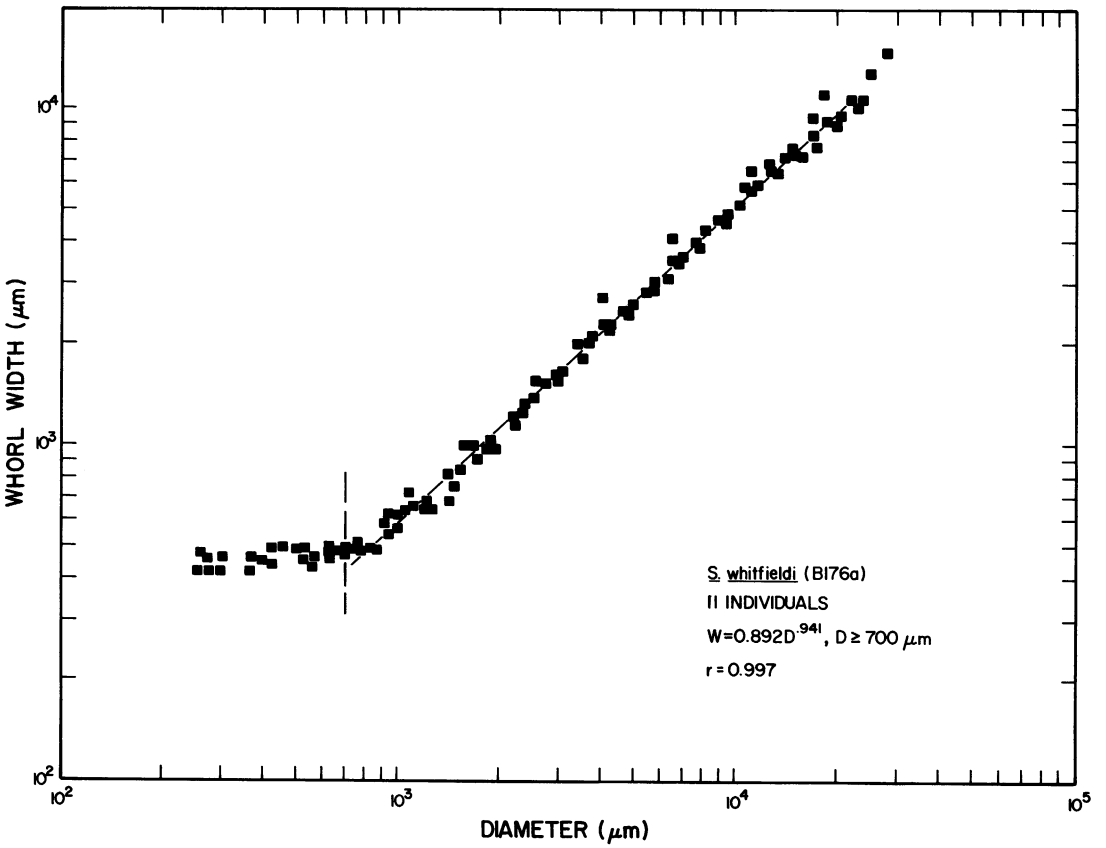

Fig. 35. Plot of whorl width versus shell diameter for 11 specimens of *Scaphites whitfieldi*. The dashed vertical line represents the boundary between embryonic and postembryonic growth.

diameter. Tanabe (1977) also detected a change in the pattern of whorl width versus shell diameter at approximately two whorls from the constriction in *Scaphites planus* and *Otoscaphites puerculus*.

Whorl Height

The growth pattern of whorl height versus shell diameter does not exhibit as dramatic a break between embryonic and postembryonic development as that of whorl width versus shell diameter. Nevertheless, the measurements of whorl height for embryonic growth display a wide dispersion and their combined slope is different from that of postembryonic growth which, as in the examples of whorl width versus shell diameter, equals approximately one. Measurements of 18 specimens of *S. larvaeformis* from locality B189 approximate a straight line on log-log paper for diameters greater than 700 μm (fig. 38). A slight departure from linearity appears with points less than 3 mm in diameter falling below the line, points between 3 and 6 mm lying above the line, and points greater than 6 mm, falling below the line again. The equation of the line is $\log H = 1.113 \log D - .709$ or the equivalent power function $H = .196D^{1.113}$ (measurements are expressed in μm). The coefficient of correlation equals .9989. Allometry is positive with 95% confidence ($Z = 19.53$, number of data points = 81). Measurements of 11 specimens of *S. whitfieldi* from locality B176a also approximate a straight line on log-log paper for diameters greater than 700 μm although a slight inflexion point appears at approximately 3–4 mm in shell diameter (fig. 39). The equation of the line is $\log H = 1.065 \log D - .516$ or the equivalent power function $H = .304D^{1.065}$ (measurements are expressed in μm). The

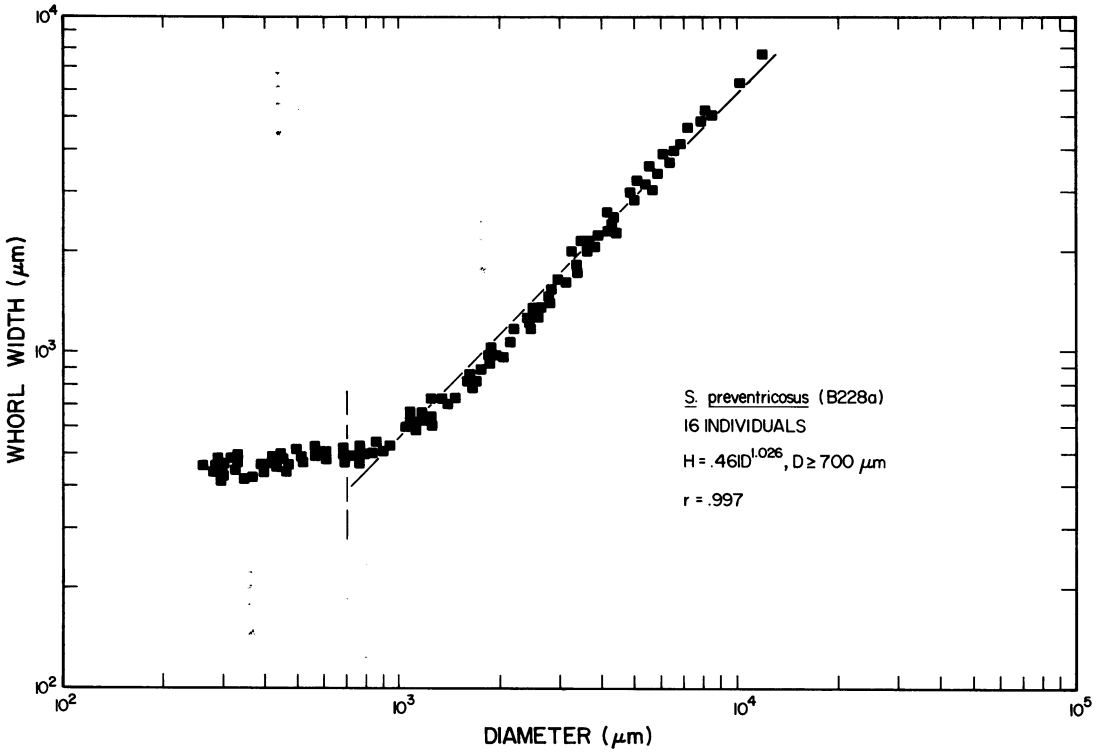

Fig. 36. Plot of whorl width versus shell diameter for 16 specimens of *Scaphites preventricosus*. The dashed vertical line represents the boundary between embryonic and postembryonic growth.

coefficient of correlation equals .9995. Allometry is positive with 95% confidence (Z = 17.90, 86 data points). In *S. preventricosus*, measurements of whorl height versus shell diameter also nearly conform to a straight line for diameters greater than 700 μm (fig. 40). A slight sinusoidal pattern appears with an inflexion point at approximately 3 mm in diameter. The equation of the line of best fit is $\log H = 1.100 \log D - .670$ or the equivalent power equation $H = .214D^{1.100}$ (measurements are expressed in μm). The coefficient of correlation equals .9971. Allometry is positive with 95% confidence (Z = 10.41, 76 data points). Similarly, the measurements of whorl height versus shell diameter for 11 specimens of *C. vermiformis* from locality B235a approximately conform to a straight line (fig. 41). A slight inflexion in the pattern of growth appears at approximately 3–4 mm diameter. The equation is $\log H = 1.107 \log D - .650$ or the equivalent power function $H = .225D^{1.107}$ (measurements are expressed in μm). The coefficient of correlation equals .9977. Allometry is positive with 95% confidence (Z = 10.36, 53 data points).

Thus, all four species exhibit positive allometry, although the pattern of postembryonic growth may depart slightly from a straight line. Comparing the patterns of growth for these four species using Imbrie's statistical test reveals that *S. whitfieldi* is significantly different at the 1% level from all the other species, which among themselves exhibit no significant differences. In fact, although *S. preventricosus* was significantly different from both *S. larvaeformis* and *C. vermiformis* in regard to whorl width versus diameter, this species is now inseparable from the other two (table 18).

Whorl Cross-sectional Area

Cross-sectional area versus shell diameter was measured on dorsoventral sections of 15 specimens of *C. vermiformis* from locality B235a (fig. 42). Note that in this instance a slope of 2.0 equals isometry because area is

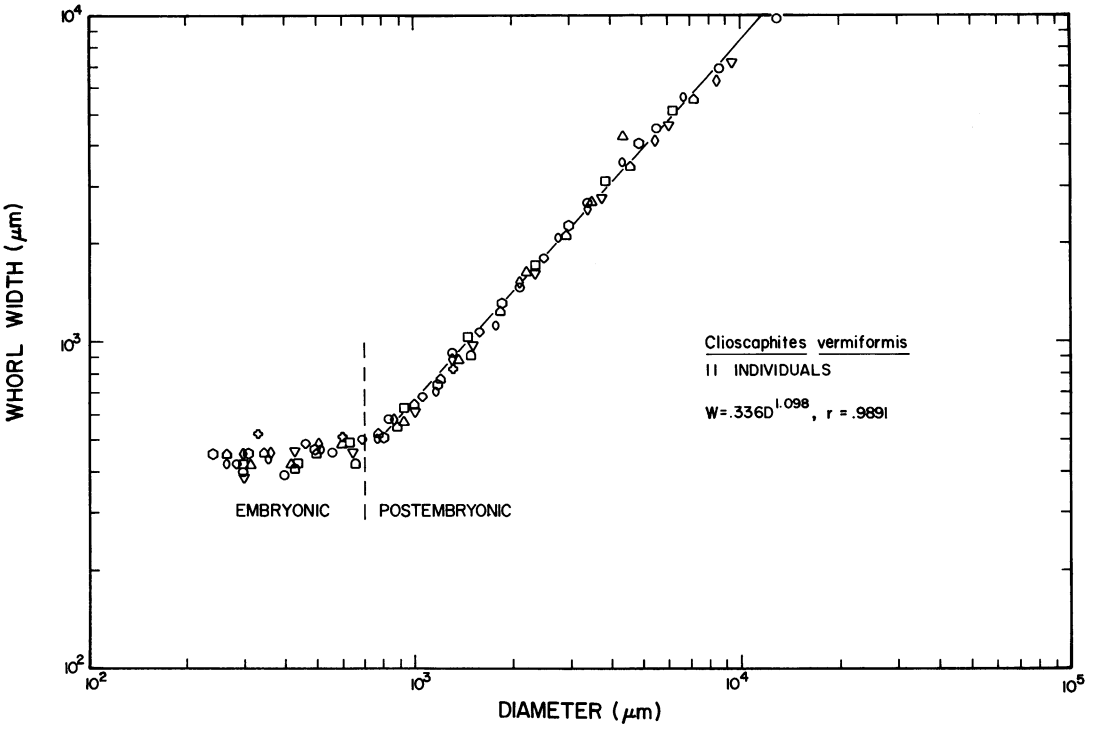

Fig. 37. Plot of whorl width versus shell diameter for 11 specimens of *Clioscaphites vermiformis*. The symbols represent different specimens. The dashed vertical line represents the boundary between embryonic and postembryonic growth.

plotted against a linear dimension. The equation of the line of best fit for postembryonic growth is log Area = 2.198 log D − 7.258 or the equivalent power function Area = $5.52 \times 10^{-8} D^{2.198}$ (measurements are expressed in mm). The coefficient of correlation equals .9982. The statistical test indicates positive allometry (Z = 12.92; 74 data points).

Umbilical Diameter

This dimension was measured on dorsoventral sections and plotted against shell diameter on log-log paper. Measurements of the umbilical diameter of 17 specimens of *S. larvaeformis* from locality B189 describe a gently sloping curve without any deviations between 0.7 and 3 mm in shell diameter (fig. 43). However, an abrupt and graphic increase in scatter occurs at approximately 3 mm in diameter and although the subsequent points may represent a continuation of the earlier curve, the disruption beginning at 3 mm is very conspicuous. On the other hand, measurements of the umbilical diameter for 33 specimens of *S. whitfieldi* from locality B176a

TABLE 17
Statistical Tests of the Allometric Slope of the Growth of Whorl Width Versus Shell Diameter

	S. whitfieldi	*S. preventricosus*	*C. vermiformis*
S. larvaeformis	Z = 9.26 sig. at 1%	Z = 4.99 sig. at 1%	Z = 1.24 nonsig.
S. whitfieldi		Z = 7.07 sig. at 1%	Z = 6.87 sig. at 1%
S. preventricosus			Z = 3.05 sig. at 1%

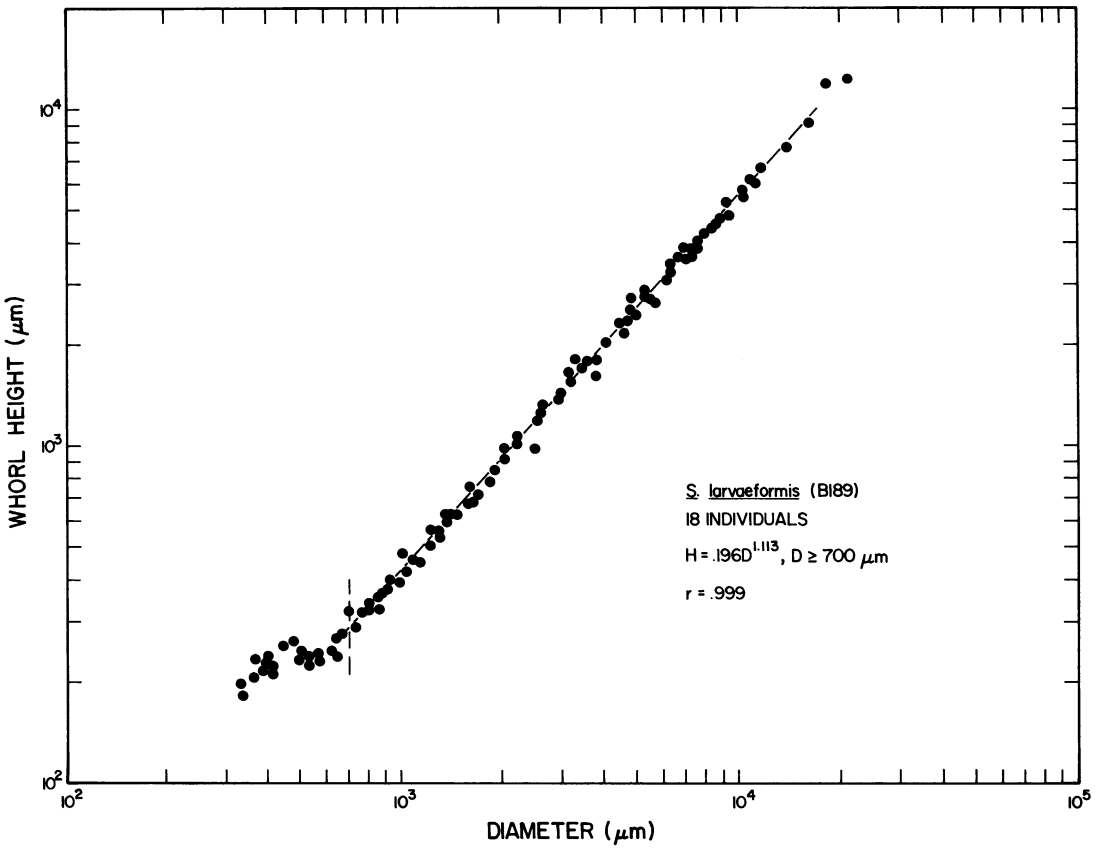

Fig. 38. Plot of whorl height versus shell diameter for 18 specimens of *Scaphites larvaeformis*. The dashed vertical line represents the boundary between embryonic and postembryonic growth.

do not suggest any apparent changes in the pattern of growth (fig. 44). In *S. preventricosus,* measurement of the umbilical diameter for 27 specimens from locality B228a describes a pattern similar to that in *S. larvaeformis.* It consists of a fairly tight curve up to 3–4 mm in shell diameter followed by a sharp and dramatic increase in scatter (fig. 45). A plot of umbilical diameter versus shell diameter for 26 specimens of *C. vermiformis* from locality B235a also reveals a change at a diameter of approximately 3–4 mm but suggests a slightly different pattern thereafter (fig. 46). In this species, the change at 3–4 mm represents a kind of inflexion point with subsequent values describing a steeper slope, although this impression is partly exaggerated by the more expanded scale used in figure 46.

Thus, at least three species indicate a change in the pattern of growth of the umbilical diameter at approximately 3–4 mm in shell diameter. Tanabe (1977) also recognized a change in the growth pattern of umbilical diameter at approximately two whorls from the constriction corresponding to 3–4 mm in shell diameter in *S. planus* and *Otoscaphites puerculus.*

Constant of Spiral Expansion

The transition from embryonic to postembryonic growth is commonly marked by a sharp increase in the length of the spiral radius (fig. 47). However, the subsequent pattern of growth is nearly uniform with only minor deviations. Figure 48 represents measurements of the growth of the spiral radius versus the total rotational angle for a juvenile specimen of *S. preventricosus* from locality

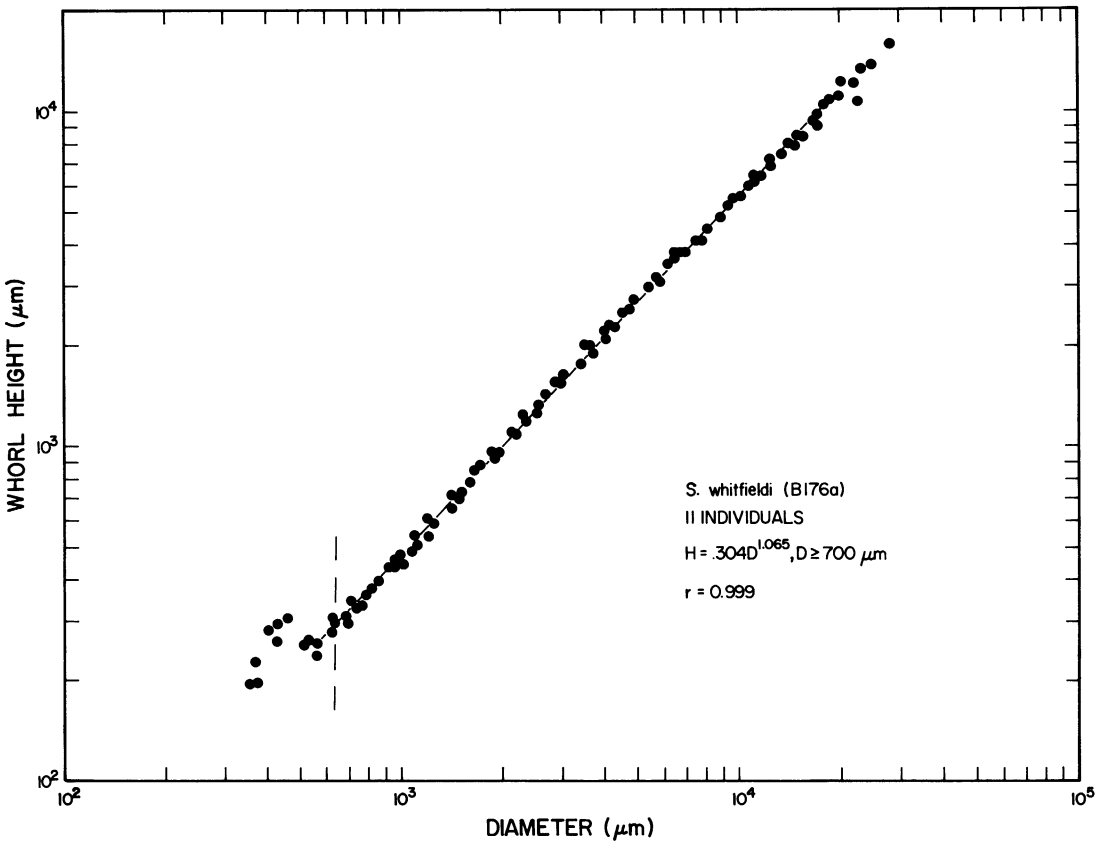

Fig. 39. Plot of whorl height versus shell diameter for 11 specimens of *Scaphites whitfieldi.* The dashed vertical line represents the boundary between embryonic and postembryonic growth.

B228a. The points, plotted on semilog paper, approximate a straight line of slope .1420, which equals the expansion constant of the spiral (k). The intercept represents the distance between the center of the spiral and its start, that is, the point at which $\theta = 0$, the beginning of the postembryonic shell.

The growth patterns for spiral radius versus total rotational angle are very similar among the four species studied (table 19). In four specimens of *S. larvaeformis* from localities B189 and B180 and USGS locality 21792, the slope averages .1391 and ranges from .1310 to .1495. The pattern of growth for each specimen approximately conforms to a straight line; the coefficients of correlation exceed .9753. In four specimens of *S. whitfieldi* from locality B176 and USGS locality 21194 the slope averages .1412 and ranges from .1299 to .1482. The pattern of growth for each specimen approximates a straight line; the coefficients of correlation exceed .9974. In nine specimens of *S. preventricosus,* the slope averages .1441 and ranges from .1373 to .1561. The pattern of growth for each specimen also conforms to a straight line; the correlation coefficients exceed .9592.The average slope for six specimens of *C. vermiformis* from localities B235a and B239a and USGS locality 21425 equals .1426 and ranges from .1349 to .1480. As in the other examples, the pattern of growth for each specimen approximately conforms to a straight line; the coefficients of correlation exceed .9574.

To investigate the ontogenetic change in the constant of spiral expansion, I calculated the expansion constant every quarter whorl in two species to obtain a plot of k versus θ (fig. 49). Changes occur throughout growth and the constant of spiral expansion is itself a function of size or rotational angle. In *S.*

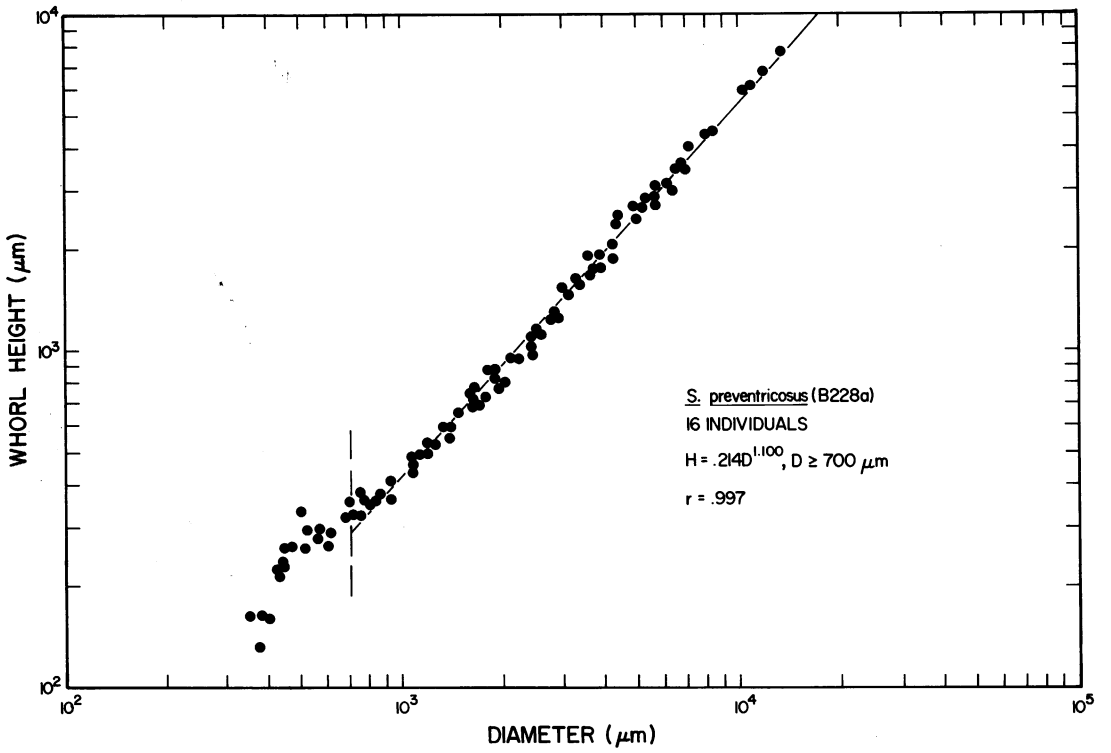

Fig. 40. Plot of whorl height versus shell diameter for 16 specimens of *Scaphites preventricosus*. The dashed vertical line represents the boundary between embryonic and postembryonic growth.

preventricosus, the constant of spiral expansion appears to increase and subsequently decrease. In *C. vermiformis*, the pattern resembles an arch with a peak at approximately two whorls from the constriction (fig. 50). Because the equation of the spiral is $r = ae^{k\theta}$, we may express k as a function of θ. The simplest approach is to fit a straight line through the scatter of points. For example, in *S. preventricosus* the equation of the line of best fit is $k = .00175\theta + .1252$. Substituting this equation into the equation of the spiral yields

$$r = ae^{(.00175\theta + .1252)\theta}$$

or

$$r = ae^{.00175\theta^2 + .1252\theta}$$

At low θ, the linear term predominates and at high θ, the quadratic. The derivative of k with respect to θ may be considered the modification rate of the constant of spiral expan-

TABLE 18
Statistical Tests of the Allometric Slope of the Growth of Whorl Height Versus Shell Diameter

	S. whitfieldi	*S. preventricosus*	*C. vermiformis*
S. larvaeformis	$Z = 7.06$ sig. at 1%	$Z = 1.18$ nonsig.	$Z = .55$ nonsig.
S. whitfieldi		$Z = 3.12$ sig. at 1%	$Z = 3.82$ sig. at 1%
S. preventricosus			$Z = .48$ nonsig.

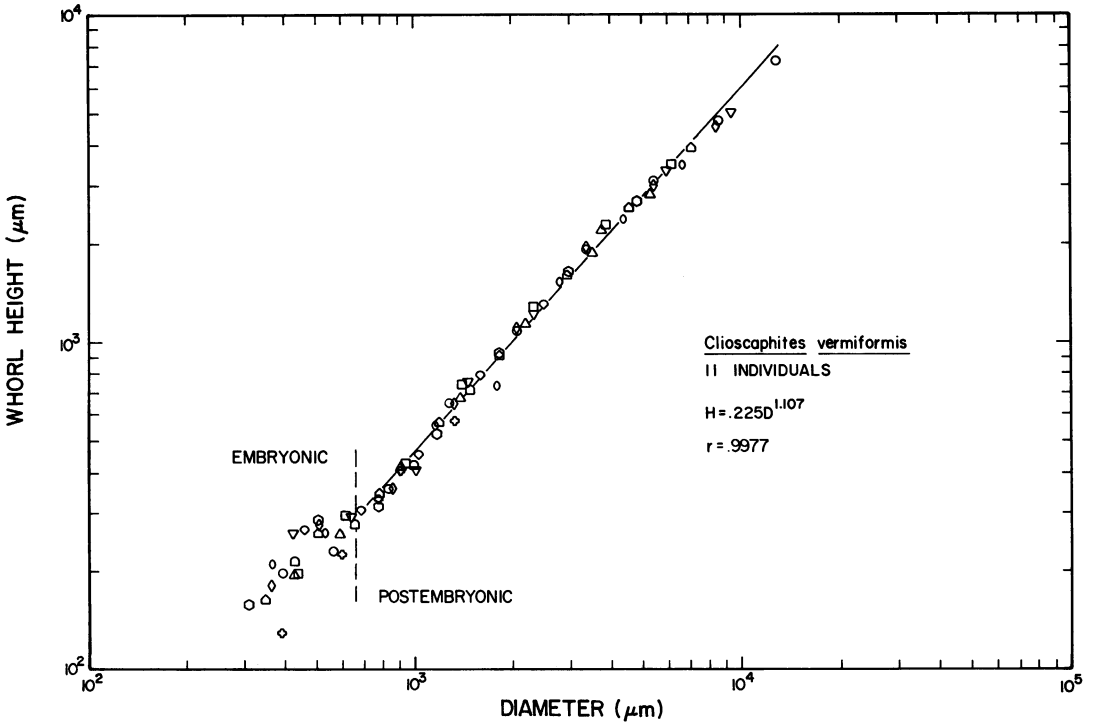

Fig. 41. Plot of whorl height versus shell diameter for 11 specimens of *Clioscaphites vermiformis*. The dashed vertical line represents the boundary between embryonic and postembryonic growth.

sion (McGhee, 1980). The measurements suggest an increase in the constant of spiral expansion after approximately two whorls from the constriction and another approach would be to construct a step function that exhibits a shift at this whorl number.

The ontogenetic change in the constant of spiral expansion may also be analyzed by plotting the natural logarithm of the ratio of consecutive diameters separated by one-half whorl against log diameter. This ratio equals the constant of spiral expansion. If postembryonic growth conformed to a perfect log spiral, this ratio would remain constant at all sizes. The ratio is related to Raup's "whorl expansion rate" and is precisely defined in the following derivation. Let D_1 represent the diameter at some $\theta + \pi$

$$D_1 = ae^{k\theta} + ae^{k(\theta+\pi)} \tag{7}$$

Let D_2 represent the diameter one-half whorl forward

$$D_2 = ae^{k(\theta+\pi)} + ae^{k(\theta+2\pi)} \tag{8}$$

The ratio of D_2 to D_1 is

$$\frac{D_2}{D_1} = \frac{ae^{k\theta+k\pi} + ae^{k\theta+2k\pi}}{ae^{k\theta} + ae^{k\theta+k\pi}} \tag{9}$$

which reduces to

$$\frac{ae^{k\theta}(e^{k\pi} + e^{2k\pi})}{ae^{k\theta}(1 + e^{k\pi})} = \frac{e^{k\pi} + e^{2k\pi}}{1 + e^{k\pi}}$$

$$= e^{k\pi}\left(\frac{1 + e^{k\pi}}{1 + e^{k\pi}}\right) \tag{10}$$

and finally

$$\frac{D_2}{D_1} = e^{k\pi} \tag{11}$$

The natural logarithm of the ratio equals $k\pi$ and dividing by π yields k, the constant of spiral expansion.

The graphs of the four species exhibit considerable scatter but certain patterns emerge. Measurements for 26 specimens of *S. larvaeformis* from localities B189 and B180 and

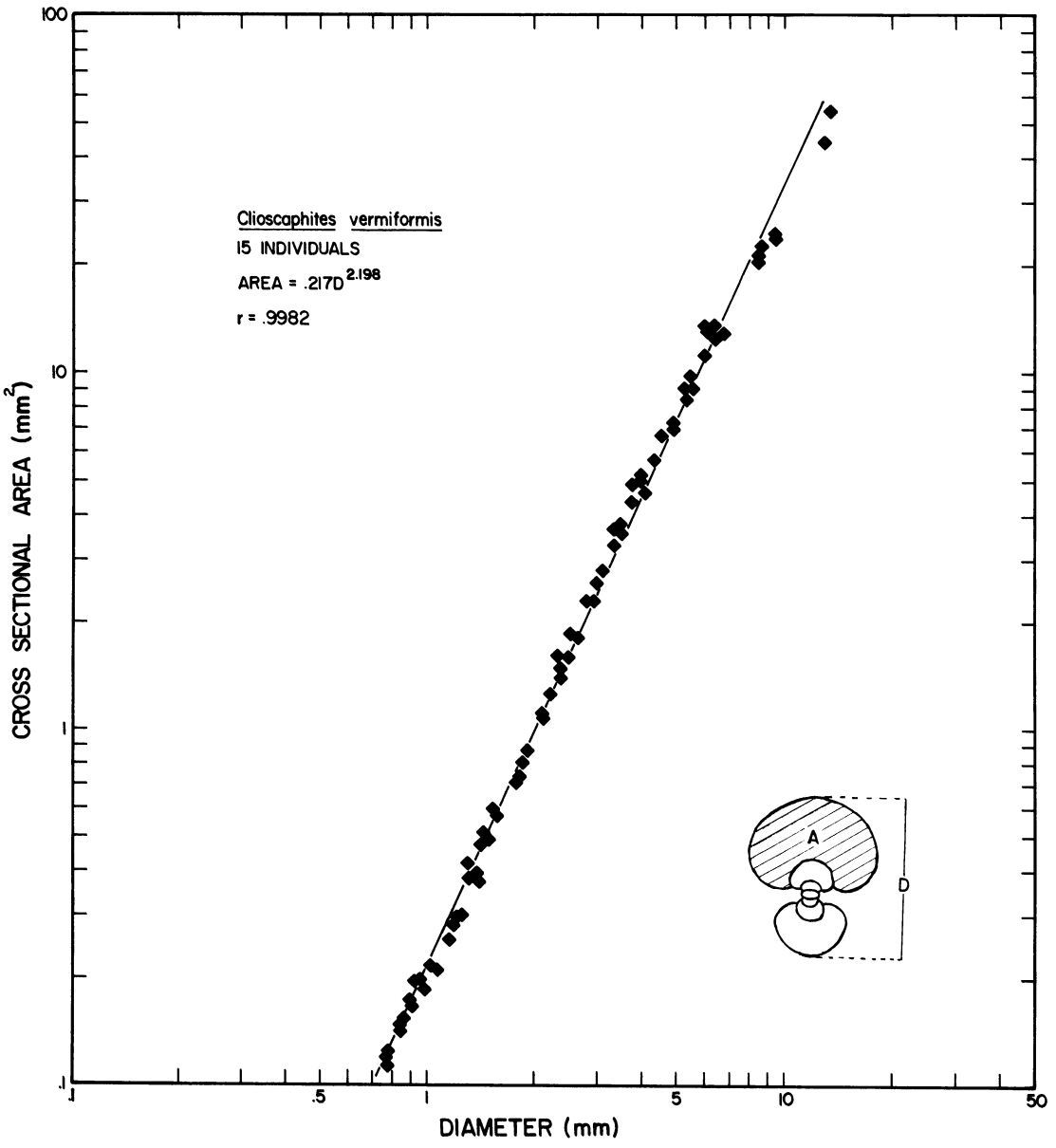

Fig. 42. Plot of whorl cross-sectional area versus shell diameter for 15 specimens of *Clioscaphites vermiformis*.

USGS localities 21792 and D203 describe a gentle arc with a peak at approximately 3 mm in shell diameter (fig. 51). The constant of spiral expansion averages .1401 for post-embryonic growth (compares to a value of .1391 calculated previously). After 3 mm in shell diameter, the constant remains approximately the same or declines slightly. On the other hand, measurements for 20 specimens of *S. whitfieldi* from locality B176a indicate no conspicuous changes except at maturity (fig. 52). The constant increases until approximately 10 mm in shell diameter and then sharply decreases at the onset of maturity. This decrease occurs over the final 0.5–1.5 whorls of the mature phragmocone and appears as a tightening of the spiral. The constant of spiral expansion averages .1408 for

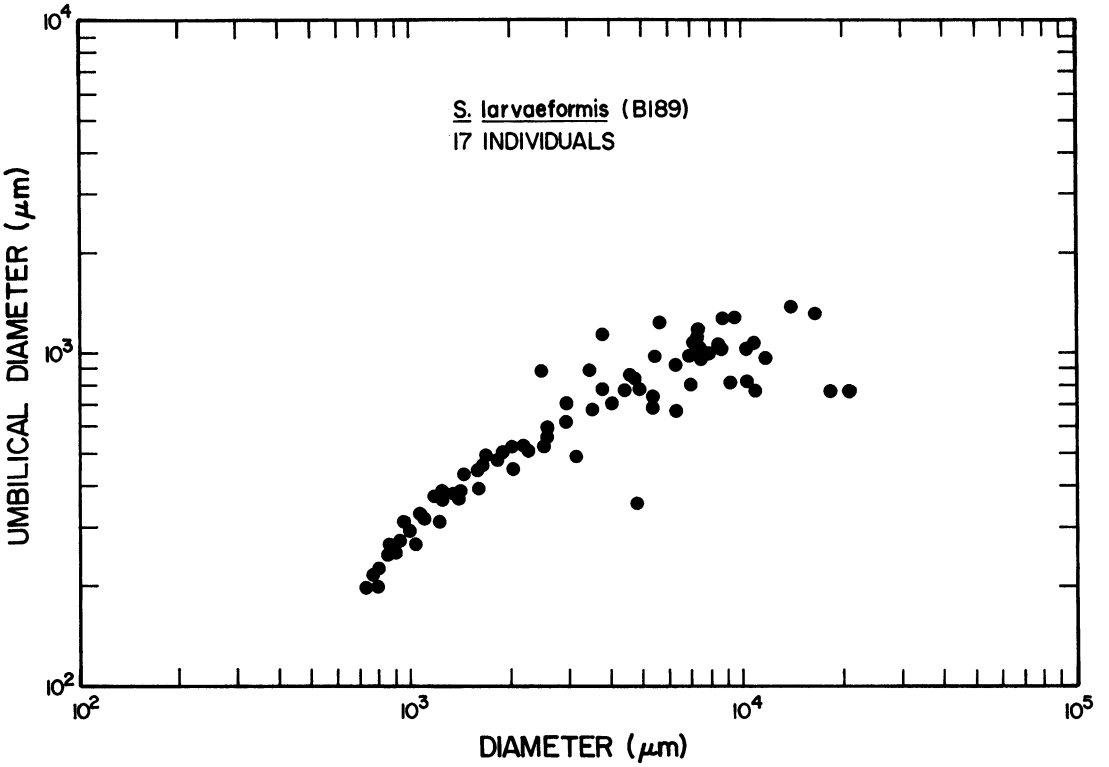

Fig. 43. Plot of umbilical diameter versus shell diameter for 17 specimens of *Scaphites larvaeformis.*

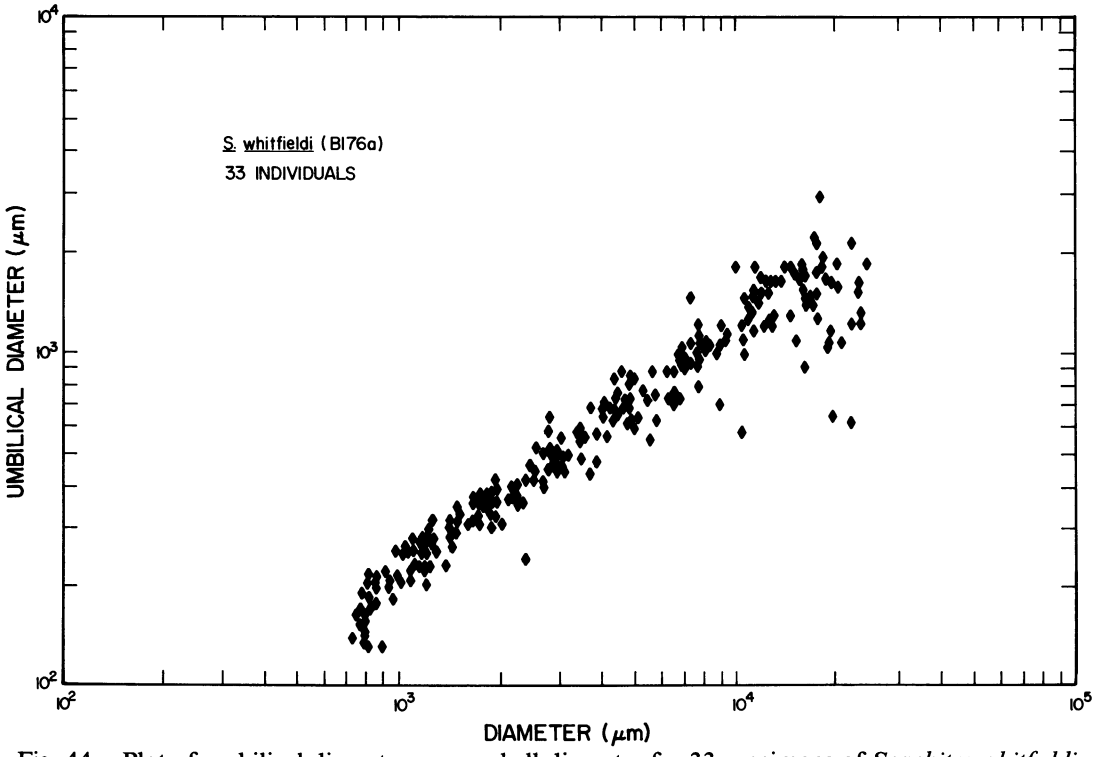

Fig. 44. Plot of umbilical diameter versus shell diameter for 33 specimens of *Scaphites whitfieldi.*

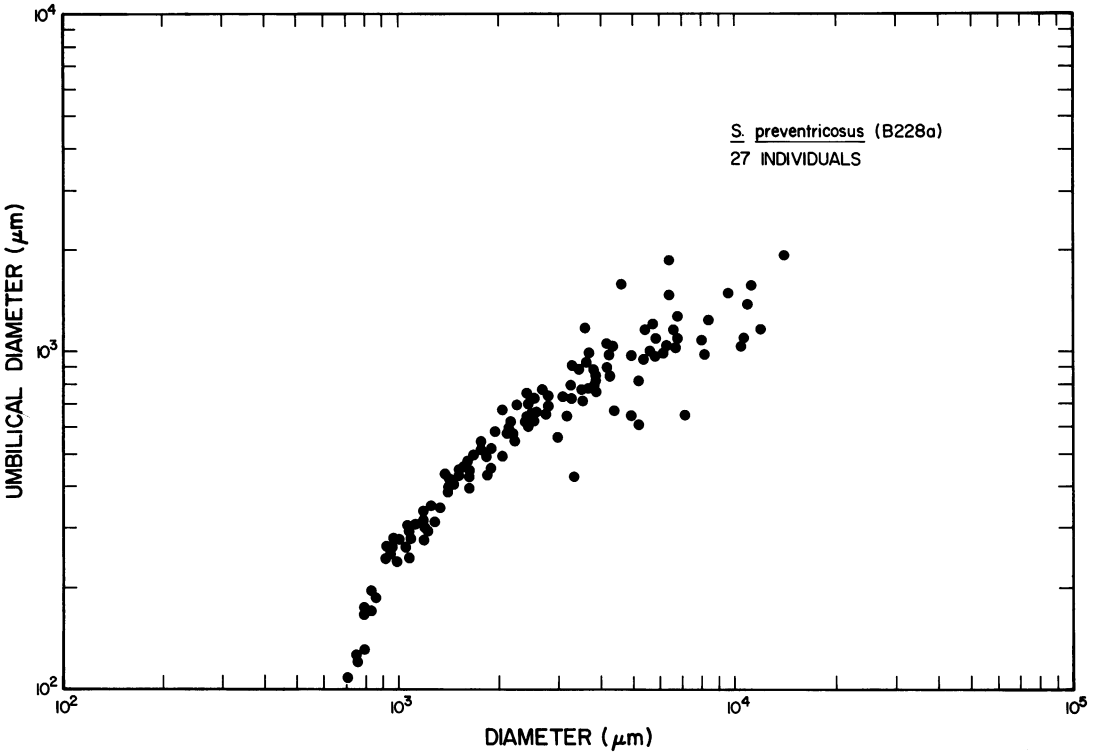

Fig. 45. Plot of umbilical diameter versus shell diameter for 27 specimens of *Scaphites preventricosus*.

postembryonic growth (compares to a value of .1412 calculated previously). Measurements for 27 specimens of *S. preventricosus* from localities B228a and B227b describe a trough with a minimum at approximately 3 mm in shell diameter (fig. 53). After this size the constant increases followed by a decrease for the final 1.5 whorls of the mature phragmocone. Inasmuch as *S. preventricosus* commonly attains a larger size at maturity than *S. whitfieldi,* the increase in *k* prior to maturity persists longer. The constant of spiral expansion averages .1396 for postembryonic growth (compares to .1441 calculated previously). Measurements for 24 specimens of *C. vermiformis* from localities B235a and B239a and USGS localities 21425 and 10888 describe an arch with a peak at approximately 4 mm in shell diameter (fig. 54). The constant of spiral expansion averages .1383 for postembryonic growth (compares to .1418 calculated previously). The pattern in this species differs from that in the other species in two respects. First, the constant of spiral expansion appears to change at approximately 1 mm in shell diameter and second, after a peak at approximately 4 mm in shell diameter, it decreases steadily toward maturity.

In summary, the average value of *k,* the expansion constant of the spiral, is similar among these four species and, in fact, resembles the average value of the expansion constant in *Otoscaphites puerculus* and *Scaphites planus* (Tanabe, 1975, 1977). However, *k* itself is not constant during growth and at least three species exhibit a change at 3–4 mm in shell diameter. After this size, the pattern differs among species. In *C. vermiformis* the expansion constant steadily decreases whereas it initially increases or remains the same in the other three species until the onset of maturity.

The values for the constant of spiral expansion may be used to solve for diameter or total rotational angle when only one variable is given. For example, how many whorls correspond to a diameter of 3.5 mm in *S. preventricosus*? The constant of spiral expan-

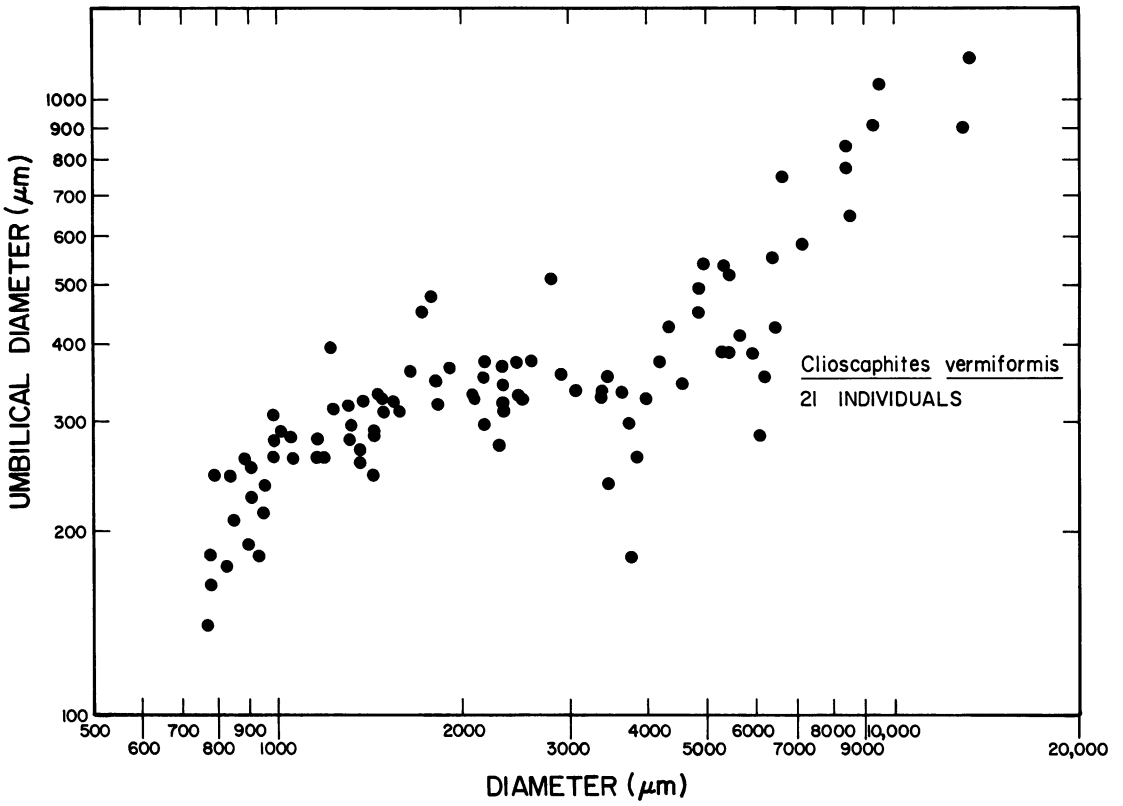

Fig. 46. Plot of umbilical diameter versus shell diameter for 21 specimens of *Clioscaphites vermiformis*.

sion may equal either $.00175\theta^2 + .1252\theta$ or, for simplicity, the average value of .1394. The distance between the center of the spiral and its start, represented by a, equals approximately 60% of the ammonitella diameter. Choosing an ammonitella of 606 μm yields a value of a equal to 362 μm. The equation is:

$$D = 362\ \mu\text{m}\ e^{.1394\theta} + 362e^{.1394(\theta+\pi)} \quad (12)$$

or 3500 μm

$$= 362\ \mu\text{m}\ e^{.1394\theta}(1 + e^{.1394\pi}) \quad (13)$$

Solving for θ,

$$\theta = \frac{1}{.1394} \ln \frac{3500\ \mu\text{m}}{362\ \mu\text{m}\ (1 + e^{.1394\pi})} \quad (14)$$

$\theta = 9.56$ radians or 548°

The angle which corresponds to a diameter of 3.5 mm is $\theta + 180°$, which equals 728° or 2.02 whorls from the primary constriction.

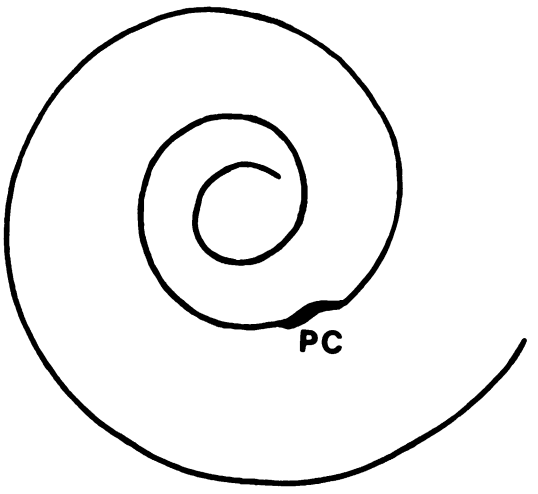

Fig. 47. Diagram of a median section of a specimen of *Clioscaphites vermiformis* showing a marked increase in the growth of the radius of the spiral following the primary constriction (PC).

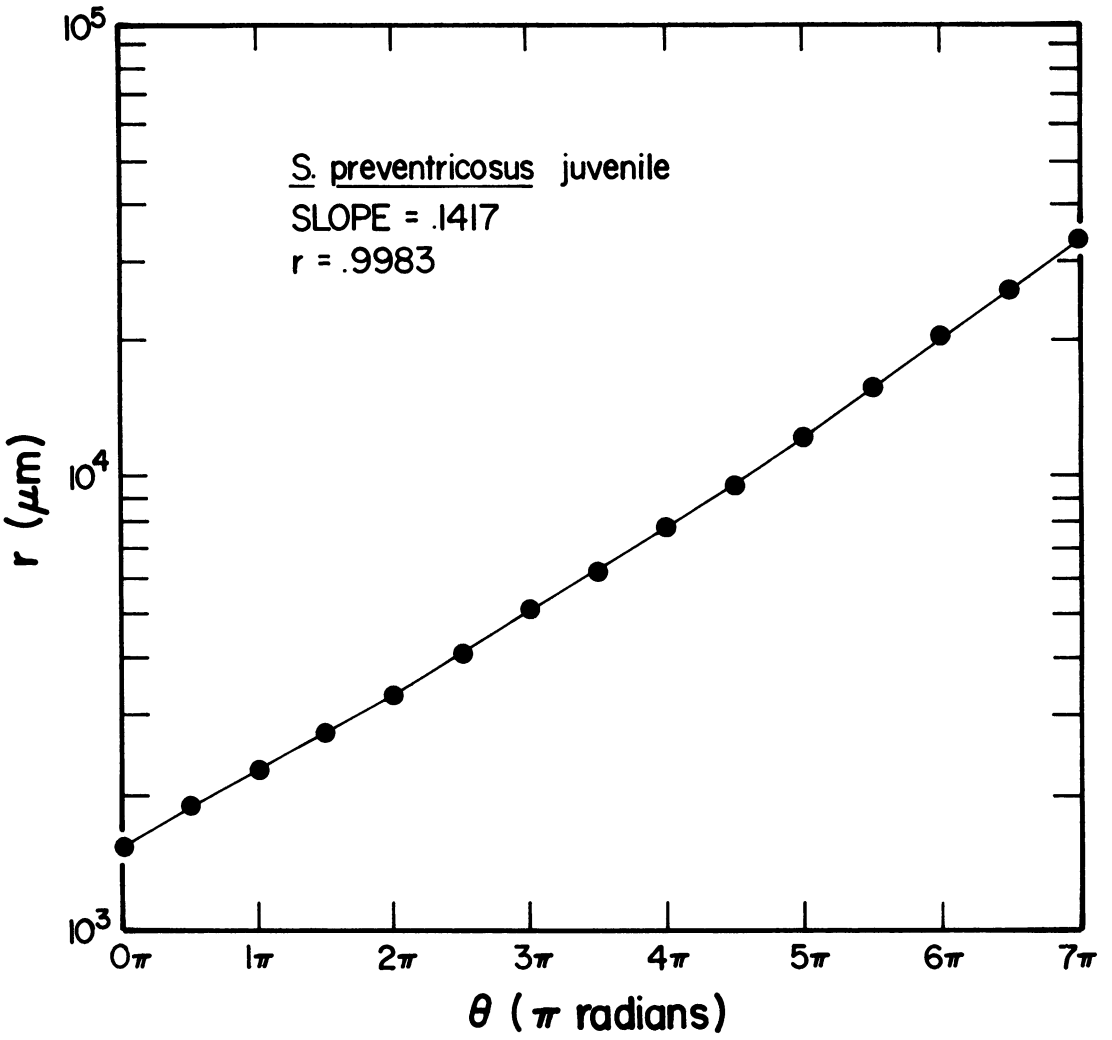

Fig. 48. Plot of the radius of the spiral (r) versus total rotational angle (θ) for a juvenile specimen of *Scaphites preventricosus* from locality B228a. (The values of r plotted are four times the actual measurements.)

Similar solutions may be calculated for the other three species. The value of k is similar among these species and slight differences in ammonitella size may result in a small range of variation in the number of whorls corresponding to a diameter of 3.5 mm.

Ornamentation

Ornamentation was observed on the venter of the shell in median section and initially consists of weak, wavy undulations less than 25 μm in amplitude. These undulations later develop into more pronounced ventral ribs. The first appearance of ornament occurs at approximately two whorls from the primary constriction. Table 20 lists the number of whorls at which ornament first appears for 17 individuals of *S. larvaeformis* from all available localities, 109 individuals of *S. whitfieldi* from locality B176a, 24 individuals of *S. preventricosus* from locality B228a, and 45 individuals of *C. vermiformis* from locality B235a. The number of whorls at the first appearance of ornament is similar for all four species and averages 2.19 whorls with a range

from 1.5 to 2.6 whorls. *S. larvaeformis* exhibits the highest average (2.26 whorls) and the smallest range (2.00–2.56 whorls). This may be due to the fact that *S. larvaeformis* possesses the smallest ammonitella. Because the constant of spiral expansion is similar among all four species, an individual that begins growing at a smaller size will have secreted more whorls to attain the same diameter at which ornament first appears.

Structure of the Outer Wall

Ontogenetic changes occur in the structure of the outer wall. After the formation of the primary varix, where nacre first appears, the shell wall consists of both prismatic and nacreous microstructure. Erben et al. (1969) reported that an inner prismatic layer appears at 2.75 whorls from the proseptum in *Acanthoscaphites nodosus* and *Discoscaphites* cf. *conradi*. This point corresponds to two whorls from the primary constriction (the angular length of the ammonitella equals approximately 0.75 whorls). However, Birkelund and Hansen (1974), in a study of *Discoscaphites* sp., noted that although the inner prismatic layer reaches a thickness greater than that of the outer prismatic layer at two whorls from the primary constriction, it first appears as a very thin layer one whorl earlier. Figure 55 is a magnified cross section of the outer wall of a specimen of *C. vermiformis* approximately three whorls from the primary constriction. The thin outer prismatic and thicker inner prismatic layers sandwich a very thick nacreous layer. Dorsally, the outer prismatic and nacreous layers wedge out and only the inner prismatic layer continues across the venter of the preceding whorl (fig. 55B; Birkelund and Hansen, 1974). Determination of the diameter at which the inner prismatic layer first appears in these Turonian-Santonian scaphites may provide additional support for recognizing a developmental change at approximately two whorls from the constriction.

Angular Length of the Juvenile Body Chamber

Are the changes in the shape of the shell and the development of ornament manifested internally in changes in the spacing of the septa and position of the siphuncle? To answer this question, we must determine the angular length of the juvenile body chamber. This information will permit us to relate an aperture at a particular diameter with the septa that formed at approximately the same time.

Ascertaining the angular length of the juvenile body chamber requires inspection of shells actually preserved at juvenile stages. There is no a priori method of inferring these data by observations of shells preserved at maturity. However, measurement of the angular length of the juvenile body chamber is subject to error because breakage of the body chamber is not always detectable, resulting in an underestimate of the actual value. Figure 56 represents a plot of the measurements of body chamber angle versus phragmocone

TABLE 19

Constants of Spiral Expansion (*k* in *S. larvaeformis, S. whitfieldi, S. preventricosus,* and *C. vermiformis*[a]

Species	Specimen	*k*	*r*
C. vermiformis	1	.1461	.9994
$\bar{k}$ = .1426	2	.1480	.9620
	3	.1460	.9993
	4	.1380	.9574
	5	.1349	.9999
	6	.1426	.9994
S. preventricosus	1	.1387	.9997
$\bar{k}$ = .1441	2	.1520	.9994
	3	.1392	.9592
	4	.1373	.9990
	5	.1561	.9996
	6	.1452	.9991
	7	.1417	.9983
	8	.1428	.9997
	9	.1440	.9946
S. whitfieldi	1	.1299	.9974
$\bar{k}$ = .1412	2	.1482	.9999
	3	.1419	.9985
	4	.1449	.9996
S. larvaeformis	1	.1310	.9753
$\bar{k}$ = .1391	2	.1495	.9998
	3	.1390	.9949
	4	.1370	.9760

[a] The constant of spiral expansion equals the slope of the line of best fit for measurements of the spiral radius versus the rotational angle plotted on semi-log paper. $\bar{k}$ = mean constant; *r* = coefficient of correlation.

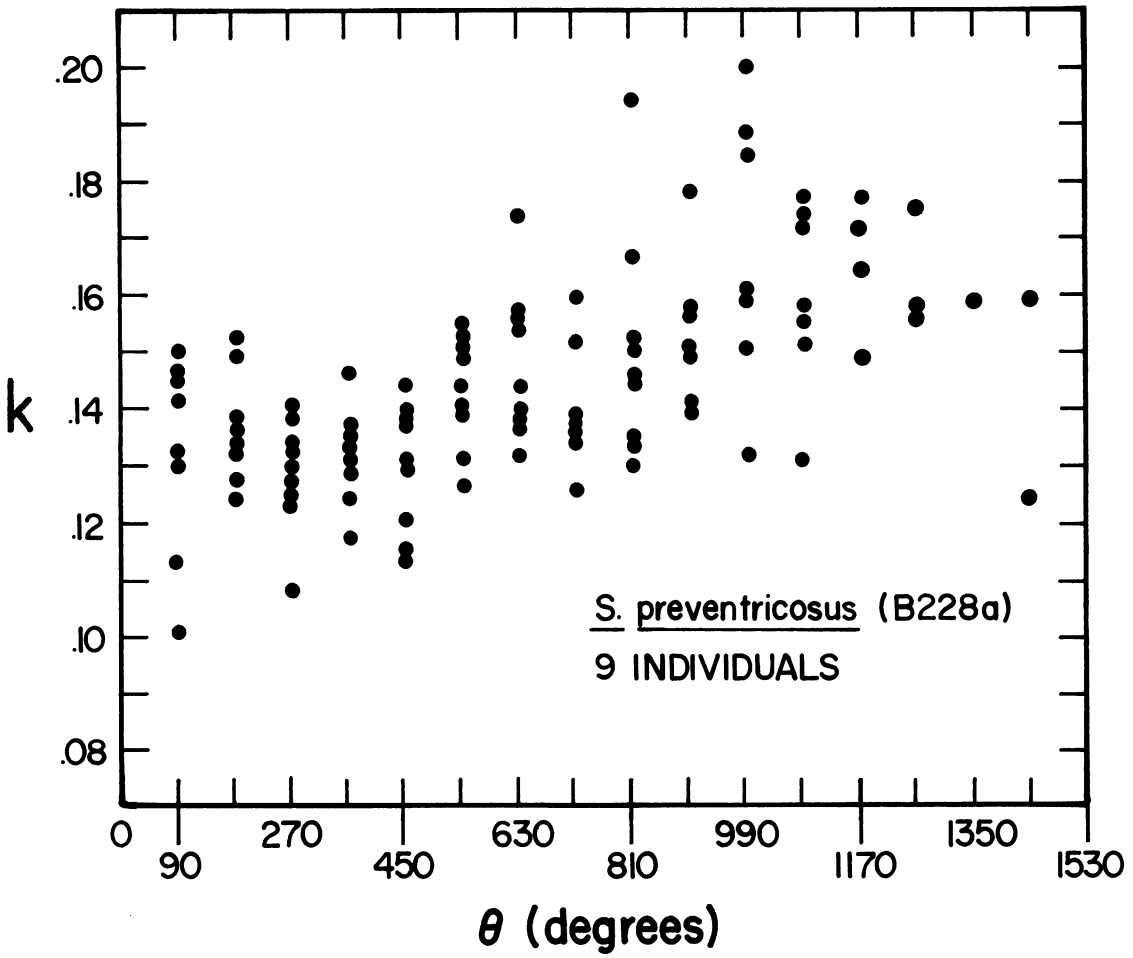

Fig. 49. Plot of the constant of spiral expansion (k) versus total rotational angle (θ) for nine juveniles of *Scaphites preventricosus*.

angle (in degrees) for 40 juveniles of *S. preventricosus* and *C. vermiformis* from localities B228a, B235a, and B239a, and USGS locality 21425. The phragmocone angle is standardized with zero at the primary constriction. In other words, the phragmocone angle is measured relative to the end of the embryonic shell. Calculation of the phragmocone angle from the proseptum requires adding the angle of the ammonitella. The angle of the body chamber exhibits no trend with increasing phragmocone angle but remains approximately the same throughout juvenile growth. The body chamber angle averages 266° and ranges from 235 to 302°; the coefficient of variation equals 7.63. This average is similar to that for the ammonitella angle although it may represent an underestimate of the actual body chamber angle.

Siphuncle

Having determined an average value for the angular length of the juvenile body chamber, we may now discuss internal changes and relate them to the aperture that formed at the same time. Let us first consider the siphuncle. The siphuncle is a posterior process of the body that permits the transfer of cameral liquid to regulate buoyancy and construct new chambers. The siphuncle is preserved in most of the scaphite species studied but its preservation varies widely. For example, in some specimens of *S. whitfieldi* free of matrix, the

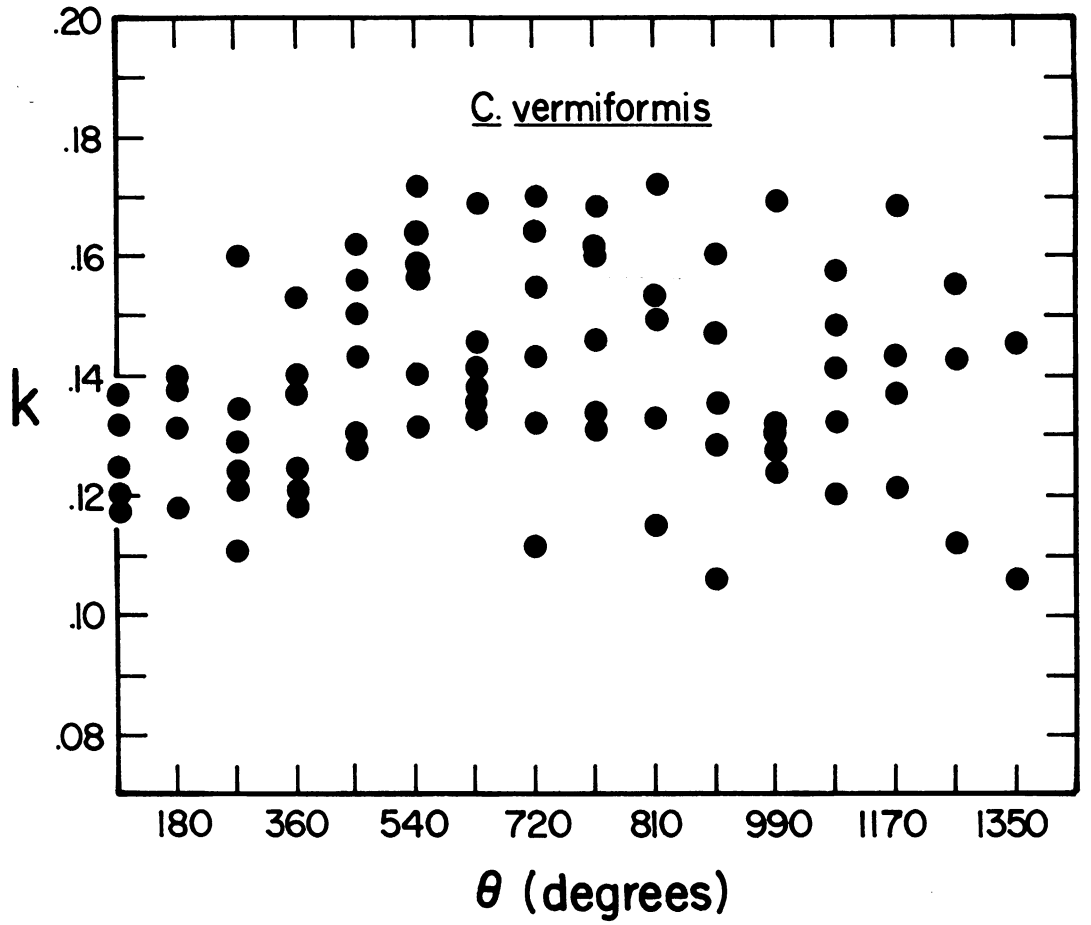

Fig. 50. Plot of the constant of spiral expansion (k) versus total rotational angle (θ) for six specimens of *Clioscaphites vermiformis*.

siphuncle is unaltered, whereas in other specimens it is shrunken (fig. 57). The condition of the siphuncle bears on the calculation of siphuncular strength as defined by Westermann (1971). This calculation relies on actual measurements of wall thickness and diameter and, therefore, requires unaltered siphuncles. The surface of the siphuncle in scaphites is smooth and bears no growth lines as reported on the siphuncles of other ammonites by Grandjean (1910). The scaphite siphuncle also exhibits a homogeneous structure on fractured surfaces (fig. 57). Its structure is similar to that of the siphuncles in *Damesites, Eupachydiscus, Mesopuzosia,* and *Scalarites* as reported by Obata et al. (1980) and interpreted as originally organic.

The growth of the diameter of the siphuncle is illustrated in figure 58. Measurements of siphuncular diameter are plotted versus shell diameter on log-log paper for four specimens of *C. vermiformis* from locality B235a and USGS localities 21425 and 10888. The measurements describe a gently sloping curve with no obvious breaks or critical points. The pattern is increasingly negatively allometric, that is, the siphuncle expands more and more slowly relative to the diameter of the shell. This pattern is similar to that in many other ammonites (Westermann, 1971).

Although the siphuncle eventually attains a ventral position in later ontogeny, initially it may occupy a subcentral position. Determination of the position of the siphuncle is subject to error, however, in specimens sectioned at an angle to or above or below the

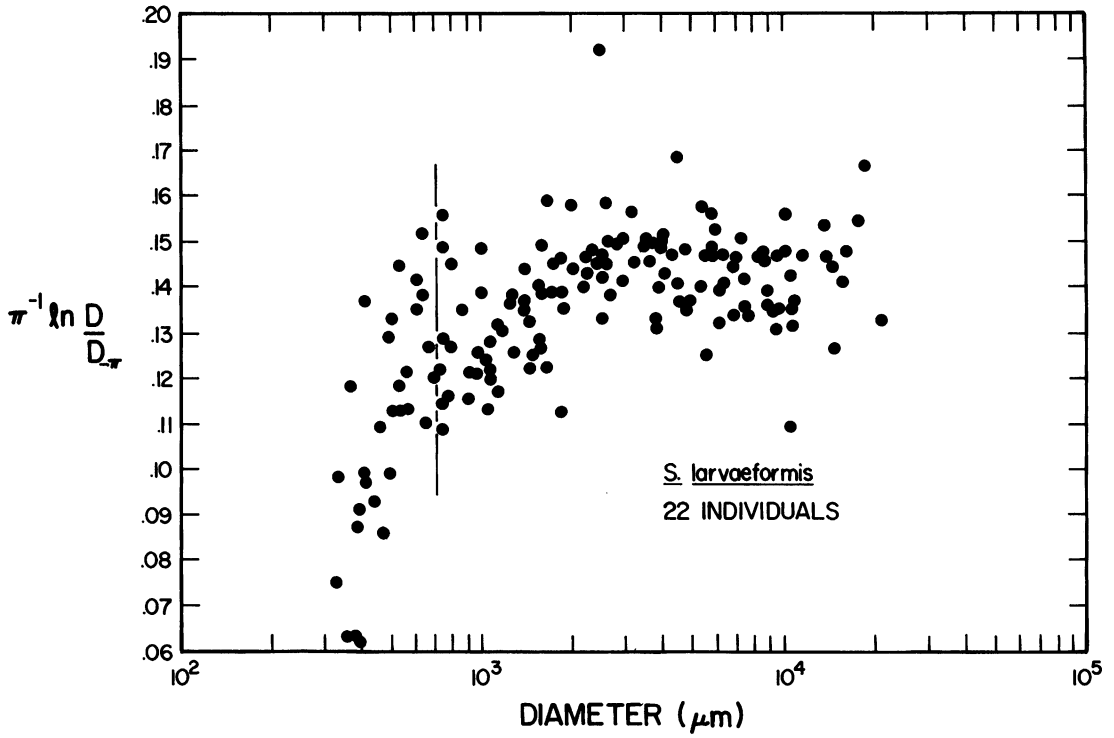

Fig. 51. Plot of $\pi^{-1}\ln(D/D_{-\pi})$ versus shell diameter for 22 specimens of *Scaphites larvaeformis*. The ratio is equivalent to the constant of spiral expansion (k). The vertical line represents the boundary between embryonic and postembryonic growth.

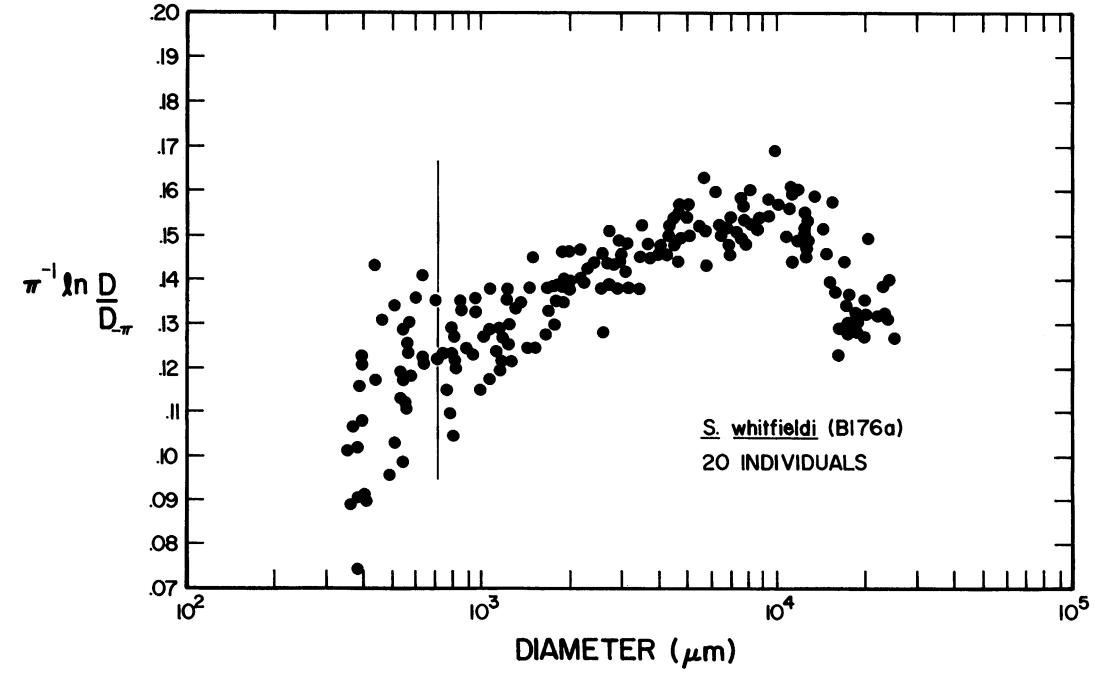

Fig. 52. Plot of $\pi^{-1}\ln(D/D_{-\pi})$ versus shell diameter for 20 specimens of *Scaphites whitfieldi*. The ratio is equivalent to the constant of spiral expansion (k). The vertical line represents the boundary between embryonic and postembryonic growth.

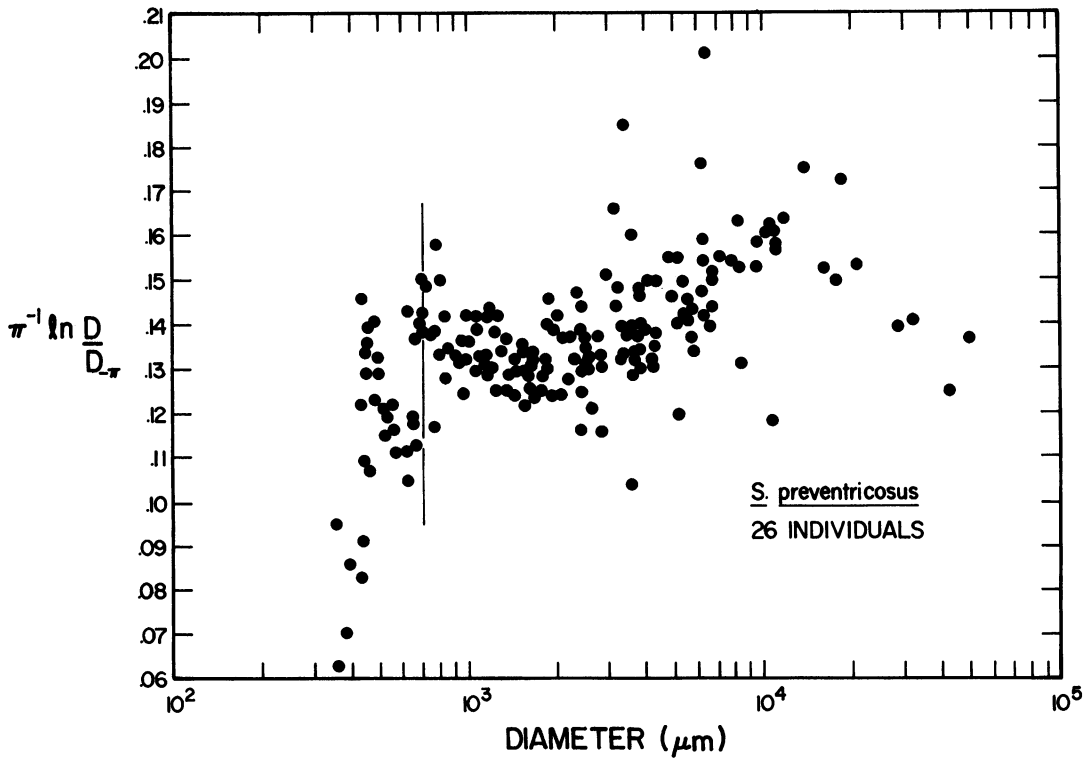

Fig. 53. Plot of $\pi^{-1}\ln(D/D_{-\pi})$ versus shell diameter for 26 specimens of *Scaphites preventricosus*. The ratio is equivalent to the constant of spiral expansion (k). The vertical line represents the boundary between embryonic and postembryonic growth.

median plane and in specimens in which the siphuncle is diagenetically altered. In median sections of five specimens of *C. vermiformis* from localities B235a and B239a and USGS locality 21425 in which the siphuncle appeared unaltered, it gradually migrated from a subcentral to ventral position. The angular length between the primary constriction and the point at which the final ventral position was established averages 498°. It ranges from 456 to 536° and the coefficient of variation equals 5.75. Adding the average angular length of the juvenile body chamber (266°) to the mean value of 498° indicates that this changeover corresponds to an aperture at 2.1 whorls from the primary constriction. Functional interpretations of such a changeover in the position of the siphuncle rely on speculations

TABLE 20
Number of Whorls at the First Appearance of Macro-ornamentation[a]

	N	$\bar{x}$	Range	CV
Scaphites larvaeformis (all available localities)	17	2.26	2.00–2.58	8.12
Scaphites whitfieldi (locality B176a)	109	2.15	1.46–2.58	13.84
Scaphites preventricosus (locality B228a)	24	2.18	1.72–2.62	8.90
Clioscaphites vermiformis (locality B235a)	45	2.16	1.72–2.58	10.19

[a] The number of whorls is measured from the primary constriction.

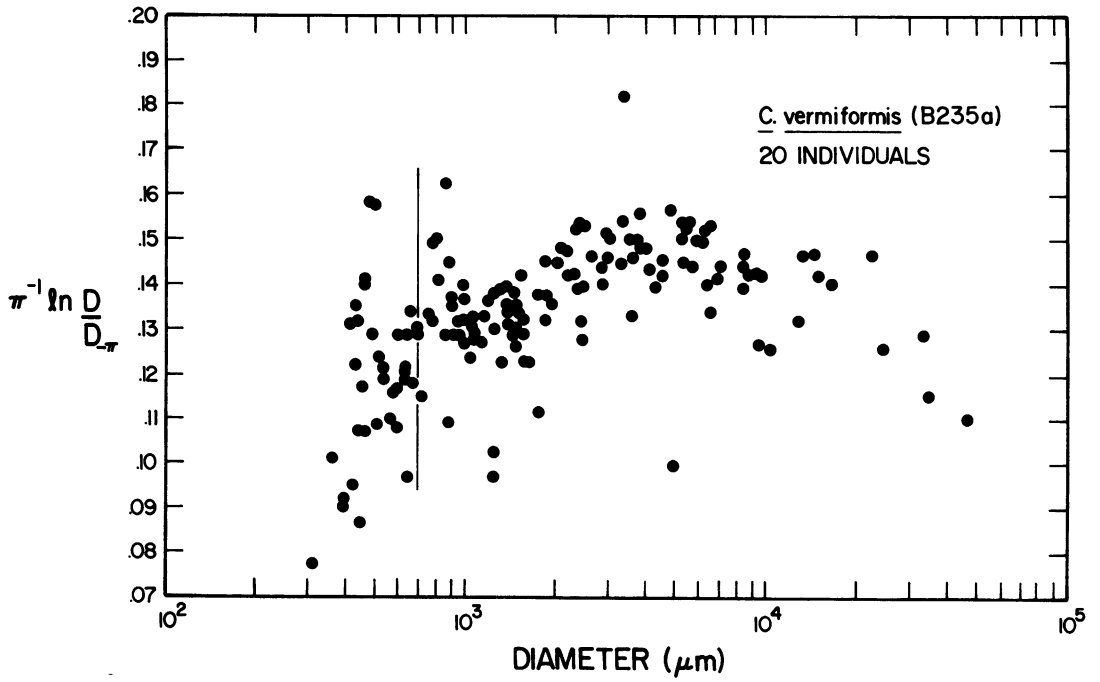

Fig. 54. Plot of $\pi^{-1}\ln(D/D_{-\pi})$ versus shell diameter for 20 specimens of *Clioscaphites vermiformis*. The ratio is equivalent to the constant of spiral expansion (k). The vertical line represents the boundary between embryonic and postembryonic growth.

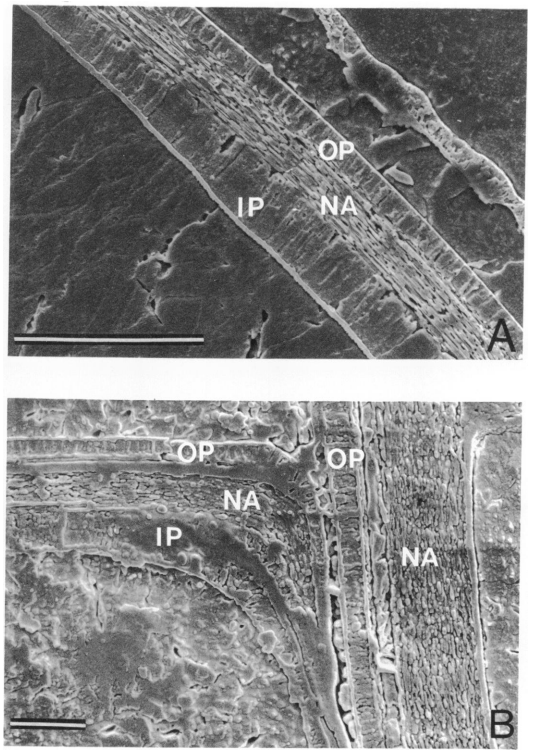

regarding the benefits of liquid decoupling between the siphuncle and cameral fluid (see Ward, 1979).

Septal Spacing

Do any of the changes in the shape of the shell correspond to changes in the spacing of the septa? Figure 59 is a plot of the measurements of septal angle versus septal number for the initial 40 septa of two specimens of *C. vermiformis* from locality B239a and USGS locality 21425. The septal angle is measured on median section with the apex of the angle located at the center of the pro-

←

Fig. 55. **A.** Microstructure of the shell wall approximately three whorls from the primary constriction in a specimen of *Clioscaphites vermiformis* (AMNH 43205). Note the nacreous (NA), outer (OP), and inner (IP) prismatic layers. **B.** Microstructure of the shell wall at the umbilical seam in a specimen of *S. preventricosus* (AMNH 43206). The outer prismatic (OP) and nacreous (NA) layers eventually wedge out.

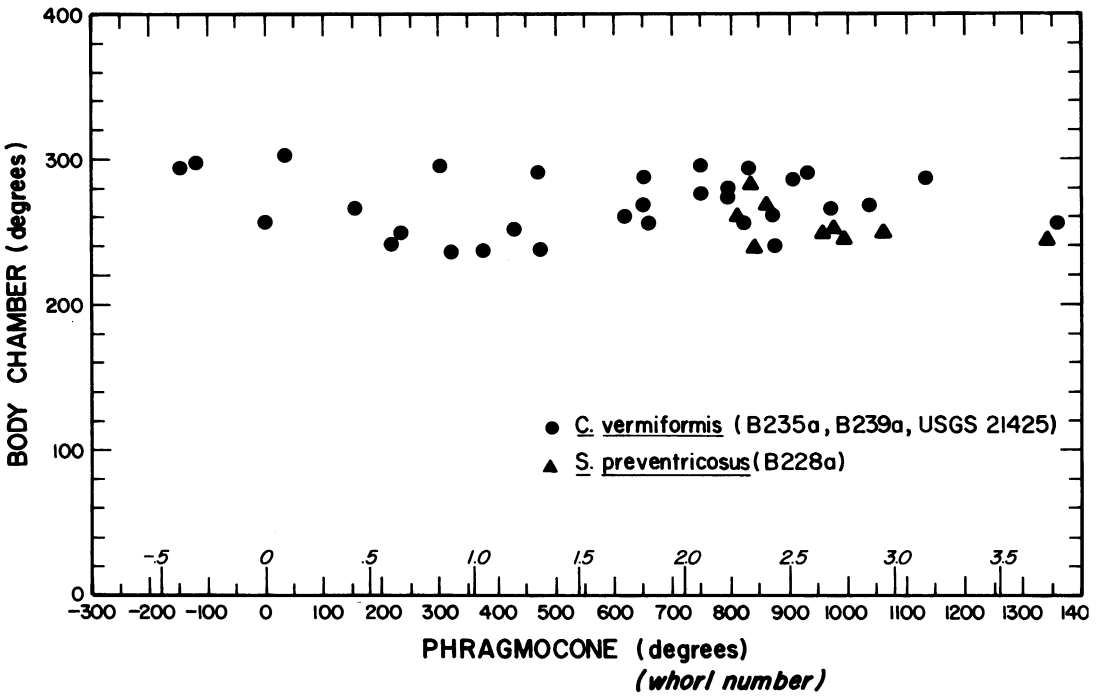

Fig. 56. Plot of body chamber angle versus phragmocone angle for 31 juveniles of *Clioscaphites vermiformis* and 9 juveniles of *Scaphites preventricosus*. The phragmocone angle is standardized starting from zero at the primary constriction.

toconch and its two legs positioned on the ventral edges of the septa. The patterns of septal spacing for the two specimens are similar although one specimen (numbered 1) displays a higher amplitude than the other (numbered 2). After the proseptum, the septal angle increases and attains a peak at approximately the seventh or eighth septum. Subsequently, the angle between septa sharply decreases and reaches a minimum at the 19th septum in one specimen and at the 26th septum in the other. Thereafter, the septal angle more or less increases, culminating in a second maximum in both specimens (septa 37 and 45, respectively). This maximum is in turn followed by a decline in septal spacing. In specimen 1, a third maximum occurs followed by a final decline (not shown on fig. 59). This final decline or "approximation" is associated with maturity.

Let us consider the patterns more closely. In specimen 1, a maximum in septal spacing occurs at septum 7, 208° from the proseptum. Adding the angular length of the juvenile body chamber indicates that this maximum corresponds to an aperture at 474° from the proseptum. Now, a minor change in the shape of the shell occurs at 700–900 μm in diameter corresponding to approximately one-half whorl from the primary constriction, which occurs in this specimen at 292° from the proseptum. Adding one-half whorl to 292° yields an aperture at 472° from the proseptum, a value remarkably close to the value of 474° calculated above. Similarly, in specimen 2 a maximum in septal spacing occurs at the eighth septum, 206° from the proseptum. Adding the angular length of the juvenile body chamber indicates that this maximum corresponds with an aperture at 472° from the proseptum. The minor change in the shape of the shell at one-half whorl from the primary constriction occurs in this specimen at 470° from the proseptum (the ammonitella angle of this specimen equals 290°), a value remarkably close to the value of 472° calculated above. However, in both specimens, these widely spaced septa also coincide with the location of the primary constriction and accompanying varix. The presence of these

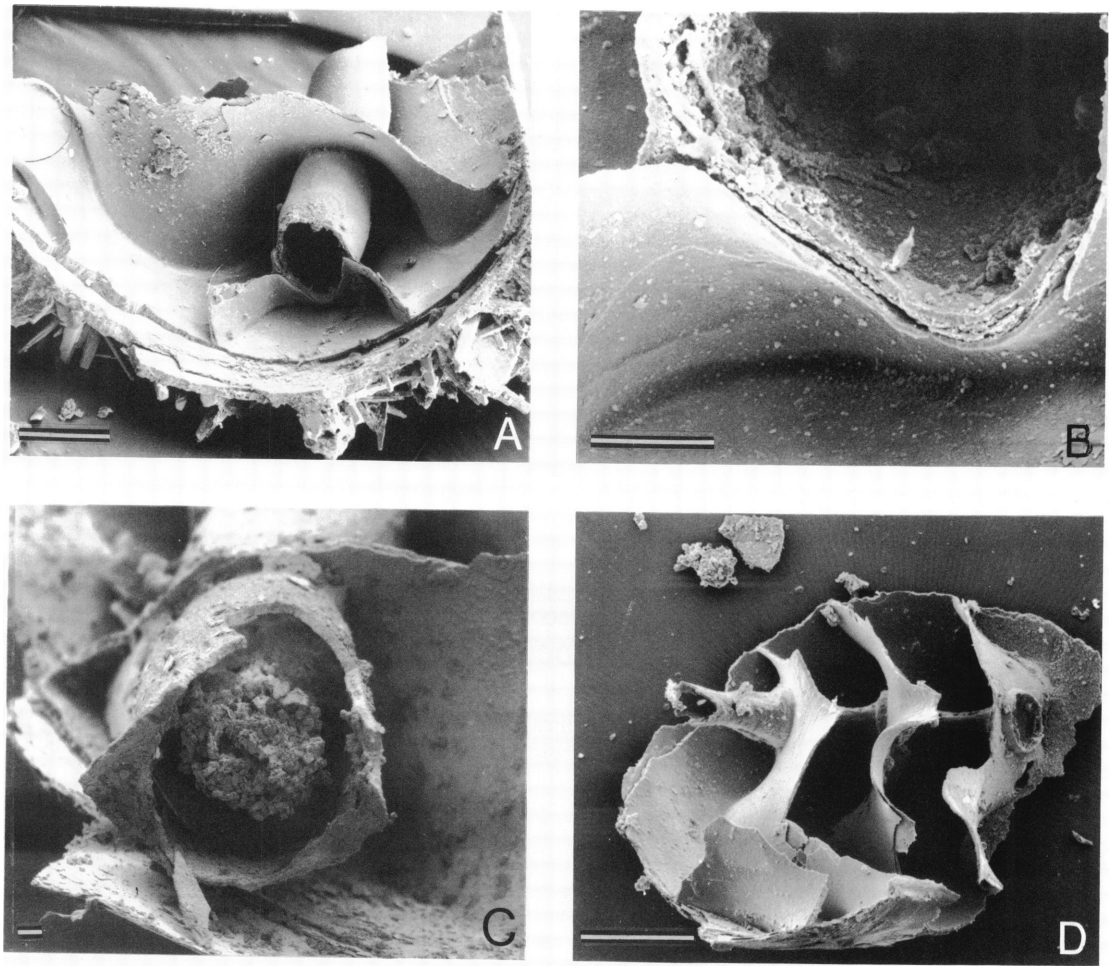

Fig. 57. **A.** Fragments of a well-preserved siphuncle from a specimen of *Scaphites whitfieldi* (AMNH 43207). Scale bar = 100 μm. **B.** Close-up of the same siphuncle. Scale bar = 20 μm. **C.** Fragment of a well-preserved siphuncle from a specimen of *S. whitfieldi* (AMNH 43208). Scale bar = 10 μm. **D.** More poorly preserved siphuncle from a specimen of *S. whitfieldi* (AMNH 43209). Scale bar = 100 μm.

features may also help explain the wider spacing at this point (see below).

The minimum in septal spacing in specimen 1 occurs between septa 16 and 19, that is, between 480 and 522° from the proseptum. The minimum in specimen 2 occurs at septum 26, 602° from the proseptum. Adding the average angular length of the juvenile body chamber to these values yields apertures at approximately 788 and 868° from the proseptum, respectively. A conspicuous change in the shape of the shell occurs at approximately 3–4 mm in diameter, corresponding to approximately 923° from the proseptum in specimen 1 and approximately 917° from the proseptum in specimen 2. In both specimens, these apertures correspond in time of formation with a few septa adoral of the minimum in septal spacing (six septa adoral in specimen 1 and two septa adoral in specimen 2).

In summary, the first peak in septal spacing corresponds in time of formation with a minor change in the shape of the aperture one-half whorl from the primary constriction. It also coincides with the location of the primary varix. The minimum in septal spacing, however, occurs slightly before the formation of a conspicuous change in the shape of the aperture at approximately 3–4 mm in diameter.

The pattern of septal spacing in these two

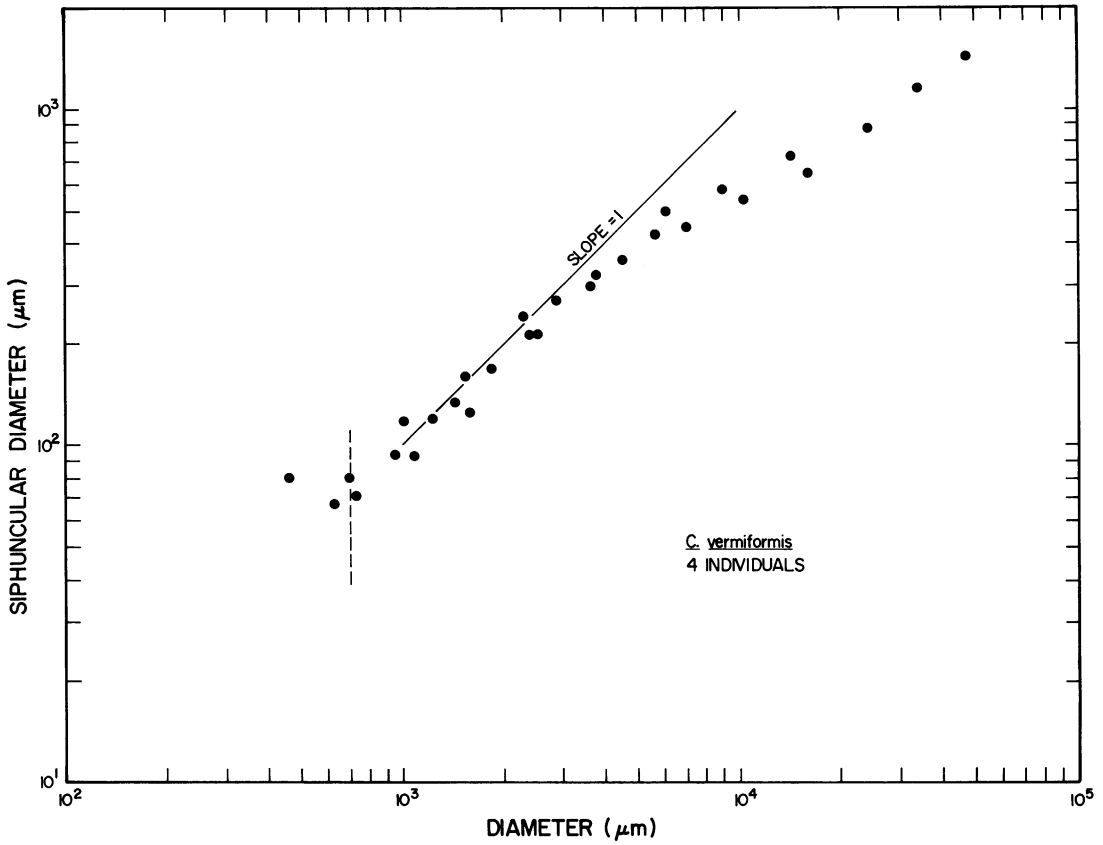

Fig. 58. Plot of siphuncular diameter versus shell diameter for four specimens of *Clioscaphites vermiformis*. The dashed vertical line represents the boundary between embryonic and postembryonic growth. The line with slope equals 1.0 is drawn for reference.

specimens also appears in other specimens of *C. vermiformis, S. preventricosus* and *Baculites* sp. cf. *B. asper, B. codyensis* measured on their coiled whorls. The pattern always consists of a steep increase for the initial approximately ten septa followed by an equally steep or gradual decrease reaching a minimum approximately 1.5 whorls from the proseptum. This may be followed in turn by a gentle uniform increase, an increase marked by steep fluctuations, or a random pattern with many small oscillations and only a slightly increasing slope. These patterns are also remarkably similar to those in Jurassic *Leioceras opalinum* (Bayer, 1972) and *Quenstedtoceras* sp. (Kulicki, 1974: 215–216). Kulicki (1974) constructed graphs of septal spacing in *Quenstedtoceras* and noted "depressions" of narrowly spaced septa, and "elevations" of widely spaced septa. He wrote:

> In all . . . a fairly steep elevation, terminating with the second depression and occurring at the beginning of the second whorl [that is, after a little more than one whorl has been completed and going into the second whorl] is situated behind the first depression [located at the proseptum]. A sector of diagram with a fairly varied trace in particular specimens is situated behind the second depression. This sector is marked by considerable amplitudes of fluctuations. Several smaller depressions and elevations, occurring on this sector, are variously situated in various specimens.

Periodicity of Septal Secretion and Spacing

The period of septal secretion in ammonites and other externally shelled cephalopods has generally been considered a constant governed by an astronomical rhythm.

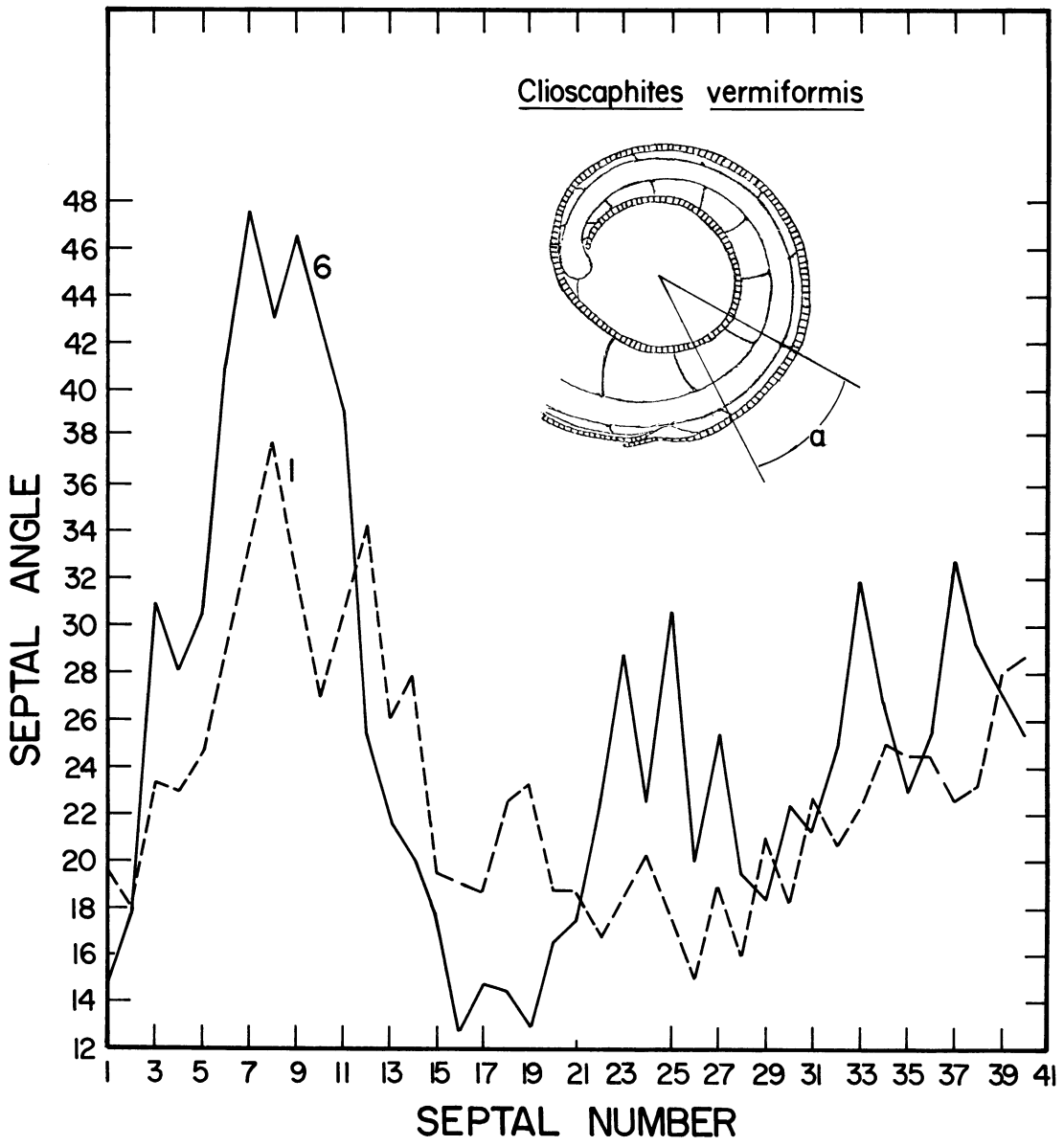

Fig. 59. Plot of septal angle versus septal number for two specimens of *Clioscaphites vermiformis*. The septal approximation at maturity is not shown.

Using this assumption, Stahl and Jordan (1969) analyzed the oxygen isotopic composition of consecutive septa in two Jurassic ammonites. The isotopic ratios yielded a sinusoidal pattern. Assuming septal secretion at equal intervals of time, this pattern was interpreted as a reflection of seasonality although it may also represent migrational behavior. I performed a similar analysis on the outermost seven septa of an adult specimen of *S. preventricosus* from locality B230 (fig. 60). However, if the underlying assumption is incorrect, that is, if septa are not secreted at equal time intervals, then even in a strongly seasonal environment, the isotopic composition of the septa may not faithfully reproduce a seasonal pattern. Clearly, starting out with one septum in the spring, if the next

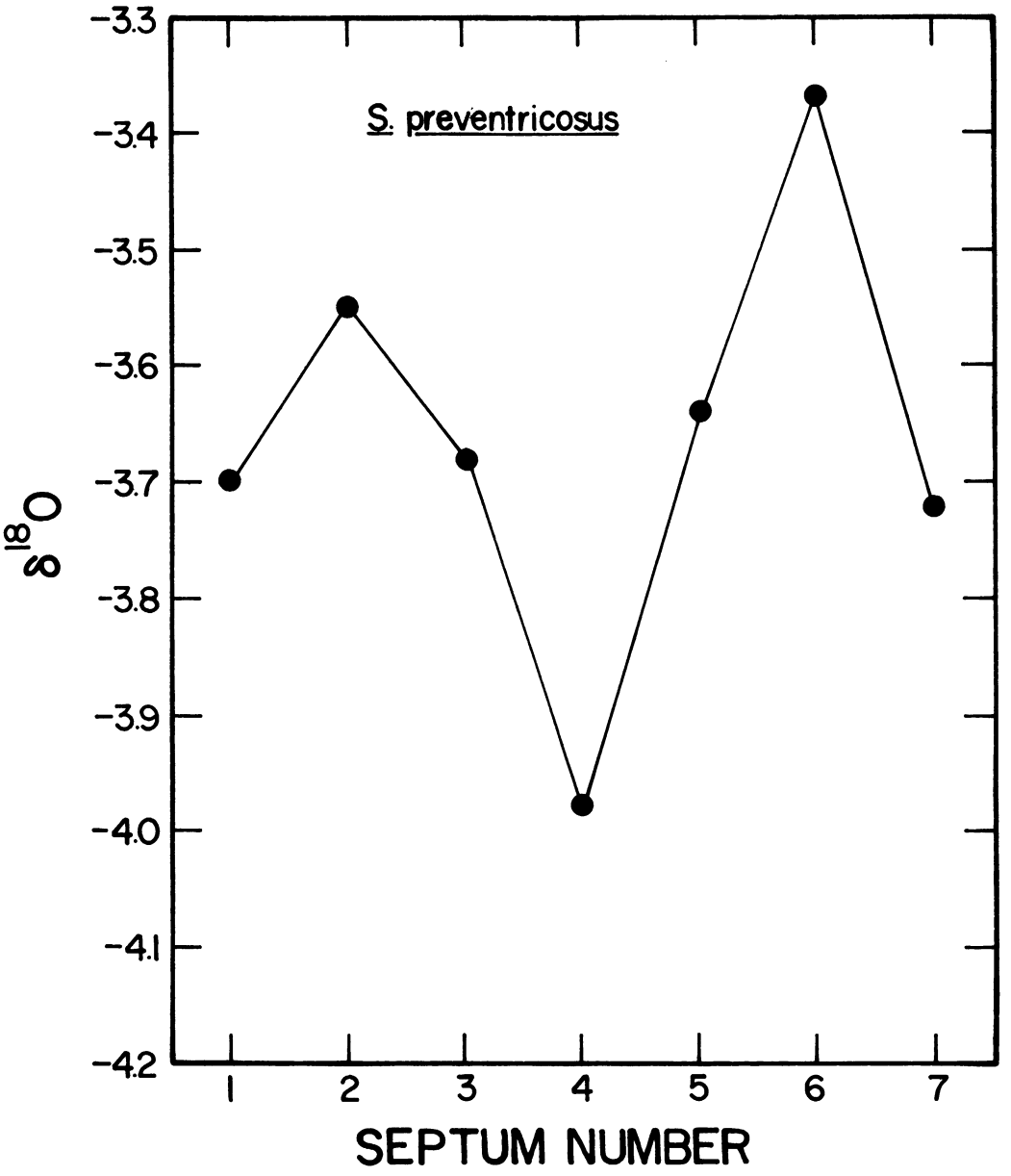

Fig. 60. Plot of $\delta^{18}O$ for the last few septa of an adult specimen of *S. preventricosus*. Septum 1 represents the final septum.

septum is secreted one month later, but the following septum three months later, any seasonal signal will be distorted.

The period of septal secretion may be studied directly in the sole surviving externally shelled cephalopod, *Nautilus*. In *Nautilus*, Denton and Gilpin-Brown (1966) and Kahn and Pompea (1978) inferred a constant time interval between septal secretion of 14 and 30 days, respectively. However, recent studies have indicated that the period of septal secretion, or chamber formation, in *Nautilus* is not constant but uniformly increases through ontogeny. This pattern was predicted on the basis of the ontogenetic decrease in the ratio of the surface area of the siphuncle

to chamber volume (Chamberlain, 1978). The period of chamber formation in specimens of *N. pompilius* in aquaria increased from a minimum of 14 to a maximum of 132 days through ontogeny (Ward and Chamberlain, 1983; Ward, 1985). Specimens of *N. macromphalus* in aquaria exhibited a similar increase from 49 to 98 days (Ward, 1985). This ontogenetic increase in the period of chamber formation appeared exponential although the period of formation for any particular chamber varied widely among individuals. Periods in nature are longer but still indicate an ontogenetic increase. In immature specimens of *N. pompilius* in nature, periods of septal formation averaged 60–90 days (Cochran et al., 1981; Landman and Cochran, 1987). Immature specimens of *N. belauensis* in nature exhibited longer periods—from 120 to 230 days, approaching a year at maturity (Saunders, 1983; Cochran and Landman, 1984).

Apparently, the period of septal secretion in *Nautilus* is not constrained by an imposed, external source such as the moon but depends instead on internal buoyancy requirements and the rate of apertural growth. As *Nautilus* adds shell at the aperture, it initiates the formation of a new chamber to maintain neutral buoyancy. This process may be effected by a complex feedback system between levels of cameral liquid and the growth of the shell at the aperture (Ward et al., 1980). At the same developmental stage within a species, variation in the rate of apertural growth may produce concomitant variation in the period of septal secretion but, in general, the period of septal secretion increases over ontogeny. The buoyancy system in scaphites and other ammonites may have been comparable to that in *Nautilus*. The ratio of the surface area of the siphuncle to chamber volume also decreases over ontogeny and, therefore, ammonites may have exhibited a similar ontogenetic increase in their period of chamber formation, independent of any astronomical rhythm (Chamberlain, 1978; Landman, 1983; Ward, 1985).

On the other hand, the patterns of septal spacing in *Nautilus* and ammonites differ markedly. In *Nautilus,* the septa tend to be equally spaced, at an average angular distance of approximately 25°. However, reductions in septal spacing coincide with hatching and maturity, and also appear immediately after shell breaks. In scaphites and other ammonites, septal spacing tends to be nonuniform and is marked by oscillations of varying amplitude although reductions in septal spacing may also coincide with hatching and maturity.

Variation in septal spacing may *directly* reflect variation in the rate of apertural growth associated with developmental or environmental changes. However, as stated, septa do not demarcate equal time intervals unlike, for example, daily growth lines. A reduction in septal spacing may, indeed, reflect a deceleration of growth at the aperture but the time interval between adjacent septa may, in fact, represent a longer period than usual. For example, traumatic breakage of the shell margin and the interruption of the normal cycle of septal formation may produce septal approximation. In an aquarium study Ward (1985) observed that a specimen of *Nautilus pompilius* that was severely broken at its edge delayed septal formation until after the apertural margin was repaired; the newly formed septum was approximated. Thus, the time interval between the secretion of adjacent septa was longer than usual. Reductions in septal spacing due to apertural breakage also appear in animals captured in the wild. The reduced chamber occurs at an angular distance of one body chamber's length from the position of the former injured and repaired apertural lip (Ward, 1985).

Variation in septal spacing may also represent an *indirect* response to the morphometric modifications coincident with developmental or environmental changes. Several parameters of the shell affect septal spacing including the thickness of the shell wall, the whorl shape, and the volume of occluded liquid (Westermann, 1973). Changes in these parameters accompanying a change in the mode of life may therefore affect the position of newly formed septa. Thus, the commonly observed septal approximation at maturity in *Nautilus,* scaphites, and many other ammonites, may reflect both a decline in the rate of apertural growth as well as modifications in the thickness of the shell wall and overall density coincident with maturation (see Westermann, 1973).

Septal spacing may also be affected by the

configuration of the whorl in which the septa are being secreted. For example, if a constriction occurs in the whorl, the chamber that forms there will be longer than previous ones to accommodate the same proportional increase in volume (Bayer, 1977a, 1977b). In other words, the newly formed septum will be more widely spaced. An example is at the primary constriction where the accompanying varix creates a constriction in the whorl shape. The septa formed at this point are commonly more widely spaced as, for example, in the two specimens plotted in figure 59.

In addition to the differences in the pattern of septal spacing between *Nautilus* and ammonites, the number of septa also differs markedly. This may be due to contrasts in septal thickness and the expansion rate of the spiral (Westermann, 1971). It may also be due to differences in the size and morphology of the embryonic shell. In ammonites, the small protoconch of the ammonitella provides an amount of bouyancy commensurate with its size and, thereafter, newly formed chambers provide buoyancy sufficient to support limited growth at the aperture.

Interpretation of Morphometric Changes

The patterns of growth in these Turonian-Santonian scaphites exhibit departures from a simple linear trend. Such departures may indicate changes in development or mode of life. In general, three kinds of departures from linearity may occur. These consist of curvilinear trends, polyphasic patterns, and rhythmic fluctuations (Reeve and Huxley, 1945; Gould, 1966). In polyphasic growth, consecutive departures from a linear trend are modeled by fitting a number of lines representing simple allometry. The inflexion points between these lines are called critical points or "Knickpunkte."

In the ontogenetic study of ammonites, polyphasic growth has been widely recognized. Kullmann and Scheuch (1972) and Kant and Kullmann (1973) identified polyphasic growth and critical points in their measurements of whorl width and whorl height for several Paleozoic ammonoids. These points were interpreted as representing the changeover points from one growth program to another. The angle between adjoining lines was interpreted as a measure of the magnitude of the changeover. These patterns were not considered curvilinear because the "allometric constant [that is, the slope] remains approximately constant over a long period of growth." In Cretaceous ammonites, Obata (1959) identified polyphasic growth in his measurements of whorl width versus diameter in *Desmoceras* sp. These phases were interpreted as representing distinctive growth stages. Later, Obata (1965) documented the patterns of growth of the spiral radius, whorl height, and whorl width in *Reesidites minimus.* He wrote, "when we carefully examine the data, we find that the change of growth ratio [that is, the slope] occurs at a few critical points in the course of growth." These "changes in the specific growth constants [that is, slopes] are a necessary consequence of . . . allometric growth." More recently, Obata et al. (1979) discriminated a number of growth phases in three specimens of *Subprionocyclus neptuni* on the basis of their measurements of the growth of the spiral radius versus the rotational angle. In an ontogenetic study of *Gaudryceras tenuiliratum,* Hirano (1975) documented the growth of the spiral radius and recognized several critical points. Similarly, Tanabe (1975, 1977) identified several "growth phases" in the ontogeny of *Otoscaphites puerculus* and *Scaphites planus* from Japan.

Departures from a linear pattern of growth require careful analysis to establish their validity. They may be due to experimental artifacts introduced by poorly prepared sections. They may also be statistically invalid. Gould (1966, personal commun. *in* Hayami and Matsukuma, 1970) has claimed that the interpretation of polyphasic growth is often based on too few points. "The so-called polyphasic allometry and critical point(s) are usually nothing but pure artifacts of an improper procedure." For example, after identifying a number of critical points, Hirano (1975) determined their "propriety" by performing a Student's *t*-test "on the growth ratios between the growth stage preceding the critical point and that succeeding . . . [it] in each sample." The size of the samples ranged from

1 to 14 specimens. However, this method may not be statistically valid if the chosen critical points are not conspicuous (Hartigan, 1982, personal commun.). In such instances, the results of these tests must first be compared to the outcomes of similar tests performed on all other sequential groupings of data, that is, between all "conceivable inflexion points" before the chosen critical points are interpreted as statistically significant.

In general, deviations from linearity are more likely to represent artifacts if they are slight, occur in only a few specimens, involve only one parameter, and only appear at very small diameters where measurements are more subject to distortion from poorly prepared sections. On the other hand, departures that are conspicuous and involve a number of parameters are more likely to be real.

In evaluating the morphometric changes in the Turonian to Santonian scaphites from the Western Interior, I have tried to reduce the number of experimental artifacts. For example, I measured the growth of the spiral radius versus the total rotational angle on median sections in which the center of the spiral had been carefully located. The first departure from linearity occurs in most species at approximately 700 μm in diameter. It appears in the plots of the measurements of whorl width versus diameter as an abrupt shift in the slope of the line of best fit. This shift is real and corresponds with a marked change from embryonic to postembryonic growth at the end of the primary constriction. However, the change in shape at approximately one-half whorl later, corresponding to 900 μm in diameter, may be an artifact. It is inconspicuous on most plots of the measurements of whorl height, whorl width, and umbilical diameter versus shell diameter although internally it corresponds to a maximum in septal spacing.

In contrast, the morphological changes at 3–4 mm in diameter appear in most species and are probably real. They occur at a sufficiently large diameter to preclude artifacts due to the mislocation of the center of the spiral. For example, the plot of the measurements of whorl height versus shell diameter in *S. larvaeformis* suggests a sinusoidal pattern with respect to the line of best fit (fig. 38). Between diameters of 0.7 and 3 mm, most points plot below the line and after 3 mm, most points plot above the line. Similarly, the plot of the measurements of whorl width versus shell diameter in *S. larvaeformis* also suggests a sinusoidal pattern (fig. 35). In fact, if the points were to be split at approximately 2.7 mm and two regression lines calculated, the slope of the line for diameters between 0.7 and 2.7 mm would be 1.0861, still positive allometry but closer to 1, with a correlation coefficient of .9880. The slope of the line for diameters greater than 2.7 mm would be .9980 with a correlation coefficient of .9898, a case of statistically significant isometry. This is an example of how a deviation, probably a real one, if neglected, can bias the overall pattern to indicate positive allometry in a log spiral form when at least part of the growth is isometric. Other species exhibit similar patterns in their measurements of whorl height and whorl width versus shell diameter. At diameters less than 3 mm, many points fall below the line of best fit and at diameters above 3 mm, many points lie above the line.

These morphological changes at 3–4 mm in diameter coincide with changes in other parameters. Measurements of umbilical diameter versus shell diameter exhibit increased scatter after approximately two whorls from the primary constriction in at least three species. Measurements of the growth of the spiral radius versus the total rotational angle also indicate changes in the constant of spiral expansion at this whorl number in at least three species. Simultaneously, macro-ornamentation gradually begins to develop. Internally, these morphological changes correspond with a broad minimum in septal spacing and the attainment of a stable, ventral position of the siphuncle. In the closely related species *Otoscaphites puerculus,* Tanabe (1975, 1977) also reported simultaneous changes in septal thickness and siphuncular diameter. These internal changes may be a direct response to metabolic and growth rate changes or may represent indirect responses to modifications occurring at the aperture.

The changes in shape at two whorls from the constriction are not abrupt, however, but gradual as, for example, in the onset of or-

namentation and the ventral migration of the siphuncle. How are these changes in shape interpreted? Because these changes appear in individuals of at least three species from a variety of localities I prefer to interpret them as indicating a change in the mode of life or development of the animals rather than a response to an environmental perturbation, for example, seasonality. As discussed in the last section, scaphites may have assumed a planktonic mode of life at hatching. For some time at least, the animals may have relied on whatever remaining yolk existed as a food source, later becoming dependent on minute plankton. The slight change in shape at approximately 1 mm in diameter may correlate with the transition from a lecithotrophic to a more planktotrophic mode with an attendant expansion in whorl width. The more conspicuous changes at 3–4 mm in diameter, however, may represent the end of the planktonic stage and the transition to a more active mode of life coincident, perhaps, with a descent from surface water. This would be equivalent to the end of the pseudolarval stage in modern cephalopods.

Other ammonites exhibit similar morphometric changes at comparable sizes and whorl numbers. *Gaudryceras tenuiliratum* exhibits three conspicuous changes in the shape of the shell at 1.25, 2.25, and 5.5 whorls from the proseptum (Hirano, 1975). The first change apparently coincides with the end of the ammonitella (the ammonitella angle exceeds one whorl as reported by Tanabe et al., 1979). The second change may reflect a juvenile growth stage, and the third probably reflects maturity. Tanabe (1975, 1977) recognized three changes in the ontogeny of *Otoscaphites puerculus* and *Scaphites planus* at 0.75, 1.75, and 2.75 whorls from the proseptum. The first change marks the end of the ammonitella. The existence of the second change is questionable but corresponds to approximately one whorl from the constriction. The third change is very conspicuous and corresponds to two whorls from the constriction, identical to the break herein described. *Reesidites minimus* exhibits two changes in growth at approximately 3.0 and 5.0 whorls from the proseptum (Obata, 1965) corresponding to 1.5 and 3.5 whorls from the constriction, respectively, after the angular length of the ammonitella is subtracted. *Subprionocyclus neptuni* exhibits two shape changes at 1.75 and 2.75 whorls from the proseptum (Obata et al., 1979) corresponding to 1.0 and 2.0 whorls from the constriction, respectively, after the angular length of the ammonitella is subtracted (approximately 0.75 whorls). Westermann (1954) identified a juvenile growth stage at approximately three whorls from the primary constriction in several species of Otoitidae and Stephanoceratidae. In *Promicroceras* and other Jurassic ammonites, Currie (1942, 1943, 1944) detected several changes in shape on the basis of her measurements of whorl height, width, and spiral angle. The most consistent changes occurred at 1.0–1.5 whorls from the proseptum, corresponding to the end of the ammonitella, and at approximately 1.5–2.0 whorls later (corresponding to approximately 2.0–3.0 mm in diameter). Hewitt (1985) has also documented a change in whorl strength and sutural complexity corresponding to approximately two to three whorls from the primary constriction in many ammonites. Finally, Kulicki (1974) recognized a break in growth in *Quenstedtoceras* corresponding internally with a decline in septal spacing, his so-called second depression.

Thus, similar morphometric changes appear in taxonomically unrelated ammonites such as *Quenstedtoceras* and *Gaudryceras* (different suborders) and may have a common explanation. In other words, just as the similarity in the morphology of the embryonic shell among all ammonites suggested a common mode of development, the similarities in the morphological patterns observed in early postembryonic growth may suggest common developmental and mode of life changes. Thus, although the kind of ornamentation may differ in different ammonites, its first appearance on the shell may indicate a similar change in mode of life. Because these changes appear in a wide variety of ammonites, they probably do not represent a response to the same environmental perturbation, but probably represent a similar change in ontogenetic development. Gross changes in ontogenetic development appear, of course, at maturity to which we now turn.

MATURITY

In the Turonian-Santonian scaphites from the Western Interior, maturity is expressed by the development of a partially or nearly completely uncoiled body chamber with a sculpture different from that of the septate whorls (Cobban, 1951). Thus, as in embryonic and early postembryonic growth, a change in shape is interpreted as indicating a change in mode of life or ontogenetic development. This change in shape is very conspicuous. The mature body chamber reflexes hooklike upon the earlier secreted phragmocone and terminates in a constricted aperture (fig. 61). The form of the body chamber precludes further development, and as in many other marine invertebrates, growth is determinate.

Among these scaphites the shape of the mature body chamber varies from a loosely uncoiled to a more tightly but still uncoiled form. Within a species, by definition, the adult shape is uniform and comparison, for example, of adult diameters among individuals comprises a valid measure of size variation. However, some species are so different from others in their adult shape, that is, the form of their mature body chamber, that few or no homologous points of comparison exist. For example, an individual of *S. carlilensis* may exhibit the same maximum length as an individual of *C. vermiformis* but in the former the measurement of maximum length includes a lot of empty space, whereas in the latter it is an accurate representation of a compact form.

Diameter of the Mature Phragmocone

To compare the adult dimensions of different species, yet circumvent the problem described above, I chose to measure the mature phragmocone. Unlike the body chamber, the phragmocone exhibits nearly the same shape, that is a logarithmic spiral, in all species. However, although the phragmocone is easily measured on whole specimens of uncoiled species, its measurement on more involute species such as *C. vermiformis* requires either broken specimens or median sections.

Histograms of mature phragmocone diameter measured as indicated on figure 61 were prepared for several species (figs. 62–67). For example, a sample of 131 individuals of *S. whitfieldi* from a single concretion from locality B176a describes a slightly skewed normal distribution with a mode between 20 and 22 mm (fig. 63). Another sample of 71 specimens of the same species from several localities just south of the Black Hills (B176, B177, B192a, B192, and B193) also describes a normal distribution with a slightly higher mode between 26 and 28 mm (fig. 63). Neither distribution is bimodal. Histograms of the other species also approximate normal distributions except for *C. vermiformis* (fig. 67). The mode, mean, and ratio of maximum to minimum diameter are listed below for six species. *S. preventricosus* and *C. vermiformis* exhibit the largest phragmocones and *S. larvaeformis* exhibits the smallest phragmocones. The ratio of maximum to minimum diameter ranges from 1.7 to 4.6.

Species	N	Mode (mm)	Mean (mm)	Ratio, max. to min. diameter
S. larvaeformis	55	12–14	13.7	4.0
S. carlilensis	34	20–22	24.5	4.6
S. warreni	47	16–20	20.2	2.3
S. whitfieldi	131	20–22	20.2	2.8
S. preventricosus	16	40–42	41.8	1.7
C. vermiformis	22	38–40	36.0	2.2

How does adult phragmocone size relate to the initial ammonitella size? A plot of measurements of ammonitella diameter versus adult phragmocone diameter for all specimens of *S. whitfieldi* from locality B176a indicates no correlation (fig. 68). A small ammonitella may develop into an adult with a small phragmocone and low whorl number or, with equal probability, an adult with a large phragmocone and high whorl number. Apparently, within species, the size of the ammonitella does not determine the final adult size. A similar plot of measurements of adult diameter versus ammonitella size for

S. larvaeformis also exhibits zero correlation (fig. 69).

The correlation between ammonitella size and adult phragmocone size improves, however, among species. According to table 10, the smallest ammonitellas appear in *S. larvaeformis, S. whitfieldi,* and *S. warreni,* and in turn, these three species exhibit the smallest adult phragmocones. At the other extreme, *C. vermiformis* possesses one of the largest ammonitellas and, consequently, one of the largest mature phragmocones. However, the average ammonitella size in *S. preventricosus* is similar to that in *S. warreni* yet the mature phragmocone of *S. preventricosus* more closely resembles that of *C. vermiformis.* These relationships are also illustrated in figure 70 in which measurements of ammonitella diameter are plotted against measurements of mature phragmocone diameter. The pooled sample means for each species are used except for *S. whitfieldi*; the coefficient of correlation equals .7698.

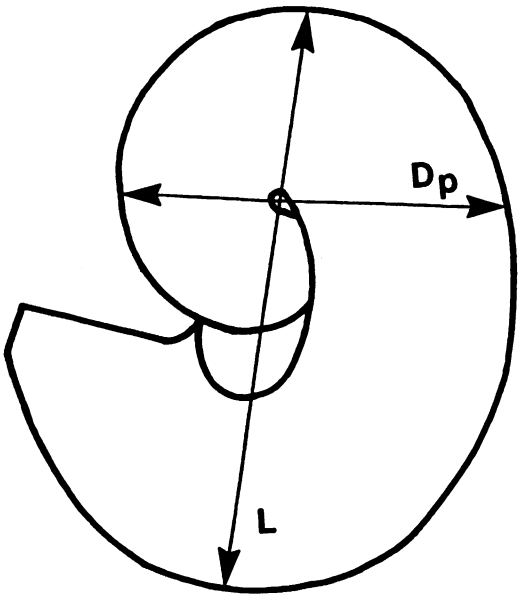

Fig. 61. Diagram of an adult scaphite illustrating the measurement of mature phragmocone diameter (*Dp*) and overall length (*L*).

Number of Whorls in the Mature Phragmocone

The number of whorls in the mature phragmocone is measured on median sections. The most complete sample available consists of 113 individuals of *S. whitfieldi* from a single concretion from locality B176a. Figure 71A represents a histogram of this sample in which the number of whorls is measured from the primary constriction. The histogram describes a normal distribution with a mode between 3.7 and 3.9 or 4.0 whorls. This mode corresponds to the mode between 16 and 22 mm in mature phragmocone diameter. Most specimens exhibit a range from 3.6 to 4.3 whorls yielding a difference of 0.7 whorls. The inclusion of two anomalously large specimens extends the range to 4.8 whorls, yielding a difference of 1.2 whorls. A similar histogram for 62 adults of *S. whitfieldi* from other localities just south of the Black Hills (localities B176, B177, B192, B192a, and B193) describes another normal distribution with a mode between 3.9 and 4.0 whorls and a range from 3.4 to 4.7 whorls, yielding a difference of 1.3 whorls (fig. 71B). Either singly or combined, the two distributions do not indicate bimodality.

Correlation Between Phragmocone Size and Whorl Number

What is the relationship between the diameter of the mature phragmocone and the number of postembryonic whorls? Figure 72 represents a plot of measurements of the natural logarithm of the diameter of the mature phragmocone versus the number of whorls, measured from the start of the postembryonic shell, for individuals of several scaphite species, namely *S. carlilensis, S. warreni, S. nigricollensis, S. corvensis, S. preventricosus, S. depressus,* and *C. vermiformis.* This plot suggests two observations, relating first to intraspecific and, second, to interspecific variation.

First, within a species, the slope of the line of best fit for measurements of whorl number versus phragmocone diameter is generally lower than that for individual growth. For example, measurements for 108 adults of *S. whitfieldi* from locality B176a approximate a straight line of slope .7190 with a correlation coefficient of .8239. Expressing whorl number in π radians, this slope converts to .1144. The inclusion of two specimens with 4.76 whorls apiece, which lie outside the general distribution, lowers the slope of the line of

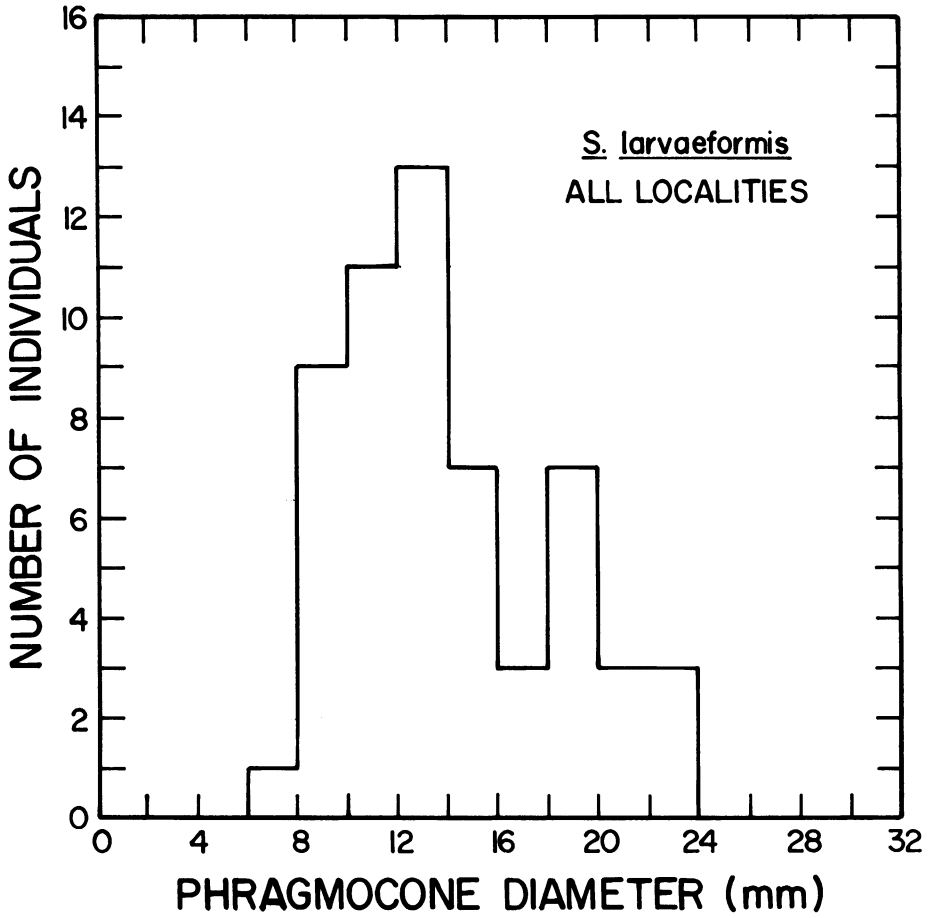

Fig. 62. Histogram of mature phragmocone diameter for 55 specimens of *Scaphites larvaeformis*.

best fit to .6684 or, using π radians, .1064. These values are lower than the mean slope of .1408 for the postembryonic growth of the spiral radius (or diameter) versus the total rotational angle in an individual specimen of *S. whitfieldi* from this locality. Similarly, measurements of the diameter of the mature phragmocone versus the number of whorls for 16 adult specimens of *S. larvaeformis* from all available localities approximate a straight line of slope .6646 with a coefficient of correlation of .8504. Expressing whorl number in π radians, this slope converts to .1058. Again, this value is lower than the mean slope of .1401 for the postembryonic growth of the spiral radius (or diameter) versus the total rotational angle in an individual specimen of *S. larvaeformis*. How do we explain this repeated discrepancy?

The difference is probably due to intraspecific variation in the size of the ammonitella and in the value of the constant of spiral expansion (k). Ammonitella size is a measure of a, the distance between the center of the spiral and its start. If all individuals of a species began postembryonic growth with the same size ammonitella, and assuming for the moment they all grew with the same spiral expansion constant (k), the plot of the measurements of mature phragmocone size versus whorl number would conform to a straight line whose slope would equal the value of the spiral expansion constant for individual growth. Whorls would accrue in larger individuals as if their addition simply represented an extrapolation of the growth of smaller individuals, short of maturity. However, the size of the ammonitella varies widely within

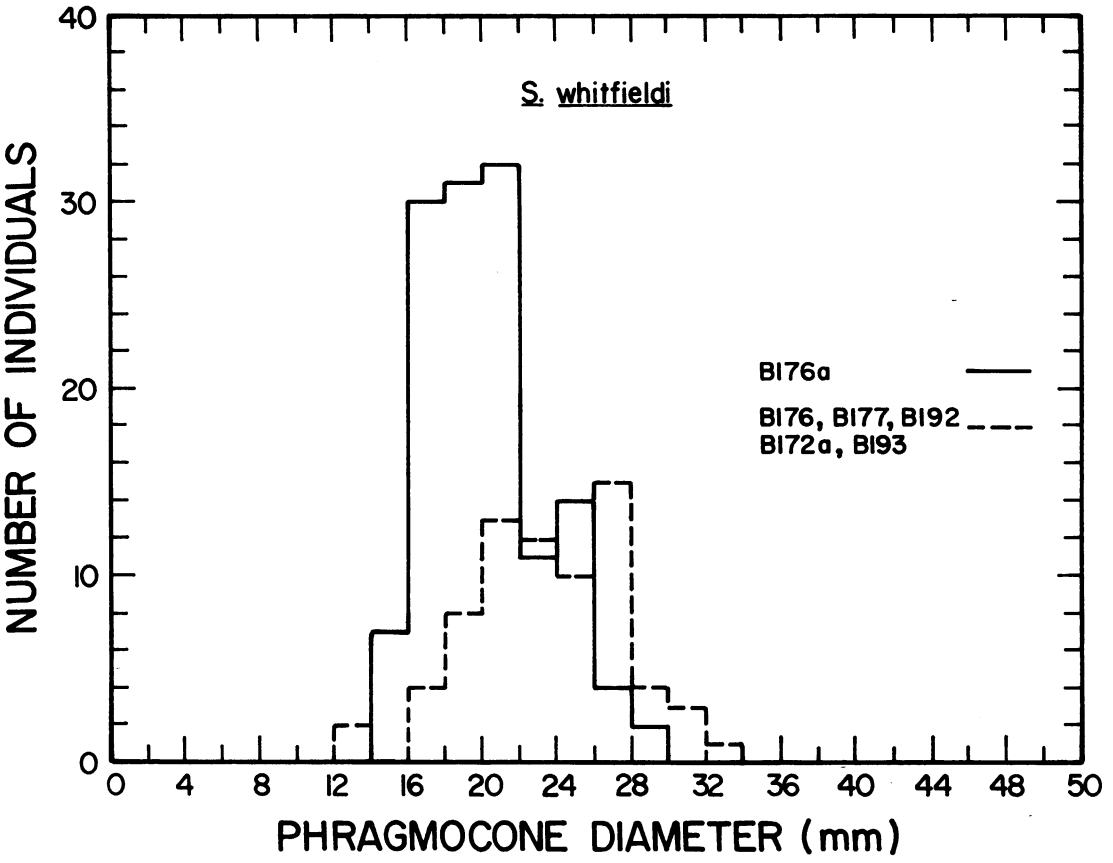

Fig. 63. Histogram of mature phragmocone diameter for 131 specimens of *Scaphites whitfieldi.*

a single species, and, therefore, specimens do not begin postembryonic growth at the same size. Thus, although previously we learned that ammonitella size exhibits no correlation

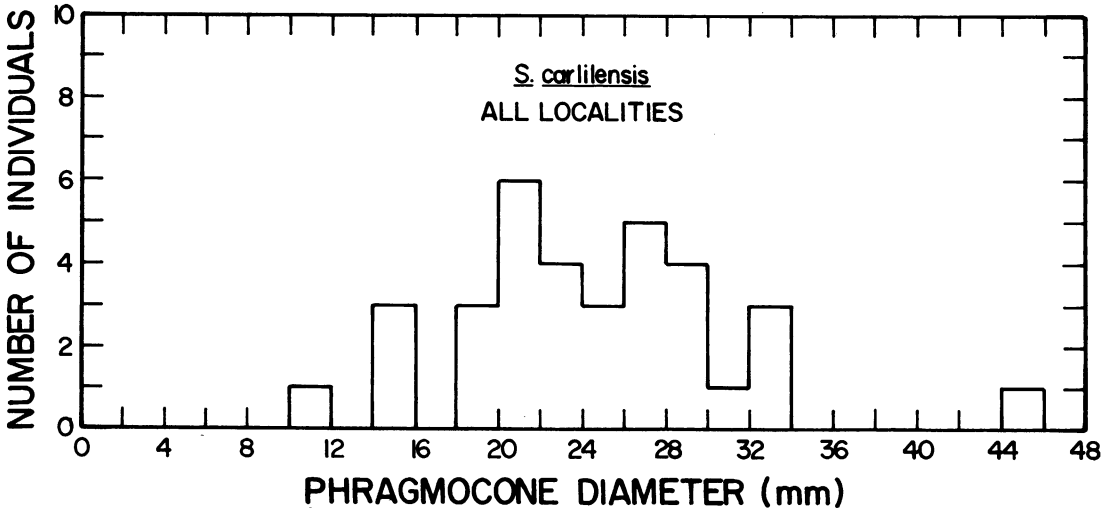

Fig. 64. Histogram of mature phragmocone diameter for 34 specimens of *Scaphites carlilensis.*

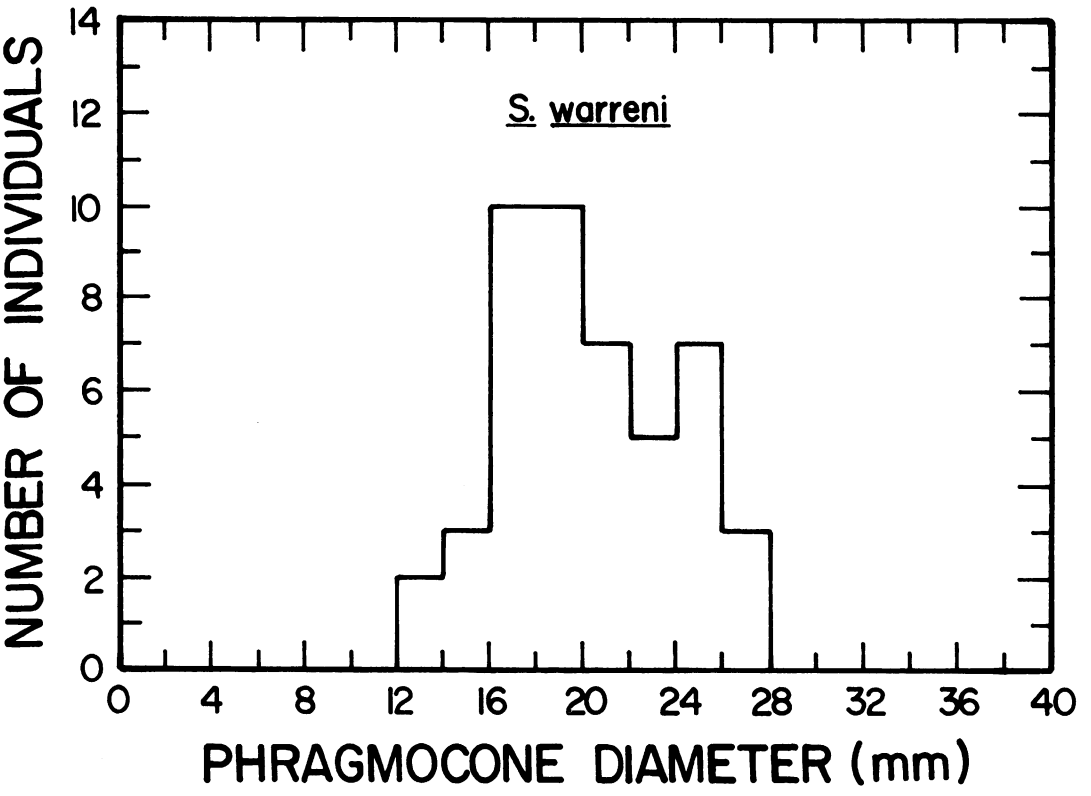

Fig. 65. Histogram of mature phragmocone diameter for 47 specimens of *Scaphites warreni.*

with final adult phragmocone size within species, at *any particular adult size,* the size of the ammonitella is inversely related to the number of adult whorls. For example, in *S. larvaeformis,* the size of the ammonitella ranges from approximately 525 to 650 μm. Ammonitellas at these two sizes will yield specimens with 3.75 and 3.5 whorls, respectively, at an average phragmocone diameter of 14 mm. The calculations are as follows:

$$\theta_1 = \pi + \frac{1}{.14} \ln \frac{14 \text{ mm}}{.315 \text{ mm } (1 + e^{.14\pi})}$$

$$= 23.56 \text{ radians},$$

$$\theta_1 = 3.75 \text{ whorls}$$

$$\theta_2 = \pi + \frac{1}{.14} \ln \frac{14 \text{ mm}}{.390 \text{ mm } (1 + e^{.14\pi})}$$

$$= 21.99 \text{ radians},$$

$$\theta_2 = 3.50 \text{ whorls}$$

where .14 = the constant of spiral expansion

.315 mm = 60% of the size of the ammonitella, which measures .525 mm

.390 mm = 60% of the size of the ammonitella, which measures .650 mm

14 mm = the mean size of the adult phragmocone.

At a phragmocone diameter of 20 mm, these two ammonitellas will yield specimens with 4.15 and 3.91 whorls, respectively.

The variation in the number of whorls at a given diameter of the adult phragmocone is further illustrated in figure 73. Measurements of phragmocone diameter versus the number of postembryonic whorls are replotted for specimens of *S. larvaeformis* with individual growth trajectories terminating at each point. These trajectories are drawn assuming a constant slope, that is, a spiral expansion constant k equal to approximately .14. The lines are parallel but not coincident and, therefore, display different y intercepts.

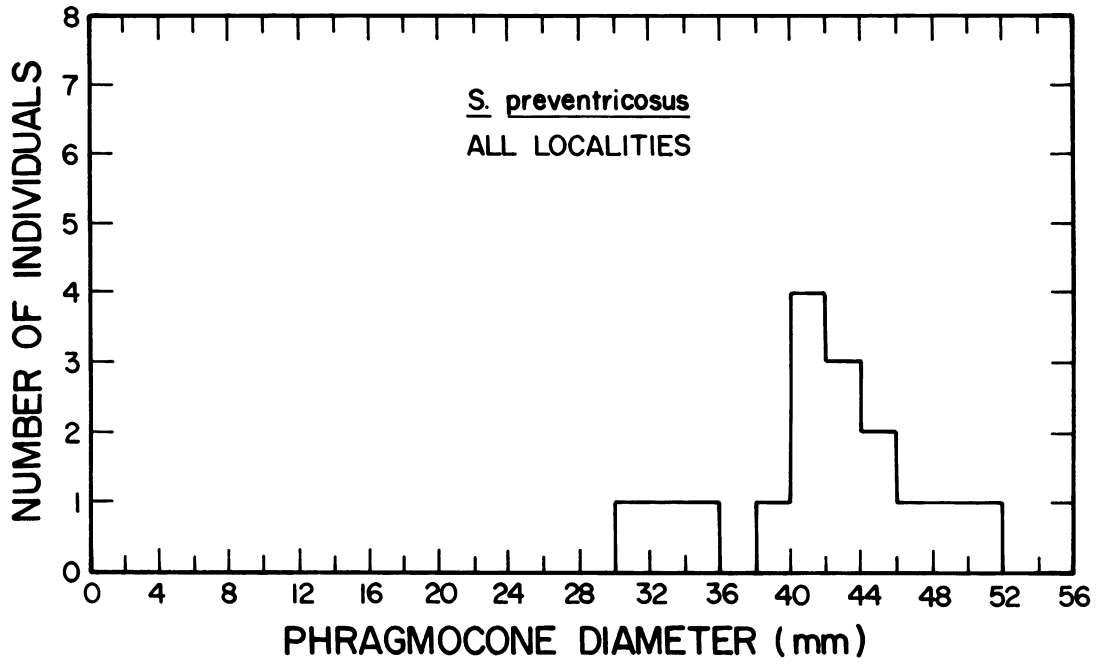

Fig. 66. Histogram of mature phragmocone diameter for 16 specimens of *Scaphites preventricosus.*

The intercepts reflect ammonitella size, and at *any particular adult diameter,* specimens with larger ammonitellas (higher y intercepts) exhibit fewer whorls. Note, however, as shown previously, that ammonitella size does not display any correlation with final adult size and whorl number, considered collectively. Specimens with small phragmocones and low

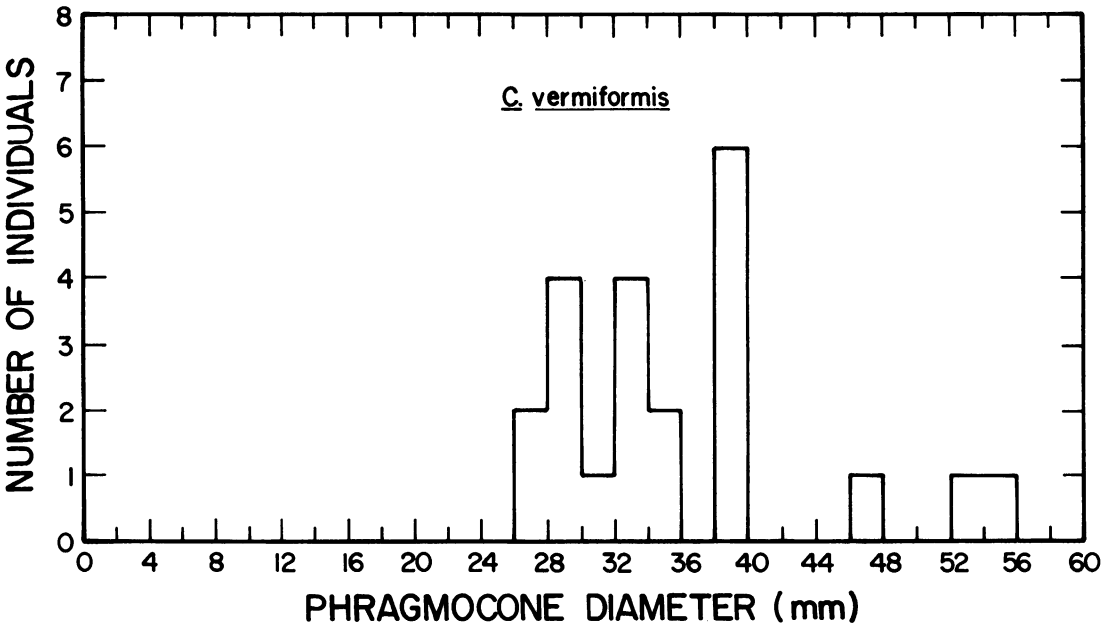

Fig. 67. Histogram of mature phragmocone diameter for 22 specimens of *Clioscaphites vermiformis.*

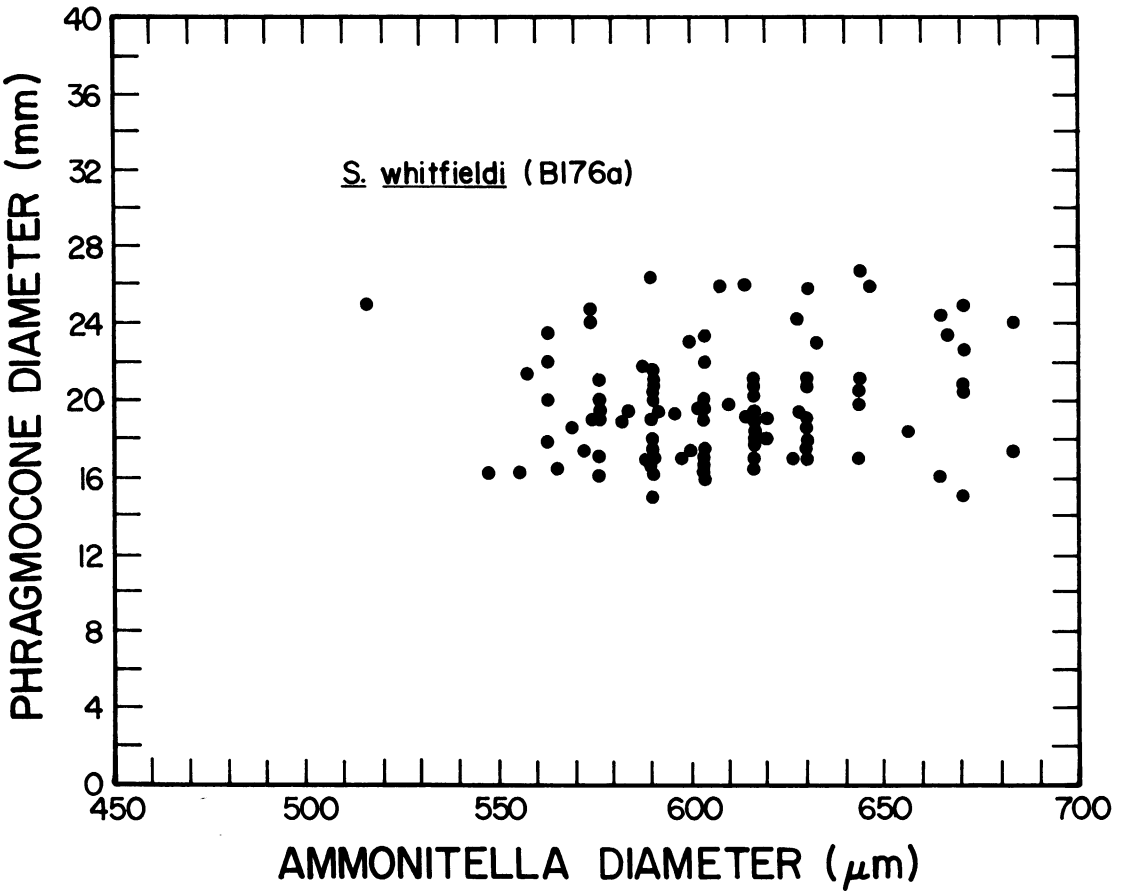

Fig. 68. Plot of mature phragmocone diameter versus ammonitella diameter for 98 specimens of *Scaphites whitfieldi*.

whorl numbers may, in fact, exhibit higher intercepts than those with larger phragmocones and greater whorl numbers. The result is that the slope of the line of best fit through the measurements of adult phragmocone diameter versus whorl number is lower than that for individual growth. (The intercepts in fig. 73 do not strictly translate as ln a because diameter rather than radius is plotted against θ. The equation $D = ae^{k\theta} + ae^{k(\theta-\pi)}$ is rendered in natural logarithms as $\ln D = k\theta + \ln a + \ln(1 + e^{-k\pi})$, and the intercept actually represents the last two terms.)

In addition to intraspecific variation in ammonitella size, variation also occurs in the value of the spiral expansion constant. For example, the spiral expansion constant in *S. larvaeformis* ranges from .1310 to .1495. Beginning with the same size ammonitella, this difference in the value of the constant of spiral expansion will yield a difference of 0.44 whorls at an adult diameter of 14 mm. The calculations are as follows:

$$\theta_1 = \pi + \frac{1}{.1310} \ln \frac{14 \text{ mm}}{.394 \text{ mm } (1 + e^{.1310\pi})}$$

$$= 23.37 \text{ radians},$$

$$\theta_1 = 3.72 \text{ whorls}$$

$$\theta_2 = \pi + \frac{1}{.1495} \ln \frac{14 \text{ mm}}{.394 \text{ mm } (1 + e^{.1495\pi})}$$

$$= 20.63 \text{ radians},$$

$$\theta_2 = 3.28 \text{ whorls}$$

where .1310 = the lower constant of spiral expansion

.1495 = the higher constant of spiral expansion

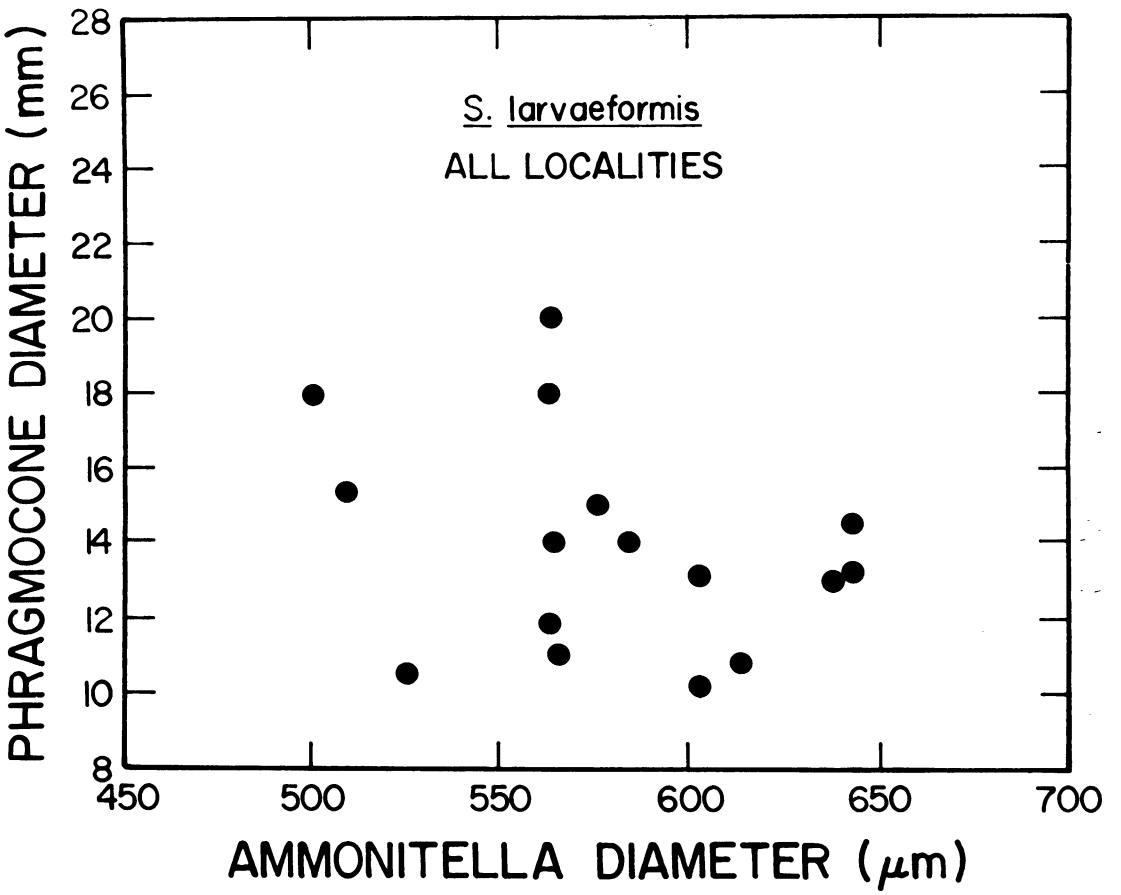

Fig. 69. Plot of mature phragmocone diameter versus ammonitella diameter for 16 specimens of *Scaphites larvaeformis.*

14 mm = the mean size of the adult phragmocone
.349 mm = 60% of the mean size of the ammonitella, which measures .582 mm in *S. larvaeformis.*

At a phragmocone diameter of 20 mm, the lower and higher values of k will yield specimens with 4.15 and 3.66 whorls, respectively. Thus, as with ammonitella diameter, the constant of spiral expansion is inversely related to the number of postembryonic whorls at *any particular adult size* and, therefore, the slope of the line of best fit through the measurements of adult phragmocone diameter versus whorl number will not match that for individual growth.

The second observation emerging from figure 72 relates to interspecific variation. The measurements of phragmocone size versus whorl number for the adults of all species approximately conform to a straight line of slope .8121 with a correlation coefficient of .8865. Expressing whorl number in π radians, this slope converts to .1292, a value approaching the mean spiral expansion constant for individual growth. This slope probably also reflects variation in ammonitella size and the spiral expansion constant. As shown previously, among species, the relationship between ammonitella size and number of postembryonic whorls and adult phragmocone size exhibits a weak positive correlation. A species starting out with a larger ammonitella tends to attain a larger size and more whorls at maturity than a species starting out with a smaller ammonitella.

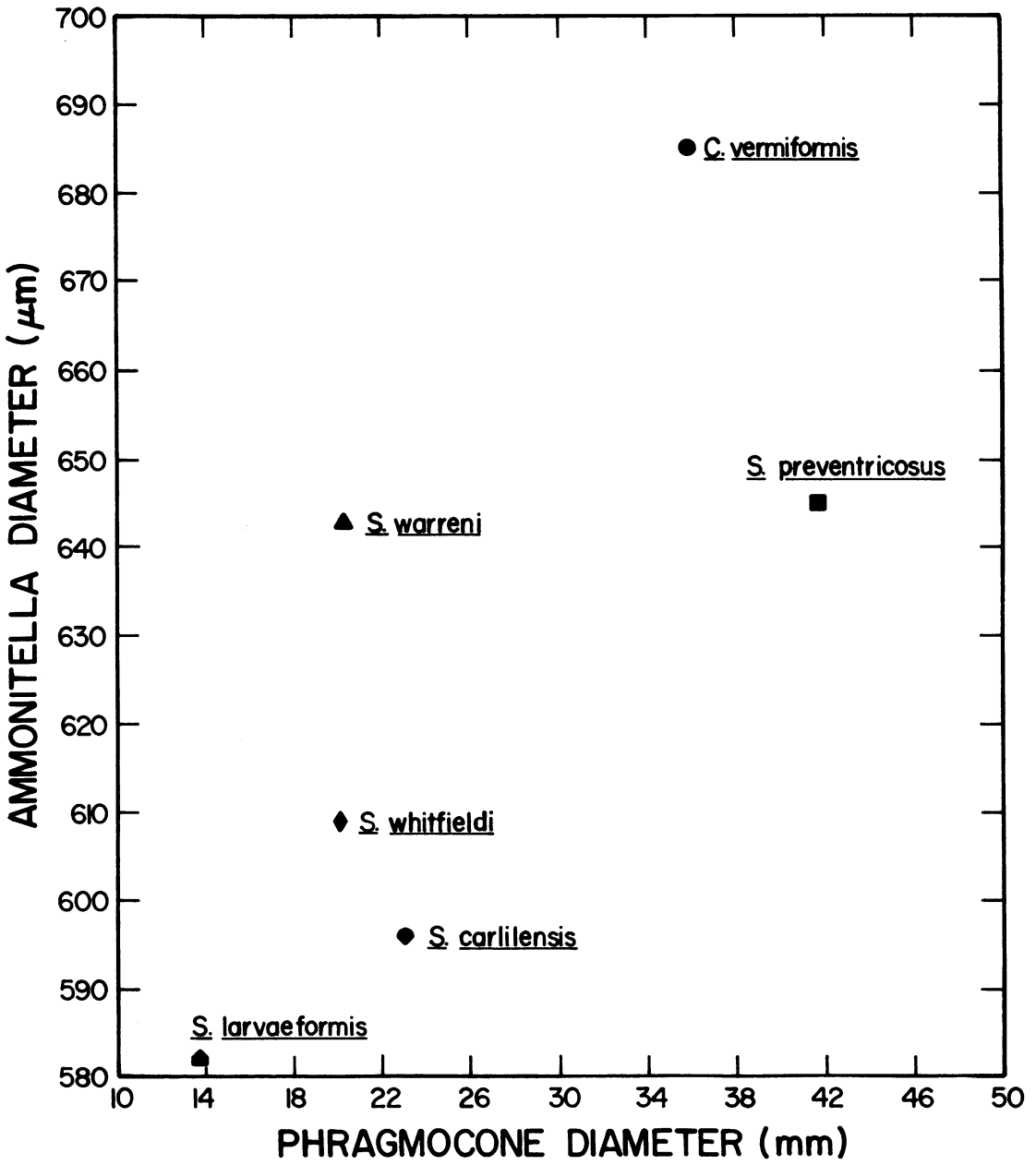

Fig. 70. Plot of mean ammonitella diameter versus mean phragmocone diameter for six species exhibits a positive correlation (correlation coefficient = .7698).

Nevertheless, at *any particular adult phragmocone size,* the size of the ammonitella is inversely related to the number of postembryonic whorls.

Likewise, although the mean value of the spiral expansion constant is similar among the four species studied, variation in k will produce concomitant variation in the number of whorls at *any particular adult phragmocone size.* The species also differ in their patterns of spiral expansion after approximately two whorls from the primary constriction. These differences are especially well marked at the onset of maturity. After two

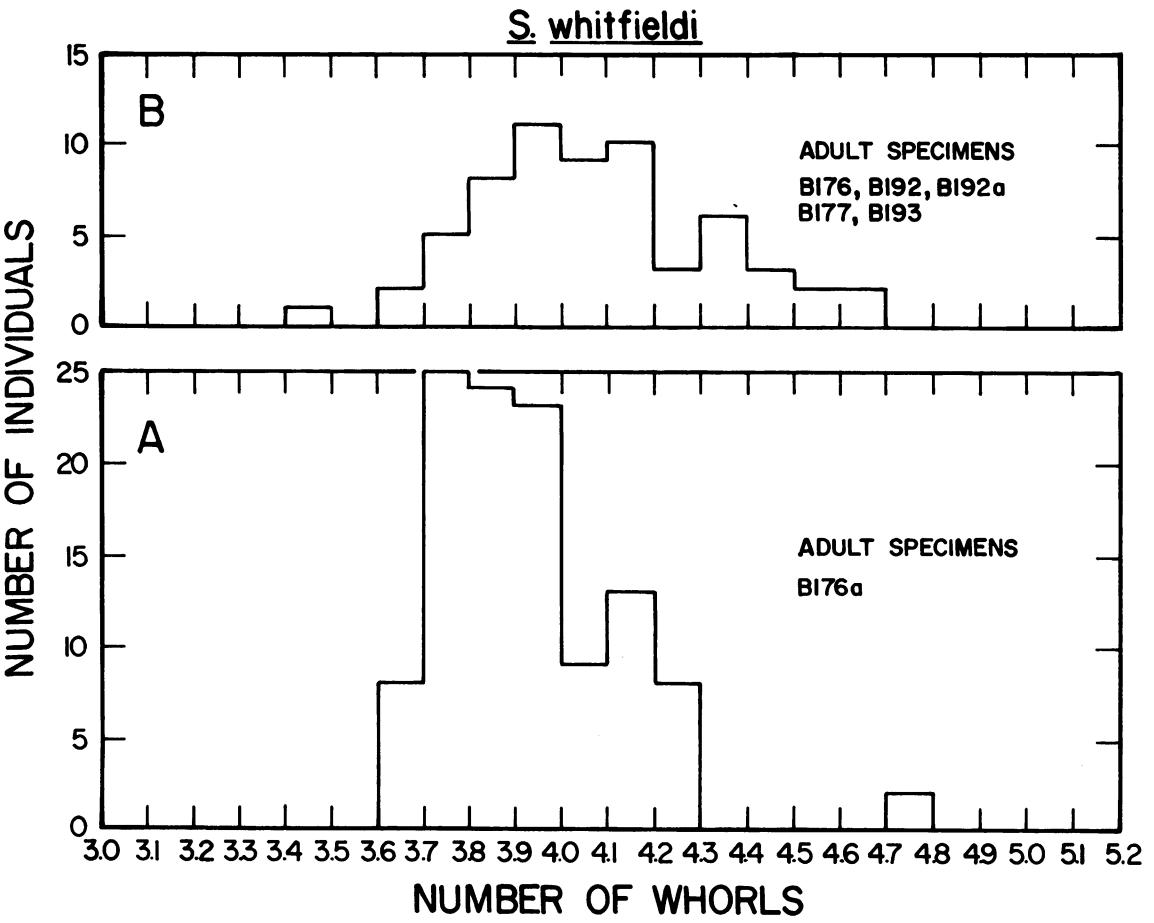

Fig. 71. Two histograms illustrating the number of postembryonic whorls in the mature phragmocone of *Scaphites whitfieldi*. **A**, 113 specimens from locality B176a. **B**, 62 specimens from localities B176, B177, B192, B192a, and B193.

whorls from the primary constriction in *S. larvaeformis* the spiral expansion constant remains the same or exhibits a slight decrease. In *S. whitfieldi*, the constant of spiral expansion increases after this whorl number but sharply decreases at maturity. In *S. preventricosus* the value of k also increases after two whorls from the constriction and subsequently exhibits a decrease for the final 1.5 whorls of the mature phragmocone. The mature phragmocone of *S. preventricosus* commonly possesses more whorls than that of *S. whitfieldi*, and, therefore, the increase in k persists longer. Finally, in *C. vermiformis*, the decrease in the spiral expansion constant that typically occurs near maturity in the other species, appears immediately after two whorls from the primary constriction in this species. Thus, the slight decline in the constant of spiral expansion at maturity in *S. larvaeformis* is accentuated in *S. whitfieldi* and *S. preventricosus* and appears even earlier in the ontogeny of *C. vermiformis*.

The fact that the slope of the line of best fit for phragmocone size versus whorl number among species approaches the mean value of the constant of spiral expansion for individual growth suggests that, on the average, differences in size among species more commonly entail differences in whorl number rather than marked disparities in the value of the spiral expansion constant. The change in k in larger species is not sufficiently large to accommodate increase in size and at the

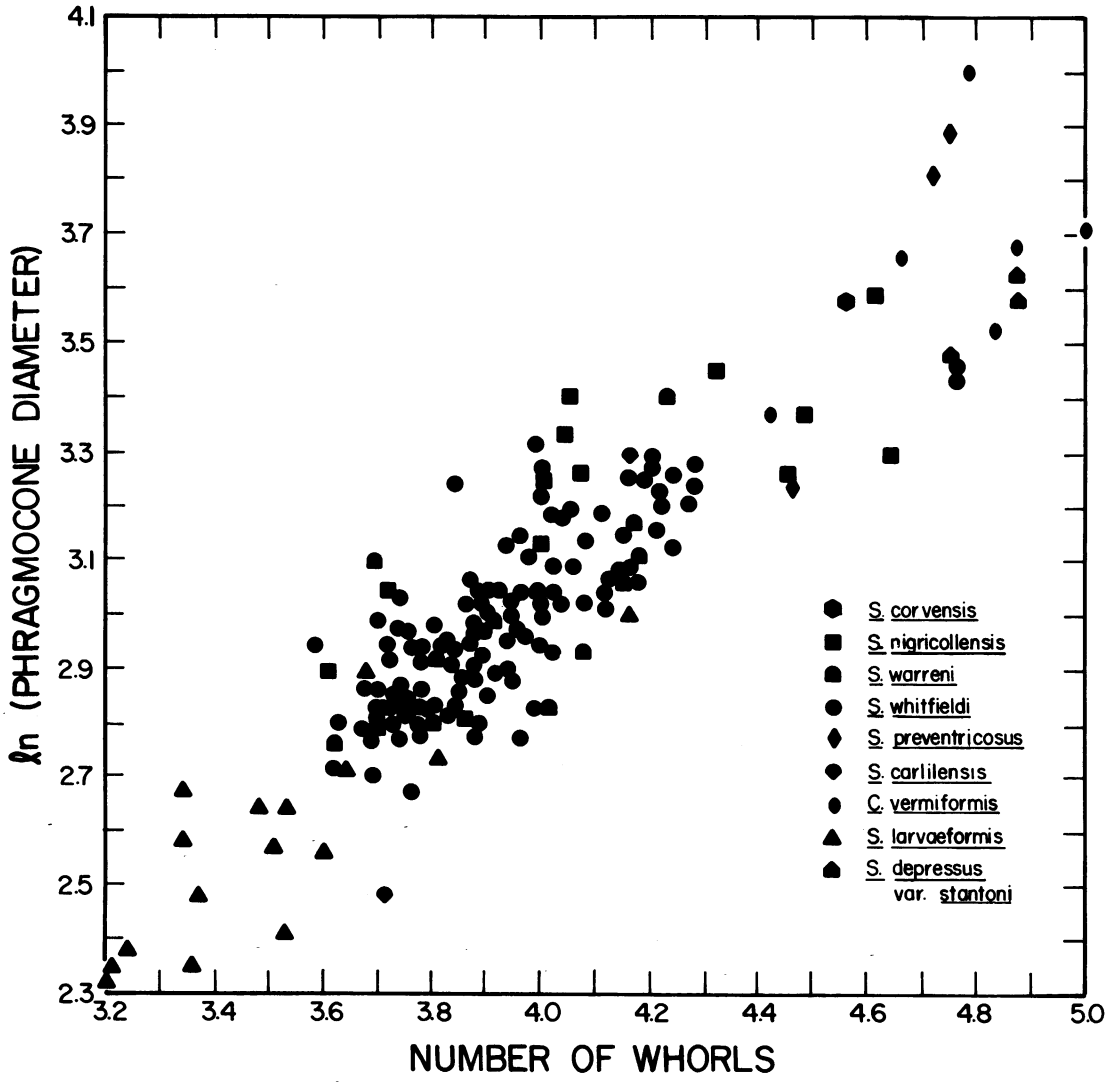

Fig. 72. Plot of the natural logarithm of the diameter of the mature phragmocone versus whorl number for several scaphite species including *S. corvensis* from an unnumbered USGS locality near Lander, Wyo. (see Appendix II); *S. nigricollensis* from localities B185–B188 and USGS localities 21198, 23666, D422, and D1363; *S. warreni* from all available localities; *S. whitfieldi* from locality B176a; *S. preventricosus* from locality B211 and USGS localities 20289 and 23280; *S. carlilensis* from locality B183 and USGS locality 21182; *C. vermiformis* from localities B204 and B205, and USGS locality 21425; *S. larvaeformis* from all available localities; and *S. depressus* var. *stantoni* from locality B253 and USGS locality 17957.

same time maintain the same number of whorls.

Number of Septa in the Adult Phragmocone and Age at Maturity

How do the numbers of septa relate to adult size? Recall that in a logarithmic spiral, if the addition of angular increments is arithmetic, then increase in diameter is exponential. Therefore, given the simplifying assumption that, on the average, septa are spaced at equal angles, say 20°, or in other words, 18 septa occur per whorl, a specimen whose phragmocone has twice the number of whorls will exhibit twice the number of septa. However, a specimen whose phragmocone is twice as large in diameter will exhibit many fewer than

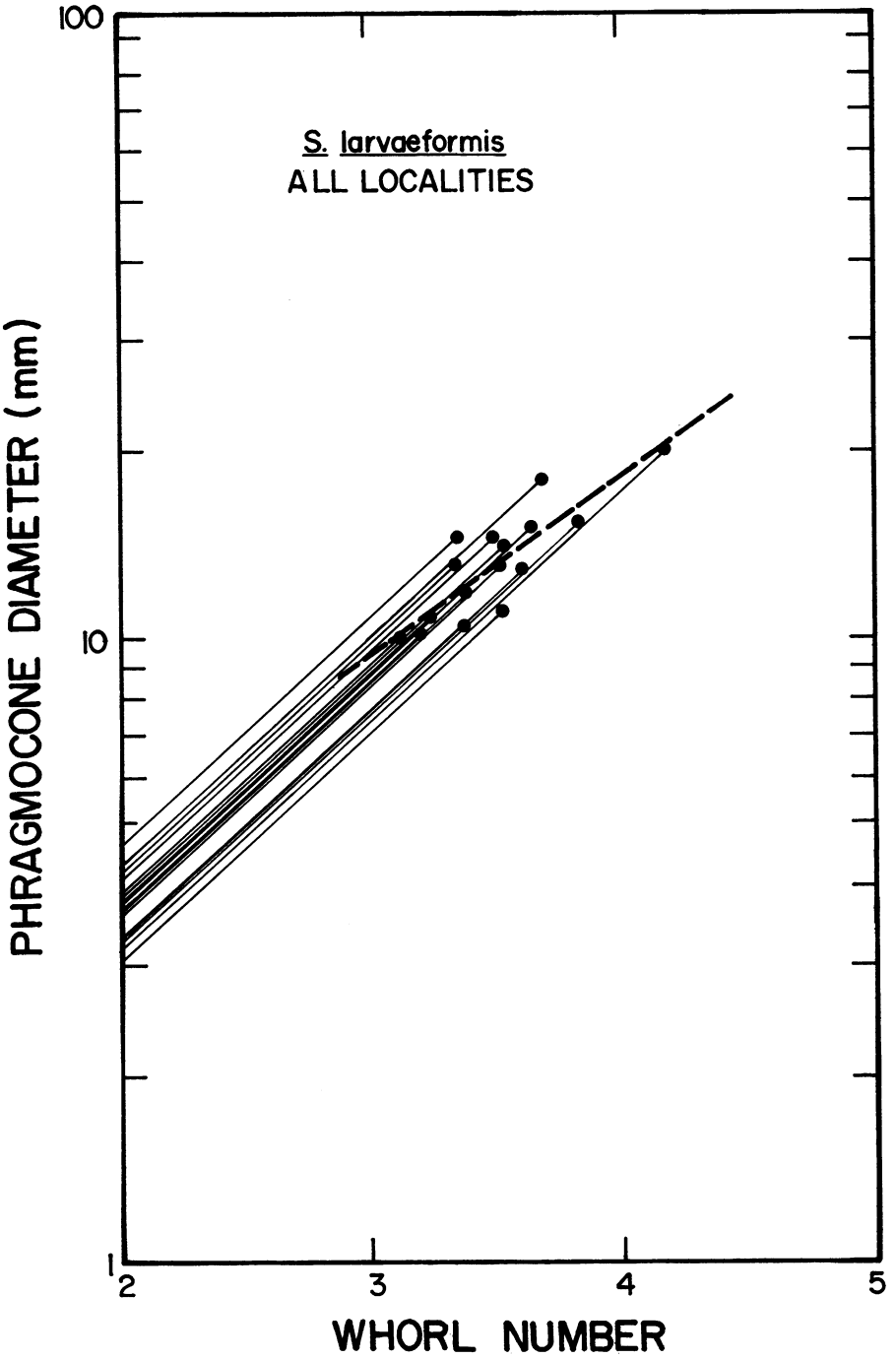

Fig. 73. Plot of the mature phragmocone diameter versus the number of postembryonic whorls in the phragmocones of 16 specimens of *Scaphites larvaeformis*. Individual growth trajectories are drawn with a slope, that is, a spiral expansion constant, equal to approximately .14. The slope of the line of best fit through the adult values is lower than the slope of the individual growth trajectory.

twice that number of septa. For example, a specimen with an adult phragmocone 5 mm in diameter, an ammonitella 670 μm in diameter, an ammonitella angle of 280°, a spiral

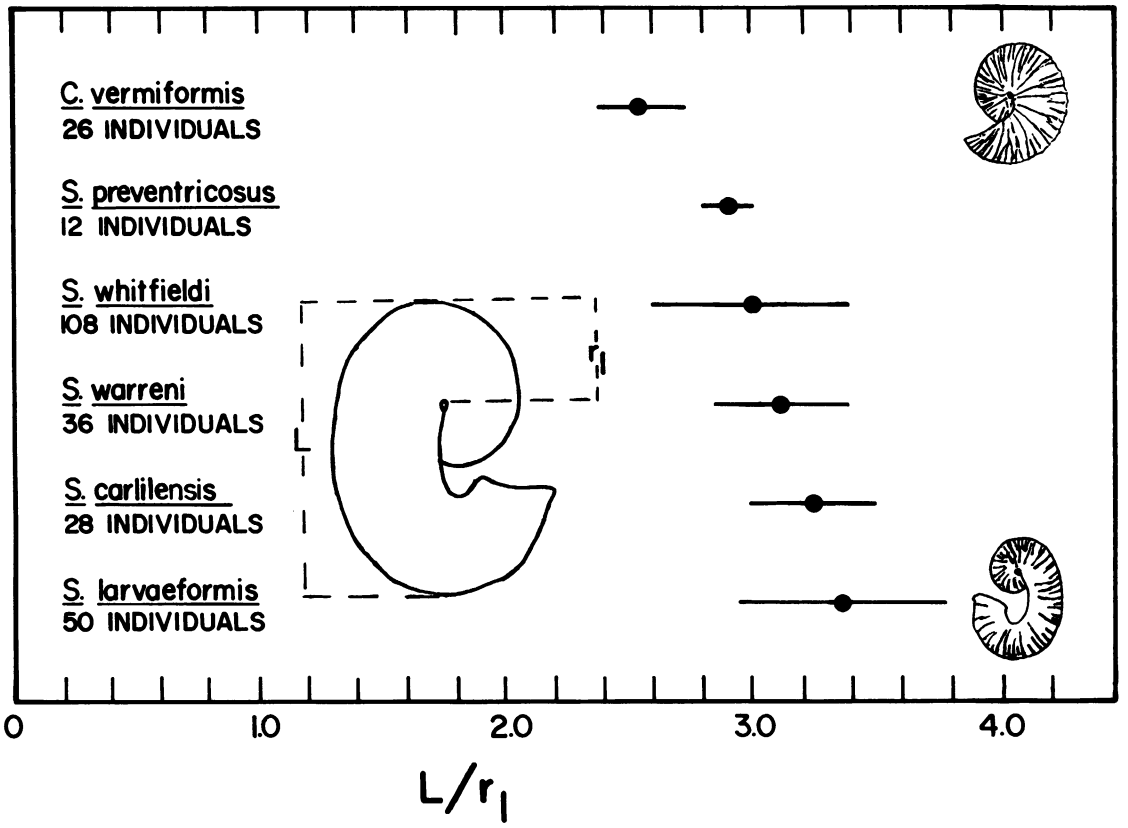

Fig. 74. Plot of the ratio of L to r_1 for six scaphite species showing the mean with one standard deviation to either side. This shape ratio indicates the extent to which the adult hook is developed. Drawings of *S. larvaeformis* and *C. vermiformis* are reduced to the same size for comparison.

expansion constant of .138, and septa that are spaced every 20° will possess a total of 56 septa. Another specimen whose adult phragmocone is twice that size, that is, 10 mm in diameter, will only display 14 septa more, and a specimen whose adult phragmocone is four times the original size will only display an additional 29 septa.

This relationship between the number of septa and the size of the adult phragmocone is well illustrated by two adults of *S. whitfieldi* from locality B176a. The first specimen displays an ammonitella angle of 285°. Its mature phragmocone measures 16.3 mm in diameter and consists of 3.68 whorls from the primary constriction. The total number of septa including the proseptum equals 92. The second specimen displays an ammonitella angle of 299°. Its mature phragmocone measures 21.4 mm in diameter and consists of 4.13 whorls from the primary constriction. The total number of septa in this specimen equals 101. In other words, although the second specimen is 1.3 times the diameter of the first specimen, it does not possess 1.3 times the number of septa (120). The actual number of septa may be estimated by the following procedure: divide the total rotational angle of the first specimen by the number of septa in that specimen:

$$\frac{3.68 \times 360° + 285°}{92} = \frac{1609.8°}{92} = 17.5°$$

Given the simplifying assumption that all septa are equally spaced, the angle between septa equals 17.5°. Dividing the total rotational angle for the second specimen by 17.5°,

$$\frac{4.13 \times 360° + 299°}{17.5°} = \frac{1785.8°}{17.5°}$$

yields 102 septa, very near the actual number.

Thus, the number of postembryonic whorls in the mature phragmocone correlates with the number of septa at maturity.

Determination of the age at maturity of these scaphites based on the number of septa is difficult. In *Nautilus,* the age at maturity is estimated at 10–15 years based on extrapolated rates of apertural growth and periods of septal secretion; animals are known to survive for several years after maturity (Saunders, 1983; Cochran and Landman, 1984; Landman and Cochran, 1987). This contrasts with other cephalopods such as octopus, squids, and cuttlefish, which rapidly reach maturity within one or two years, reproduce, and die (Wells and Wells, 1983). Attempts to determine the rate of growth and longevity in ammonites have, in general, relied on the study and interpretation of patterns of growth, using *Nautilus* as an analogy (Westermann, 1971; Kennedy and Cobban, 1976; Hirano, 1981; Doguzhayeva, 1982; Landman, 1983; Landman, 1986). Growth rate estimates have also been based on the known growth rates of encrusting organisms that grew while the ammonite was still alive (Schindewolf, 1934; Seilacher, 1960, 1982; Merkt, 1966; Meischner, 1968; Westermann, 1971; Hirano, 1981) and the identification of size or year classes within preserved fossil assemblages (Trueman, 1941). These methods have yielded a range of estimates that suggest a slow rate of growth and an extended longevity more similar to that of *Nautilus* than that of modern dibranchiates. This similarity may reflect the common "costs" of growing a large external shell (Ward, 1985).

Mature Body Chamber

Whatever modifications in shape occur in the scaphite phragmocone prior to maturity, they are small compared to the shape changes coincident with the development of the final body chamber. Moreover, as already stated, the shape of the adult body chamber itself varies among species. Comparing the adult shapes of different species by conventional measures of length and width fails to convey or adequately describe this variation. A simple, alternate shape ratio is illustrated in figure 74. The maximum length L of a specimen is measured and divided by the radial distance r_1. This ratio is a measure of evoluteness and the extent to which a hooklike body chamber is developed. In a logarithmic spiral, this is equivalent to dividing a diameter at rotational angle θ by the radius at angle $\theta - \pi$ and the quotient will always remain constant. For example, if $k = .14$, the approximate value for the constant of spiral expansion in these scaphites, and $a = .4$, then

$$\frac{D_\theta}{r_{\theta-\pi}} = \frac{.4e^{.14\theta} + .4e^{.14(\theta-\pi)}}{.4e^{.14(\theta-\pi)}}$$

$$= \frac{.4e^{.14(\theta-\pi)}(1 + e^{.14\pi})}{.4e^{.14(\theta-\pi)}}$$

$$\frac{D_\theta}{r_{\theta-\pi}} = 1 + e^{.14\pi}$$

$$= 2.55$$

Figure 74 illustrates the mean and standard deviation of this ratio for six scaphite species. *S. larvaeformis* displays a mean of 3.31, *S. carlilensis* 3.19, *S. warreni* 3.10, *S. whitfieldi* 3.00, *S. preventricosus* 2.90, and *C. vermiformis* 2.55. The incremental decrease by tenths starting from *S. larvaeformis* and ending with *S. preventricosus* reflects a relative decrease in the uncoiling of the mature body chamber. The mean of 2.55 for *C. vermiformis* matches that of a perfect logarithmic spiral (assuming $k = .14$) and indicates minimal uncoiling.

The degree of uncoiling and the size of the adult shell exhibit a positive correlation among species. Small slender evolute species contrast with large, robust, involute species. A quantitative measure of this correlation is illustrated in figure 75. The same measurements that were previously used to calculate the shape ratio are slightly modified and consist of two radii, r_1 and r_2, measured along the line of maximum length. They are plotted against one another on log-log paper for several species. If the shape of the adult shell, including the body chamber, conformed to a perfect logarithmic spiral, these two measurements would represent radii separated by one-half whorl and their ratio would equal a constant. This would be true of all species, regardless of their adult size, if their adult shape conformed to the same logarithmic spiral. A plot of these measurements on log-log

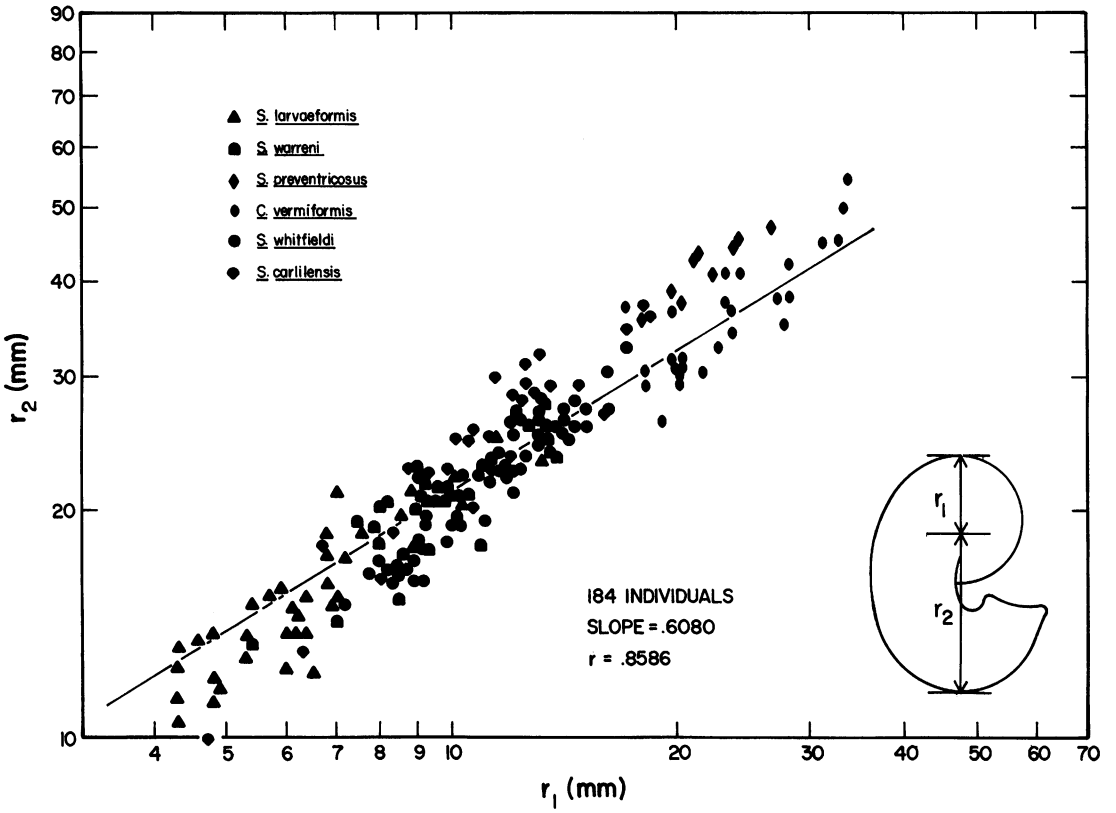

Fig. 75. Plot of r_2 versus r_1 for six scaphite species illustrating the tendency toward greater involuteness with increasing size (slope = .6080).

paper would exhibit a slope of 1, that is, isometry. Similarly, even if the adult shape did not conform to a logarithmic spiral, which is, in fact, more the norm than the exception among these scaphites—but, nevertheless, adults of larger species displayed the scaled-up proportions of adults of smaller species—a plot of these measurements would still exhibit a slope of 1, indicating no change in shape. However, in these Turonian-Santonian scaphites, the ratio of r_2 versus r_1 on log-log paper displays a slope of approximately .6, indicating negative allometry. As r_1 increases in size, r_2 does not keep pace and the result is an increase in coiling, that is, involuteness.

Due to this negative allometry, the adult shapes of larger species closely resemble those of their juvenile shells. In their evolution, these species exhibit a trend toward larger size and greater involuteness (Cobban, 1951). This evolutionary pattern may indicate neoteny in which shape is retarded with respect to developmental stage. Adults of larger species also possess more whorls than those of smaller species, suggesting a delay in maturity. Thus, adult descendants are larger but exhibit a shape characteristic of their ancestors at a juvenile stage of ontogeny; they never develop an extended hooklike body chamber.

How does the angular length of the uncoiled body chamber, for example, in *S. whitfieldi,* compare with the angular length of the body chamber in juveniles of the same species or in adults of coiled species such as *C. vermiformis*? One approach is to treat the uncoiled body chamber as if it were coiled in a normal logarithmic spiral. How is an uncoiled body chamber transformed into a coiled body chamber? Tanabe (1977) described a method called reconstituted spiral length which posed the question: if a scaphite were to continue coiling in a logarithmic spi-

ral, what rotational angle would correspond to the ventral length of the uncoiled body chamber? The length of the uncoiled body chamber is measured along the ventral periphery. However, we require an equation for the length of a logarithmic spiral. The general formula for arc length is

$$L = \int \sqrt{dx^2 + dy^2} \tag{15}$$

The polar equation of the logarithmic spiral $r = ae^{k\theta}$ may be converted into cartesian coordinates, remembering that $x = r\cos\theta$ and $y = r\sin\theta$. The new expression is

$$x = ae^{k\theta}\cos\theta$$

and

$$y = ae^{k\theta}\sin\theta \tag{16}$$

The derivatives are

$$dx/d\theta = -ae^{k\theta}\sin\theta + ake^{k\theta}\cos\theta$$

and

$$dy/d\theta = ae^{k\theta}\cos\theta + ake^{k\theta}\sin\theta$$

Substituting the squares of the derivatives in formula 15 and simplifying yields

$$L = \int \sqrt{a^2e^{2k\theta}(\sin^2\theta + \cos^2\theta) + a^2k^2e^{2k\theta}(\cos^2\theta \sin^2\theta)} \tag{17}$$

which further simplifies to

$$L = \int \sqrt{a^2e^{2k\theta}(k^2 + 1)} \tag{18}$$

and

$$L = \int ae^{k\theta}\sqrt{k^2 + 1} \tag{19}$$

Integrating yields the final expression

$$L = \frac{a}{k}e^{k\theta}\sqrt{k^2 + 1}\Bigg|_{\theta_i}^{\theta_f} \tag{20}$$

This formula expresses arc length as a function of rotational angle.

Thompson (1917) presented a formula for the length of a logarithmic spiral which at first glance appears to be different from equation (20). It is

$$L = r\sec\alpha \tag{21}$$

where α is the constant angle of the spiral, the cotangent of which equals k. However, remembering the trigonometric identity $\tan^2\alpha + 1 = \sec^2\alpha$ and substituting $1/k^2$ for $\tan^2\alpha$ yields

$$L = r\sqrt{(1/k^2) + 1} \tag{22}$$

which simplifies to

$$L = (r/k)\sqrt{k^2 + 1} \tag{23}$$

This is equivalent to equation (20), remembering that $r = ae^{k\theta}$.

Equation (20) may be used to calculate the reconstituted angular body length in two specimens of *S. whitfieldi*. In the first specimen, the length of the body chamber measured along the ventral periphery equals approximately 50 mm. The base of the body chamber occurs at 4.13 whorls or 25.95 radians from the primary constriction. The distance between the center and the start of the spiral a equals .335 mm, and the mean value for the constant of spiral expansion k equals .1408. Substituting in equation (20) and solving for θ_f yields

$$50 = \frac{.335}{.1408}e^{.1408\theta_f}\sqrt{(.1408)^2 + 1} - \frac{.335}{.1408}e^{.1408(25.95)}\sqrt{(.1408)^2 + 1}$$

$$50 = 2.403e^{.1408\theta_f} - 2.403(38.62)$$

$$\frac{142.803}{2.403} = e^{.1408\theta_f}$$

$$59.427 = e^{.1408\theta_f}$$

$$\theta_f = 29.011 \text{ radians or } 1662.2°$$

The difference between θ_f and θ_i, that is, the reconstituted body chamber angle, equals 175.4°. In the second specimen, the length of the body chamber measured along the ventral periphery equals approximately 39 mm. The base of the body chamber occurs at 3.69 whorls or 23.18 radians from the primary constriction. The distance between the center and the start of the spiral a equals .398 mm, and the mean value of the constant of spiral expansion k equals .1408. Solving the equation for θ_f equals 26.16 radians or 1499.2°. The reconstituted body chamber angle for this specimen equals 170.8°.

Tanabe (1977) modified this technique by

considering the length of the body chamber as the average of the ventral and dorsal periphery. In the second specimen of *S. whitfieldi,* for example, this average equals 27 mm. The calculated body chamber angle reduces to 125.6°. These values compare to Tanabe's values of 216–270° for the reconstituted body chamber angles in *Otoscaphites puerculus* and 234° in *Scaphites planus.*

In *S. whitfieldi,* the method of reconstituted angular length of the body chamber yields body chamber angles smaller than those in juveniles, which average 266°, or in adults of tightly coiled species such as *C. vermiformis,* which average 255° and range from 210 to 310°. Thus, although this method may provide a descriptive basis for comparing individuals within a single species, it may be less meaningful for interspecific comparisons. Even within a single species, however, do the results really represent the angle of the body chamber if the body chamber remained coiled? One obvious drawback is that the calculated angle only depends on the length of the body chamber as measured along the ventral periphery and neglects variation in body chamber volume. In addition, body chambers of the same length, as measured along the ventral periphery, attached to larger phragmocones, will yield smaller reconstituted body chamber angles. For example, in the first specimen of *S. whitfieldi* the length of the body chamber equals 50 mm and the number of postembryonic whorls in the phragmocone equals 4.13; the calculated body chamber angle equals 175.4°. The same body chamber length in a specimen with a smaller phragmocone consisting of, for example, 3.69 whorls, yields the larger angle of 208.6°. Tanabe (1977) also documented an inverse relationship between reconstituted angular body length and phragmocone size.

Measurement of the angle of the body chamber generally provides a convenient description and comparison of similarly shaped shells. For example, in embryonic and juvenile shells, body chamber angles are routinely measured and compared because the shape of the body chamber is similar, nearly conforming to a logarithmic spiral. The persistence of the same body chamber angle in small and large juveniles may imply that a constant volumetric relationship between the phragmocone and body chamber is maintained, perhaps in order to preserve neutral buoyancy. In other words, measurement of the body chamber angle may provide a convenient means for documenting the volumetric relationship between the phragmocone and body chamber in species that maintain the same shape through ontogeny. However, once a marked change in shape occurs, the angle of the body chamber is no longer an appropriate parameter to measure. The body chamber and phragmocone of an adult specimen of *S. whitfieldi* may exhibit the same volumetric ratio as that of the body chamber and phragmocone of a juvenile specimen but this will not be evident from angular measurements.

An alternative approach is to measure volume, or as an approximation, area. Area is easily measured on median sections of specimens with a planimeter. Figure 76 represents a plot of the measurements of body chamber area versus phragmocone area for eight adults belonging to *S. whitfieldi, S. preventricosus, S. depressus,* and *C. vermiformis*; two juveniles of *C. vermiformis*; and three ammonitellas of *S. preventricosus* and *C. vermiformis.* The slope of the line of best fit through these points equals .8839 and the coefficient of correlation equals .9764. This slope indicates slightly negative allometry, that is, the absolute ratio of body chamber area to phragmocone area decreases with increasing phragmocone area. This area relationship may reflect a volumetric relationship that is maintained to preserve near neutral buoyancy. The negative allometry suggests a tendency toward increased buoyancy in larger specimens, and, indeed, Tanabe (1977) interpreted a similar pattern in *Scaphites planus* as indicating a transition from a benthic to a planktonic mode of life. However, other parameters such as shell wall and septal thickness and the volume of occluded cameral water must also be considered in assessing buoyancy changes (see Westermann, 1973).

Microstructure, Ornament, and Attachment Scars at Maturity

Throughout most of ontogeny, the dorsal shell consists of the inner prismatic layer; the outer prismatic and nacreous layers wedge

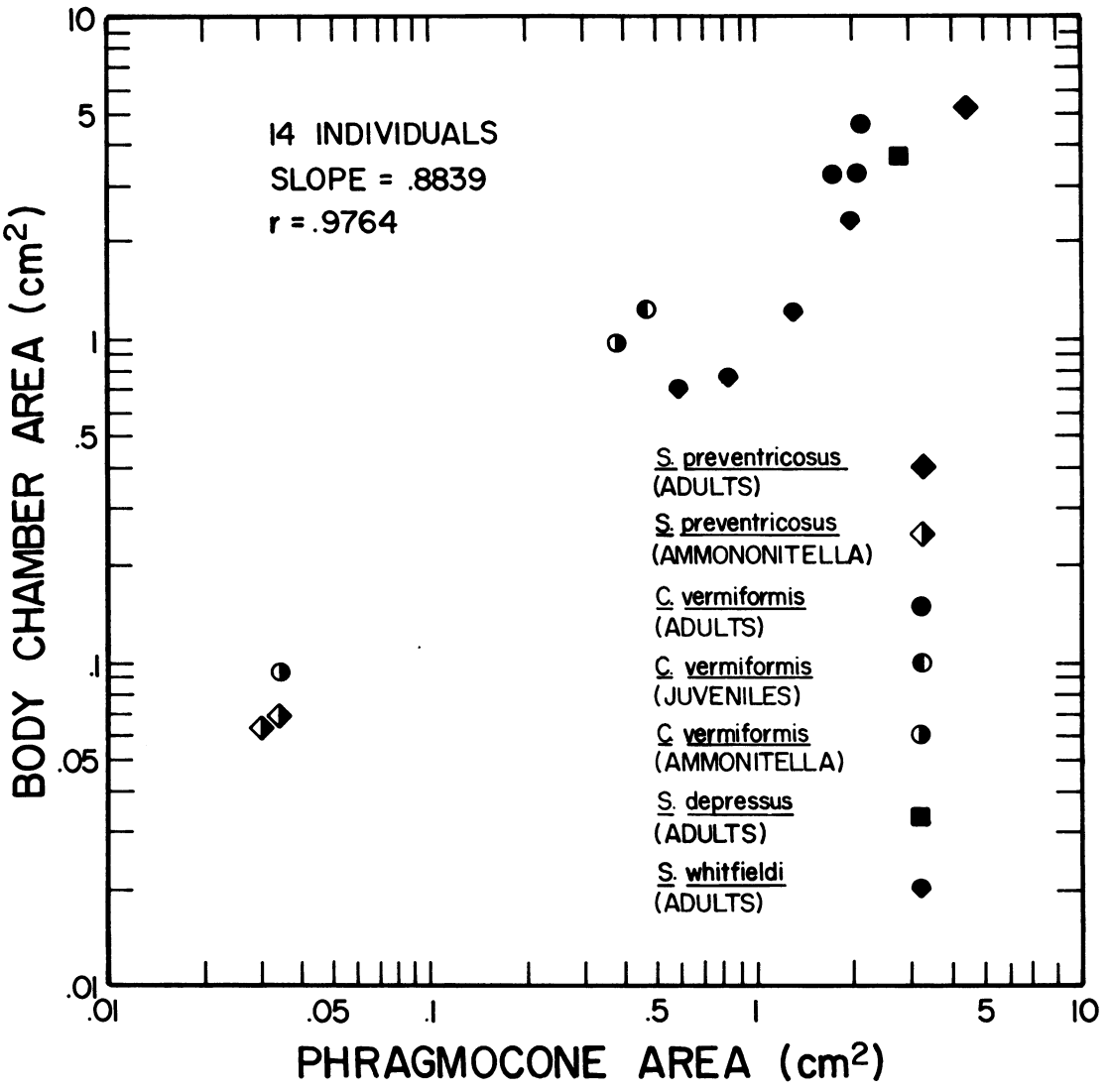

Fig. 76. Plot of body chamber area versus phragmocone area for 14 specimens representing various developmental stages in four scaphite species.

out at the umbilical shoulder (Birkelund and Hansen, 1974). However, at maturity the body chamber detaches from the coiled septate whorls but retains an impressed dorsal zone. The dorsal shell increases in thickness because the final body chamber is not supported by the buttressing of juxtaposed whorls, as in earlier ontogeny. This increase in dorsal shell thickness appears slightly before uncoiling and, as in the uncoiled shafts of *Baculites* and other heteromorphs, the dorsal wall of the scaphite body chamber consists of all three shell layers (see also Doguzhayeva and Mikhailova, 1982).

An interruption in ribbing or an attenuated sector of shell with subdued ornament commonly occurs near the base of the body chamber, which coincides in many species with the transition from a coiled to uncoiled shape. This pattern is especially common in species with an extended hooklike body chamber. For example, in *S. warreni* the base of the body chamber exhibits a wider spacing of ventral ribs (Cobban, 1951). In some indi-

viduals of *S. larvaeformis,* the ornament disappears altogether for a short distance immediately adoral of the base of the body chamber. This pattern of subdued ornamentation, called "stretch pathology" by Landman and Waage (1986), also appears on younger scaphites such as *S. hippocrepis* and *Hoploscaphites nicolleti* (see Cobban, 1969). Its presence is unclear but may indicate that this part of the mature body chamber was secreted rapidly. Indeed, specimens of scaphites with half-formed mature body chambers are virtually unknown.

Internal molds of scaphite body chambers also commonly display an isolated, oval-shaped muscle scar. It occurs on the midventer at the base of the body chamber and has been documented in many other ammonites. A midventral line or track sometimes appears adoral of the scar and persists for a variable distance beyond it. This track also appears on the body chambers of preserved juveniles. Jordan (1968) refers to this impression as a "sipho-strucktur" but its relation to a similar tracklike feature on the venter of the septate whorls is unclear.

Sexual Dimorphism

Like many other ammonites, scaphites exhibit sexual dimorphism (Cobban, 1969; Jeletzky and Waage, 1978; Crick, 1978). The dimorphs are referred to as microconchs and macroconchs and have been tentatively interpreted as males and females, respectively (Kennedy and Cobban, 1976). In addition to size, they are distinguished on the basis of the presence or absence of umbilical swellings at the base of the mature body chamber, the diameter of the umbilicus, the curvature of the umbilical seam, the profile of the umbilical shoulder, and the ratio of whorl width to whorl height at the base of the mature body chamber.

Among scaphites, size alone is not a definitive criterion for dimorphic separation. In the Maastrichtian species *Discoscaphites conradi,* "size is not a primary distinguishing characteristic owing to the great variability in size of both sexes" (Jeletzky and Waage, 1978). Similarly, size varies widely within dimorphs of *S. hippocrepis* and *S. leei* which are largely identified on the basis of size-independent criteria. Cobban (1969) indicated that "the range in size is such that the largest males [microconchs] are larger than the smallest females [macroconchs] but not as large as the largest females [macroconchs]." The largest macroconch is approximately five times the size of the smallest microconch. Within these dimorphs, the ratio of maximum size equals approximately 4:1. Cobban constructed two size histograms of *S. leei* III and *S. hippocrepis* I (the Roman numerals indicate chronologic subspecies) illustrating the size distributions of microconchs and macroconchs which were already diagnosed on criteria other than size. Size was defined as maximum length, including the body chamber, as illustrated in figure 61 (Cobban, 1969: fig. 2). Within species, the dimorphs overlap in size and, in fact, in *S. leei* III, a combined histogram for microconchs and macroconchs would exhibit only a single mode although a combined histogram for the smaller sample of *S. hippocrepis* I would suggest bimodality. Within species, larger specimens exhibit as much as one more whorl than smaller specimens. Size histograms for several scaphite species from Greenland, unsegregated with respect to sex, exhibit both unimodal and bimodal distributions (Birkelund, 1965). Within *S. cobbani,* the maximum size ratio equals 6:1. Larger specimens of *S. cobbani* and *S. rosenkrantzi* exhibit fewer whorls than smaller specimens, although intermediate size specimens occur which exhibit an intermediate number of whorls. In *Hoploscaphites constrictus,* dimorphism was identified based on the presence of two nonoverlapping size groups that exhibited a difference of one whorl (Makowski, 1962).

Within the Turonian-Santonian scaphites from the Western Interior, a well-marked dimorphism occurs in many species. Cobban (1951) assigned varietal names to these dimorphs when they were especially distinctive and later interpreted them as sexual in origin (Cobban, 1969). He based his diagnosis largely on size, stoutness, and the relative degree of uncoiling. Small, slender, evolute forms (microconchs) were interpreted as males whereas large, robust relatively involute forms (macroconchs) were interpreted as females. In some species such as *S. impendicostatus,* the macroconch possesses a prominent um-

bilical swelling at the base of the body chamber (Cobban, 1951: pl. 11, figs. 1–28) whereas in other species, such as *C. montanensis,* the umbilical swelling commonly appears in both dimorphs (Cobban, 1951: pls. 16, 17) and in still other species it is absent altogether.

As in other scaphites, size does not provide a firm basis for dimorphic separation in these species, except perhaps at the extreme ends of the spectrum. The ratio of maximum to minimum phragmocone diameter within species ranges from 1.7 in *S. preventricosus* to 4.6 in *S. carlilensis.* [Because within-species ratios are being compared among species, measurement of maximum length as employed by Cobban (1969) and Birkelund (1965) would do equally well and generally is more often used.] However, the size frequency distributions of phragmocone diameter are generally unimodal although the shape of the distribution is sensitive to sample size (figs. 62–67). Nevertheless, even in species that exhibit bimodal distributions, such as *S. larvaeformis,* specimens of intermediate size commonly occur between the modes.

The largest and perhaps most instructive sample consists of several hundred specimens of *S. whitfieldi* from a single concretion (B176a) and from several localities just south of the Black Hills (B176, B177, B192, B193). Both separate locality and combined locality histograms of phragmocone diameter describe normal distributions with a maximum size ratio of 2.8 (fig. 62). The histogram of the number of postembryonic whorls indicates a maximum difference of approximately one whorl between large and small specimens although intermediate size specimens appear (fig. 71). A histogram of maximum length, including the body chamber, of 266 specimens yields a skewed distribution with one prominent peak at 29 mm and successively smaller peaks at 35 and 49 mm (fig. 77). The maximum size ratio equals 2.21. Separation of these specimens into dimorphs based on a number of criteria other than size, including robustness, relative involuteness, inflation of the mature body chamber, curvature of the umbilical seam, diameter of the umbilicus, and the ratio of whorl width to whorl height at the base of the mature body chamber is represented in figure 77. The dimorphs overlap in size (maximum length) and the ratio of maximum size within each dimorph is reduced relative to that of the unsegregated population. The ratio equals 1.88 in microconchs and 1.65 in macroconchs. The maximum degree of overlap occurs between 32 and 38 mm in maximum length. The dimorphs themselves are intergradational in shape over this size range and the morphological criteria previously used to discriminate dimorphs are ineffective at these sizes. This ambiguity may be the result of analyzing a large sample with implications about the ease with which dimorphs are distinguished in very small samples or, and perhaps more likely, a phenomenon common to *S. whitfieldi* and several other scaphite species.

Mode of Life at Maturity

The mode of life of adult scaphites has been variously interpreted. Lehmann (1981) proposed that the adult scaphite leads a benthic existence shoveling up sediment. Tanabe (1977) suggested a benthic mode for loosely coiled forms and a planktonic mode for more tightly coiled forms. Later, however, Tanabe et al. (1978) favored a nektobenthic or mobile benthic mode of life for both forms. Chamberlain (1981: 320) does "not find any severe problems in accepting the view that . . . many of the heteromorphs were nektobenthonic . . . . In this regard, the similarity in overall shape between a scaphitid and a sea horse is uncanny." On the other hand, Klinger (1982: 346), following Ward and Westermann (1977), concluded that the most likely "mode of life is . . . that of a planktonic floater."

Presumably, if changes in shell shape indicate changes in mode of life, then the distinctive uncoiling of the adult body chamber must mark a change in the mode of life from that of the submature form. Similarly, an involute adult shape closely resembling that of the subadult shell must indicate the persistence of the same mode of life. When speculating on mode of life, the question of buoyancy arises. Superficially, measurements of phragmocone area versus body chamber area suggest that increased buoyancy correlates with involuteness (fig. 76). However, buoyancy is also dependent on the amount of cam-

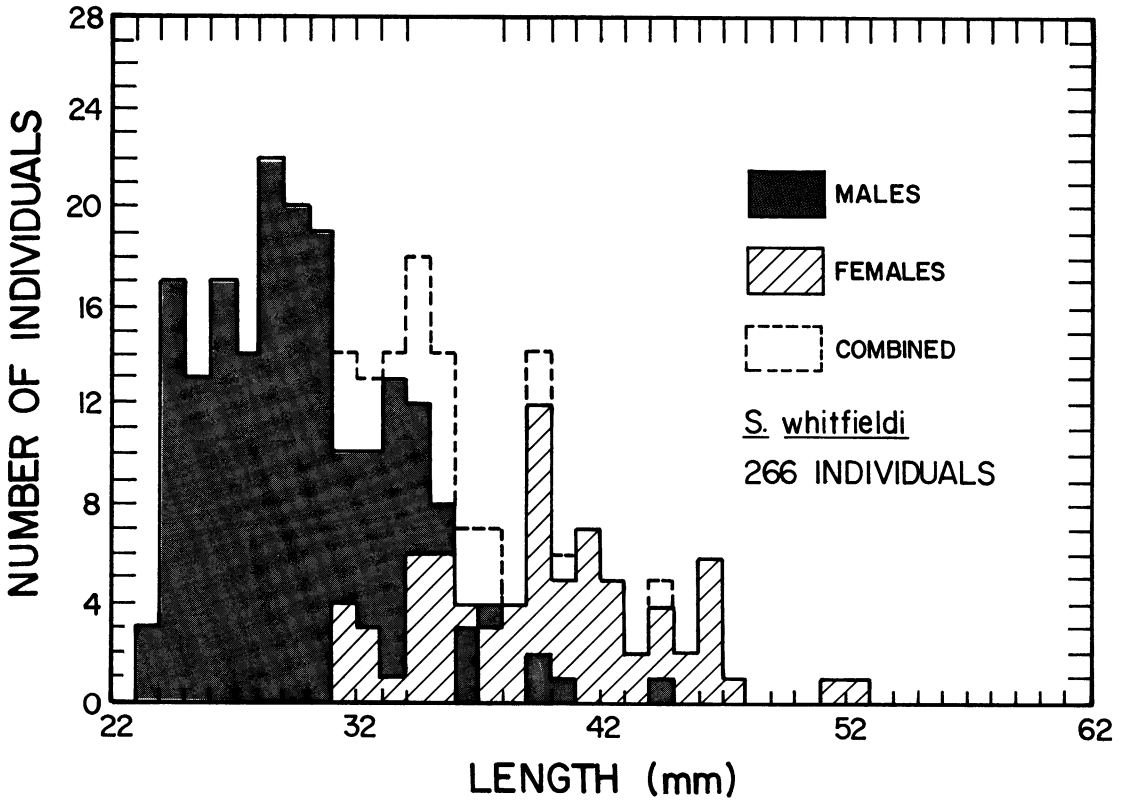

Fig. 77. Histogram of maximum length in dimorphically segregated and combined samples of *Scaphites whitfieldi*.

eral liquid occluded in the phragmocone and the growth pattern of shell and septal thickness.

It is perhaps more reasonable to argue from the standpoint of swimming capability and maneuverability. The submature scaphite with its planispirally coiled shell would presumably have been capable of some swimming, although the shape of the shell is not streamlined; the mode of life may have been nektobenthic. Uncoiling results in an increase in stability and a decrease in maneuverability because the distance between the centers of buoyancy and gravity diverges. This consequence of uncoiling seems to be implicit in all of the suggested modes of adult animals: benthic crawlers, near-bottom floaters or vagrants, and near-surface floaters.

However, the shells of larger species do not represent geometrically scaled-up versions of the shells of smaller species. For example, figure 75 illustrates that larger species tend to be more tightly coiled. Would a specimen of *S. depressus* at a diameter of 10 cm be inadaptive as a geometrically scaled-up version of *S. whitfieldi*? Would it pursue the same mode of life? One relevant point is that scaphites are never preserved with their adult body chambers half completed, or, in other words, with only half their long shaft formed. This may be due to an acceleration in the rate of growth at that point, but, in any event, hypotheses of shell orientations never consider the animal at this submature stage. Nevertheless, this stage was successfully incorporated as part of the ontogenetic development. Would a similarly long shaft be inadaptive in a scaled-up version of *S. whitfieldi*? Other heteromorphs exhibit long shafts at large sizes but this may not have been a viable combination within the scaphite Bauplan.

TABLE 21
Dimensions of the Protoconch and Ammonitella in 11 Specimens of *Pteroscaphites* sp.

Species	Protoconch width (μm)	Protoconch diameter (μm)	Ammonitella diameter (μm)	Ammonitella diameter / Protoconch diameter	Ammonitella angle (°)
P. praecoquus					
N = 1					
USGS locality D203		314.9	536.0	1.70	262
P. pisinnus					
N = 7					
locality B176a	427.7				
locality B176a	427.7				
locality B176a		314.9	589.6	1.87	296
locality B176a		299.5	558.0	1.86	277
locality B240a		348.4	670.0	1.92	265
locality B240b		348.4	643.2	1.85	294
locality B240c		361.8	656.6	1.81	260
P. auriculatus					
N = 3					
locality B228a	493.5				
locality B228a		308.2	575.4	1.87	278
locality B226					262

MICROMORPHS

Micromorphs display the same shape at maturity as other scaphites but are reduced in size. They are represented in the Turonian to Santonian of the Western Interior by the endemic genus *Pteroscaphites* Wright, which consists of six species. These species are rare and co-occur with many of the more normally sized scaphites. Several species develop lappets or auricles at the mature aperture although these features are smaller and less conspicuous than those in Jurassic ammonites (Cobban, 1951).

The early ontogeny of *Pteroscaphites* is similar to that in the co-occurring larger scaphite species. Its reduced adult size is not reflected in a proportionally smaller ammonitella. Table 21 lists the width and diameter of the protoconch, the diameter of the ammonitella, the ratio of ammonitella diameter to protoconch diameter, and the ammonitella angle for three species of *Pteroscaphites*, namely *P. praecoquus* (Cobban), *P. pisinnus* (Cobban), and *P. auriculatus* (Cobban). *P. praecoquus* co-occurs with *S. larvaeformis* and these two species display similarities in the sizes of their protoconch and ammonitella. *P. pisinnus* co-occurs with *S. whitfieldi* (locality B176a) and *S. nigricollensis* (locality B240). At locality B176a, the size of the embryonic shell of *P. pisinnus* is similar to that of the embryonic shell of *S. whitfieldi*. At locality B240, the size of the embryonic shell of *P. pisinnus* coincides more closely with that of the embryonic shell of *S. nigricollensis*. *P. auriculatus* co-occurs with *S. preventricosus* at localities B228a and B226 and these two species also display similarities in the sizes of their embryonic shell.

The growth patterns of whorl height and whorl width are approximately isometric based on four specimens of *P. pisinnus* and *P. auriculatus*. The measurements of whorl height versus shell diameter exhibit a slope of 1.032. Growth is isometric ($Z = .0007$) and the coefficient of correlation equals .9949 (fig. 78). The measurements of whorl width versus shell diameter exhibit a slope of .9604. Growth is also isometric ($Z = -.5630$) and

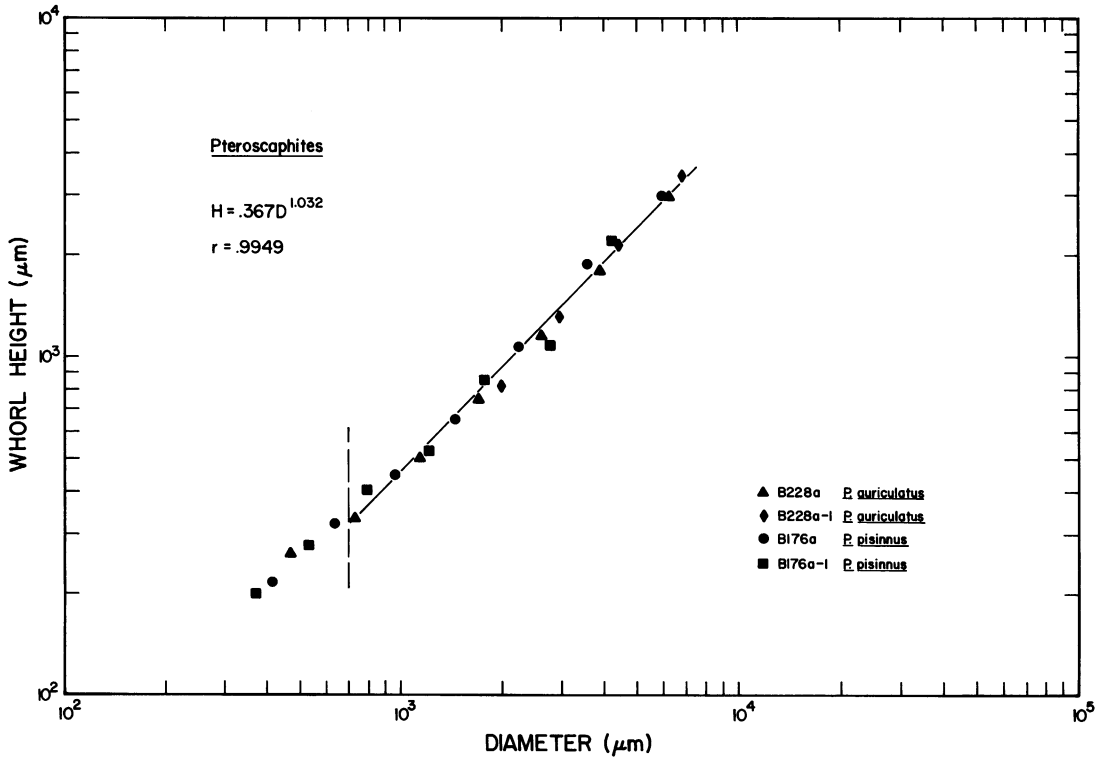

Fig. 78. Plot of whorl height versus shell diameter for four specimens of *Pteroscaphites auriculatus* and *P. pisinnus*. Dashed vertical line demarcates boundary of embryonic and postembryonic growth.

the coefficient of correlation equals .9449 (fig. 79). Nevertheless, as in the other scaphite species, these patterns of growth exhibit changes at 1 and 3–4 mm in diameter corresponding to approximately one-half and two whorls from the constriction, respectively. Measurements of umbilical diameter versus shell diameter, however, exhibit only a slight increase in scatter after approximately 3 mm in shell diameter (fig. 80). The measurement of $1/\pi$ multiplied by the natural logarithm of the ratio of shell diameters separated by one-half whorl versus shell diameter, which is equivalent to the constant of spiral expansion versus shell diameter, exhibits an increase after approximately 3 mm, particularly in *P. pisinnus* (fig. 81). The average value of k in these two species equals .1358, which is lower than that in the two co-occurring species, *S. whitfieldi* and *S. preventricosus*. Unlike the patterns in these latter two species, the constant of spiral expansion does not decrease abruptly at maturity.

As in the larger scaphite species, the change in shape at approximately two whorls from the constriction is nearly coincident with the first appearance of ornamentation. In three specimens of *P. pisinnus* the ornament first appears at 2.25, 2.27, and 2.39 whorls from the constriction. More remarkably, however, this number of whorls coincides approximately with the end of the mature phragmocone and the beginning of the adult body chamber. In fact, in most specimens the ornament first appears on the body chamber.

That the morphometric changes at approximately two whorls from the constriction correspond to the start of maturity in micromorphs lends additional support to the inference that a change in development or mode of life also occurs in the larger scaphites at approximately this same whorl number and size. Up to approximately two whorls from the constriction, both the micromorphs and the co-occurring larger species share a similar ontogenetic pattern interpreted as indicating direct development followed by a planktonic stage. The end of the presumed planktonic

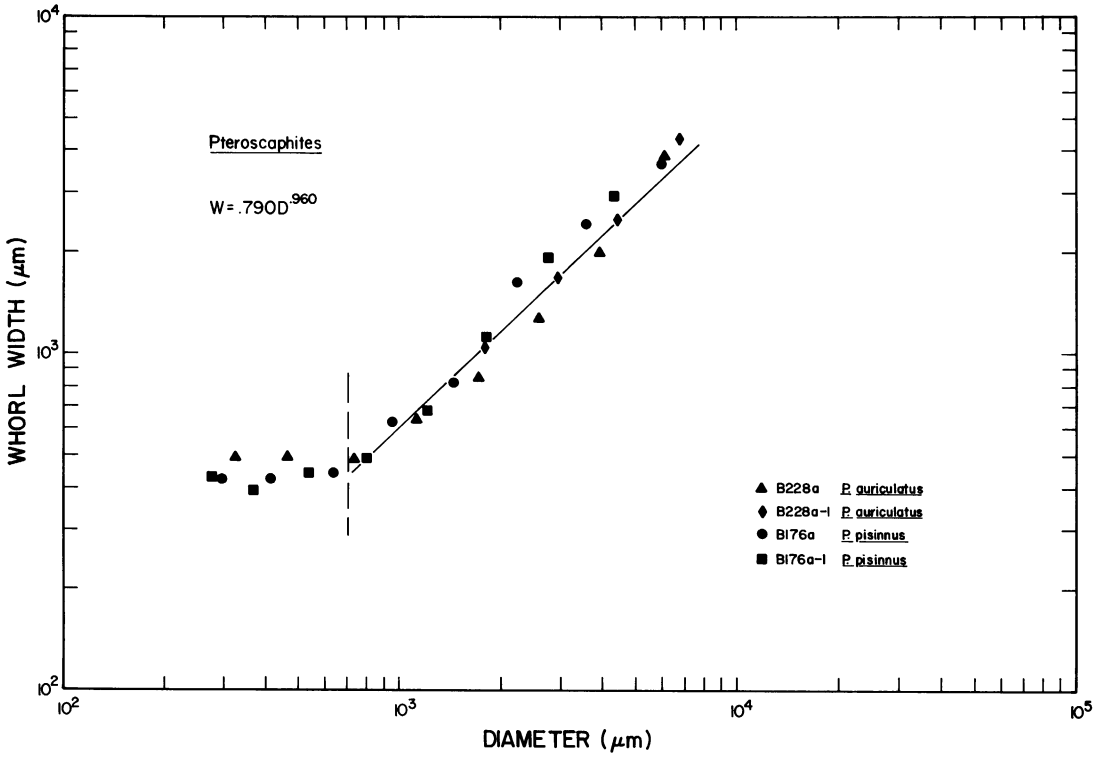

Fig. 79. Plot of whorl width versus shell diameter for four specimens of *Pteroscaphites auriculatus* and *P. pisinnus*. Dashed vertical line demarcates boundary of embryonic and postembryonic growth.

stage is marked by a gradual change in shape and the development of macro-ornamentation. At this point, *Scaphites* and *Cliioscaphites* may have assumed a nektobenthic mode of life but, in any event, maturity did not occur for at least another whorl. The micromorphs, however, accelerated into maturity at this point and developed their hook-like body chamber. This accelerated maturity at a juvenile size may have occurred via progenesis. The fact that maturity does not occur at a smaller size suggests that this size and whorl number represent a point of flexibility at which different developmental pathways may emerge.

The number of postembryonic whorls in the mature phragmocones of five specimens of *P. pisinnus* averages 2.38 and ranges from 2.25 to 2.52. In three specimens of *P. auriculatus,* the number of postembryonic whorls averages 2.58 and ranges from 2.25 to 2.89. In one specimen of *P. praecoquus* the number of whorls equals 2.23. Within species, the maximum whorl difference is 0.66 whorls. This value compares to a maximum difference of 1.4 whorls in the largest sample of *S. whitfieldi.* The number of postembryonic whorls in the adult phragmocones of the micromorphs may be compared to the minimum number in the adult phragmocones of the four co-occurring species: *S. larvaeformis,* 3.12; *S. whitfieldi,* 3.4; *S. nigricollensis,* 3.61; and *S. preventricosus,* 4.46. The minimum whorl difference between the micromorphs and the co-occurring larger species ranges from a little less to a little more than one whorl.

The maximum length of five specimens of *P. praecoquus* averages 9.5 mm (SD = 2.38) and ranges from 6.8 mm for one of the smallest mature scaphites ever observed, to 12.3 mm, nearly the same size as that of the smallest specimen of *S. larvaeformis.* The ratio of the largest to smallest specimen is 1.81. The maximum length of 14 specimens of *P. pisinnus* averages 8.8 mm (SD = .973) and ranges from 7.3 to 10.1 mm. The ratio of the largest to smallest specimen equals 1.4. The

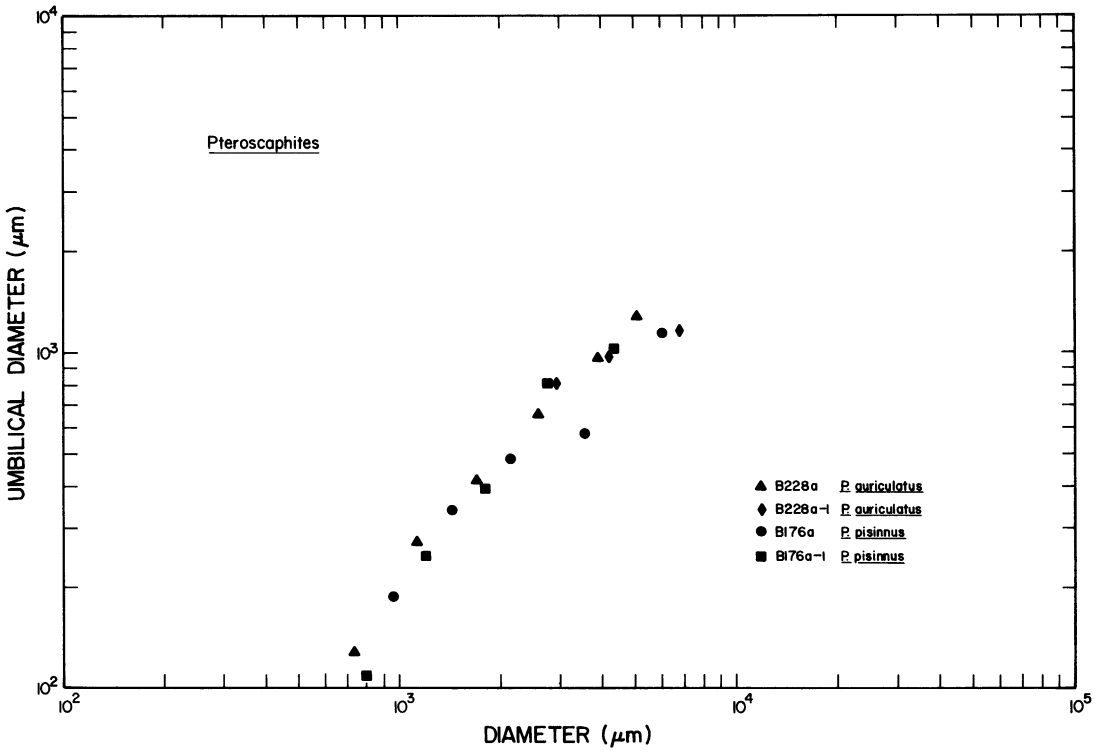

Fig. 80. Plot of umbilical diameter versus shell diameter for four specimens of *Pteroscaphites auriculatus* and *P. pisinnus.*

largest specimen is less than half the length of the smallest specimen of *S. whitfieldi.* The maximum length of 11 specimens of *P. auriculatus* averages 9.9 mm and ranges from 7.5 to 11.5 mm (SD = 1.233). The ratio of the largest to smallest individual equals 1.53. The largest specimen is approximately one-fifth the size of the smallest specimen of *S. preventricosus.*

P. auriculatus exhibits a weak dimorphism. This dimorphism is not based on size but rather on the diameter of the umbilicus, the curvature of the umbilical seam, and the profile of the umbilical shoulder (fig. 82). As in the larger scaphite species, these dimorphs consist of a robust relatively involute form (macroconch) and a slender relatively evolute form (microconch), which may represent the female and male, respectively.

The systematic relationship between *Pteroscaphites,* on the one hand, and *Scaphites* and *Clioscaphites,* on the other, is still unclear. Wiedmann (1965) has suggested, based mainly on the presence of lappets, that the micromorphs may represent the microconchs of the larger size scaphites. In Jurassic ammonites, lappets are invariably associated with microconchs. In addition, as I have indicated, the ontogenetic development of these three genera is very similar until 3–4 mm in shell diameter. Moreover, sexual dimorphism is weak in many species of *Scaphites* and *Clioscaphites,* whereas in the Maastrichtian genera *Hoploscaphites* and *Discoscaphites,* sexual dimorphism is well marked and, at the same time pteroscaphite-like forms are absent.

This interpretation is weakened, however, by (1) morphological differences between the lappets in *Pteroscaphites* and those in Jurassic ammonites suggesting differences in functional significance, (2) an apparent dimorphism within the larger scaphite species and *Pteroscaphites* itself, and (3) the rarity of *Pteroscaphites* and the lack of co-occurrence with all of the larger scaphite species. However, two new occurrences have been documented. A single individual assigned to *P. inaffectus* Crick was discovered in the range zone of *S. carlilensis* in Kansas (Crick, 1979). Another

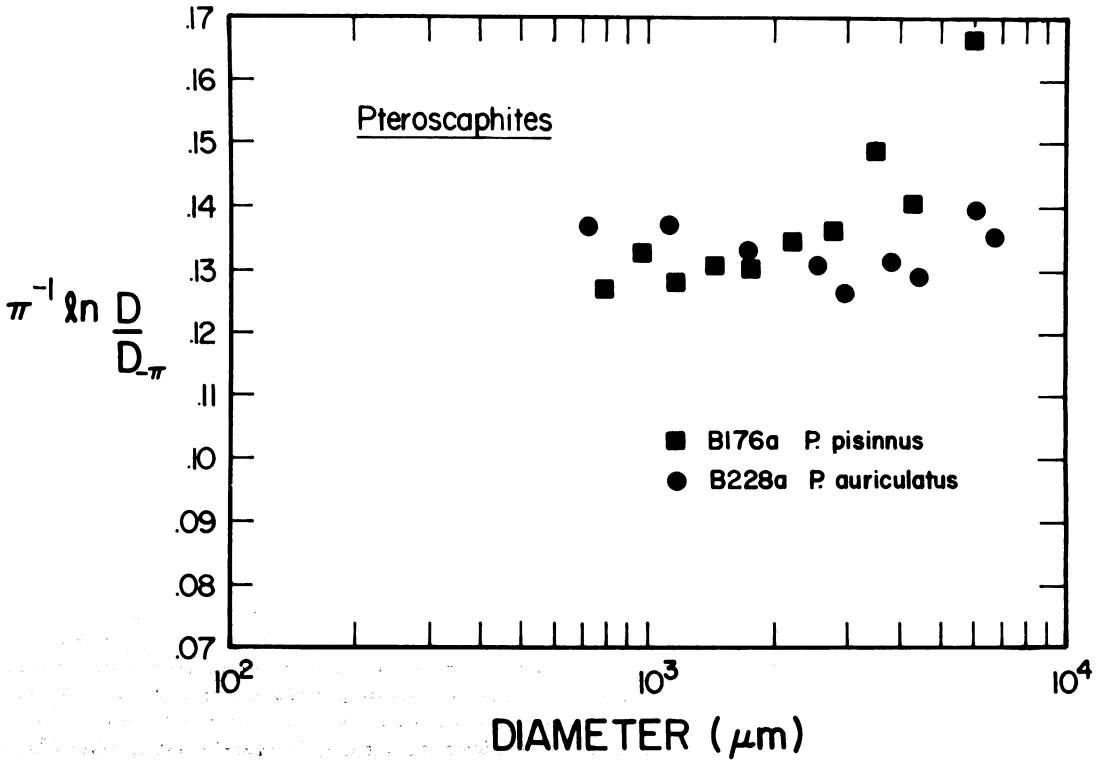

Fig. 81. Plot of $\pi^{-1}\ln(D/D_{-\pi})$ versus shell diameter for four specimens of *Pteroscaphites auriculatus* and *P. pisinnus*. The ratio is equivalent to the constant of spiral expansion (k).

individual probably belonging to the species *P. auriculatus* was discovered in the range zone of *S. ventricosus* on the Sweetgrass arch, Montana.

If the pteroscaphites do not represent microconchs, then they comprise a separate group. Is this group monophyletic as suggested by Cobban (1951) or polyphyletic? The interpretation that they represent a polyphyletic accumulation of iterative offshoots relies on the observation that the ontogeny of each species of *Pteroscaphites* most closely resembles that of the co-occurring larger scaphite species. However, species of *Pteroscaphites* associated with large species of *Clioscaphites* are approximately the same size as those associated with small species of *Scaphites*. Nor are species of *Pteroscaphites* more closely coiled when associated with more closely coiled species of *Clioscaphites*. In addition, the lappets, one of the defining characters of the group, is unlikely to have repeatedly evolved. Further work is required to resolve this perplexing problem.

CONCLUSIONS

The scaphites studied are endemic to the Western Interior and range from the Turonian to the Santonian. Their adult size, shape, and suture are distinctive and differentiate them from scaphites outside this region (Cobban, 1951). Their abundance and excellent preservation permit a detailed study of their ontogenetic development.

The ammonitellas of all these species are basically similar although they display interspecific variation in size and shape. The ammonitella consists of a protoconch and approximately 0.75 whorls, terminating in the primary constriction. The morphology of the caecum and prosiphon is also similar among species and may, in fact, characterize the entire order Ancyloceratina, although this requires further study. On the other hand, the

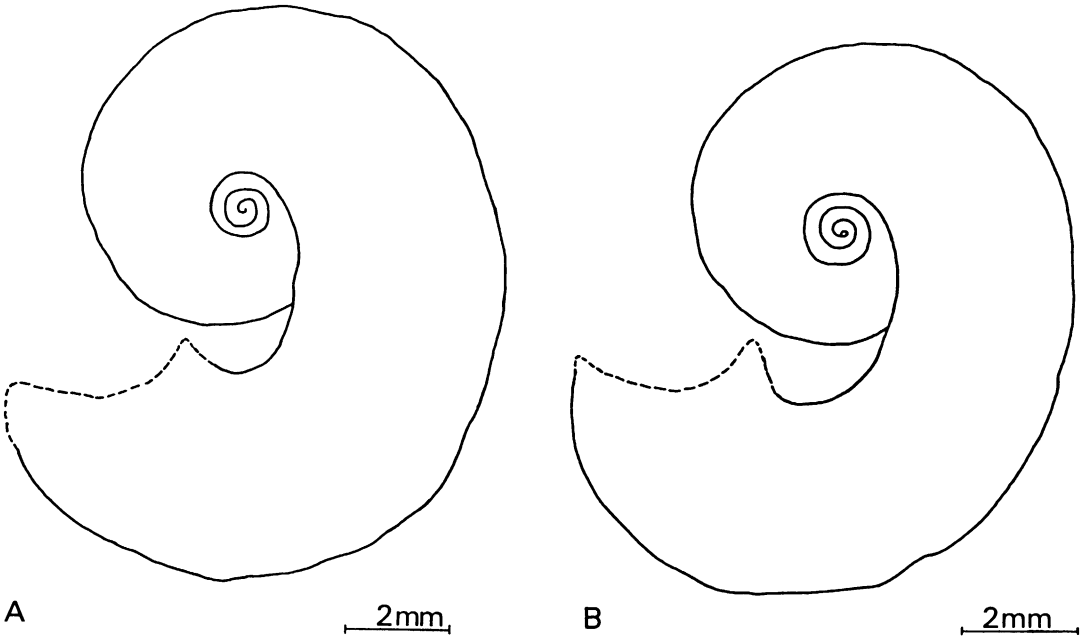

Fig. 82. Diagram illustrating macroconch (**A**) and microconch (**B**) of *Pteroscaphites auriculatus.*

necklike attachment of the proseptum appears to represent a distinctive scaphitid feature. The scaphite ammonitella closely resembles that of other ammonites and implies a common developmental scheme. Based on the uniform microstructure and micro-ornamentation of the ammonitella, development in Mesozoic ammonites may have been direct without an intervening larval stage. Finds of newly hatched scaphites and other ammonites suggest that hatching may have occurred after the proseptum had formed although additional septa may also have developed. The newly hatched animal may have followed a planktonic mode of life.

Subsequently, many of the scaphite species exhibit a morphological change at approximately two whorls from the primary constriction, corresponding to 3–4 mm in shell diameter. This change is well expressed in the growth patterns of the umbilical diameter and the constant of spiral expansion. The first appearance of macro-ornamentation also occurs at this diameter and correlates with a closer spacing of septa and attainment of a ventral position of the siphuncle. This change in morphology may mark the end of the planktonic stage and a gradual transition to a more active swimming role. In the pteroscaphites, it coincides with an abrupt transition to maturity, possibly via progenesis. Other ammonites display similar morphological changes at comparable sizes and whorl numbers, which may indicate similar changes in mode of development. Additional studies of shell microstructure and the growth of septal thickness and siphuncular diameter may lend further support to this interpretation.

The uncoiling of the final body chamber indicates the attainment of maturity. The ratio of the maximum to minimum diameter of the adult phragmocone ranges from a low of 1.7 in *S. preventricosus* to a high of 4.6 in *S. carlilensis.* A positive correlation occurs between mature phragmocone diameter and the number of postembryonic whorls, with larger individuals displaying more whorls. However, discrepancies in the size of the ammonitella and the constant of spiral expansion introduce variation into this relationship. The final adult size and the degree of uncoiling of the mature body chamber covary within and among species. Small, slender shells with relatively evolute body chambers contrast with large, robust shells with relatively involute body chambers. Within species, these morphs may represent males and females. Among species, more involute

forms tend to exhibit more whorls and attain a larger size before reaching maturity. At this stage, they closely resemble the shape of their juvenile shell and the juvenile shells of presumed ancestors. These patterns may suggest that shape is retarded with respect to developmental stage if a hypothesized evolutionary trend toward involuteness is correct.

SYSTEMATIC DESCRIPTIONS

SUBORDER ANCYLOCERATINA WIEDMANN, 1966

SUPERFAMILY ANCYLOCERATACEA MEEK, 1876

FAMILY SCAPHITIDAE MEEK, 1876

GENUS *SCAPHITES* PARKINSON, 1811

TYPE SPECIES: *Scaphites equalis* J. Sowerby designated by Meek (1876).

DIAGNOSIS: Early whorls in close contact; mature body chamber partially uncoils and reflexes hooklike upon the phragmocone; whorl section ranges from compressed to depressed. Ornament consists of simple ribs on the whorl flanks that branch and cross the venter and become separated by intercalary ribs. Umbilical and ventrolateral tubercles may occur on the mature body chamber. Aperture is constricted, commonly collared and may bear lappets. Dimorphism is well expressed in many species.

Scaphites larvaeformis Meek and Hayden

Scaphites larvaeformis Meek and Hayden, 1859: 58. Meek, 1876: 418, pl. 6, fig. 6a–c. Stanton, 1893: 182, pl. 44, fig. 2. Logan, 1898: 473, pl. 104, fig. 2. Reeside, 1927: 31. Cobban, 1951: 19–20, pl. 1, figs. 4–22. Cobban et al., 1956: text fig. 1A. Easton, 1960: text figs. 11.28-1a, b. Kennedy, 1977: text fig. 18 (3, 4). Kaufmann, 1977: 261, pl. 23, figs. 1, 2.

Scaphites larvaeformis Meek [and Hayden]. Frech, 1915: 556, fig. 1.

Holcoscaphites larvaeformis (Meek and Hayden). Nowak, 1916: 66.

HOLOTYPE: USNM 229; plesiotypes, USNM 106743–106745.

DESCRIPTION: *S. larvaeformis* Meek and Hayden consists of a small, slender morph (microconch, interpreted as the male) and a relatively large, inflated morph (macroconch, interpreted as the female) called *S. larvaeformis* Meek and Hayden var. *obesus* Cobban (1951: 20, pl. 1, figs. 16–22). Several aspects of the ontogenetic development of this species may be added to Cobban's (1951) description. The maximum diameter of the protoconch (D_1) averages 319 μm and ranges from 281 to 362 μm. The maximum width of the protoconch averages 404 μm and ranges from 362 to 461 μm. The ratio of average protoconch width to average protoconch diameter equals 1.27. The diameter of the ammonitella averages 582 μm and ranges from 525 to 649 μm. The ammonitella angle averages 280° and ranges from 266 to 300°. The average whorl widths, whorl heights, whorl width to whorl height ratios, umbilical diameters, and umbilical diameter to shell diameter ratios are listed for shell diameters between 1 and 10 mm in table 22. The average whorl width to whorl height ratios range from 1.37 to 1.45 between 1 and 10 mm indicating a depressed whorl section. The ratio of umbilical diameter to shell diameter decreases over ontogeny with the sharpest decrease in the initial 3 mm of shell diameter. The number of whorls at the first appearance of ventral ribs averages 2.26 whorls from the primary constriction and ranges from 2.00 to 2.58 whorls, approximately corresponding to a diameter of 4 mm.

Measurements of the diameter of the mature phragmocone of 55 specimens from various localities conform to a normal distribution with a mode between 12 and 14 mm, a mean of 13.7 mm, and a range from 6 to 24 mm. The ratio of the maximum to minimum values equals 4.0. The number of postembryonic whorls of 16 adult specimens ranges from 3.2 to 4.15 with a maximum difference of .95 whorls. The average shape ratio (L/r_1) of a sample of 50 adult specimens equals 3.31 indicating marked uncoiling of the adult body chamber and departure from a logarithmic spiral.

MATERIAL: Approximately 70 adults and

TABLE 22

Average Measurements of the Whorl Width (*W*), Whorl Height (*H*), the Ratio of Whorl Width to Whorl Height (*W/H*), Umbilical Diameter (*U*), and the Ratio of Umbilical Diameter to Shell Diameter (*U/D*), at Shell Diameters between 1 and 10 mm in *S. larvaeformis*[a]

D	*W*	*H*	*W/H*	*U*	*U/D*
1	0.59	0.43	1.37	0.30	0.30
2	1.33	0.93	1.43	0.52	0.26
3	2.07	1.47	1.41	0.67	0.22
4	2.87	2.05	1.40	0.79	0.20
5	3.70	2.60	1.42	0.86	0.17
6	4.55	3.17	1.44	0.94	0.16
7	5.45	3.78	1.44	0.99	0.14
8	6.32	4.36	1.45	1.04	0.13
9	7.20	4.99	1.44	1.07	0.12
10	8.10	5.58	1.45	1.10	0.10

[a] All measurements in mm.

TABLE 23

Average Measurements of the Whorl Width (*W*), Whorl Height (*H*), the Ratio of Whorl Width to Whorl Height (*W/H*), Umbilical Diameter (*U*), and the Ratio of Umbilical Diameter to Shell Diameter (*U/D*), at Shell Diameters between 1 and 10 mm in *S. whitfieldi*[a]

D	*W*	*H*	*W/H*	*U*	*U/D*
1	0.59	0.47	1.26	0.22	0.22
2	1.13	1.00	1.13	0.38	0.19
3	1.65	1.55	1.06	0.50	0.17
4	2.15	2.10	1.02	0.62	0.16
5	2.65	2.65	1.00	0.72	0.14
6	3.18	3.20	0.99	0.82	0.14
7	3.70	3.80	0.97	0.92	0.13
8	4.18	4.30	0.97	1.00	0.12
9	4.60	4.90	0.94	1.09	0.12
10	5.10	5.50	0.93	1.15	0.12

[a] All measurements in mm.

20 juveniles from various localities listed in the appendix.

DISTRIBUTION: *S. larvaeformis* is middle Turonian in age and occurs in the *Collignoniceras woollgari regulare* (Haas) subzone in the Western Interior of North America. It is present in the Pool Creek Member of the Carlile Shale along the flanks of the Black Hills in western South Dakota and northeastern Wyoming. Associated ammonites include *Tragodesmoceras carlilense* Cobban, *Binneyites carlilensis* Cobban, and rare specimens of *Hamites* sp. Other fossils include *Pseudomelania hendricksoni* Henderson, *Anisomyon apicalis* Sidwell, and *Inoceramus fragilis* Hall and Meek.

Scaphites whitfieldi Cobban, 1951

Scaphites warreni Meek and Hayden. Whitfield, 1880: 444, pl. 13, figs. 1–4. Stanton, 1893: pl. 40, figs. 5–7. Logan, 1898: pl. 104, figs. 5–7. Logan, 1899: pl. 23, fig. 5.

Scaphites warreni Meek [and Hayden]. Frech, 1915: pl. 557, fig. 4a, 4b.

Scaphites wyomingensis Meek. Whitfield, 1880: 446, pl. 13, figs. 5–7.

Scaphites whitfieldi Cobban. Cobban, 1951: 24, pl. 4, figs. 30–40; pl. 5, figs. 1–4. Kennedy and Cobban, 1976: pl. 8, fig. 1. Kauffman, 1977: 260, pl. 22, figs. 9, 10; pl. 23, figs. 9, 10. Hook and Cobban, 1979: 40, text fig. 3A–D.

HOLOTYPE: USNM 106735; paratypes, USNM 12258a, 106736, 106737, 106738a–b.

DESCRIPTION: Cobban (1951) provided a comprehensive description of this species. It is marked by dense and evenly spaced ribbing on the adult body chamber. Several points may be added concerning its ontogenetic development. The maximum diameter of the protoconch (D_1) averages 320 μm and ranges from 250 to 400 μm. The protoconch width averages 444 μm and ranges from approximately 360 to 520 μm. The ratio of average protoconch width to average protoconch diameter equals 1.39. The diameter of the ammonitella averages 620 μm and ranges from approximately 550 to 740 μm. The angle of the ammonitella averages 284° and ranges from 260 to 308°. The average whorl widths, whorl heights, whorl width to whorl height ratios indicate that after 5 mm in shell diameter to shell diameter ratios are listed for shell diameters between 1 and 10 mm in table 23. The average whorl width to whorl height ratios indicate that after 5 mm in shell diameter, the whorl section is slightly compressed (ratios equal slightly less than 1.0). The ratio of umbilical diameter to shell diameter decreases over ontogeny with the sharpest decrease in the initial 3 mm of shell diameter. The number of whorls at the first appearance of ventral ribs averages 2.15 whorls from the primary constriction and ranges from 1.46 to 2.58 whorls, approximately corresponding to 4 mm in shell diameter.

Measurements of the diameter of the mature phragmocone of 131 specimens from a single concretion (locality B176a) describe a slightly skewed normal distribution with a single mode between 20 and 22 mm or more broadly between 16 and 22 mm. Another sample of 71 specimens from other localities just south of the Black Hills (B176, B177, B192a, B192, and B193) also describes a normal distribution with a slightly higher mode between 26 and 28 mm. Altogether, the diameter of the mature phragmocone ranges from 12 to 34 mm and the ratio of maximum to minimum values equals 2.8. Measurements of the number of postembryonic whorls in the adult phragmocones of the sample from locality B176a describe a normal distribution with a single mode between 3.7 and 3.9 whorls or more broadly between 3.7 and 4.0 whorls, corresponding to the mode between 16 and 22 mm in phragmocone diameter. Most specimens exhibit a range between 3.6 and 4.3 whorls, yielding a difference of 0.7 whorls although the maximum difference equals 1.2 whorls. In another sample of 62 specimens of *S. whitfieldi* from other localities just south of the Black Hills (localities B176, B177, B192, B192a, and B193), measurements of the number of postembryonic whorls also conform to a normal distribution with a single mode between 3.9 and 4.0 whorls. The number of postembryonic whorls in this sample ranges from 3.4 to 4.7 whorls with a maximum difference of 1.3 whorls.

Measurements of maximum length (diameter) of a sample of 266 adults from various localities describe a right skewed distribution with one prominent peak at 29 mm and successively smaller peaks at 35 and 49 mm. The ratio of maximum to minimum values equals 2.21. *S. whitfieldi* exhibits dimorphism although size is not the sole, nor best, discriminating criterion except at the extreme ends of the spectrum. Cobban (1951, 1969) interpreted large, robust, relatively involute morphs as macroconchs or females and small, slender, evolute morphs as microconchs or males. Microconchs commonly range from 23 to 38 mm in overall length; macroconchs commonly range from 31 to 48 mm in overall length. The ratio of maximum to minimum size within each morph equals 1.88 in microconchs and 1.65 in macroconchs. However, between 32 and 38 mm in maximum length, the dimorphs intergrade in shape. The average shape ratio (L/r_1) of a sample of 108 specimens equals 3.0, indicating marked uncoiling of the body chamber and departure from a logarithmic spiral.

MATERIAL: Several hundred adults and numerous juveniles from various localities listed in the appendix.

DISTRIBUTION: *S. whitfieldi* is late Turonian in age and represents an important biostratigraphic zone in the Western Interior of North America (Cobban, 1984). It ranges from south-central Montana to southern New Mexico. Cobban (1984) summarizes its distribution as follows: in south-central Montana, the Carlile Member of the Cody Shale; along the flanks of the Black Hills, the Turner Sandy Member of the Carlile Shale; in north-central, south-central, and southeastern Wyoming, the Frontier Formation; in northwestern Colorado and northeastern Utah, the Mancos Shale; in east-central Utah, western Colorado, and northern New Mexico, the Juana Lopez Member of the Mancos Shale; in west-central and southern New Mexico, the D-Cross Tongue of the Mancos Shale; and in southeastern Colorado, an unnamed calcareous shale member at the top of the Carlile Shale. Associated fauna include *Inoceramus perplexus* Whitfield, *Prionocyclus novimexicanus* (Marcou), *Pteroscaphites pisinnus* (Cobban), *Baculites yokoyamai* Tokunaga and Shimiza, and *Lopha lugubris* (Conrad).

Scaphites preventricosus Cobban, 1951

Scaphites preventricosus Cobban, 1951: 26, pl. 9, figs. 1–16. Casanova, 1970: text fig. 79. Cobban, 1976: 124, pl. 1, figs. 8, 9. Kauffman, 1977: 263, pl. 24, figs. 1, 2. Cobban, 1983: 10, pl. 8, figs. 11–13.

HOLOTYPE: USNM 106675; paratypes, USNM 106676a–d, 106679.

DESCRIPTION: Cobban (1951) provided a comprehensive description of this species and its varietal form *sweetgrassensis* Cobban (1951: 27, pl. 10, figs. 18–25). The latter is more slender than the type species with a comparatively more uncoiled body chamber at maturity. It has been interpreted as the microconch of the dimorphic pair (Cobban,

TABLE 24
Average Measurements of the Whorl Width (*W*), Whorl Height (*H*), the Ratio of Whorl Width to Whorl Height (*W/H*), Umbilical Diameter (*U*), and the Ratio of Umbilical Diameter to Shell Diameter (*U/D*), at Shell Diameters between 1 and 10 mm in *S. preventricosus*[a]

D	*W*	*H*	*W/H*	*U*	*U/D*
1	0.56	0.42	1.33	0.27	0.27
2	1.14	0.91	1.25	0.54	0.27
3	1.72	1.43	1.20	0.75	0.25
4	2.30	1.95	1.18	0.91	0.23
5	2.90	2.53	1.15	1.02	0.20
6	3.50	3.10	1.13	1.10	0.18
7	4.10	3.67	1.12	1.16	0.16
8	4.70	4.20	1.12	1.21	0.15
9	5.28	4.80	1.10	1.26	0.14
10	5.85	5.40	1.08	1.30	0.13

[a] All measurements in mm.

1983). Several aspects of the ontogenetic development of this species may be added to Cobban's (1951) description. The maximum diameter of the protoconch (D_1) averages 344 μm and ranges from 295 to 415 μm. Protoconch width averages 460 μm and ranges from 395 to 559 μm. The ratio of average protoconch width to average protoconch diameter equals 1.34. The diameter of the ammonitella averages 645 μm and ranges from 575 to 714 μm. The ammonitella angle averages 274° and ranges from 257 to 292°. The average whorl widths, whorl heights, whorl width to whorl height ratios, umbilical diameters, and umbilical diameter to shell diameter ratios are listed for shell diameters between 1 and 10 mm in table 24. The average whorl width to whorl height ratios range from 1.08 to 1.33 indicating a slightly depressed whorl section especially at 1 to 3 mm in shell diameter. The ratio of umbilical diameter to shell diameter is largest at small diameters and steadily declines thereafter. The number of whorls at the first appearance of ventral ribs averages 2.18 whorls from the primary constriction and ranges from 1.72 to 2.62 whorls, corresponding to a diameter of 3 to 4 mm.

Measurements of the diameter of the mature phragmocone of a sample of 16 adults nearly conform to a normal distribution with a mode between 40 and 42 mm and a mean of 41.8 mm. The diameter of the phragmocone ranges from 30 to 52 mm; the ratio of maximum to minimum values equals 1.7. The number of postembryonic whorls in a sample of three adults ranges from 4.45 to 4.75 whorls with a maximum difference of approximately 0.3 whorls. The average shape ratio (L/r_1) of a sample of 12 adults equals 2.90, indicating moderate uncoiling of the adult body chamber and departure from a logarithmic spiral.

MATERIAL: Approximately 60 adults and juveniles from various localities listed in the appendix.

DISTRIBUTION: *S. preventricosus* is early Coniacian in age and comprises an important biostratigraphic zone in the Western Interior of North America. It occurs in the lower part of the Kevin Member of the Marias River Shale in north-central and northwestern Montana (Cobban et al., 1976). It also occurs in the upper part of the Frontier Formation in central and western Wyoming and in glacial drift in southwestern Minnesota. In the Kevin Member of the Marias River Shale in north-central Montana, the associated ammonites include *Scaphites mariasensis* Cobban, *S. impendicostatus* Cobban, *Pteroscaphites auriculatus* (Cobban), and *Baculites mariasensis* Cobban. Other fossils include *Inoceramus waltersdorfensis* Andert, *I. erectus* Meek, *Cremnoceramus deformis* (Meek), and *Actinocamax* sp.

GENUS *CLIOSCAPHITES* COBBAN, 1951

TYPE SPECIES: *Clioscaphites montanensis* Cobban, 1951.

DIAGNOSIS: Early whorls in close contact; mature body chamber tightly enrolled compared to the typical scaphitoid shape; whorl section commonly depressed. Ornament consists of simple ribs on the whorl flanks that branch and cross the venter and become separated by intercalary ribs. Ventrolateral tubercles and bullae may occur on the mature body chamber. Aperture is constricted and collared; suture displays trifid or asymmetrically bifid first lateral lobe. Dimorphism is well expressed in many species.

DISCUSSION: Cobban (1951) considered this genus as polyphyletic, originating from three independent lineages in the mid-Santonian.

However, the question of multiple origins requires further study.

Clioscaphites vermiformis (Meek and Hayden, 1862)

Scaphites vermiformis Meek and Hayden, 1862: 22. Meek, 1876: 423, pl. 6, fig. 4. Stanton, 1893: 183, pl. 44, fig. 3. Logan, 1898: 474, pl. 104, fig. 3. Reeside, 1927: 7, pl. 6, figs. 9, 10.
Holcoscaphites vermiformis (Meek and Hayden). Nowak, 1916: 66.
Clioscaphites vermiformis (Meek and Hayden). Cobban, 1951: 35–36, pl. 18, figs. 30–40. Wright, 1957: L228, fig. 255, 7a, b. Scott and Cobban, 1964: pl. 7, figs. 10–12. Miller, 1968: 44. Cobban, 1976: pl. 125, pl. 2, figs. 3, 4. Kennedy and Cobban, 1976: pl. 10, fig. 6; text fig. 17. Kauffman, 1977: 263, pl. 24, figs. 7, 8. Hattin, 1982: pl. 8, figs. 4, 5.

HOLOTYPE: USNM 1902; plesiotypes USNM 106713a–f.

DESCRIPTION: Like other Turonian-Santonian scaphites from the Western Interior, *C. vermiformis* consists of a relatively small, slender morph (microconch, interpreted as the male) and a more inflated, larger morph (macroconch, interpreted as the female) that was previously described as *C. vermiformis* var. *toolensis* Cobban (1951: 36, pl. 19, figs. 1–10). In addition to overall size, these dimorphs are differentiated on the basis of the umbilical diameter and the curvature of the umbilical seam of the mature body chamber. In microconchs, the umbilical diameter is larger and the umbilical seam is curved in side view. Several aspects of the ontogenetic development of this species may be added to Cobban's (1951) description. The maximum diameter of the protoconch (D_1) averages 338 μm and ranges from 289 to 436 μm. The minimum diameter of the protoconch (D_2) averages 270 μm and ranges from 233 to 372 μm. The ratio of the average maximum to average minimum diameter of the protoconch equals 1.24. Protoconch width averages 443 μm and ranges from 428 to 461 μm. The ratio of average protoconch width to average protoconch maximum diameter equals 1.31. The diameter of the ammonitella averages 685 μm and ranges from 603 to 817 μm. The ammonitella angle averages 286° and ranges from 259 to 306°. The average whorl widths, whorl heights, whorl width to whorl height ratios, umbilical diameters, and umbilical diameter to shell diameter ratios are listed for shell diameters between 1 and 10 mm in table 25. The whorl width to whorl height ratios range from 1.40 to 1.42 between 1 and 10 mm indicating a depressed whorl section. The ratio of umbilical diameter to shell diameter decreases with an accelerated decrease in the initial 3 mm of shell diameter. The number of whorls at the first appearance of ventral ribs averages 2.16 whorls from the primary constriction and ranges from 1.72 to 2.58 whorls, corresponding to approximately 4 mm in shell diameter.

TABLE 25
Average Measurements of the Whorl Width (*W*), Whorl Height (*H*), the Ratio of Whorl Width to Whorl Height (*W/H*), Umbilical Diameter (*U*), and the Ratio of Umbilical Diameter to Shell Diameter (*U/D*), at Shell Diameters between 1 and 10 mm in *C. vermiformis*[a]

D	*W*	*H*	*W/H*	*U*	*U/D*
1	0.67	0.47	1.42	0.25	0.25
2	1.44	1.01	1.42	0.34	0.17
3	2.25	1.58	1.42	0.35	0.12
4	3.04	2.16	1.41	0.34	0.08
5	3.90	2.78	1.40	0.38	0.08
6	4.78	3.40	1.40	0.47	0.08
7	5.65	4.02	1.40	0.58	0.08
8	6.56	4.67	1.40	0.70	0.09
9	7.40	5.30	1.40	0.82	0.09
10	8.30	5.95	1.40	0.93	0.09

[a] All measurements in mm.

Measurements of the diameter of the mature phragmocone of a sample of 22 adults yield a discontinuous histogram with a mode between 38 and 40 mm and a range between 26 and 56 mm. The ratio of maximum to minimum values equals 2.2. The number of postembryonic whorls in the mature phragmocone in a sample of six adults ranges from 4.4 to 5.0 whorls with a maximum difference of 0.6 whorls. The average shape ratio (L/r_1) of a sample of 26 adults equals 2.55 indicating a tightly coiled adult body chamber. However, in median section, the dorsum of the body chamber does not touch the phragmocone for a short distance.

MATERIAL: Approximately 90 adults and juveniles from various localities listed in the appendix.

DISTRIBUTION: *C. vermiformis* is middle Santonian in age and represents an important biostratigraphic zone in the Western Interior of North America. It ranges from northwestern New Mexico to north-central Montana. In north-central Montana it occurs in the upper part of the Kevin Member of the Marias River Shale (Cobban et al., 1976). In central and western Wyoming, it occurs in the Cody Shale. In southwestern Wyoming it is present in the Hilliard Shale. In western Colorado, central and northeastern Utah, and northwestern New Mexico, it occurs in the Mancos Shale. Associated ammonites include *Clioscaphites montanensis* Cobban, *Pteroscaphites coloradensis* (Cobban), *Baculites asper* Morton, and *B. codyensis* Reeside. Other fossils include *Inoceramus* (*Cordiceramus*) *cordiformis* Sowerby and *Pseudoperna congesta* (Conrad).

APPENDIX I
Fossil Localities

Locality no. on fig. 1	Yale Peabody Museum no.; USGS Mesozoic locality no.; other designation	Collector; year of collection; geographic description; stratigraphic assignment
1	B175	N. H. Landman and K. M. Waage, 1977, SE¼ sec. 12, T. 36 N, R. 62 W, Niobrara County, Wyo. Carlile Shale, 16½ ft above base of Turner Sandy Member.
1	B176 B176a, b	Same as B175. Carlile Shale, 8 ft septarian concretionary interval 27.5 ft above base of Turner Sandy Member. "a" and "b" refer to individual concretions.
1	B177	Same as B175. Carlile Shale, ledge 41.5 ft above base of Turner Sandy Member.
2	B178	N. H. Landman and K. M. Waage, 1977. Near Newcastle, in the NE¼ SW¼ sec. 33, T. 45 N, R. 61 W, Weston County, Wyo. Carlile Shale, limestone concretion layer 37 ft below base of Turner Sandy Member.
3	B180	N. H. Landman and K. M. Waage, 1977. Near Newcastle, in the W½ sec. 31, T. 45 N, R. 61 W, Weston County, Wyo. Carlile Shale, limestone concretions in upper 39.1 ft of Pool Creek Member.
4	21792	W. A. Cobban, 1948. One mile west of Newcastle, Weston County, Wyo. Carlile Shale, light grey limestone concretions 62 to 70 ft above base.
5	B183	N. H. Landman and K. M. Waage, 1977. Near Belle Fourche, in the NE¼ sec. 15, T. 9 N, R. 2 E, Butte County, S.Dak. Carlile Shale, ferruginous concretions in Pool Creek Member 28 or more ft below base of Turner Sandy Member.
6	B185 B185a, b, c, d	N. H. Landman and K. M. Waage, 1977. Near Belle Fourche, in the SW¼ sec. 33, T. 10 N, R. 2 E, Butte County, S.Dak. Carlile Shale, 20 ft interval in Turner Sandy Member 90.5 ft above base. "a" and "b" refer to interval 90.5–98.5 ft above base, and "c" and "d" refer to rusty weathering concretionary ledge 110.5 ft above base.
7	B186	N. H. Landman and K. M. Waage, 1977. Near Belle Fourche, in the NE¼ NW¼ sec. 10, T. 9 N, R. 2 E, Butte County, S.Dak. Carlile Shale, rusty weathering concretionary ledge 110.5 ft above base of Turner Sandy Member.
8	B187	N. H. Landman and K. M. Waage, 1977. Near Belle Fourche, in the center S½ sec. 29 and center N½ sec. 32, T. 10 N, R. 2 E, Butte County, S.Dak. Carlile Shale, concretionary interval 90.5–98.5 ft above base of Turner Sandy Member.
8	B188	Same as B187. Carlile Shale, concretionary ledge 110.5 ft above base of Turner Sandy Member.
9	21182	W. A. Cobban, 1947. Five miles north of Belle Fourche, in the SW¼ SE¼ SW¼ sec. 11, T. 9 N, R. 2 E, Butte County, S.Dak. Carlile Shale, in ferruginous concretions 57 to 81 ft above base.
9	21187	Same as 21182. Carlile Shale, from large calcareous concretions 14.5 ft above base of Turner Sandy Member.
10	21194	W. A. Cobban, 1947. Six miles north of Belle Fourche, in the N½ sec. 10, T. 9 N, R. 2 E, Butte County, S.Dak. Carlile Shale, 164 ft above base.

APPENDIX I—(*Continued*)

Locality no. on fig. 1	Yale Peabody Museum no.; USGS Mesozoic locality no.; other designation	Collector; year of collection; geographic description; stratigraphic assignment
11	21195	W. A. Cobban, 1947. Six miles north of Belle Fourche, in the NE¼ NE¼ NW¼ sec. 10, T. 9 N, R. 2 E, Butte County, S.Dak. Carlile Shale, 272 to 274 ft above base.
11	21198	Same as 21195. Carlile Shale, 293 ft above base.
12	B197 B197a, b	N. H. Landman and K. M. Waage, 1977. Near the Belle Fourche Reservoir, in the NE¼ SE¼ NE¼ sec. 18, T. 9 N, R. 4 E, Butte County, S.Dak. Carlile Shale, limestone concretions in Turner Sandy Member. "a" and "b" refer to individual concretions.
12	B198	Same as B197. Carlile Shale, small red weathering concretions in Turner Sandy Member.
13	D1166	E. Post, 1956. E½ sec. 19, T. 9 S, R. 5 E, Fall River County, S.Dak. Carlile Shale, sandy limestone concretions.
14	B189 B189a	N. H. Landman and K. M. Waage, 1977. Near Edgemont, in sec. 7, T. 9 S, R. 2 E, Fall River County, S.Dak. Carlile Shale, limestone concretions in Pool Creek Member 30–50 ft below base of Turner Sandy Member. "a" refers to single concretion.
14	B190	Same as B189. Carlile Shale, limestone concretions in Pool Creek Member 10–15 ft below base of Turner Sandy Member.
14	B191a, b, c, d	Same as B189. Carlile Shale, basal ledge of Turner Sandy Member. "a" refers to ledge and "b," "c," and "d" refer to concretions within ledge.
14	B192 B192a, b, c, d, e, f, g	Same as B189. Carlile Shale, 8 ft septarian concretionary interval 27.5 ft above base of Turner Sandy Member. Letters refer to individual concretions.
14	B193	Same as B189. Carlile Shale, ledge 41.5 ft above base of Turner Sandy Member.
15	D1524	D. E. Wolcott and C. E. Price, 1957. SE¼ SW¼ SW¼ sec. 35, T. 7 S, R. 6 E, Fall River County, S.Dak. Carlile Shale, base of Turner Sandy Member.
16	D203	R. J. Dunham, 1954. NE¼ NW¼ sec. 28, T. 35 N, R. 47 W, Dawes County, Nebr. Carlile Shale, large concretions of laminated silty limestone 131–133 ft above Greenhorn Limestone.
17	Conlin collection (USGS)	Ten miles northeast of Rock River, Albany County, Wyo.
18	D6928	W. A. Cobban, 1969. E½ NE¼ SW¼ sec. 31, T. 22 N, R. 75 W, Albany County, Wyo. Frontier Formation, Wall Creek Sandstone Member.
19	Lander, Wyo. (USGS collections)	Near Lander, in N½ SW¼ sec. 31, T. 2 N, R. 2 W, Freemont County, Wyo. Frontier Formation, 694 ft above base.
20	17956	W. G. Pierce and J. B. Reeside, Jr., 1938. SW¼ SW¼ sec. 26, T. 58 N, R. 103 W, Park County, Wyo. Cody Shale, 590 ft above base.
21	17957	W. G. Pierce and J. B. Reeside, Jr., 1938. Line Creek, in the SE¼ SW¼ sec. 26, T. 58 N, R. 103 W, Park County, Wyo. Cody Shale, 760 to 810 ft above base.
22	D4630	J. R. Gill and W. A. Cobban, 1964. At stream bend in SW¼ NE¼ SE¼ SW¼ sec. 26, T. 58 N, R. 103 W, Park County, Wyo. Cody Shale, small brownish-weathering limestone concretions and reddish ironstone concretions 760–810 ft above base.
23	B253	N. H. Landman and S. M. Kidwell, 1978. Line Creek, 40 miles north of Cody, in sec. 26, T. 58 N, R. 103 W, Park County, Wyo. Cody Shale.
24	D4636	J. R. Gill and C. R. Givens, 1964. NW¼ NW¼ SW¼ sec. 16, T. 8 S, R. 24 E, Carbon County, Mont. Colorado Shale, from lower third.
25	10888	G. F. Moulton, 1921. 17 miles southwest of Lodge Grass, near center of sec. 21, T. 7 S, R. 33 E, Big Horn County, Mont. Cody Shale, Niobrara Member.
26	21372	W. A. Cobban and R. W. Imlay, 1946. Two miles north of Fort Shaw, in the S½ secs. 35 and 36, T. 21 N, R. 2 W, Cascade County, Mont. Colorado Shale, 184 to 208 ft above top of calcareous shale of Greenhorn age.

APPENDIX I—(*Continued*)

Locality no. on fig. 1	Yale Peabody Museum no.; USGS Mesozoic locality no.; other designation	Collector; year of collection; geographic description; stratigraphic assignment
27	B203	N. H. Landman and S. M. Kidwell, 1978. Northwest of Kevin, in the secs. 3 and 4, T. 35 N, R. 3 W, Toole County, Mont. Marias River Shale, Kevin Member, corresponds stratigraphically to bed no. 139 in middle unit of type section (Cobban et al., 1976).
27	B204	Same as B203. Marias River Shale, Kevin Member, corresponds stratigraphically to USGS Mesozoic locality 21665 in middle unit of type section (Cobban et al., 1976).
27	B205	Same as B203. Marias River Shale, Kevin Member, corresponds stratigraphically to USGS Mesozoic locality D1244 in top unit of type section (Cobban et al., 1976).
28	B211	N. H. Landman and S. M. Kidwell, 1978. Northwest of Kevin, in the N½ sec. 15, T. 35 N, R. 3 W, Toole County, Mont. Marias River Shale, Kevin Member, corresponds stratigraphically to bed no. 20 in lower unit of type section (Cobban et al., 1976).
28	B212	Same as B211. Marias River Shale, Kevin Member, corresponds stratigraphically to bed no. 28 in lower unit of type section (Cobban et al., 1976).
29	20289	C. E. Erdmann and J. T. Gist, 1944. Three miles north of Kevin, in the SW¼ NE¼ NW¼ sec. 15, T. 35 N, R. 3 W, Toole County, Mont. Colorado Shale, about 600 ft below top.
30	D1245	W. A. Cobban, 1956. NE¼ NE¼ sec. 17, T. 35 N, R. 3 W, Toole County, Mont. Colorado Shale, 2.5 ft below bed D or 166 ft below top of formation (Cobban et al., 1976).
30	21665	C. E. Erdmann, 1956. Same geographic locality as D1245. Marias River Shale, brown to dusky red weathering concretionary dolostone 196 ft below top of Kevin Member.
31	23666	W. A. Cobban, C. E. Erdmann, R. W. Lemke, and E. K. Maughan. SW¼ NW¼ sec. 13, T. 35 N, R. 2 W, Toole County, Mont. Marias River Shale, 78.5 ft below top of Ferdig Member.
32	B240 B240a, b, c, d	N. H. Landman and S. M. Kidwell, 1978. North of Shelby, in sec. 3, T. 35 N, R. 2 W, Toole County, Mont. Marias River Shale, Ferdig Member, corresponds stratigraphically to bed no. 30 in middle unit of type section (Cobban et al., 1976). "a" and "b" refer to individual concretions and "c" and "d" to float.
32	B241	Same as B240. Marias River Shale, Ferdig Member, corresponds stratigraphically to bed no. 44 (USGS Mesozoic localtiy 20912) in upper unit of type section (Cobban et al., 1976).
33	D1253	C. E. Erdmann, 1956. SW¼ NE¼ SW¼ sec. 12, T. 35 N, R. 2 W, Toole County, Mont. Colorado Shale, 21 ft below bed O or 693 ft below top of formation (see Cobban et al., 1976).
34	D1363	W. A. Cobban, 1957, 1964. Ten miles north of Shelby, in SW¼ NE¼ NW¼ sec. 4, T. 33 N, R. 2 W, Toole County, Mont. Colorado Shale, from grey limestone concretion in sandy member.
35	D4485	W. A. Cobban, 1964. NE¼ NE¼ SE¼ sec. 16, T. 32 N, R. 2 W, Toole County, Mont. Marias River Shale, from 5 ft shale interval overlying D4484 which consists of limestone and ironstone concretions 8.5 ft below cone in cone layer.
36	23280	K. H. Holmes, 1951. SW¼ sec. 8, T. 30 N, R. 1 W, Toole County, Mont. Colorado Shale.
37	B217	N. H. Landman and S. M. Kidwell, 1978. Marias River, 8 miles south of Shelby, in the sec. 26, T. 31 N, R. 2 W, Toole County, Mont. Marias River Shale, lower of two limestone concretion layers in lower part of Kevin Member.
37	B218	Same as B217. Marias River Shale, upper of two limestone concretion layers in lower part of Kevin Member.
38	B225	N. H. Landman and S. M. Kidwell, 1978. Marias River, 5 miles south of Shelby, in

APPENDIX I—(*Continued*)

Locality no. on fig. 1	Yale Peabody Museum no.; USGS Mesozoic locality no.; other designation	Collector; year of collection; geographic description; stratigraphic assignment
	B225a	sec. 19, T. 31 N, R. 2 W, Toole County, Mont. Marias River Shale, upper of three fossiliferous limestone concretion layers in lower third of Kevin Member. "a" refers to a single concretion.
38	B226	Same as B225. Marias River Shale, middle of three fossiliferous limestone concretion layers in lower third of Kevin Member.
38	B227 B227a	Same as B225. Marias River Shale, lower of three fossiliferous limestone concretion layers in lower third of Kevin Member. "a" refers to single concretion.
39	B229	N. H. Landman and S. M. Kidwell, 1978. Marias River, 5 miles south of Shelby, in sec. 20, T. 31 N, R. 2 W, Toole County, Mont. Marias River Shale, Kevin Member, limestone concretions above large septarian concretions.
39	B230	Same as B229. Marias River Shale, Kevin Member, limestone concretions below large septarian concretions.
40	21421, 21422	W. A. Cobban, 1935. North bank of Marias River, 5.5 miles south of Shelby, in the NE¼ sec. 20, T. 31 N, R. 2 W, Toole County, Mont. Colorado Shale, 617 to 634 ft below top.
41	B228 B228a	N. H. Landman and S. M. Kidwell, 1978. Marias River, 5 miles south of Shelby, in the SE¼ sec. 13, T. 31 N, R. 3 W, Toole County, Mont. Marias River Shale, nonseptarian, fossiliferous, grey limestone concretions immediately below large septarian, nonfossiliferous, grey limestone concretions in lower third of Kevin Member. "a" refers to single concretion.
42	B233	N. H. Landman and S. M. Kidwell, 1978. Marias River, southwest of Shelby, in sec. 13, T. 31 N, R. 4 W, Toole County, Mont. Marias River Shale, Kevin Member, limestone concretions below lowest ironstone layer.
42	B234	Same as B233. Marias River Shale, Kevin Member, lowest ironstone layer.
42	B235 B235a	Same as B233. Marias River Shale, Kevin Member, large, orange weathering concretions and large, flat grey weathering concretions above lowest ironstone layer. "a" refers to a single concretion.
42	B236 B236a	Same as B233. Marias River Shale, Kevin Member, limestone concretions between lower and upper ironstone layers. "a" refers to float.
42	B237	Same as B233. Marias River Shale, Kevin Member, limestone concretions immediately below upper ironstone layer.
42	B238 B238a	Same as B233. Marias River Shale, Kevin Member, upper ironstone layer. "a" refers to float.
42	B239 B239a	Same as B233. Marias River Shale, Kevin Member, limestone concretions above upper ironstone layer. "a" refers to single concretion.
43	21425	W. A. Cobban, 1940. East bank of Marias River, 11 miles southwest of Shelby, in the W½ NE¼ SE¼ sec. 14, T. 31 N, R. 4 W, Toole County, Mont. Colorado Shale, 234 to 252 ft below top.
44	D422	B. R. Alto, 1956. Right bank of Summit Creek 175 ft south of Rocky Mountain Tavern, in the NE¼ SE¼ sec. 12, T. 30 N, R. 13 W, Glacier County, Mont. Colorado Shale.
45	D7230	J. R. Gill, Blanchard, and W. A. Cobban, 1969. North of Ivie Creek near center of sec. 13, T. 23 S, R. 6 E, Sevier County, Utah. Mancos Shale, from teepee-butte limestone masses about 100 ft above top of Ferron Sandstone Member.
46	D7227	J. R. Gill, Blanchard, and W. A. Cobban, 1969. Five miles east of Ferron, in the NW¼ sec. 9, T. 20 S, R. 8 E, Emery County, Utah. Mancos Shale, from a grey limestone concretion about 100 ft above the Ferron Sandstone Member.
47	23938	Seven miles south-southwest of Emery, Emery County, Utah. Mancos Shale.
48	D3684	W. A. Cobban, 1961. Highway 84, 0.3 miles north of state boundary, Tierra Amarilla Grant, Archuleta County, Colo. Mancos Shale, limestone concretions about 20 ft below marly bed.

APPENDIX I—(*Continued*)

Locality no. on fig. 1	Yale Peabody Museum no.; USGS Mesozoic locality no.; other designation	Collector; year of collection; geographic description; stratigraphic assignment
49	D4398	G. O. Bachman, 1961. North of Rio Gallena, in SE¼ sec. 15, T. 25 N, R. 1 E, Rio Arriba County, New Mex. Juana Lopez Member, about 75 ft above base.
50	D4083	G. R. Scott, 1963. Roadcut about 200 ft northwest of top of hill 1.6 miles southeast of junction of U.S. 84 and Colorado 17, Rio Arriba County, New Mex. Carlile Shale.
51	22608	Renfro collection. East of power plant on Mountain Creek Lake and east side of road and along hillside, Dallas County, Tex. Eagle Ford Group, Arcadia Park Formation.
52	6245	Conlin, 1934. Dallas County, Tex. Eagle Ford Group, Arcadia Park Formation.
53	21838	W. A. Cobban, 1948. Three miles south-southeast of Tipton, in the SE¼ sec. 4, T. 9 S, R. 10 W, Mitchell County, Kans. Carlile Shale, in upper part of Blue Hill Shale Member.

APPENDIX II
List of Scaphite Species Studied by Locality

Species	Localities
S. larvaeformis	B178, B180, 21792, B189, B189a, B190, D1166, D203
S. carlilensis	B183, 21182, 22608, 6245, 21838
S. warreni	21187, B191, B191a–d, D1524, D3684, D4398, D4083
S. whitfieldi	B175, B176, B176a, b, B177, 21194, B197, B197a, b, B198, B192, B192a–g, B193, Conlin collection (USGS), D6982, D7227
S. nigricollensis	B185, B185a–d, B186, B187, B188, 21195, 21198, 23666, B240, B240a–d, D1253, D1363, D422
S. corvensis	Lander, Wyo. (USGS), B241
S. preventricosus	21372, B211, B212, 20289, D4485, 23280, B217, B218, B225, B225a, B226, B227, B227a, B229, B230, 21421, 21422, B228, B228a
S. impendicostatus	B225a, B226, B228, D7230, 23938
S. depressus	17956, 17957, D4630, B253, D4636
C. vermiformis	10888, B203, B204, B205, 21665, B233, B234, B235, B235a, B236, B236a, B237, B238, B238a, B239, B239a, 21425
C. montanensis	B203, B204, B205, D1245, 21665, B238, B239
P. praecoquus	B189, B189a, B190, D203
P. pisinnus	B176a, B240a, b, c
P. auriculatus	B226, B228a

LITERATURE CITED

Arkell, W. J.
1957. Introduction to Mesozoic Ammonoidea. *In* R. C. Moore (ed.), *Treatise on invertebrate paleontology, part L.* Lawrence, Kansas: Geol. Soc. Am. and Univ. Kansas Press, pp. 81–129.

Arnold, J. M., and B. A. Carlson
1986. Living *Nautilus* embryos: preliminary observations. *Science, 232*:73–76.

Arnold, J. M., and L. D. Williams-Arnold
1977. Cephalopods: Decapoda. *In* A. C. Giese and J. S. Pearse (eds.), *Reproduction of marine invertebrates,* vol. 4. New York: Academic Press, pp. 243–284.

Bandel, K.
1975. Embryonalgehaeuse Karibischer Meso- und Neogastropoden (Mollusca). *Abh. Akad. Wiss. DDR, Abt. Math., Naturwiss. Tech., 1*:1–133.
1982. Morphologie und Bildung der fruehontogenetischen Gehaeuse bei conchiferen Mollusken. *Facies, 7*:1–198.

1986. The ammonitella: a model of formation with the aid of the embryonic shell of archaeogastropods. *Lethaia, 19*:171–180.

Bandel, K., and S. V. Boletzky
1979. A comparative study of the structure, development, and morphological relationships of chambered cephalopod shells. *Veliger, 21*:313–354.

Bandel, K., N. H. Landman, and K. M. Waage
1982. Micro-ornament on early whorls of Mesozoic ammonites: implications for early ontogeny. *J. Paleontol., 56(2)*:386–391.

Bayer, U.
1972. Zur Ontogenie und Variabilitaet des Jurassischen Ammoniten *Leioceras opalinum. N. Jahrb. Geol. Palaeontol. Abh., 140(3)*:306–327.
1977a. Cephalopoden-Septen Teil 1: Konstruktionsmorphologie des Ammoniten-Septums. *N. Jahrb. Geol. Palaeontol. Abh., 154*:290–366.
1977b. Cephalopoden-Septen Teil 2: Regel mechanismen in Gehaeuse und Septenbau der Ammoniten. *N. Jahrb. Geol. Palaeontol. Abh., 155*:162–215.

Birkelund, T.
1965. Ammonites from the Upper Cretaceous of West Greenland. *Medd. om Grønland 179*:1–192.
1979. The last Maastrichtian ammonites. *In* T. Birkelund and R. G. Bromley (eds.), *Cretaceous-Tertiary boundary events.* Copenhagen: Univ. of Copenhagen, pp. 51–57.

Birkelund, T., and H. J. Hansen
1968. Early shell growth and structures of the septa and the siphuncular tube in some Maastrichtian ammonites. *Medd. fra Dansk Geol. Forening Kobenhavn, 18*: 71–78.
1974. Shell ultrastructures of some Maastrichtian Ammonoidea and Coleoidea and their taxonomic implications. *Kong. Danske. Videnskab. Sel. Biol. Skr., 20(6)*:2–34.

Blind, W.
1979. The early ontogenetic development of ammonoids by investigation of shell structures. In *Symposium on Ammonoidea.* Systematics Assoc. York, Abstr., p. 32.

Boletzky, S. V.
1974. The "larvae" of Cephalopoda: a review. *Thalassia Jugoslavica, 10*:45–76.
1977. Post-hatching behavior and mode of life in Cephalopoda. *Zool. Soc. London Symp., 38*:557–567.

Branco, W.
1879–1880. Beitraege zur Entwickelungs Geschichte der fossilen Cephalopoden. *Palaeontographica (Stuttgart), 26(1879)*: 15–50; *27(1880)*:17–81.

Brown, A.
1892. The development of the shell in the coiled stage of *Baculites compressus* Say. *Proc. Acad. Nat. Sci. Philadelphia, 44*: 136–142.

Byers, C. W.
1979. Biogenic structures of black shale paleoenvironments. *Postilla, 174*:1–43.

Casanova, R.
1970. *An illustrated guide to fossil collecting.* Healdsburg, Calif.: Naturegraph Publishers, 128 pp.

Chamberlain, J. A.
1978. Permeability of the siphuncular tube of *Nautilus*: its ecologic and paleoecologic implications. *N. Jahrb. Geol. Palaeontol. Monatsh., 3*:129–142.
1981. Hydromechanical design of fossil cephalopods. *In* M. R. House and J. R. Senior (eds.), *The Ammonoidea. Systematics Assoc.* Special vol. 18. New York: Academic Press, pp. 289–336

Cobban, W. A.
1951. Scaphitoid cephalopods of the Colorado Group. *U.S. Geol. Surv. Prof. Pap. 239*: 39 pp.
1956. Cretaceous rocks along part of southeast boundary of Glacier National Park, Montana. *Am. Assoc. Petroleum Geol. Bull., 40(5)*:1001–1004.
1969. The Late Cretaceous ammonites *Scaphites leei* and *Scaphites hippocrepis* (DeKay) in the Western Interior of the United States. *U.S. Geol. Survey Prof. Pap. 618*:29 pp.
1976. Ammonite record from the Mancos Shale of the Castle Valley-Price-Woodside area, east-central Utah. *Brigham Young Univ. Geology Studies, 22(3)*: 117–126.
1983. Stratigraphy and paleontology of mid-Cretaceous rocks in Minnesota and contiguous areas. Molluscan fossil record from the northeastern part of the Upper Cretaceous seaway, Western Interior. *U.S. Geol. Surv. Prof. Pap. 1253-A*:25 pp.
1984. Mid-Cretaceous ammonite zones, Western Interior, United States. *Bull. Geol. Soc. Denmark, 3*:71–89.

Cobban, W. A., C. E. Erdmann, B. R. Alto, and C. H. Clark
1958. *Scaphites depressus* zone (Cretaceous)

in northwestern Montana. *Am. Assoc. Petroleum Geol. Bull., 42(3)*:656–664.

Cobban, W. A., C. E. Erdmann, R. W. Lemke, and E. K. Maughan
1959. Revision of Colorado Group on Sweetgrass arch, Montana. *Am. Assoc. Petroleum Geol. Bull., 43(12)*:2786–2796.
1976. Type sections and stratigraphy of the Members of the Blackleaf and Marias River Formations (Cretaceous) of the Sweetgrass arch, Montana. *U.S. Geol. Surv. Prof. Pap. 974*:66 pp.

Cobban, W. A., W. L. Rohrer, and C. E. Erdmann
1956. Discovery of the Carlile (Turonian) ammonite *Collignoniceras woollgari* in northwestern Montana. *J. Paleontol., 30(5)*:1269–1272.

Cochran, J. K., and N. H. Landman
1984. Radiometric determination of the growth rate of *Nautilus* in nature. *Nature, 308*:725–727.

Cochran, J. K., D. M. Rye, and N. H. Landman
1981. Growth rate and habitat of *Nautilus pompilius* inferred from radioactive and stable isotope studies. *Paleobiology, 7(4)*: 469–480.

Crick, R. E.
1978. Morphological variations in the ammonite *Scaphites* of the Blue Hill Member, Carlile Shale, Upper Cretaceous, Kansas. *Univ. Kansas Paleontol. Contrib., Pap. 88*. 28 pp.
1979. A pteroscaphitid (Cephalopoda, Ammonoidea) from the Upper Cretaceous (Turonian) of Kansas. *J. Paleontol., 53(1)*:98–102.

Crickmay, C. H.
1925. The discovery of the prosiphon in Cretaceous ammonites from California, with remarks upon the function of the organ. *Am. J. Sci., 9*:229–232.

Crocker, K. C., M. J. DeNiro, and P. D. Ward
1985. Stable isotopic investigations of early development in extant and fossil chambered cephalopods I. Oxygen isotopic composition of eggwater and carbon isotopic composition of siphuncle organic matter in *Nautilus*. *Geochim. Cosmochim. Acta, 49*:2527–2532.

Currie, E. D.
1942. Growth changes in the ammonite *Promicroceras marstanense* Spath. *Proc. Roy. Soc. Edin., B*:344–367.
1943. Growth stage in some species of *Promicroceras*. *Geol. Mag., 80*:15–22.
1944. Growth stages in some Jurassic ammonites. *Trans. Proc. Roy. Soc. Edin., 61(6)*:171–198.

Cutbill, J. L., and C. L. Forbes
1967. Graphical aids for the description and analysis of variation in fusuline foraminifera. *Palaeontology, 10(2)*:322–337.

Davis, R. A., and W. Mohorter
1973. Juvenile *Nautilus* from the Fiji Islands. *J. Paleontol., 47*:925–928.

Denton, E. J., and J. P. Gilpin-Brown
1966. On the buoyancy of the pearly *Nautilus*. *J. Mar. Biol. Assoc. (UK), 46*:723–759.

Doguzhayeva, L.
1982. Rhythms of ammonoid shell secretion. *Lethaia, 15*:385–394.

Doguzhayeva, L., and I. Mikailova
1982. The genus *Luppovia* and the phylogeny of Cretaceous heteromorph ammonoids. *Lethaia, 15*:55–65.

Druschits, V. V., and L. A. Doguzhayeva
1974. Some morphogenetic characteristics of phylloceratids and lytoceratids (Ammonoidea). *Paleontol. J., 1*:37–48.

Druschits, V. V., L. A. Doguzhayeva, and I. A. Mikhaylova
1977a. The structure of the ammonitella and the direct development of ammonites. *Paleontol. J., 2*:188–199.

Druschits, V. V., L. A. Doguzhayeva, and T. A. Lominadze
1977b. Internal structural features of the shell of Middle Callovian ammonites. *Paleontol. J., 3*:271–284.

Druschits, V. V., and N. Khiami
1970. Structure of the septa, protoconch walls and initial whorls in early Cretaceous ammonites. *Paleontol. J., 1*:26–38.

Dunbar, C. O., and J. W. Skinner
1937. Permian Fusulinidae of Texas. *Bull. Univ. Tex. Sci. Ser., 3701*:517–825.

Easton, W. H.
1960. *Invertebrate paleontology*. New York: Harper and Brothers, 701 pp.

Erben, H. K., G. Flajs, and A. Siehl
1969. Die fruehontogenetische Entwicklung der Schallenstruktur ectocochleaten Cephalopoden. *Palaeontogr. Abt. A, 132*: 1–54.

Frech, F.
1915. Ueber *Scaphites*. *Centralbl. Mineralogie, Jahrb., 21*:553–568.

Gill, J. R., and W. A. Cobban
1966. The Red Bird section of the Upper Cretaceous Pierre Shale in Wyoming. *U.S. Geol. Surv. Prof. Pap. 393-A*:73 pp.

Gould, S. J.
1966. Allometry and size in ontogeny and phylogeny. *Biol. Rev., 41*:587–640.
1977. *Ontogeny and phylogeny*. Cambridge, Mass.: Belknap Press of Harvard Univ. 501 pp.

Grandjean, F.
1910. Le siphon des ammonites et des belémnites. *Soc. Géol. Fr., Bull. 10*:496–519.
Gutjahr, A. L., and S. C. Hook
1981. Statistical method for analysis of planispiral coiling in shelled invertebrates. *New Mexico Bur. Mines and Mineral Resources Circular 173*. 14 pp.
Hamada, T., and S. Mikami
1977. A fundamental assumption on the habitat condition of *Nautilus* and its application to the rearing of *N. macromphalus*. *Sci. Pap. Coll. Gen. Educ., Univ. Tokyo, 27(1)*:31–39.
Hattin, D. E.
1982. Stratigraphy and depositional environment of Smoky Hill Chalk Member, Niobrara Chalk (Upper Cretaceous) of the type area, western Kansas. *Kansas Geol. Surv. Bull. 225*, 108 pp.
Hayami, I., and A. Matsukuma
1970. Variation of bivariate characters from the standpoint of allometry. *Palaeontology, 13(4)*:588–605.
Henderson, R. A.
1973. Clarence and Raukumara Series (Albian-?Santonian) Ammonoidea from New Zealand. *J. Roy. Soc. N.Z., 3*:71–123.
Hewitt, R. A.
1985. Significance of early septal ontogeny in ammonoids and other ectocochliates. *Second Int. Cephalopod Symp., Tuebingen, Abst.*, p. 16.
Hirano, H.
1975. Ontogenetic study of Late Cretaceous *Gaudryceras tenuiliratum*. *Mem. Fac. Sci., Kyushu Univ., Ser. D., Geol., 22*: 165–192.
1981. Growth rates in *Nautilus macromphalus* and ammonoids: its implications. *Int. Symp. Concept. Meth. Paleontol., Barcelona, 1981*:141–146.
Hook, S. C., and W. A. Cobban
1979. *Prionocyclus novimexicanus* (Marcou)—common Cretaceous guide fossil in New Mexico. *In* F. E. Kottlowski et al., *New Mexico Bur. Mines and Mineral Resources Ann. Rept., 1977–1978*, pp. 34–42.
House, M. R.
1965. A study in the Tornoceratidae: the succession of *Tornoceras* and related genera in the North American Devonian. *Phil. Trans. Roy. Soc. London, Ser. B, 250(763)*:79–130.
Huxley, J. S.
1932. *Problems of relative growth*. New York: Dial Press, 276 pp.
Hyatt, A.
1894. Phylogeny of an acquired characteristic. *Proc. Am. Phil. Soc., 32(143)*:349–647.
Imbrie, J.
1956. Biometrical methods in the study of invertebrate fossils. *Bull. Am. Mus. Nat. Hist., 108*:215–252.
Jablonski, D., and R. A. Lutz
1980. Larval shell morphology: ecology and paleoecological applications. *In* D. C. Rhoads and R. A. Lutz (eds.), *Skeletal growth of aquatic organisms*. New York: Plenum, pp. 323–377.
Jackson, R. T.
1890. Phylogeny of the Pelecypoda, the Aviculidae and their allies. *Mem. Bos. Soc. Nat. Hist., 4(8)*:277–400.
Jeletzky, J. A., and K. M. Waage
1978. Revision of *Ammonites conradi* Morton, 1834 and the concept of *Discoscaphites* Meek 1870. *J. Paleontol., 52(5)*:1119–1132.
Jordan, R.
1968. Zur Anatomie mesozoischer Ammoniten nach den Strukturelementen der Gehaeuse—Innenwand. *Beih. Geol. Jahrb., 77*:1–64.
Kahn, P. G., and S. M. Pompea
1978. Nautiloid growth rhythms and dynamical evolution of the earth-moon system. *Nature, 275*:606–611.
Kant, R., and J. Kullmann
1973. "Knickpunkte" in allometrischen Wachstum von Cephalopoden-Gehaeusen. *N. Jahrb. Geol. Palaeontol. Abh., 142(1)*:97–114.
Kaufmann, E. G.
1977. Illustrated guide to biostratigraphically important macrofossils, Western Interior Basin, U.S.A. *The Mountain Geologist, 14(3–4)*:225–274.
1979. Cretaceous. *In* R. A. Robison and C. Teichert (eds.), *Treatise on invertebrate paleontology, part A. Introduction*. Lawrence, Kansas: Geol. Soc. Am. and Univ. Kansas Press, pp. 418–487.
Kennedy, W. J.
1977. Ammonite evolution. *In* A. Hallam (ed.), *Developments in paleontology and stratigraphy*, vol. 5. Amsterdam: Elsevier, pp. 251–302.
Kennedy, W. J., and W. A. Cobban
1976. Aspects of ammonite biology, biogeography, and biostratigraphy. *Spec. Pap. Palaeontol., 17*:133 pp.
Klinger, H. C.
1982. Speculations on buoyancy control and ecology in some heteromorph ammonites. *In* M. R. House and J. R. Senior

(eds.), *Systematics Assoc.* Special vol. 18. New York: Academic Press, pp. 337–355.

Kulicki, C.
1974. Remarks on the embryogeny and post-embryonal development of ammonites. *Acta Palaeontol. Polonica, 20*:201–224.
1979. The ammonite shell: its structure, development and biological significance. *Acta Palaeontol. Polonica, 39*:97–142.

Kulicki, C., and A. Wierzbowski
1983. The Jurassic juvenile ammonites of the Jagua Formation, Cuba. *Acta Palaeontol. Polonica, 28(3, 4)*:369–384.

Kullmann, J., and J. Scheuch
1972. Absolutes und relatives Wachstum bei Ammonoideen. *Lethaia, 5*:128–146.

Landman, N. H.
1982. Embryonic shells of *Baculites. J. Paleontol., 56(5)*:1235–1241.
1983. Ammonoid growth rhythms. *Lethaia, 16*:248.
1985. Preserved ammonitellas of *Scaphites* (Ammonoidea, Ancyloceratina). *Am. Mus. Novitates, 2815*:1–10.
1987. Early ontogeny of Mesozoic ammonites and nautilids. *N. Jahrb. Geol. Palaeontol.* In press.

Landman, N. H., and K. Bandel
1985. Internal structures in the early whorls of Mesozoic ammonites. *Am. Mus. Novitates, 2823*:1–21.

Landman, N. H., and J. K. Cochran
1987. Growth and longevity. *In* W. B. Saunders and N. H. Landman (eds.), *Living Nautilus.* In press.

Landman, N. H., D. M. Rye, and K. Shelton
1983. Early ontogeny of *Eutrephoceras* compared to Recent *Nautilus* and Mesozoic ammonites: evidence from shell morphology and light stable isotopes. *Paleobiology, 9(3)*:269–279.

Landman, N. H., and K. M. Waage
1982. Terminology of structures in embryonic shells of Mesozoic ammonites. *J. Paleontol., 56(5)*:1293–1295.
1986. Shell abnormalities in scaphitid ammonites. *Lethaia, 19*:211–224.

Lehmann, U.
1981. *The ammonites: their life and their world,* J. Lettau, translator. Cambridge: Cambridge University Press, 246 pp.

Logan, W. N.
1898. The invertebrates of the Benton, Niobrara, and Fort Pierre Groups. *Kansas Univ. Geol. Surv., 4(8)*:431–578.
1899. Contributions to the paleontology of the Upper Cretaceous series. *Field Mus. Nat. Hist. Pub. 36, Geol. ser. 1*:207–211.

Makowski, H.
1962. Problems of sexual dimorphism in ammonites. *Acta Palaeontol. Polonica, 12*: 1–92.

McGhee, G. R.
1980. Shell form in the biconvex articulate Brachiopoda: a geometric analysis. *Paleobiology, 6(1)*:57–76.

Meek, F. B.
1876. Invertebrate Cretaceous and Tertiary fossils of the Upper Missouri Country. *U.S. Geol. Surv. Terr. Rep. 9*:629 pp.

Meek, F. B., and F. V. Hayden
1859. Descriptions of new organic remains collected in Nebraska Territory in the year 1857 by Dr. F. V. Hayden. *Acad. Nat. Sci. Philadelphia Proc. 10*:41–59.
1862. Descriptions of new Cretaceous fossils from Nebraska Territory, collected by the expedition sent out by the Government under the command of Lieut. John Mullon, U.S. Topographical Engineers, for the location and construction of a wagon road from the sources of the Missouri to the Pacific Ocean. *Acad. Nat. Sci. Philadelphia Proc.*:21–28.

Meischner, D.
1968. Pernicioese Epoeke von *Placunopsis* auf *Ceratites. Lethaia, 1*:156–174.

Merkt, J.
1966. Über Austern und Serpeln als Epoeken auf Ammonitengehaeusen. *N. Jhrb. Geol. Palaeontol. Abh., 125*:467–479.

Miller, H. W., Jr.
1968. Invertebrate fauna and environment of deposition of the Niobrara Formation (Cretaceous) of Kansas. *Fort Hays Studies, Science Series, 8*:90 pp.

Moseley, H.
1838. On the geometrical forms of turbinated and discoid shells. *Roy. Soc. London Phil. Trans.*:351–370.

Naef, A.
1923. *Fauna and flora of the Bay of Naples. Monograph 35.* Berlin: Friedlander and Son, pp. 55–76. [Trans. Israel Program for Scientific Translations; Jerusalem, 1972.]

Nowak, J.
1916. Zur Bedeutung von *Scaphites* für die Gleiderung der Oberkreide. *K. k. Geol. Reichsanstalt Verh., Jahrb., 3*:56–67.

Obata, I.
1959. Croissance relative sur quelques espèces des Desmoceratidae. *Mem. Fac. Sci., Kyushu Univ., Ser. D. (Geol.), 9(1)*:33–45.

1965. Allometry of *Reesidites minimus*, a Cretaceous ammonite species. *Trans. Proc. Palaeontol. Soc. Japan, New Ser., 58*: 39–63.

Obata, I., K. Tanabe, and Y. Fukuda
1980. The ammonite siphuncular wall: its microstructure and functional significance. *Bull. Natl. Sci. Mus., Ser. C (Geol.), 6(2)*: 59–72.

Obata, I., K. Tanabe, and H. Futakami
1979. Ontogeny and variation in *Subprionocyclus neptuni*, an Upper Cretaceous collignoniceratid ammonite. *Bull. Natl. Sci. Mus., Ser. C (Geol.), 5(2)*:51–88.

Obradovich, J. D., and W. A. Cobban
1975. A time scale for the Late Cretaceous of the Western Interior of North America. *Geol. Assoc. Can. Spec. Pap. 13*:31–54.

Palframan, D. F. B.
1967. Mode of early shell growth in the ammonite *Promicroceras marstonense* Spath. *Nature, 216*:1128–1130.

Parkinson, J.
1811. *Organic remains of a former world*, vol. 3. London: Sherwood, Neely and Jones, xvi + 479 pp.

Raup, D. M.
1966. Geometric analysis of shell coiling: general problems. *J. Paleontol., 40*:1178–1190.
1967. Geometric analysis of shell coiling: coiling in ammonoids. *J. Paleontol., 41*:43–65.

Reeside, J. B.
1927. The scaphites, an Upper Cretaceous ammonite group. *U.S. Geol. Surv. Prof. Pap. 150-B*:21–36.

Reeve, E. C. R., and J. S. Huxley
1945. Some problems in the study of allometric growth. *In* W. E. Le Gros Clark and P. B. Medawar (eds.), *Essays on growth and form.* Oxford, pp. 121–156.

Rice, D. D., and W. A. Cobban
1977. Cretaceous stratigraphy of the Glacier National Park area, northwestern Montana. *Bull. Can. Petrol. Geol., 25(4)*:828–841.

Saunders, W. B.
1983. Natural rates of growth and longevity of *Nautilus belauensis. Paleobiology, 9*: 280–288.
1984. The role and status of *Nautilus* in its natural habitat: evidence from deep-water remote camera photosequences. *Paleobiology, 10(4)*:469–486.

Schindewolf, O. H.
1929. Vergleichende Studien zur Phylogenie, Morphogenie und Terminologie der Ammoneenlobenlinie. *Abh. Preuss. Geol. Landesanst., 115*:102 pp.
1934. Über Epoeken auf Cephalopoden-Gehaeuse. *Palaeontol. Z., 16*:15–31.
1954. On development, evolution and terminology of ammonoid suture line. *Bull. Mus. Comp. Zool., 112(3)*:217–237.

Scott, G. R., and W. A. Cobban
1964. Stratigraphy of the Niobrara Formation at Pueblo, Colorado. *U.S. Geol. Surv. Prof. Pap. 454-L*:30 pp.

Seilacher, A.
1960. Epizoans as a key to ammonoid ecology. *J. Paleontol., 34*:189–193.
1982. Ammonite shells as habitats in the Posidonia shales of Holzmaden—floats or benthic islands? *N. Jahrb. Geol. Palaeontol. Monatsh., 159*:98–114.

Shimizu, S.
1929. On siphuncle in some Upper Cretaceous ammonites. *Saitohoonkai Publ.* (in Japanese), *4*:91–116.

Shuto, T.
1974. Larval ecology of prosobranch gastropods and its bearing on biogeography and paleontology. *Lethaia, 7(3)*:239–256.

Smith, J. P.
1898. The development of *Lytoceras* and *Phylloceras. Proc. Calif. Acad. Sci. (Geol.), 1(4)*:129–160.
1901. The larval coil of *Baculites. Am. Nat., 35(409)*:39–49.

Smith, W. D.
1905. The development of *Scaphites. J. Geol., 13*:635–654.

Stahl, W., and R. Jordan
1969. General considerations on isotopic paleotemperature determinations and analyses on Jurassic ammonites. *Earth Planet. Sci. Letters, 6*:173–178.

Stanton, T. W.
1893. The Colorado Formation and its invertebrate fauna. *U.S. Geol. Surv. Bull. 106*: 288 pp.

Stenzel, H. B.
1964. Living *Nautilus. In* R. C. Moore (ed.), *Treatise on invertebrate paleontology, part K.* Lawrence, Kansas: Geol. Soc. Am. and Univ. Kansas Press, pp. 59–93.

Stumbur, H.
1975. Biometrical characteristics of the shell of a living *Nautilus. Bull. Acad. Sci. Estonian SSR, Chem., Geol., 24(1)*:78–89.

Tanabe, K.
1975. Functional morphology of *Otoscaphites puerculus* (Jimbo), an Upper Cretaceous

ammonite. *Trans. Proc. Palaeontol. Soc. Japan, New Ser. 99*:109–132.

1977. Functional evolution of *Otoscaphites puerculus* (Jimbo) and *Scaphites planus* (Yabe), Upper Cretaceous ammonites. *Mem. Fac. Sci., Kyushu Univ., Ser. D (Geol.), 23*:367–407.

Tanabe, K., Y. Fukuda, and I. Obata

1980. Ontogenetic development and functional morphology in the early growth-stages of three Cretaceous ammonites. *Bull. Natl. Sci. Mus., Ser. C. (Geol.), 6(1)*:9–26.

Tanabe, K., I. Obata, Y. Fukuda, and M. Futakami

1979. Early shell growth in some Upper Cretaceous ammonites and its implications to major taxonomy. *Bull. Natl. Sci. Mus., Ser. C (Geol.), 5(4)*:153–176.

Tanabe, K., I. Obata, and M. Futakami

1978. Analysis of ammonoid assemblages in the Upper Turonian of the Manji area, central Hokkaido. *Bull. Natl. Sci. Mus. Ser. C (Geol.), 4(2)*:37–62.

1981. Early shell morphology in some Upper Cretaceous heteromorph ammonites. *Trans. Proc. Palaeontol. Soc. Japan, New Ser. 124*:215–234.

Tanabe, K., and Y. Ohtsuka

1985. Ammonoid early internal shell structure: its bearing on early life history. *Paleobiology, 11(3)*:310–322.

Taylor, B. E., and P. O. Ward.

1983. Stable isotope studies. *Nautilus macromphalus* Sowerby (New Caledonia) and *Nautilus pompilius* L. (Fiji). *Palaeogeogr., Palaeoclimat., Palaeoecol., 41*:1–16.

Thompson, D. W.

1917. *On growth and form.* London: Cambridge Univ. Press, 1116 pp.

Trueman, A. E.

1941. The ammonite body chamber with special reference to the buoyancy and mode of life of the living ammonite. *Q. J. Geol. Soc. London, 96*:339–383.

Ward, P. D.

1979. Cameral liquid in *Nautilus* and ammonites. *Paleobiology, 5*:40–49.

1985. Periodicity of chamber formation in chambered cephalopods: evidence from *Nautilus macromphalus* and *Nautilus pompilius. Paleobiology, 11(4)*:438–450.

Ward, P. D., and J. Chamberlain

1983. Radiographic observation of chamber formation in *Nautilus pompilius. Nature, 304*:57–59.

Ward, P. D., L. Greenwald, and O. E. Greenwald

1980. The buoyancy of the chambered *Nautilus. Sci. Am., 243*:190–203.

Ward, P. D., and G. E. G. Westermann

1977. First occurrence, systematics and functional morphology of *Nipponites* (Cretaceous Lytoceratina) from the Americas. *J. Paleontol., 51*:367–372.

Wells, H. J., and J. Wells

1977. Cephalopoda: Octopoda. *In* A. C. Geise and J. S. Pearse (eds.), *Reproduction of marine invertebrates,* vol. 4. New York: Academic Press, pp. 291–330.

1983. Cephalopods do it differently. *New Scientist, 100*:332–338.

Westermann, G. E. G.

1954. Monographie der Otoitidae (Ammonoidea). *Beih. Geol. Jahrb. Heft., 15*:1–364.

1971. Form, structure and function of shell and siphuncle in coiled Mesozoic ammonoids. *Life Sci. Contr. Roy. Ontario Mus., 78*:39 pp.

1973. Strength of concave septa and depth limits of fossil cephalopods. *Lethaia, 6*: 383–393.

Wetzel, W.

1959. Über Ammoniten-Larven. *N. Jahrb. Geol. Palaeontol., Abh. 107(2)*:240–252.

Whitfield, R. P.

1880. Paleontology of the Black Hills of Dakota. *In* Henry Newton and W. P. Jenny, Report on the geology and resources of the Black Hills of South Dakota. *U.S. Geog. Geol. Surv. Rocky Mtn. Reg.*:325–468.

Wiedmann, J.

1965. Origin, limits, and systematic position of *Scaphites. Palaeontology, 8(3)*:397–453.

1966. Stammesgeschichte und System der posttriadischen Ammonoideen. Ein Ueberblick (2 parts). *N. Jahrb. Geol. Palaeontol., Abh., 125*:49–79; *127*:13–81.

Willey, A

1897a. The embryology of the *Nautilus. Nature, 55*:402–403.

1897b. On the nepionic shell of Recent *Nautilus* (Zoological observations in the South Pacific). *Q. J. Micro. Sci. New Ser., 39*: 219–231.

Wright, C. W.

1953. Notes on Cretaceous ammonites. I. Scaphitidae. *Ann. Mag. Nat. Hist., Ser. 12, 6*:473–476.

1957. *In* R. C. Moore (ed.), *Treatise on invertebrate paleontology, part L. Mollusca 4*. Lawrence, Kansas: Geol. Soc. Am. and Univ. Kansas Press, pp. L80–L436.

Zakharov, Y. D.
1972. Formation of the caecum and prosiphon in ammonoids. *Paleontol. J., 6*: 201–206.